A feasibility study of stationary and dual-axis tracking grid-connected photovoltaic systems in the Upper Midwest

by

Ryan Duwain Warren

A dissertation submitted to the graduate faculty

in partial fulfillment of the requirements for the degree of

DOCTOR OF PHILOSOPHY

Major: Mechanical Engineering

Program of Study Committee:
Michael Pate, Co-Major Professor
Ron Nelson, Co-Major Professor
Gregory Maxwell
Palaniappa Molian
Howard Meeks

Iowa State University

Ames, Iowa

2008

TABLE OF CONTENTS

LIST OF FIGURES

LIST OF TABLES

ABSTRACT

Three primary objectives were defined for this work. The first objective was to determine, assess, and compare the performance, heat transfer characteristics, economics, and feasibility of real-world stationary and dual-axis tracking grid-connected photovoltaic (PV) systems in the Upper Midwest. This objective was achieved by installing two grid-connected PV systems with different mounting schemes in central Iowa, implementing extensive data acquisition systems, monitoring operation of the PV systems for one full year, and performing detailed experimental performance and economic studies. The two PV systems that were installed, monitored, and analyzed included a 4.59 kW_p roof-mounted stationary system oriented for maximum annual energy production, and a 1.02 kW_p pole-mounted actively controlled dual-axis tracking system. The second objective was to demonstrate the actual use and performance of real-world stationary and dual-axis tracking grid-connected PV systems used for building energy generation applications. This objective was achieved by offering the installed PV systems to the public for demonstration purposes and through the development of three computer-based tools: a software interface that has the ability to display real-time and historical performance and meteorological data of both systems side-by-side, a software interface that shows real-time and historical video and photographs of each system, and a calculator that can predict performance and economics of stationary and dual-axis tracking grid-connected PV systems at various locations in the United States. The final objective was to disseminate this work to social, professional, scientific, and academic communities in a way that is applicable, objective, accurate, accessible, and comprehensible. This final objective will be addressed by publishing the results of this work and making the computer-based tools available on a public website (www.energy.iastate.edu/Renewable/solar).

Detailed experimental performance analyses were performed for both systems; results were quantified and compared between systems, focusing on measures of solar resource, energy generation, power production, and efficiency. This work also presents heat transfer characteristics of both arrays and quantifies the affects of operating temperature on PV system performance in terms of overall heat transfer coefficients and temperature coefficients for power. To assess potential performance of PV in the Upper Midwest, models were built to predict performance of the PV systems operating at lower temperatures. Economic analyses were performed for both systems focusing on measures of life-cycle cost, payback period, internal rate of return, and average

incremental cost of solar energy. The potential economic feasibility of grid-connected stationary PV systems used for building energy generation in the Upper Midwest was assessed under assumptions of higher utility energy costs, lower initial installed costs, and different metering agreements.

The annual average daily solar insolation seen by the stationary and dual-axis tracking systems was found to be 4.37 and 5.95 kWh/m^2, respectively. In terms of energy generation, the tracking system outperformed the stationary system on annual, monthly, and often daily bases; normalized annual energy generation for the tracking and stationary systems were found to be 1,779 and 1,264 kWh/kW_p, respectively. The annual average conversion efficiencies of the tracking and stationary systems were found to be approximately 11 and 10.7 percent, respectively. Annual performance ratio values of the tracking and stationary system were found to be 0.819 and 0.792, respectively.

The net present values of both systems under all assumed discount rates were determined to be negative. Further, neither system was found to have a payback period less than the assumed system life of 25 years. The rate-of-return of the stationary and tracking systems were found to be -3.3 and -4.9 percent, respectively. Furthermore, the average incremental cost of energy provided by the stationary and dual-axis tracking systems over their assumed useful life is projected to be $0.31 and $0.37 dollars per kWh, respectively. Results of this study suggest that grid-connected PV systems used for building energy generation in the Upper Midwest are not yet economically feasible when compared to a range of alternative investments; however, PV systems could show feasibility under more favorable economic scenarios.

Throughout the year of monitoring, array operating temperatures ranged from -24.7 ^oC (-12.4^oF) to 61.7 ^oC (143.1 ^oF) for the stationary system and -23.9 ^oC (-11 ^oF) to 52.7 ^oC (126.9 ^oF) for the dual-axis tracking system during periods of system operation. The hourly average overall heat transfer coefficients for solar irradiance levels greater than 200 W/m^2 for the stationary and dual-axis tracking systems were found to be 20.8 and 29.4 W/$m^{2o}C$, respectively. The experimental temperature coefficients for power for the stationary and dual-axis tracking systems at a solar irradiance level of 1,000 W/m^2 were -0.30 and -0.38 %/^oC, respectively. Simulations of the stationary and dual-axis tracking systems operating at lower temperatures suggest that annual conversion efficiencies could potentially be increased by to up 4.3 and 4.6 percent, respectively.

CHAPTER 1 - GENERAL INTRODUCTION

THESIS ORGANIZATION

The contents of this dissertation are organized into chapters and appendices. Chapters 2-6 present journal papers in preparation to be submitted for publication. Each paper focuses on a different aspect of the experimental testing done in this work. Chapter 1 presents an overview of the work completed and a literature review of topics relevant to this project. Chapters 2 and 3 describe the design and present the experimental performance of two grid-connected PV systems used in this research: a roof-mounted stationary and a pole-mounted dual-axis tracking PV system. The performance analysis primarily focuses on measures of power production, energy generation, and efficiency. Chapter 4 presents comparisons of performance between the systems, highlighting differences in fixed and tracking mounting schemes. Chapter 5 presents a detailed economic analysis of both PV systems. Economic parameters that are considered include: life-cycle costs, payback period, internal rate of return, and average incremental costs of solar energy. Additionally, the potential economic feasibility of grid-connected PV systems in the Upper Midwest was assessed assuming scenarios of higher utility energy costs and more favorable incentive programs. Chapter 6 presents an assessment of heat transfer characteristics of the stationary and tracking arrays and quantifies the affects of operating temperature on PV system performance. Further, simulations were performed to estimate how each system might perform while operating at lower temperatures. Metrics used to assess heat transfer characteristics and affects of operating temperature on PV system performance include overall heat transfer coefficients and the temperature coefficients for power. Chapter 7 offers detailed descriptions of a real-time and historical online interactive data interface, web cameras and software interface, and a PV calculator all developed as a part of this work. Finally, Chapters 8 and 9 include general conclusions of this work and suggestions for future study, respectively. The appendices include uncertainty analysis and bid specification documents for the systems and software.

OBJECTIVES

The primary objectives of this work are to:

1. Determine, assess, and compare the performance, heat transfer characteristics, economics, and feasibility of real-world stationary and dual-axis tracking grid-connected PV systems used for building energy generation applications in the Upper Midwest

2. Demonstrate the actual use and performance of real-world stationary and dual-axis tracking grid-connected PV systems used for building energy generation applications

3. Disseminate this work in a way that is applicable, objective, accurate, accessible, and comprehensible

These primary objectives were met through the completion of the following general tasks:

1. Design, procure, install, and commission complete stationary and tracking real-world grid-connected PV systems in similar geographical locations using equipment considered standard for residential and commercial building energy generation applications

2. Design, procure, install, and commission a research-grade data acquisition system with the capability of collecting extensive and accurate performance and weather data at high sampling intervals from the installed PV systems, and archiving data in a central repository

3. Quantify, compare, and document experimental performance of the stationary and dual-axis tracking grid-connected PV systems operating in the Upper Midwest's climate using measures of power production, energy generation, and efficiency

4. Perform detailed economic analyses on both systems focusing on measures of life-cycle cost, payback period, internal rate of return, and average incremental costs of solar energy. In addition, assess potential economic feasibility of the grid-connected PV systems operating in the Upper Midwest under assumptions of varying utility energy costs, initial installed costs, and metering agreements

5. Evaluate heat transfer characteristics of the stationary and dual-axis tracking systems and quantify the affects of operating temperature on PV system performance by determining overall heat transfer coefficients of the arrays and temperature coefficients for power under outdoor conditions inherent to the Upper Midwest. Additionally, assess potential performance improvements for both systems in terms of energy generation and efficiency by modeling the systems operating at lower, yet achievable temperatures

6. Design and implement an online interface to simultaneously display real-time and historical performance data of the stationary and dual-axis tracking systems

7. Design, procure, and install web cameras and software interface to display real-time and historical video and photographs of the stationary and dual-axis tracking PV systems

8. Design, develop, and implement a Windows based interactive application having the ability to predict/model the performance and economics of stationary and dual-axis grid-connected PV systems

9. Offer results of this work and developed tools on a publically available website

CONTRIBUTIONS

The PV and data acquisition systems implemented in this work are unique in several ways. The stationary system was designed as three side-by-side, identical, and independently operating systems. This unique design offers the opportunity to assess the effects of a particular variable introduced to one or more subsystems by simultaneously comparing performance in real-time to the other(s) operating in the same environment. The tracking system is designed to have the ability to operate as either a single-axis or dual-axis tracking system; thus, this system allows for comparisons between both common tracking schemes. Further, both systems are located in similar geographical locations and use similar equipment. As a result, all common mounting schemes of PV systems can be evaluated and compared directly. The setup of these systems allow for detailed performance, feasibility, and comparative studies on mounting schemes, components, and variables affecting system and component performance (e.g., soiling, shading, etc.). Both systems are available as demonstration units. The research-grade DAQ equipment and instrumentation has the ability to collect accurate and extensive performance and meteorological data at a high sampling rate. The comprehensive and experimental data set built in this work could allow for opportunities in the development, validation, and improvement of computer simulation tools.

Operating characteristics of PV in the Upper Midwest based on experimental efforts are not well-established. In this work, the performance and economics of real-world grid-connected stationary and dual-axis tracking PV systems used in Iowa for building energy generation was evaluated in detail. The results and conclusions drawn in this work are based on onsite experimental testing and reflect what would be experienced in practice as opposed to model-based or laboratory generated simulations and predictions. Advantages and disadvantages of the different mounting schemes in terms of performance and economics are presented. The estimation of potential performance of the systems operating at lower temperatures offers insight to limits of achievable performance through the removal of

reasonable amounts of heat. Levels of utility energy costs, initial installed costs, and types of metering agreements were identified as potential conditions that may result in economic competitiveness of PV with other common investment alternatives. All results found in this work can be used to set appropriate expectations for PV systems operating in the Upper Midwest allowing design professionals and consumers to make more informed decisions. Practicing professionals could use the results of this study to better understand PV which could lead to better system selection, more intelligent system design, and improved system integration/installation.

The interactive data interface developed in this work was custom designed. This interface has the capability to simultaneously displaying actual and normalized (i.e., per square meter of PV) real-time and historical performance data from both systems. Therefore, a user can monitor the performance of the stationary and tracking systems in real-time, view historical performance of both systems, and make direct comparisons of performance between systems. Additionally, the interface is designed with a "dashboard" approach using gauges, digital values, and plots that gives a user a feel for the magnitude of each field. The webcams and software interface offers the unique ability to visually observe the operation of each system and on-site meteorological conditions while evaluating real-time performance data through the interface simultaneously. The interface and webcams offer a distinctive educational opportunity focused on PV performance in the Upper Midwest. The solar calculator developed in this work could benefit both PV professionals and consumers. This tool will enable dealers to quickly and efficiently estimate performance and economics of a proposed PV system. The user could then use the results to make an informed decision as to whether or not they are interested in pursuing the purchase and implementation of a photovoltaic system.

Surveys indicate the general public possesses little knowledge in regards to most aspects of PV; the unfamiliarity with and lack of understanding of PV technology, performance, and economics is suggested to be one reason the use of PV for building energy generation is not more widespread. There currently exists a lack of information on PV specific to the Upper Midwest that is applicable, objective, quantitative, accurate, publically available, and easily accessible. Moreover, the Upper Midwest possesses an insufficient number of grid-connected PV systems used for building energy generation available to the public for demonstration. A portion of this work aims to address these shortcomings by offering the installed PV systems as demonstration units and by expanding a publically available website to present general information about the systems themselves, performance and economic data, and other tools for learning about and increasing awareness of PV.

BACKGROUND/LITERATURE REVIEW

A general overview of U.S. electricity generation and consumption, PV markets, the fundamentals of PV, and a general survey of literature relating to this project is presented herein.

US Electricity Generation and Consumption

Conventional methods for energy generation using fossil-fuel based sources in the U.S. are negatively impacting our economy, national security, environment, natural resources, and public health. Additionally, negative impacts resulting from the use of fossil-fuels are intensifying due to the Nation's increasing demand of energy; total electricity consumption in the U.S. (considering both electric power producers and on-site distributed generation) is projected to increase at an average annual rate of 1.1 percent [1]. Thus, the increasing demand of energy must be met while decreasing the use of fossil-fuels. Conventional energy generation methods must be reformed by using sources that are renewable, domestic, distributed, and environmentally friendly; solar-photovoltaic (PV) systems are an alternative to conventional methods for energy generation possessing these characteristics.

U.S. electricity generation in 2006 by fuel source is shown in Figure 1.1. Approximately 71 percent of all electrical energy consumed in the U.S. in 2006 was derived from fossil fuels; namely, coal, petroleum, and natural gas [2]. Only 9.5 percent of the total electrical energy supply in 2006 was derived from renewable sources (including hydroelectric); further, only approximately 0.13 percent of the renewable energy supplied was generated through solar-photovoltaics [2, 3].

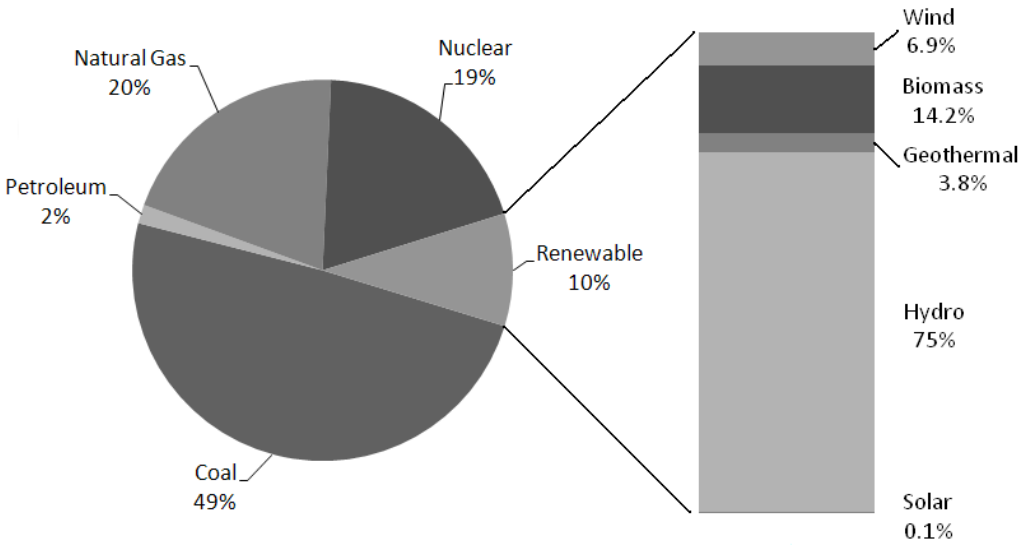

Figure 1.1. 2006 U.S. electricity generation by source [2, 3]

In 2006, the total energy consumption in the U.S. by end-use sector was as follows: 32 percent industrial, 29 percent transportation, 21 percent residential, and 18 percent commercial [4]. If the energy use by sector is examined in greater detail, 48 percent of the total energy generated in 2006 was consumed in buildings [5]. In terms of electricity consumption, 75 percent of the total went to operate buildings [5]. Additionally, it has been estimated that in the year 2035, approximately 75 percent of the built environment in the U.S. will either be new or renovated [5]. Thus, buildings are both one of the largest problems, and opportunities in terms of energy [5].

To reduce energy use or improve energy utilization in buildings, the most immediate cost effective strategy is focusing on reducing energy use through improving energy efficiency. Current energy utilization research is taking place in all facets of buildings and includes areas such as building envelopes, lighting, daylighting, heating ventilating and air-conditioning (HVAC) equipment and controls, and water heating, to name a few. A group of organizations led by the American Society of Heating, Refrigerating and Air-Conditioning Engineers, Inc. (ASHRAE) recently released publications with strategies for reducing energy consumption in buildings by 30 percent over a standard code compliant building built to the requirements of ANSI/ASHRAE/IESNA Standard 90.1-1999 [6-9]. However, even with loads reduced dramatically, buildings will still require electric power.

PV and Other Renewables for Onsite Building Energy Generation

Current renewable energy systems that are utilized in buildings include geothermal, wind, and solar energy systems. Although geothermal systems can reduce the consumption of energy, these systems do not generate energy, and thus, still require auxiliary power to operate. Additionally, geothermal energy systems can be difficult to integrate into existing buildings and can require significant amounts of space for a well field. Furthermore, these systems require routine maintenance due to moving parts and circulating fluid of the system.

Wind energy systems also have vast potential for local building energy generation, yet have some inherent disadvantages in comparison to other forms of renewable energy sources. Wind turbines and towers are large and require extensive capital and engineering to design and install. These systems have moving parts and are prone to regular maintenance requirements. In addition, many cities have regulations that restrict towers within city limits. Moreover, wind resources can be greatly minimized due to surrounding structures/ground cover to the site, which degrades their effectiveness in urban areas. Wind energy systems are most conducive to rural settings.

Solar energy systems could show the most promise for existing and new building integration for electrical energy generation applications. PV systems can often be installed directly to a building without further strengthening the existing structure. These systems have no moving parts and maintenance requirements are relatively minimal. Additionally, in comparison to wind, PV systems can be simpler to design. Solar energy systems are currently more expensive on a peak Watt basis to implement in comparison to wind and geothermal systems. However, government incentives, technological advances, and the potential for PV equipment to replace building materials increase economic feasibility.

PV Markets

The demand for PV is highly concentrated in certain regions of the world. The world demand for PV modules by region is shown in Figure 1.2.

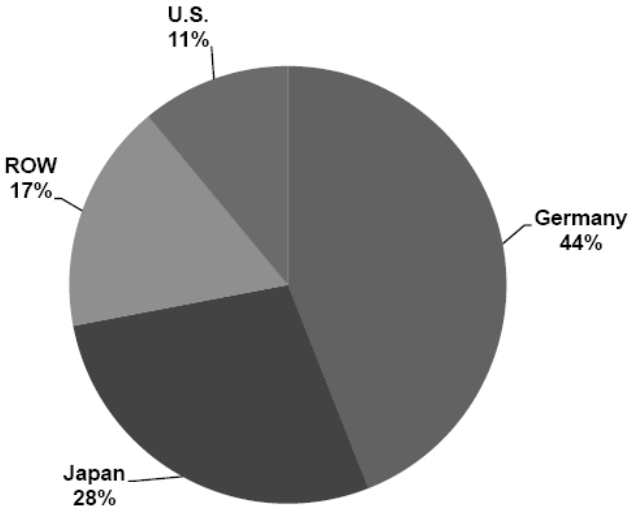

Figure 1.2. World demand of PV by region in 2005 (in terms of regional shipments) [10]

In 2005, approximately 44 percent of all PV modules were shipped to Germany, 28 percent were shipped to Japan, and 11 percent were consumed in the U.S. [10].

Markets for solar photovoltaic systems are growing at exponential rates worldwide and in the United States. Annual shipments of PV (in peak kilowatts) in the U.S. between 1997 and 2007 can be seen in Figure 1.3.

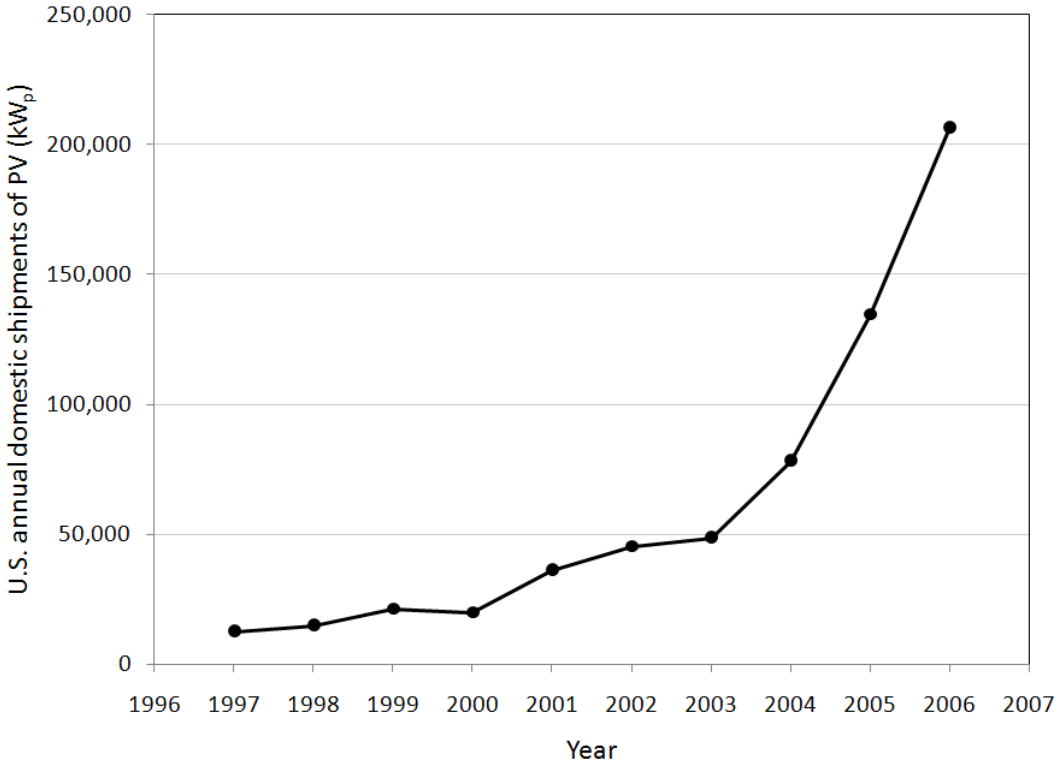

Figure 1.3. Annual domestic shipments of PV in the U.S. [11]

Annual domestic shipments of PV in the U.S. have increased at an annual average rate of 36 percent between the years 1997 and 2006 [11].

A breakdown of PV cell and module shipments by type between the years of 2004 and 2006 is shown in Figure 1.4.

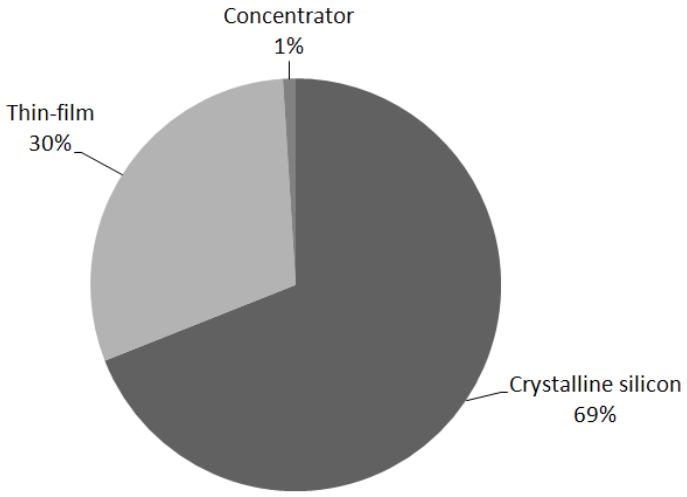

Figure 1.4. Photovoltaic cell and module shipments by type, 2004-2006 [12]

The U.S. demand for PV by type and sector in 2006 can be seen in Table 1.1.

Table 1.1. U.S. demand for PV by type in 2006 [12]

Sector Market	Crystalline Silicon (kW_p)	Thin-Film Silicon (kW_p)	Concentrator Silicon (kW_p)	2006 Total (kW_p)
Industrial	22,018	6,600	0	28,618
Residential	84,930	9,801	1,084	95,815
Commercial	97,949	82,603	300	180,852
Transportation	2,455	3	0	2,458
Utility	1,314	2,067	600	3,981
Government	7,130	558	0	7,688
Other	17,723	134	0	17,857
Total	233,519	101,766	1,984	337,269

The use of PV is most prevalent in the commercial, residential, and industrial sectors consuming approximately 91 percent of the overall demand [12]. Further, crystalline silicon PV technology dominates the market when compared to thin-film and concentrator type PV. However, when considering only the commercial sector, the use of crystalline silicon is comparable to thin film.

PV is used in a wide variety of applications. The U.S. demand for PV by end-use sector in 2006 is shown in Table 1.2.

Table 1.2. U.S. demand for PV by end-use in 2006 [12]

End Use	Crystalline Silicon (kW_p)	Thin-Film Silicon (kW_p)	Concentrator Silicon (kW_p)	2006 Total (kW_p)
Electricity Generation	201,254	88,962	1,984	292,200
Grid Interactive	186,894	86,319	984	274,197
Remote	14,360	2,643	1,000	18,003
Communication	6,767	121	0	6,888
Consumer Goods	1,170	2,860	0	4,030
Transportation	2,435	3	0	2,438
Water Pumping	2,093	0	0	2,093
Cells/Modules to OEM	2,644	3,488	0	6,132
Health	0	0	0	0
Other	17,156	6,332	0	23,488
Total	233,519	101,766	1,984	337,269

PV is primarily used for building energy generation applications. Eighty-six percent of all PV used in 2006 was used for grid-connected and remote energy generation systems [12].

The installed PV capacity in the U.S. was approximately 0.03 Gigawatts in 2006 [1]. Within the U.S., approximately 80 percent of the installed PV capacity is located in California.

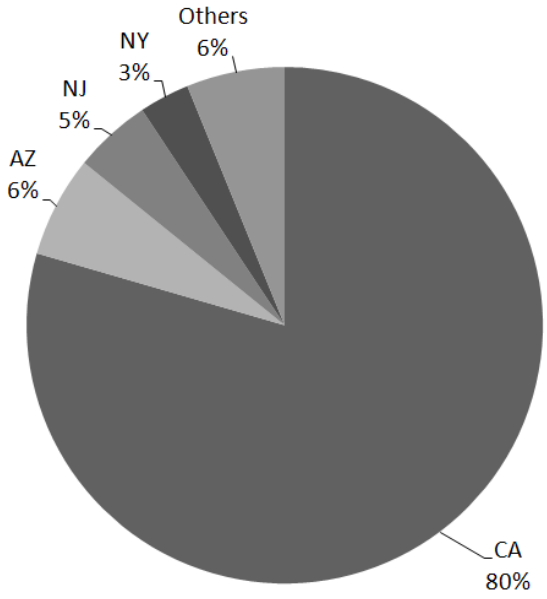

Figure 1.5. U.S. distribution of PV [13]

The cumulative installed capacity of grid-connected PV systems in Iowa as of 2007 was approximately 0.1 MW_{DC} [13].

In summary, as of 2006, the U.S. holds only an 11 percent market share of PV shipments, whereas Germany and Japan support 76 percent of the market, collectively [10]. However, the use of PV in the U.S. is increasing at an annual average rate of 36 percent per year (between 1997 and 2006) [11]. Most PV in the U.S. is used in the residential and commercial sectors for building energy generation applications and is dominated by crystalline silicon and thin film technologies. The distribution of PV in the U.S. is heavily imbalanced; approximately 80 percent of the installed PV capacity in the U.S. resides in California [13].

Solar Resource in U.S. and Iowa

The solar resource (on a horizontal plane) in Iowa ranges from 3.6 to 4.2 $kWh/m^2/day$ [14]; the distribution of solar resource on a horizontal plane in Iowa is shown in Figure 1.6.

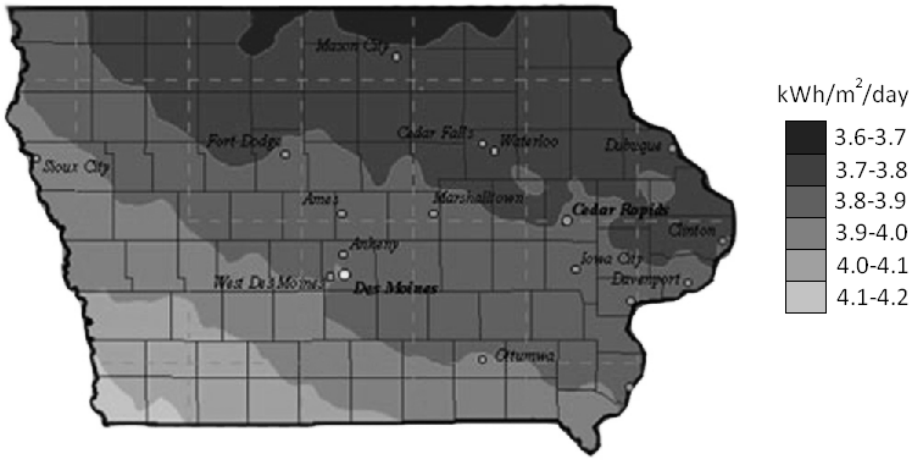

Figure 1.6. Iowa annual average solar resource on a horizontal plane [14]

The solar resource available to stationary (oriented at a slope equal to the latitude of the location) and dual-axis tracking systems on a national basis can be seen in Figure 1.7.

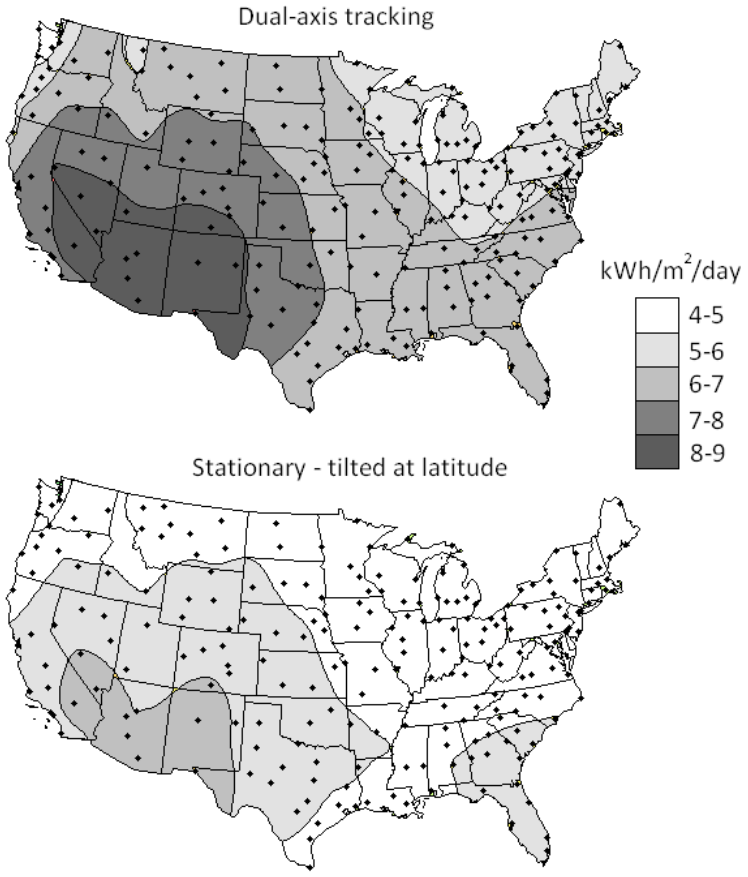

Figure 1.7. U.S. annual average daily solar resource [15]

The solar resource available in Iowa ranges from 4.4 to 5.3 kWh/m^2/day for stationary systems (oriented at a slope equal to the latitude) and 5.9 to 7.3 kWh/m^2/day for dual-axis tracking systems based on solar insolation observed over a 30 year period [16].

Solar Energy and the Photoelectric Effect

Solar photovoltaic cells are devices that convert solar energy into usable electrical energy via the photoelectric effect. The photoelectric effect was first observed by a French physicist, Alexandre Edmond Becquerel in 1839 [17]. The first PV cell was developed at Bell Laboratories in 1954 [18]. The sun emits energy in the form of electromagnetic radiation. Electromagnetic radiation, including sunlight, is made up of photons traveling in a wave-like pattern and moving at the speed of light [19]. The wave-like pattern of electromagnetic radiation can be characterized in terms of wavelength or frequency. The moving photons that make up electromagnetic radiation have an associated amount of energy which is a function of the wavelength or frequency at which they are moving. The energy of a photon can be calculated by

$$E_{photon} = \frac{hc}{\lambda} \tag{1.1}$$

where h = Planck's constant, 6.626 x 10^{-34} Js

c = Speed of photon (speed of light), 3 x 10^8 m/s

λ = Wavelength

The entire range of wavelengths or frequencies of electromagnetic waves is referred to as the electromagnetic spectrum. Most of the energy emitted from the sun is in a range of wavelengths from approximately 2x10^{-7} to 4x10^{-6} meters, which is primarily in the visible light region, shown in Figure 1.8 [20].

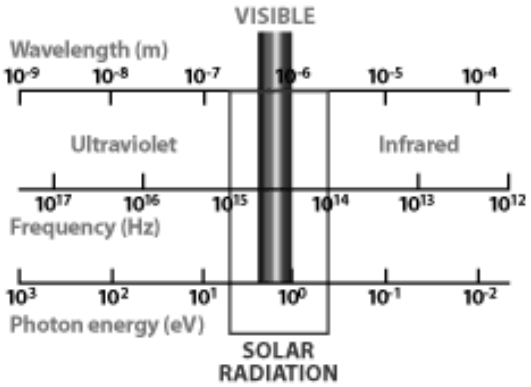

Figure 1.8. Solar wavelength, frequency, and photon energy [20]

Photovoltaic devices are made of semiconductor materials; the most common type of material used for PV devices is silicon. Impurities such as phosphorous and boron are added to a semiconductor, such as silicon, to change properties of the material through a process known as doping. Silicon material doped with phosphorous is an n-type semiconductor, whereas silicon doped with boron is a p-type semiconductor. Phosphorous atoms have five valance electrons, four of which covalently bond with neighboring electrons of silicon atoms; the remaining electron is loosely bound to the positive charge of the nucleus in the phosphorous atom [18]. In contrast, boron atoms have three valance electrons; each of these electrons form a strong covalent bond to neighboring electrons on silicon atoms leaving one silicon electron available for bonding. Thus, the n-type semiconductor has an excess of electrons and a negative charge, while the p-type semiconductor has a positive charge and a deficient number of electrons. A photovoltaic device can then be constructed by joining n-type and p-type semiconductors; the region where the n-type and p-type semiconductors are joined is called the p-n junction [21]. When a p-n junction is formed, free electrons in phosphorus atoms from the n-type side bond with available silicon electrons on the p-type side and form what is known as the depletion zone [22]. An electric potential (or electric field) is formed across the depletion zone by the organization of these charges and inhibits any further electrons from crossing the p-n junction (or depletion zone) [22, 23].

Electromagnetic radiation from the sun that strikes a photovoltaic device is reflected, absorbed, or transmitted through. The absorbed energy is either transformed into thermal energy or initiates the photovoltaic effect and creates usable electrical energy. Photons that do not have enough energy to break an electron bond pass through the cell with no interaction [23]. Photons absorbed into the photovoltaic device with energy levels equal to or greater than the band gap energy (i.e., the amount of energy required to break an electron from its covalent bond) of the device can break apart an electron pair; thus, a negative electron and a positive hole are created [18]. The electric field surrounding the p-n junction then pushes the negative electron to one side of the junction and new hole to the other [18]. If an electron bond is broken in the n-type semiconductor, then the electron is attracted/pushed to the p-type semiconductor through an external electrical circuit; in contrast, if an electron bond is broken in the p-type semiconductor, then the electron is attracted/pushed to the n-type semiconductor through the n-p junction via the electrical field. This redistribution of electrons and holes through the junction and electric circuit is the means for which electrical energy is generated in a photovoltaic device.

Types of PV Cell/Module Materials and Structures

The primary technologies utilized in PV devices can be divided into two types by semiconductor material: crystalline silicon and thin film [24, 25]. The two main types of crystalline silicon PV cells are monocrystalline which is also known as singlecrystalline (sc-Si), and multicrystalline silicon (mc-Si) [24, 26]. Materials used for thin film cells can be divided into two types: amorphous silicon and polycrystalline materials [24]. Polycrystalline materials can include: cadmium telluride (CdTe) and copper indium (gallium) diselenide (CIS or CIGS) [24, 27].

Crystalline silicon is the most prominent type of solar cell/module in current markets; in 2006, crystalline silicon made up 69 percent of all shipments of PV [12, 28]. Monocrystalline (or singlecrystalline) silicon cells have a uniform molecular structure that is ideal for transferring electrons efficiently through the material [25, 29]. These cells are primarily produced using the Czochralski (CZ) method where a crystal seed is submersed into molten silicon and withdrawn slowly as the silicon crystallizes [25, 29, 30]. Multicrystalline silicon can be produced using several different techniques; the most common methods involve casting processes [29]. The ingot is typically created from a square mold and cut into square shaped cells that can be assembled together into a module [29]. Multicrystalline silicon cells are of lower-grade than monocrystalline silicon and are generally less efficient; however, they are more cost effective to produce [25, 29]. Monocrystalline and multicrystalline silicon semiconductor materials used in the construction of PV cells and modules are required to be of considerable thickness (several hundred microns) in comparison to thin film [24].

Materials used for thin film PV are typically characterized as efficient light absorbers; additionally, the semiconductor material is only required to be approximately one micron thick [24]. The use of thin-film PV is not as prevalent compared to crystalline silicon. In general, thin-film conversion efficiencies range from 5-7 percent compared to 12-14 percent conversion efficiencies commonly experienced with crystalline silicon modules [31]. Due to lower conversion efficiencies, additional space is required for a thin-film based system to meet design energy demand. Often, demand for thin-film PV is application-based. Thin film PV is used in building energy generation applications and also for small devices such as calculators, watches, etc. Thin film PV does have some advantages when compared to typical crystalline silicon modules. Laminates made from thin film can be integrated into a building roof structure having the appearance of shingles which can improve the overall aesthetics of the structure. Additionally, thin film PV is generally thinner, flexible, and has less weight than conventional panels. Thin film PV can be easily transported and used in remote areas to power small devices. Less material is required in thin

film PV in comparison to other technologies which aid in reducing manufacturing costs; thin film PV can also be manufactured in large volumes and can be deposited on flexible materials [24, 32]. Amorphous silicon is the leading thin film PV material and has the ability to absorb solar radiation approximately 40 times more efficiently than single-crystalline [24, 25, 29]. However, amorphous silicon is a non-crystalline form of silicon that does not have structural uniformity and contains many bonding defects [29]. Certain bonding defects provide places where electrons can bond instead of moving to the external circuit to form electricity; however, some defects can be minimized through hydrogenation where hydrogen atoms are introduced to fill these holes and permit electrons to move through the material [29]. Polycrystalline materials including CdTe and CIS are also commonly utilized in thin film cells. These materials are known to have high absorptivity of light; however, CdTe and CIS materials tend to have high electrical resistivity, which results in high resistive losses in the cell [32].

Four types of cell structure designs are typically considered with common PV modules: homojunction, heterojunction, p-i-n or n-i-p, and multijunction. Homojunction devices are those PV devices that join two of the same materials (e.g., silicon) each having been doped so that one is a p-type and the other n-type. Most often, homojunction devices are made of crystalline silicon-based materials. Homojunction devices are designed so that the maximum amount of light is absorbed near the p-n junction; this design allows the electron-hole pair to effectively separate and reduces recombination affects [33].

Heterojunction devices are those devices that join two dissimilar semiconductor materials together, each having a different band gap. In these devices the top layer material is typically selected to have a high band gap so that much of the solar energy is transmitted to the bottom layer, which typically has a low band gap absorbing light very effectively [33]. With this design, the electron-hole pairs are mostly created near the junction, as with homojunction devices, to promote separation and reduce recombination. Common examples of materials used in heterojunction devices are cadmium sulfide (Cds) and copper indium diselenide ($CuInSe_2$ or otherwise denoted as CIS) [33].

P-i-n and n-i-p structures are created using three layers; these layers can be made of similar or dissimilar materials. As suggested in the name, the three layers consist of an n-type, p-type, and an i-type (undoped) material in the middle [33]. The electric field is created by the interactions between the n-type and p-type materials across the intrinsic layer. For these cell structures, the depletion region makes up a significant fraction of the total cell thickness [28]. Photons with enough energy then form electron-hole pairs in the intrinsic layer/region which are then separated by the electric field. One characteristic of these structures that sets it apart from the others is that the electron-holes pairs are

formed within the depletion zone instead of outside of it and is subject to the diffusion of the electron and hole [33].

Multijunction structures consist of multiple layers of semiconductor materials, each having differing band gaps to utilize as much of the solar spectrum as possible [33]. The top layer always has the highest band gap and each layer thereafter has progressively lower band gaps to allow the largest amount of energy to penetrate the cell. Multijunction cells can be manufactured in two ways: mechanically and monolithically [33]. In a mechanical design, two solar cells are made independently and stacked on one another; in a monolithic design, a solar cell is made and layers of remainder cells are grown or deposited directly on the first [33]. Many multijunction cells utilize gallium arsenide as the primary material [33].

In summary, homojunction structures use two layers of the same material but doped with different atoms making one side n-type and the other p-type; heterojunction structures use two dissimilar materials with the top having high band gap and the lower an efficient light absorber; n-i-p or p-i-n structures use similar or dissimilar materials in three layers where the depletion zone stretches across the intrinsic layer; and multijunction structures use similar and dissimilar materials in multiple layers having different band gaps to utilize a greater amount of the solar spectrum [33].

Types of PV systems

PV systems can be divided into two types: standalone and grid-connected. Standalone systems are much less common than grid-connected systems; as shown in Table 1.2, standalone systems represent 5.34 percent of the shipments of PV in the U.S. in 2006 [12]. These systems are most often utilized in remote areas where either an electrical service is not available or it is not economically feasible to bring an electrical service to the site. Standalone systems often require additional equipment, which can include battery banks and charge controllers. This additional equipment increases costs and maintenance requirements. Common applications for standalone systems can include: building energy generation, remote water-pumping systems for livestock, remote weather stations, road-side signs, etc.

Grid-connected PV systems are the most common type for building energy generation; in 2006 grid-connected represent approximately 81.3 percent of the installed PV capacity in the U.S [12]. These systems are connected directly to the utility grid and building electrical system. Thus, building electrical demand can be supported by either the PV system or utility, or both simultaneously. These systems typically consist of a PV array, mounting structure, inverter, wiring, and general hardware such as disconnects, conduit, ground rod, etc.

Electrical loads in buildings with grid-connected PV systems are met in one of three ways (i) all of the load is met with utility supplied power (e.g., during non-sunlight periods), (ii) a portion of the load is met with utility supplied power and a portion of the load is met with power produced by the PV system (e.g., when building load is greater than power output of PV system), (iii) or all of the load is met with power produced by the PV system (e.g., when the load of the building is either equal to or less than the output power of the PV system). When the PV system is generating more power than is demanded by the building, the excess power is fed into the utility grid. The excess quantity of energy fed back into the grid is then accounted for by either measuring it directly (using a second meter) or crediting it in terms of net energy usage at the site (using one meter with the ability to turn backwards), depending on the specific grid-connect agreement with the local utility.

Quantifying the excess energy generated in terms of net energy usage is known as "net metering" (also known as net billing). The net energy is typically measured using an electric meter that has the ability to run backwards during periods where the renewable energy system is generating more power than what is demanded onsite. In a net metering agreement, the utility credits the accumulated excess energy to the consumer for later use to offset future electrical energy consumption. The credited excess electrical energy is credited to the consumer at retail prices. However, not all states and utilities offer net metering agreements to consumers. As of August 2008, 42 states including the District of Columbia have adopted net metering for renewable energy systems. Net metering programs offered in the U.S. vary considerably [34]; specific restrictions and rules for net metering agreements by state are well documented [35].

Some utilities are opposed to net metering due to potential negative financial impacts [36]. Yet, under federal law, if net metering is not offered, utilities are obligated to allow independent power producers to interconnect with the grid and purchase excess generated energy [36]. However, excess energy may only be purchased by the utility at their wholesale cost of electricity, which may be significantly less than the retail rate imposed to the customer [37]. Under this type of agreement, excess energy is typically quantified using a second meter to monitor only energy fed into the grid.

Costs of PV

The national average installed cost of a grid-connected, stationary, multicrystalline, flat-plate PV system is approximately 9 $/W$_p$ [38-40]; typical costs in Iowa range from 8-10 $/W$_p$. A breakdown of typical installed costs for a residential system is shown in Figure 1.9.

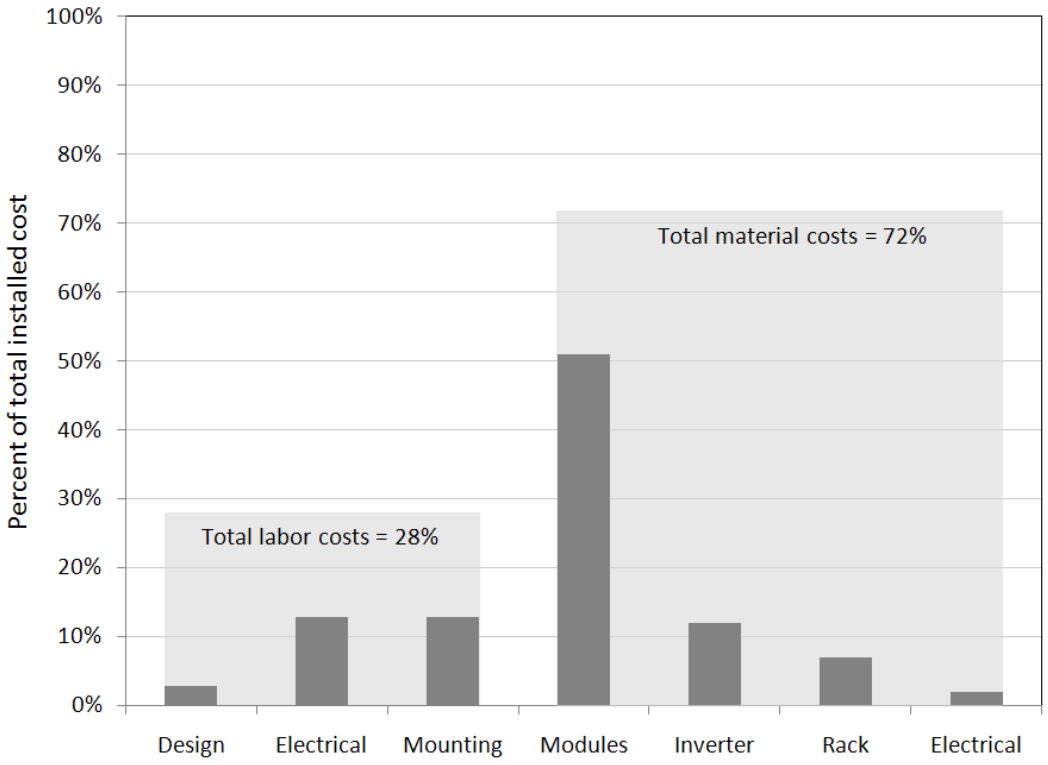

Figure 1.9. Breakdown of typical installed costs for residential system [41]

Module costs, set in a worldwide market, are heavily influenced by factors outside of the U.S., (e.g., demand for PV in Japan and Germany) and have not shown significant price declines in the past few years [38]. The costs of typical multicrystalline PV modules used in residential and commercial installations, which may represent 50 to 60 percent of the installed cost, are approximately 4.85 $\$/W_p$ (as of October 2008) [42]. The average retail cost of PV modules to the consumer has remained fairly constant since 2001 [38]. Module prices declined slightly between 2001 and 2005 but have shown slight increases in recent years from 2005 to 2008, shown in Figure 1.10.

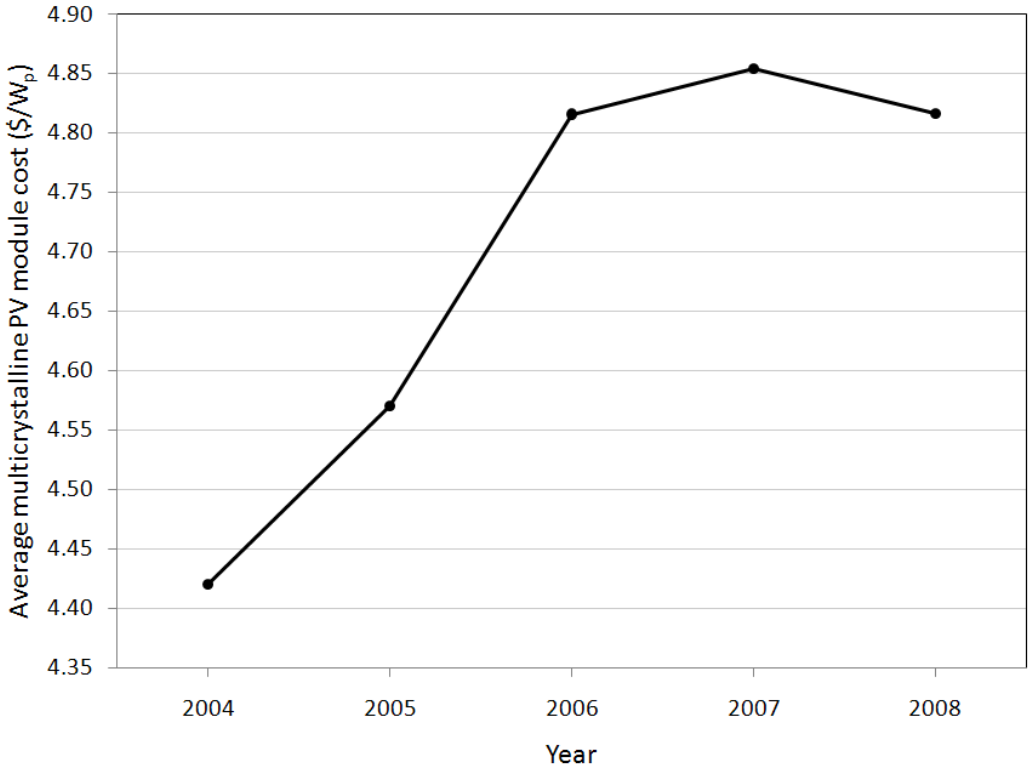

Figure 1.10. Average annual costs for multicrystalline PV modules in U.S. [42]

Inverter costs can represent 10-20 percent of the initial cost of the system [43]. The current cost of an inverter in the 1-3 kW range is approximately 1 $/Watt [43]. Inverter prices are predicted to decrease by approximately 35 percent in 10 years and 50 percent in 20 years [43]. Studies have shown that inverters may fail requiring replacement every 5 to 10 years [43]. As a result, a new inverter may be required 2 to 5 times over the life of a PV system (assuming a 25 year system life). Furthermore, major inverter manufacturers do not foresee increasing inverter lifetime to 20 years as a practical goal [43].

The installed costs of PV systems show some economies of scale, which is most evident for systems less than 10 kW_p in size [38]. Average costs for systems less than 2 kW_p were found to be approximately 9 $\$/W_p$ while systems larger than 25 kW_p were found to average approximately 7.1 $\$/W_p$ (assuming a derate factor of 0.84) in 2004 [38]. The average size of grid-connected PV systems in the residential sector in the U.S. in 2005 was approximately 4.7 kW_p [13].

To make PV more economical to the consumer, reducing non-module costs (e.g., installation, balance of system equipment) may be the most appropriate goal [38]. A significant portion in cost reductions of PV systems in the recent past have come from non-module costs [38]. Studies indicate that non-module

costs may be decreased locally by implementing programmatic activities such as providing business development funding to installers, supporting standardized PV products, offering installer training and certifications, and making performance data more publically accessible to further encourage supply competition [38].

Several financial incentives targeting the use of PV systems for energy generation are available in the Upper Midwest. Incentives are offered at federal, state, and local levels and may vary depending on the system location, type, size, and end-use sector (e.g., residential, commercial, industrial, agricultural, etc.). Incentives applicable to qualified PV systems in Iowa may include: property and sales tax exemption, accelerated depreciation tax deductions, production tax credits, low interest financing, rebates (in limited areas), net-metering, and the exclusion of subsidies provided by utilities from gross income [44].

Incentives offered to reduce the cost of PV making these systems more economical are the most significant drivers for current PV markets [38]. To illustrate this point, consider the distribution of installed PV systems in the United States. As of 2006, roughly 80 percent of the installed PV systems in the U.S. reside in California [45]. This imbalance is not entirely due to insufficient solar resources elsewhere. In fact, sites exist in the Upper Midwest where equal or more solar energy is available than portions of California. The driving factor that explains the widespread use of PV in California is attractive economics for these systems due to state incentives and relatively expensive energy. California has adopted a combination of financial and regulatory incentives that promote owning and operating PV systems. The most important of these incentives is the "buydown" or rebate programs that pay between 3 and 4.5 $\$/W_p$, which can be roughly half of the total installed cost to utility customers who invest in PV [46].

Barriers to Widespread Use of PV

The widespread use of PV in the Upper Midwest and elsewhere is being inhibited by a number of barriers. Some prominent barriers that have been identified include: high initial costs, unfamiliarity with and lack of understanding of PV technology amongst the public, economics of PV for building energy generation applications are not competitive with other sources of energy or alternative investments, lack of performance and reliability data, and a lack of financial incentives promoting the use and implementation of PV. In addition to the these barriers, common conceptions and beliefs of surveyed respondents have identified the following barriers to adoption (percentage of respondents surveyed that believe in barrier is noted): likely fuel savings not worth the cost (40%), insufficient electricity from

the system (28%), difficulty finding a reputable installer (24%), difficulties connecting to existing electricity systems (24%), new technology with uncertain performance and reliability (19%), and difficulty finding suitable location for system (16%) [47].

In Iowa, a grid-connected stationary system oriented for maximum annual energy generation would produce approximately 1,300 kWh/kWp/year [48]. Further, typical installed costs for these systems range from 8-10 $/W$_p$. Using future electric costs estimated by NIST [49] and assuming a 25 year system life, solar energy costs would be approximately 29 cents per kWh over the life of the system. It has been estimated that for the solar industry to penetrate the electricity segment, installed solar system costs will need to drop from approximately 8-10 $/W$_p$ to 3 $/W$_p$ [39]. Using a similar analysis, if the incremental installed cost of PV were to drop to 3 $/W$_p$, solar energy costs would drop from approximately 29 cents per kWh to 9.2 cents per kWh over the life of the system, which would be competitive with Iowa's current energy costs from a local utility. In order for prices to drop from current levels to 3 $/W$_p$, the cost of PV would need to drop 10 percent per year for the next 11 to 13 consecutive years.

The Iowa Department of Natural Resources has formed an advisory committee to create a strategic plan to increase the use of PV technologies. The committee commissioned a survey to determine barriers and potential solutions to the increased use of PV technologies in the Midwest. Respondents to this survey included 1,206 architects, contractors, developers, engineers, college instructors, and realtors in the Midwestern states. It was concluded that currently, basic information about costs, brands and installation is not available in a central clearinghouse [50]. In addition, it was indicated that there currently exists low familiarity with and understanding of PV and that most professionals believe that the general public was not at all informed about PV systems [50]. Respondents of the survey felt that potential solutions to increased use of PV are to disseminate information of PV technology, create case studies and payback as well as price information, and develop demonstrations to show actual operation of PV systems used for building energy generation applications [50]. The strategic plan developed by the DNR's committee includes creating a PV Yellow Pages with information on educational resources, developing case studies of applications in the Midwest and provide technical information, deploying a web site with PV information for the public and practicing professionals, and organizing public tours of existing PV systems to show the applicability of PV in the Midwest [50].

The Sandia National Laboratory offers information on what they feel are current technical, market, and institutional barriers to the widespread use of PV [51]. This organization has also identified the lack of

PV education and awareness to be a barrier. However, more specifically, they feel that information and education on PV must be targeted to specific end-user groups. For example, information geared to the general consumer should be focused on presenting the practicality and performance of PV systems over time and not on the underlying physics and theory [51]. Correspondingly, information offered to practicing professionals in the field should be more focused on components so that they can select, install, and maintain systems for consumers [51]. Lastly, the Sandia National Laboratory stresses the importance of beginning consumer awareness of and familiarity with solar technologies at an early age in educational institutions [51]. The underlying idea of targeted information to specific groups is that through appropriate information distribution, each particular group can better do their part to support a more widespread use of PV [51].

Drivers to the Widespread Use of PV

The use of PV for energy generation has many benefits. PV is renewable, domestic, environmentally friendly, distributed, modular, versatile, easy to maintain, and reliable. Additionally, the production of electrical energy using PV coincides with peak electrical demand, and the user can avoid fuel price and supply risks.

Sharp Electronics Corporation in Japan conducted a survey of 1,004 adults to measure perceptions of solar power. Results of this survey show that 80 percent of Americans believe solar power should be offered as an option for all new home construction [52]. Additionally, the survey found that 66 percent of Americans would be willing to pay a premium for homes with solar systems when told that these homes have a proven higher resale value [52]. One-half of the respondents surveyed would spend up to ten percent more for a solar-equipped house. This is a very interesting result if the net worth of utilizing PV for residential energy generation is analyzed in greater detail. The national average installed cost of a PV system in the U.S. is approximately 9 dollars per peak Watt. Therefore, a ten percent premium for a solar equipped residence would allow a consumer to install roughly 0.011 peak Watts of installed PV per dollar of home value (i.e., [1Wp PV/$9]*[$1 PV premium/$10 home value]). In Iowa, a typical stationary, grid-connected PV system produces approximately 1.30 kWh/Wp of energy. Also, the average retail rate of electricity for the residential sector in Iowa in February 2008 was 8.27 cents per kWh [53]. Consequently, the consumer may save approximately $0.001195 dollars in energy savings per year per dollar of home value (i.e., [$0.011/$1 home value]*[1.3 kWh/Wp/yr.]*[$0.0827/kWh]). According to the Appraisal Journal, home value increases approximately twenty dollars for every one dollar reduction in annual utility bills [40]; as a result, the consumer's home would increase in value due

to PV energy savings by $0.02389 per dollar of home value. Thus, a ten percent premium for PV would only yield about 24 percent in increased home value. In other words, the consumer is willing to pay 4.2 times more for a PV system than the resulting additional worth of the home due to the estimated energy savings. This result shows that although economics play a significant role in adoption PV technology, economics alone are not the only drivers.

The Design Innovation Group conducted a survey to gain insight to key reasons consumers feel PV is important. Respondents to this survey indicated the reasons for implementing PV include (percentage of respondents indicating each driver is noted): environmental concern (56%), funds available (43%), saving energy (31%), saving money on energy bills (25%), try out an innovative technology (19%) [47]. This survey additionally surveyed consumers that had PV systems to gain insight to benefits consumers felt they experience through the use of PV and included (percentage of respondents agreeing with benefit is noted): greater concern about saving energy (38%), satisfied or very satisfied with system (31%), pleasure of using a renewable energy (31%), greater energy efficiency/lower energy use (25%), and lower fuel bills (19%) [47].

PV Performance

Manufacturers rate the performance of PV modules under conditions known as Standard Reporting Conditions (SRC) or Standard Test Conditions (STC) [54]. The specific standard test conditions used by manufacturers are: solar irradiance of 1,000 W/m^2, reference air mass of 1.5 (ASTM Standard Spectrum), a zero-degree angle of incidence (AOI), and cell junction temperature of 25 degrees Centigrade. However, operating conditions experienced in practice rarely occur at STC. Additionally, systems do not output rated DC power to the inverter at STC due to losses and inefficiencies. Furthermore, the inverter, and AC-side wiring and connections introduce additional losses causing AC power output to the building or grid to be less than DC power input to the inverter. Thus, the performance of PV systems must be evaluated for a range of conditions and requires looking further than manufacturer's specifications.

Past studies characterizing performance of PV systems have been conducted in both indoor laboratory environments and outdoor conditions. The performance of PV systems is typically characterized using measures of energy generation, power production, and conversion efficiency. Energy generation is typically presented on monthly and annual bases; power production is often shown as a function of solar irradiance level; and efficiency is commonly presented in terms of average conversion efficiency or performance ratio. Additionally, the effects of other parameters on performance, such as operating temperature and incidence angle, are often evaluated.

Cueto [55] analyzed experimental outdoor performance of stationary flat-plate modules, including crystalline silicon, in terms of energy production, effective efficiency and performance ratio. Average daily energy generation results are shown verses average daily solar insolation; annual energy generation for crystalline silicon modules evaluated ranged from 192-243 kWh/m^2. Performance ratio values for crystalline silicon modules were found to range from 84-88% in the summertime and 95-101% in the winter season. The seasonal variations found in performance ratios were attributed to differences in operating temperature. Daily average conversion efficiency of the crystalline modules was found to range from 9.5-12.8% at an operating temperature of 20 degrees Centigrade. Cueto concluded that conversion efficiency for crystalline silicon is strongly temperature-dependent.

King et al. [56] studied factors that influence annual energy production of multicrystalline PV modules at a system level. This study is model based and for conditions experienced in Albuquerque, Sacramento, and Buffalo. Factors King identified having most significance on annual energy production include: cumulative solar irradiance, module power rating at the Standard Reporting Condition, operating temperature (temperature coefficient influence), maximum-power-voltage dependence on solar irradiance level, soiling, variation in solar spectrum, and optical losses when sunlight is at a high angle-of-incidence. Modeled results for stationary (oriented at a slope equal to latitude) and dual-axis tracking systems in the locations considered show a tracking system may outperform a stationary system by 23-31 percent in terms of annual energy generation. The influence of module temperature was estimated to decrease annual energy generation from 1 and 6 percent in Buffalo and Albuquerque, respectively. Further conclusions suggest that annual energy production of a module is relatively insensitive to solar spectral variation and angle of incidence. Table 1.3 shows estimated ranges by King et al. for the influence of module and system-level factors on the annual ac-energy generation of PV systems.

Table 1.3. Estimated ranges for the influence of module and system-level factors on the annual ac-energy generated by PV systems [56]

Factor	Range (%)
Module orientation	-25 to +30
Array utilization losses (MPPT)	-30 to -5
Power conditioning hardware	-20 to -5
Module power specification	-15 to 0
Module temperature coefficients	-10 to 0
Module (array) degradation (%/year)	-7 to -0.5
Module V_{mp} vs. Irradiance	-5 to +5
Module soiling (annual average)	-10 to 0
Angle-of-incidence optical losses	-5 to 0
Module mismatch in array	-5 to 0
Solar spectral variation	-3 to +1

During operation, photovoltaic (PV) systems accumulate unwanted heat from the surroundings and through the absorption of solar energy that is not converted to usable electricity. As solar cells increase in temperature, the electrons and atoms vibrate at a higher rate [18]. As the vibration of electrons and atoms increases, the randomly directed kinetic energy of the electrons and atoms becomes a greater factor in which direction the atoms and electrons move; as a result, the effectiveness of the electrical field to separate the electrons and holes diminishes which degrades the overall performance of the module [18]. The net amount of heat transferred to a PV array during operation and corresponding array temperatures are primarily functions of the type, orientation, and installation of the array and meteorological conditions under which the array operates. An understanding of the heat transfer characteristics of a PV array and the affects of operating temperature on a PV system during operation is important when considering different PV technologies, installation practices, and performance.

In the past, studies have been performed investigating the affects of module temperature on PV performance. Whitaker et al. [54] quantified experimental temperature coefficients for power for monocrystalline, amorphous, and polycrystalline type modules while operating in indoor and outdoor settings. Temperature coefficients for power were found for each module type at various levels of solar irradiance. Additional work in this study focused on the affects of incidence angle on experimental temperature coefficients. Outdoor experimental results showed that the temperature coefficient of power was sensitive to solar irradiance level, which is contrary to common belief. Indoor testing support the notion that temperature coefficients for power are in fact constant at normal operating ranges of solar irradiance. Whitaker et at. offers suggestions to explain the sensitivity of temperature coefficients of power experimentally determined under outdoor conditions focusing on sources of error which include: spectral effects, soiling, dew, and instrumentation idiosyncrasies.

Methods for estimating the overall heat transfer coefficient are presented by Duffie and Beckman [57]. In addition, Duffie and Beckman [57] present methods for calculating the normal operating temperature of a cell which can then be used to determine heat transfer characteristics of a module or array. Similar methods are presented by Tiwari et al. [58]. Experimental and theoretical modeling efforts have been made to quantify heat transfer characteristics of PV modules. However, much of this work focuses on heat exchangers coupled to PV (PV-T hybrid systems) modules or PV modules integrated into a building structure (BIPV).

A few models exist for estimating the performance and energy savings of PV systems. The National Renewable Energy Laboratory has developed a calculator known as PVWatts [48] that can be used to

estimate monthly and annual energy production and energy savings of stationary and tracking grid-connected PV systems. PVWatts is a model that uses TMY2 data to estimate solar insolation on a tilted surface and an overall derate factor to estimate energy output. The energy savings are presented monthly for one year of operation. The New Solar Homes Partnership (NSHP) program as part of the California Energy Commission also has developed a solar calculator, CECPV Calculator Version 2.3, to estimate monthly and annual energy generation and available incentives for PV systems in California [59]. The calculator developed uses weather data for 16 climate zones in California and is based on a 5-parameter model developed by the Solar Energy Laboratory at the University of Wisconsin. Incentives predicted by the calculator are for California exclusively. Another calculator found specific to California is the Clean Power Estimator® developed by the California Energy Commission [60]. This model estimates both energy generation and economics for residential and commercial sectors in California exclusively. Economics and performance are estimated over the assumed life of the system and include annual escalations of energy costs and financing for the system. No calculator found was designed to estimate the economics further than first year energy savings for states in the U.S. other than California.

CHAPTER 2 - EXPERIMENTAL PERFORMANCE OF A GRID-CONNECTED STATIONARY PHOTOVOLTAIC SYSTEM IN THE UPPER MIDWEST

A paper in preparation for submission to *American Society of Mechanical Engineers – Journal of Solar Energy Engineering*

Ryan Warren, Michael Pate, Ron Nelson

ABSTRACT

Two grid-connected photovoltaic (PV) systems comprised of multicrystalline silicon (mc-Si) modules with different mounting schemes were installed in central Iowa and monitored for one year; one roof-mounted stationary system and one pole-mounted dual-axis tracking system. These systems serve as real-world applications of PV for building energy generation in the Upper Midwest and are used for research, demonstration, and education purposes. Both systems are equipped with extensive data acquisition capable of collecting performance and meteorological data and visually displaying real-time and historical data through an interactive online interface. Additionally, web cameras and general project information are also available online (www.energy.iastate.edu/Renewable/solar).

Experimental performance and economic analyses of the systems were performed and the results are presented in a five-part series of studies. Experimental data was collected and analyzed for the systems over a one-year period from September 2007 through August 2008. This paper presents the performance of the stationary system, and primarily focuses on measures of power production, energy generation, and efficiency. The stationary system, comprised of flat-plate multicrystalline PV modules, has an installed capacity of 4.59 kWp (34.02 m^2 of PV) and is located in Ames, Iowa. During the first year of operation, the PV system received 1,594 kWh/m^2 (4.37 kWh/m^2 on average per day) of solar insolation and generated 5,801 kWh (1,264 kWh/kWp) of usable AC electrical energy. The system was found to operate at an annual average conversion efficiency and performance ratio of 10.6 percent and 0.79, respectively. The annual average DC to AC conversion efficiency of the inverter was found to be 94 percent.

INTRODUCTION

Conventional methods for energy generation using fossil-fuel based sources in the U.S. are negatively impacting our economy, national security, environment, natural resources, and public health. Additionally, negative impacts resulting from the use of fossil-fuels are intensifying due to the Nation's increasing demand of energy. Thus, the increasing demand of energy must be met while decreasing the

use of fossil-fuels. Conventional energy generation methods must be reformed by using sources that are renewable, domestic, distributed, and environmentally friendly.

The use of photovoltaic (PV) technology for generating electrical energy is one approach that could serve as a solution to help alleviate some of the nation's energy-related problems. However, the use of PV is not currently widespread in the U.S. and, more specifically, in the Midwestern states. Several barriers to the widespread use of PV have been identified in a number of studies. A survey conducted by the Iowa Department of Natural Resources (DNR) showed that there exists a lack of familiarity, awareness, and understanding of PV technology in the Midwest [50]. A different survey conducted in the United Kingdom (U.K.) found that 88 percent of respondents would consider the use of integrated photovoltaic building products (BIPV) given greater evidence for the performance and reliability of these products [61]. This U.K. study also showed that 49 percent of those surveyed would consider the use of BIPV technology only after they had witnessed the actual use of it in demonstration sites [61]. Studies show that consumers and design professionals are often reluctant to adopt a particular technology without first observing the application of that technology [62]. Although this survey was conducted in the U.K. for BIPV, it is expected that the acceptance of non-building integrated PV in the US would closely follow these trends [61].

In an attempt to overcome the barriers to the use of PV as described in the previous paragraphs, two grid-connected PV systems with different mounting schemes were installed in central Iowa, USA; one roof-mounted stationary system and one pole-mounted dual-axis tracking system. Both systems were designed as "turn-key" installations for building energy generation applications. The orientation of the stationary system was selected to optimize for annual energy generation. All PV and Balance-Of-System (BOS) equipment used in the installations are considered standard for residential and commercial applications. For example, flat-plate PV modules made of silicon nitride multicrystalline silicon (mc-Si) cells were used. The PV systems are equipped with extensive data acquisition (DAQ) systems capable of collecting accurate performance and meteorological data, archiving data in a central repository, and visually displaying real-time and historical data through an interactive online interface. Additionally, webcams are installed at each site to show real-time and historical streaming video and photographs that can be compared to the data presented in the interface.

The experimental performance and economics of both systems have been analyzed in detail based on experimental data taken over one full year and are presented in a five-part series of studies. The performance analysis of the systems primarily focuses on measures of power production, energy

generation, and efficiency. Results are shown on instantaneous, daily, monthly, and annual bases. Two papers of the series present performance results for the stationary system and dual-axis tracking system, respectively [63, 64]. A third paper presents a comparison of normalized measures between the two systems by highlighting the performance differences due to the different mounting schemes [65]. The fourth paper presents an economic analysis of both systems by focusing on life-cycle-cost, payback period, internal rate of return, and the incremental cost of solar energy [66]. The final study investigates heat transfer characteristics of the stationary and tracking arrays and quantifies the affects of operating temperature on PV system performance [67]. Further, simulations were performed to estimate how each system might perform while operating at lower temperatures. Metrics used to assess heat transfer characteristics and affects of operating temperature on PV system performance include overall heat transfer coefficients and the temperature coefficient for power.

As mentioned, this work serves several important purposes aimed at alleviating some of the current barriers to the widespread use of PV. The PV systems serve as demonstrations of real-world stationary and tracking PV applications for building energy generation in the Upper Midwest and are used for research, demonstration, and education purposes. The performance and economic results of this work are based on onsite experimental testing and reflect what would be experienced in practice as opposed to model-based or laboratory generated simulations and predictions. These results can be used to set appropriate expectations for PV systems operating in the Upper Midwest allowing design professionals and consumers to make more informed decisions. Additionally, the experimental data collected can be used in the development, validation, and improvement of computer simulation tools. The test systems are available to the public for observation and to the scientific community for future research. The interactive data interface, webcam, and general project information can be found online through the Iowa Energy Center's website at [68].

PV SYSTEM DESCRIPTION

The stationary system is located in Ames, Iowa, at a latitude of 42 degrees 2 minutes north and a longitude of 93 degrees 48 minutes west. The system has a total installed capacity of 4.59 kW_p (rated at standard operating conditions) and total PV array area of 34.02 m^2 (366.2 ft^2). This system is designed as three side-by-side, identical, and independently operating sub-systems. Each subsystem consists of nine, 170 Watt modules operated at their peak power point and wired in series to a single inverter; all three inverters are identical. All modules are attached directly to a south-facing standing-seam white metal roof at a slope of 36 degrees, shown in Figure 2.1.

Figure 2.1. Photograph of stationary PV system

The system configuration presented in a one-line diagram can be seen in Figure 2.2.

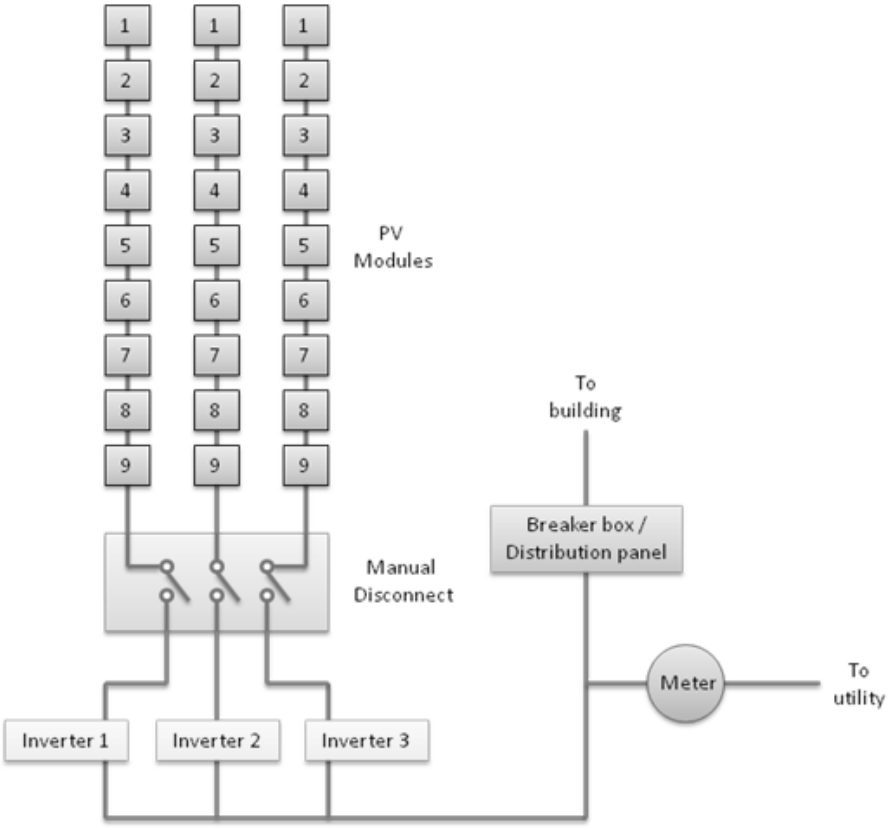

Figure 2.2. One-line diagram of PV system

The flat-plate PV modules are made of silicon nitride multicrystalline silicon cells. Electrical and mechanical specifications for these modules can be seen in Table 2.1.

Table 2.1. Electrical and mechanical characteristics of photovoltaic modules

Rated power	170 Watts
Voltage at rated power	35.4 VDC
Current at rated power	4.8 Amps
Short-circuit current	5.0 Amps
Open-circuit voltage	44.2 VDC
Temperature coefficient of short circuit current	(0.065 $\pm$ 0.015)%/^{o}C
Temperature coefficient of open circuit voltage	-(160 $\pm$ 20) mV/^{o}C
Temperature coefficient of power	-(0.5 $\pm$ 0.05)%/^{o}C
NOCT (Air 20 ^{o}C; sun 0.8 kW/m^{2}, wind 1 m/s)	47 $\pm$ 2 ^{o}C (116.6 $\pm$ 3.6 ^{o}F)
Size (length x width x depth)	1593 x 790 x 50 mm (62.8 x 31.1 x 1.97 in.)
Weight	15.0 kg (33.1 lb.)
Solar Cells	72 cells (125 mm x 125 mm) in a 6 x 12 matrix connected in series

All three grid-tied inverters are identical and utilize maximum power point tracking during operation. The inverters accept the DC electricity from the PV arrays and output single phase AC electricity to the building and utility at a nominal 208 volts AC. The manufacturer's stated conversion efficiency for each inverter is 94.4 percent. Each inverter consumes less than 0.15 Watts of electrical power in stand-by mode and approximately 7 Watts during operation. Electrical and mechanical specifications of the inverters can be found in Table 2.2.

Table 2.2. Electrical and mechanical characteristics of inverters

Maximum PV input power	3,000 Watts
Operating DC voltage range	150 – 450 Volts DC
Maximum DC input voltage	450 Volts DC
Maximum DC input current	16.9 Amps DC
Maximum output power	2,350 Watts
Nominal output voltage	208 VAC
Utility output voltage range	196 – 218 Volts AC
Maximum current	11.25 Amps AC
Nominal operating frequency range	60 Hz
Power factor	1
Peak efficiency	94.4%
Power consumption in stand-by	< 0.15 Watts (night)
Power consumption during operation	7 Watts
Size (length x width x height)	470 x 418 x 223 mm. (18.5 x 16.46 x 8.78 in.)
Weight	11.79 kg. (26 lbs.)
Certifications and compliance	UL 1741, IEEE 929, ISO 9001:2000, FCC regulations

The PV system is equipped with an extensive data acquisition system (DAQ). The DAQ is capable of collecting accurate data at a high sampling rate, archiving data in a central repository, and visually displaying real-time and historical data through an interactive online interface. All data is measured at

ten second intervals, and stored as one-minute averages. To adequately characterize the performance of the PV system, both operating parameters of the array and meteorological conditions were monitored. The specific performance parameters that were monitored include the following:

- DC voltage produced by the arrays of modules (measured at input of inverters)
- DC current produced by the arrays of modules (measured at input of inverters)
- AC voltage output by the inverters (measured at output of inverters)
- AC current output by the inverters (measured at output of inverters)
- Module temperatures

The meteorological parameters that were monitored include:

- Solar irradiance (measured at plane of array)
- Ambient air temperature
- Wind speed
- Wind direction

The placement of each instrument within the system can be seen in Figure 2.3.

The operating range and specified accuracy of each instrument can be seen in Table 2.3.

Table 2.3. Instrument specifications

Measurement	Operating Range	Accuracy
AC current to utility	0 – 10 AAC	0.5% of full scale
DC current to inverter	0 – 5 ADC	1% of full scale
AC voltage to utility	0 – 300 VAC	0.5% of full scale
DC voltage to inverter	0 – 400 VDC	0.5% of full scale
Module temperatures	0 – 260 ^{0}C (0 – 500 ^{0}F)	$\pm$0.083 ^{0}C at 0 ^{0}C ($\pm$0.15^0 F at 32 ^{0}F)
Ambient air temperature	0 – 260 ^{0}C (0 – 500 ^{0}F)	$\pm$0.083 ^{0}C at 0 ^{0}C ($\pm$0.54^0 F at 32 ^{0}F)
Solar irradiance	0 – 1,500 W/m^2	Temp: $\pm$1% from -20 – 40 ^{0}C (-4 – 104 ^{0}F) Linearity: $\pm$5% from 0 – 1,500 W/m^2 Cosine: $\pm$1% from 0^0 – 70^0 or $\pm$3%
Wind speed	1 – 100 m/s (2.2 – 224 mph)	$\pm$ 0.27 m/s ($\pm$0.6 mph) or 1% of reading
Wind direction	355^0 electrical	$\pm$3^0

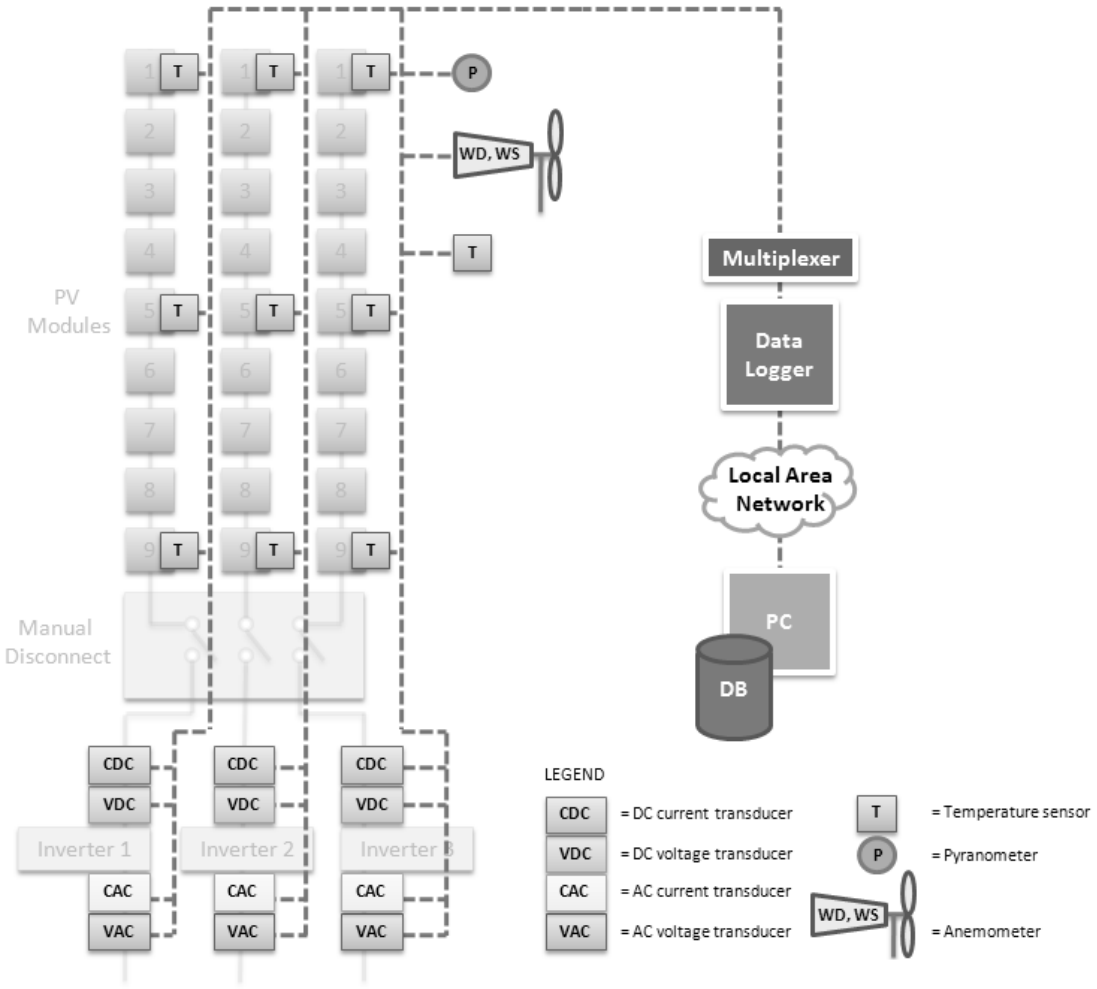

Figure 2.3. One-line diagram of data acquisition system

The DC wiring length between the modules and inverter for the first, second, and third array are 53, 65, and 74 m (174, 213, and 244 ft.), respectively. The length of DC wiring is important due to resistive losses that decrease the usable power generated by the array; however, a relatively large diameter wire was specified to minimize these effects. All DC wiring is insulated, uncoated 8 gauge stranded (7 conductors) copper wiring. The DC voltage and current transducers were installed at the input to the inverter. Thus, data collected by these instruments represent the actual "usable" DC electricity that could be input to an inverter, battery bank, or DC powered device and include all losses and inefficiencies between the array and inverter. The AC voltage and current were measured at the output of the inverters. However, due to the presence of reactive power in the AC current measurement, this data was not used for performance characterizations. Instead, inverter efficiency curves were generated using data taken in a stand-alone test from a power logger capable of individually measuring

working, reactive, and apparent power. The inverter efficiency model allows calculation of instantaneous inverter DC to AC conversion efficiency as a function of DC power input. Consequently, the working AC power generated by the system was calculated for each data point as a function of DC power input and inverter conversion efficiency.

Module temperatures were measured using flexible surface stick-on type three-wire 100 Ohm RTDs. These RTD's were affixed to the backside of six modules in the array (two modules per string or sub-system). A small amount of foam insulation was applied to the back of each temperature sensor to reduce influences from the roof and outdoor air on the temperature measurement. All array temperature data presented in this work represent an average of all six measurements. The outdoor air temperature was measured using a three-wire platinum 100 Ohm RTD (DIN B). The sensor is mounted vertically in a PVC weather resistant housing with sun shield and open slots allowing air flow across the sensor. The ambient air temperature is measured in Nevada, Iowa (site of the dual-axis tracking system) which is located approximately 14 kilometers (8.7 miles) from the stationary PV system. Wind speed and direction were measured by a four-blade helicoid propeller and vane anemometer. A thermopile-type pyranometer was used to measure the solar irradiance incident upon the arrays and was mounted at an in-plane orientation to the array. Thermopile pyranometers are commonly used for establishing solar resource for PV systems [69, 70]. This device measures irradiance over the entire solar spectrum (0.285 to 2.8 μm). All findings in this work for solar resource are presented in terms of the total solar resource measured by this pyranometer.

EXPERIMENTAL ANALYSIS AND RESULTS

Experimental data was collected for one full year with performance parameters and meteorological conditions being monitored from September 2007 through August 2008. Data was sampled at 10 second intervals and stored as one-minute averages. The PV system was new at the onset of data collection. During the test period, the system was allowed to operate as a real-world system; modules were never cleaned of snow or soiling, and operation was not purposely interrupted for any reason.

A detailed analysis of system performance is presented. Meteorological conditions experienced at the site during the one-year monitoring period are shown and include solar resource, ambient air temperature, wind speed and direction, and snow fall. Experimental performance of the PV system is quantified in terms of array current-voltage characteristics, power production, energy generation, and system and inverter efficiencies. Results are presented on hourly, daily, monthly, and annual bases where applicable.

Meteorological Conditions

To assess and characterize the performance of a PV system, it is important to first establish the solar resource available to the system. The solar resource to a PV system is primarily a function of geographical location, surrounding ground cover, array orientation, and atmospheric/meteorological conditions. For this research, the in-plane solar resource available to the test system was evaluated on monthly and annual bases. Monthly solar resource is presented in terms of average daily solar insolation, shown in Figure 2.4. Monthly average daily solar insolation and annual average daily solar insolation values are common parameters quantified in literature and often used in PV system design. Modeled values for these parameters are documented for different collector types, orientations, and locations in the U.S. [16].

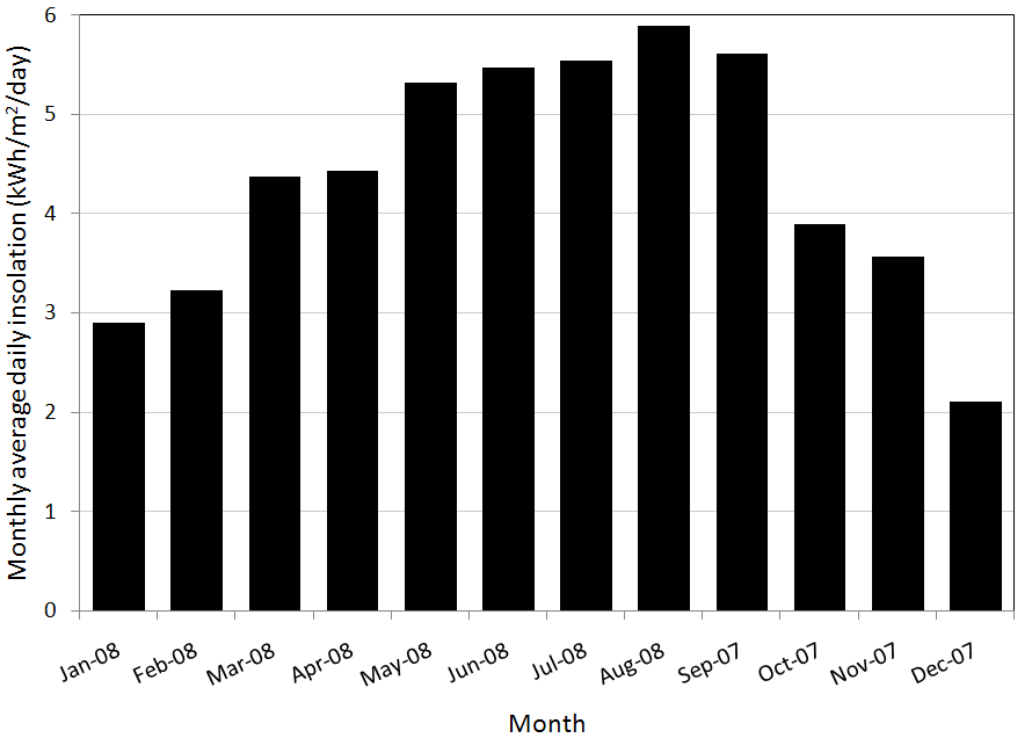

Figure 2.4. Monthly average daily solar insolation

Monthly average daily solar insolation ranged from 2.1 kWh/m^2 in December to 5.9 kWh/m^2 in August. The annual average daily solar insolation for the system was found to be 4.37 kWh/m^2.

Ambient air temperature and wind affects module/array operating temperatures, which in turn influences PV system performance. The hourly average ambient air temperature experienced during the monitoring period is shown in Figure 2.5.

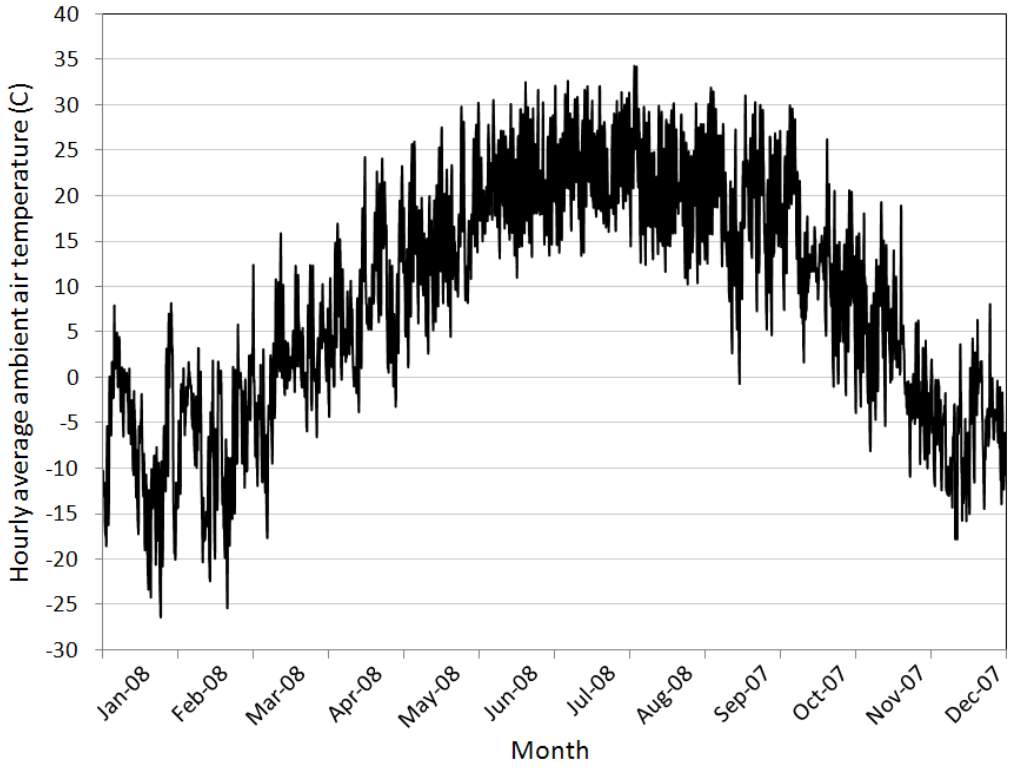

Figure 2.5. Hourly average ambient air temperature

The average monthly wind speed and prevailing direction (at a height of 10 meters) during the year of monitoring measured in Des Moines, Iowa (which is 56 kilometers (35 miles) from the site of the stationary system) is shown in Table 2.4.

Table 2.4. Average monthly wind speed

Month	Average wind speed at 10 meters, m/s (mph)
Jan-08	4.5 (10.0)
Feb-08	4.3 (9.7)
Mar-08	4.2 (9.5)
Apr-08	5.1 (11.3)
May-08	4..5 (10.1)
Jun-08	3.9 (8.8)
Jul-08	3.3 (7.3)
Aug-08	2.9 (6.4)
Sep-07	3.8 (8.6)
Oct-07	4.2 (9.4)
Nov-07	4.5 (10.1)
Dec-07	3.9 (8.6)

Source: National Weather Service Forecast Office [71]

Snow significantly affects PV system performance. Snow cover surrounding a PV array can increase the available solar energy incident upon the array via reflection. However, snow covering the array can degrade system performance considerably. Monthly snow fall measured in Des Moines, Iowa is documented in Table 2.5.

Table 2.5. Monthly snow fall

Month	Snow fall, cm. (in.)
Jan-08	28 (11)
Feb-08	57.7 (22.7)
Mar-08	12.2 (4.8)
Apr-08	2.8 (1.1)
May-08	0
Jun-08	0
Jul-08	0
Aug-08	0
Sep-07	0
Oct-07	0
Nov-07	12.2 (4.8)
Dec-07	35.8 (14.1)

Source: National Weather Service Forecast Office [71]

System Performance at Standard Test Conditions

Manufacturers rate the performance of PV modules under conditions known as Standard Reporting Conditions (SRC) or Standard Test Conditions (STC) [54]. The rated capacity of a PV system (multiple modules) is found by summing the rated DC power of each module in the array operating under STC. The specific standard test conditions used by manufacturers are: solar irradiance of 1,000 W/m^2, reference air mass of 1.5 (ASTM Standard Spectrum), a zero-degree angle of incidence (AOI), and cell junction temperature of 25 degrees Centigrade. However, operating conditions experienced in practice rarely occur at STC. Additionally, systems do not output rated DC power to the inverter at STC due to losses and inefficiencies. Furthermore, the inverter, and AC-side wiring and connections introduce additional losses causing AC power output to the building or grid to be less than DC power input to the inverter.

During the one year of monitoring, 9 instances were found where the system was operating at full-sun ($\pm$ 3 W/m^2) and 25^{o}C ($\pm$ 0.25^{o}C). The measured DC and AC electrical performance data for all instances were averaged to a single value and results are presented in Table 2.6.

Table 2.6. Performance of PV system operating at 1,000 W/m^2 and 25^{o}C

Parameter description	Value at STC	Units
System DC power output (system rating 4,600 Watts DC)	4,029	Watts DC
Average DC power output per sub-system (sub-system rating 1,530 Watts DC)	1,343	Watts DC/sub-system
Average DC power output per square meter (per m^2 rating 134.92 Watts DC)	118	Watts DC/m^2
Average DC power output per module (module rating 170 WDC)	149	Watts DC/module
Average output voltage DC per sub-system	304	Volts DC
Average output voltage DC per module	34	Volts DC
Average output current DC per sub-system	4.42	Amps DC
System AC power output	3,853	Watts AC
Average AC power output per sub-system	1,284	Watts AC/sub-system
Average AC power output per square meter	113	Watts AC/m^2
Average AC power output per module (module rating 170 WDC)	143	Watts AC/module
Derate factor to inverter (DC side)	0.876	fraction of rated cap.
Derate factor to utility (System)	0.838	fraction of rated cap.
Conversion efficiency of sun energy to electrical energy to inverter (DC side)	0.119	%/100
Conversion efficiency of sun energy to electrical energy to utility (System)	0.113	%/100

The DC electrical parameters were measured at the input of the inverter. Thus, these values represent the actual "usable" DC electricity that could be input to an inverter, battery bank, or DC powered device and include all losses and inefficiencies before the inverter. Data in this study indicates the system outputs DC power at roughly 87 percent of its rated capacity when subjected to near STC. The average angle of incidence (AOI) calculated for the instances operating full-sun and 25^{o}C were found to be 16 degrees. Angle of incidence values were calculated by using methods presented by Duffie and Beckman [57]. The AOI values do not exactly represent STC; however, past research shows this parameter to have little effect on performance at AOI's of less than approximately 60 degrees [56].

System Current-Voltage Curves

A common way to characterize the electrical performance of a PV device is by measuring the current-voltage curve (I-V) at standard conditions [55]. However, this is most often done in an indoor laboratory setting where the operating environment is controlled to specific conditions and performance is unaffected by external hardware, such as a battery bank or inverter. In this research, system I-V curves were generated to show actual operating performance when the array is subjected to outdoor conditions and when it is affected by inverter power point tracking. Electrical operating characteristics of the array are dictated by the maximum power point tracking (MPPT) software embedded in the inverters. The MPPT software optimizes the operating voltage of the array to achieve maximum power output at all times. Array DC voltage and current were monitored at the input of the inverter. Array operating I-V curves were generated for solar irradiance values of 200, 400, 600, 800, and 1,000 W/m^2 ($\pm$

3 W/m^2) and include data for all other operating conditions experienced throughout the year. The operating current and voltage for each of the three arrays were found and averaged for each minute of data collected at the specified levels of solar irradiance, shown in Figure 2.6.

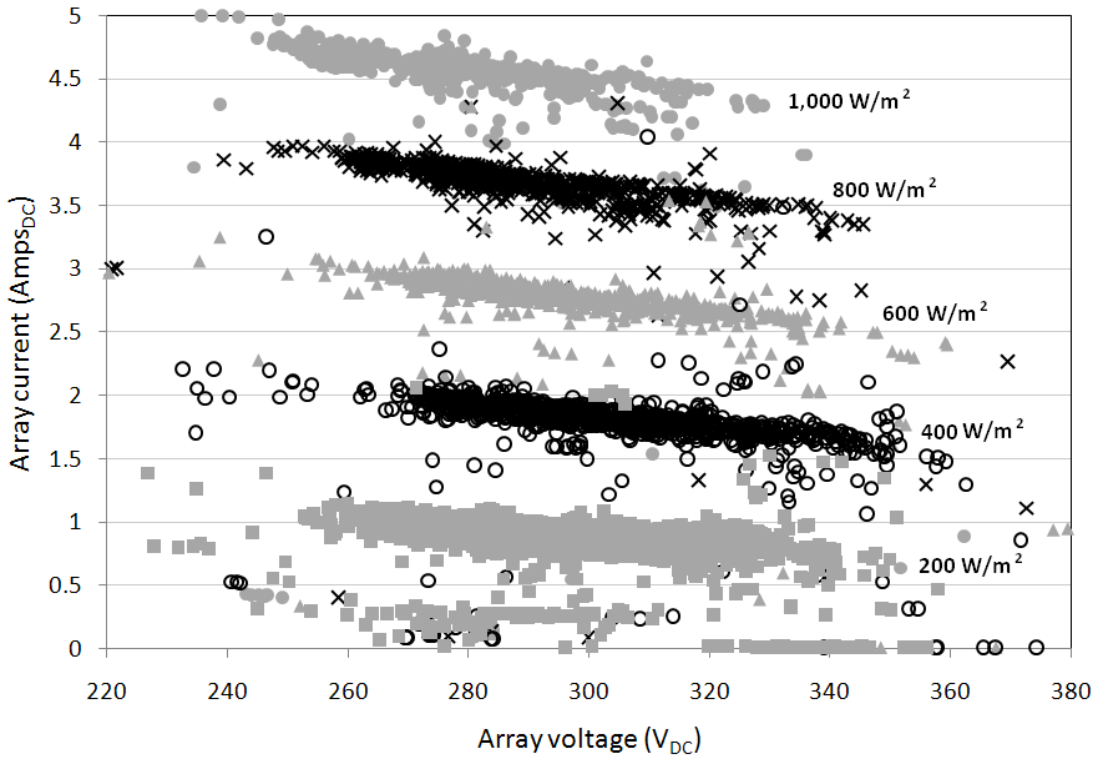

Figure 2.6. I-V curves for various levels of solar irradiance

Data points on Figure 2.6 that do not follow the general trends correspond to times where snow partially or fully covered the array and/or the pyranometer, which was verified by comparing the sampled data points to days the site experienced snow fall [71].

Power Production

The instantaneous DC and AC power production of the array was calculated from data rather than being directly measured by a single instrument. Direct current power output of the array, P_{DC}, was determined by the product of DC current and DC voltage. The AC power output of the array, P_{AC}, was found using the DC power input to the inverter and the inverter efficiency model by

$$P_{AC} = P_{DC}(\eta_{inverter}) \tag{2.1}$$

where $\eta_{inverter}$ is the instantaneous inverter efficiency to the corresponding DC power input. The method used for calculating inverter efficiency discussed in the section, Efficiency Measures.

The average DC power output of the system for each hour of the one-year monitoring period is plotted against corresponding hourly average in-plane solar irradiance values, seen in Figure 2.7. The AC power output would be slightly lower for all data points due to the inverter efficiencies.

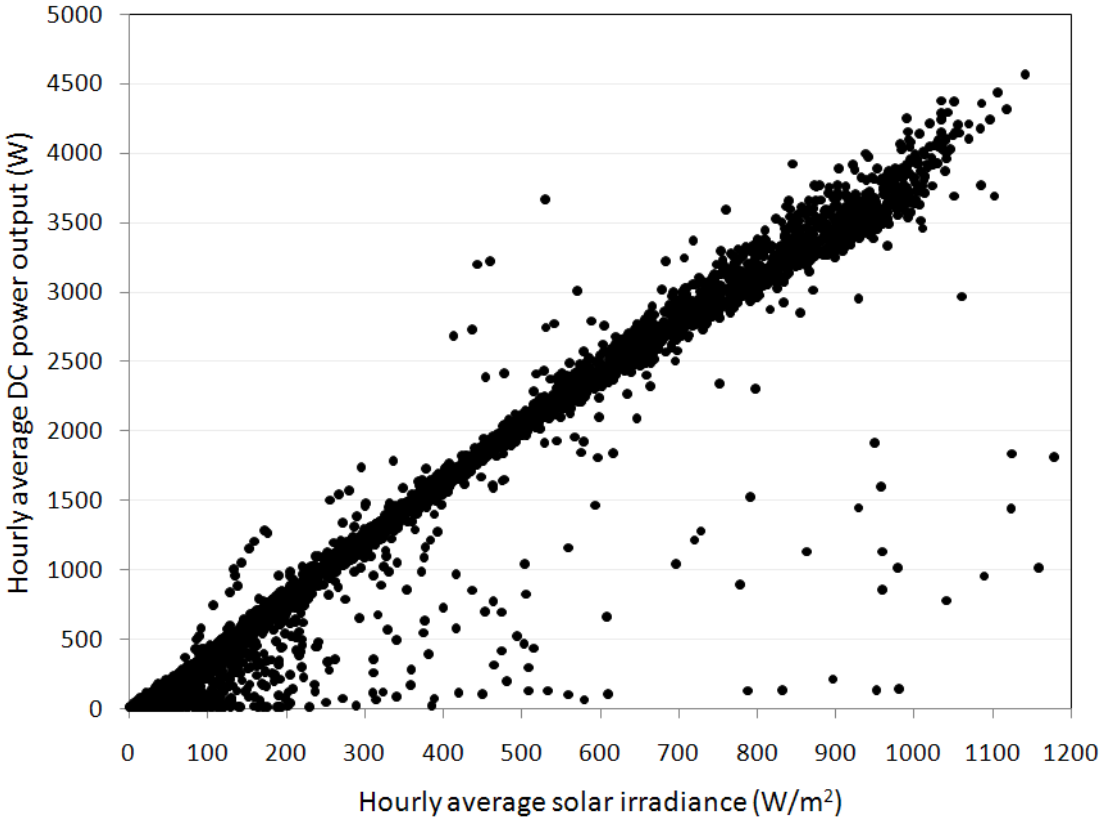

Figure 2.7. Power production vs. solar irradiance

The data shown in Figure 2.7 represents power production of the system for all operating conditions experienced at the site throughout the year. Figure 2.7 shows data points that deviate from the general trend; these particular points correspond to times where snow partially or fully covered the array and/or pyranometer and illustrate its effect on power production or measured irradiance. The maximum hourly average AC and DC power output by the system was measured to be 4,362 and 4,575 Watts (corresponding to a solar irradiance of 1,141 W/m^2 and an average array temperature of 18 ^{o}C (64 ^{o}F)), respectively. The average AC and DC power output of the system at full sun (i.e., 1,000 W/m^2) was found to be 3,646 and 3,812 Watts, respectively.

Energy Generation

The array performance was also characterized in terms of energy generation. Energy generation was evaluated for different time intervals (i.e., monthly and annually) and against solar energy input to the

system. Monthly and annual AC and DC energy generation was calculated by multiplying the instantaneous power production value by the time-interval for which the power was produced, and then summing those values over the month or year. Results for monthly energy generation are shown in Figure 2.8.

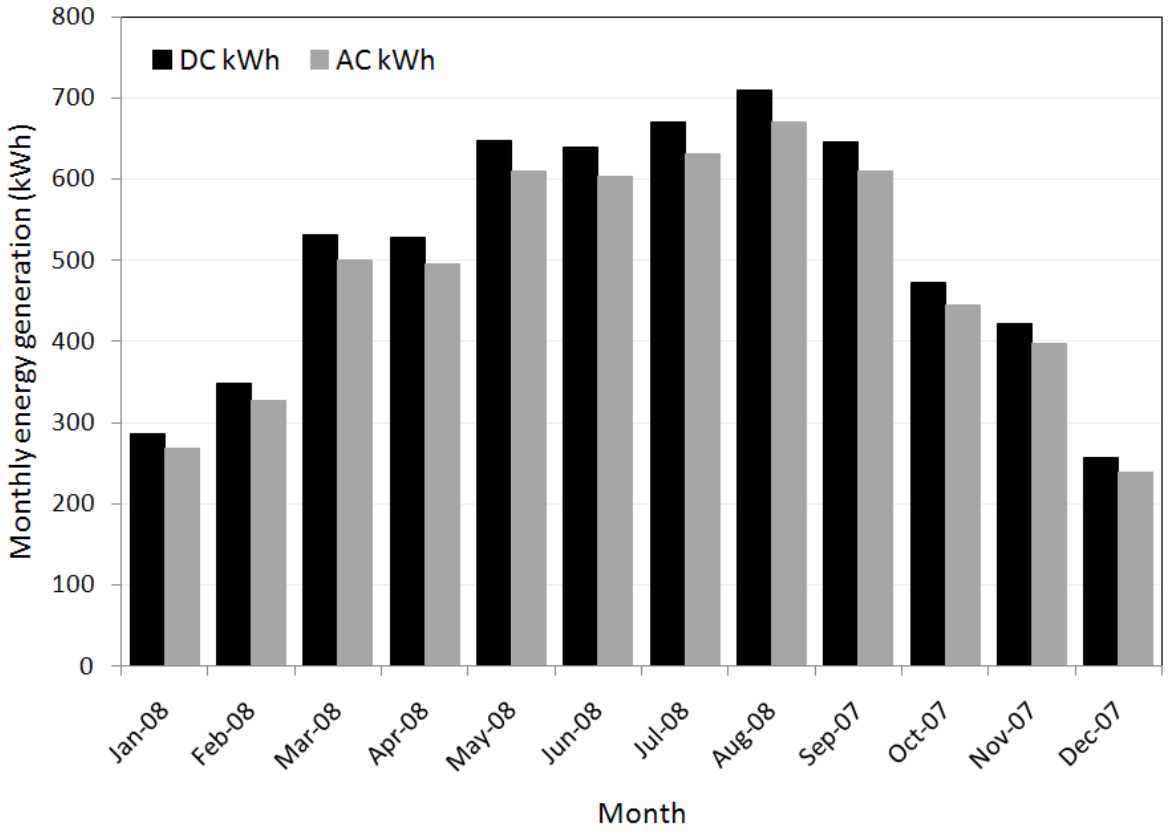

Figure 2.8. Monthly energy generation

The annual AC and DC energy generation for the system was found to be 5,801 and 6,162 kWh (1,264 and 1,342 kWh/kWp), respectively.

The daily DC energy generation of the system was evaluated against the daily in-plane solar insolation incident on the array, shown in Figure 2.9.

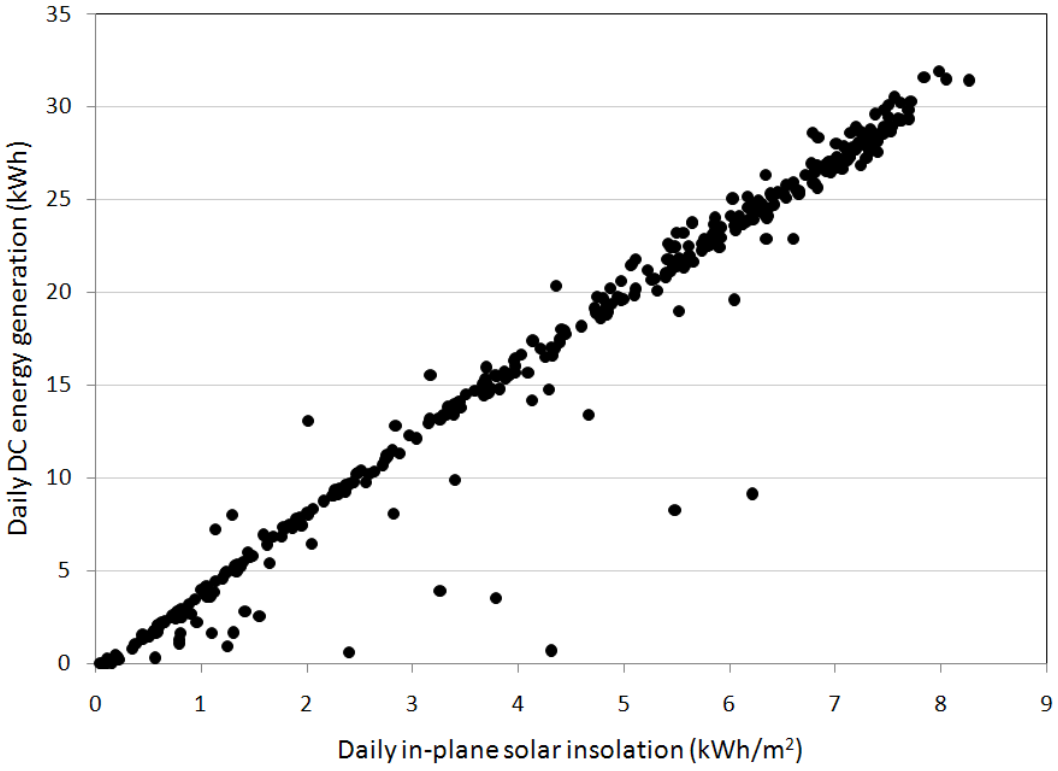

Figure 2.9. Daily DC energy generation vs. daily in-plane solar insolation

The effects of snow cover can be seen by points below the main trend line. The relationship between daily DC energy generation and daily solar insolation was observed to be approximately linear.

Efficiency Measures

System and component efficiencies are important to consider when characterizing performance of PV systems. Efficiency assessments offer insight to where and to what magnitude losses are experienced and to how well the system coverts the available solar resource to useable electrical energy. Losses and inefficiencies resulting in performance less than rated can be attributed to: inaccurate nameplate rating, conversion from DC to AC electricity in the inverter, module mismatch, diodes, wiring and connection losses, soiling, snow cover, age, high operating temperatures, and other losses from converting solar energy to usable electrical energy [48]. As shown in Table 2.7, system efficiency was quantified in terms of average monthly and annual DC and AC system conversion efficiency. System conversion efficiency is defined as the ratio of the total DC or AC generated energy to the total solar insolation incident on the array.

Table 2.7. Monthly and annual average system conversion efficiencies

Month	Conversion efficiency from sun energy to DC electrical energy	Conversion efficiency from sun energy to AC electrical energy
Jan-08	0.090	0.085
Feb-08	0.113	0.106
Mar-08	0.115	0.109
Apr-08	0.117	0.110
May-08	0.115	0.109
Jun-08	0.115	0.108
Jul-08	0.114	0.108
Aug-08	0.114	0.108
Sep-07	0.113	0.107
Oct-07	0.115	0.109
Nov-07	0.116	0.109
Dec-07	0.115	0.107
Annual	0.113	0.107

Slight seasonal variations in system efficiency can be observed in this study. System efficiencies in the summer months were found to be slightly lower when compared to Spring and Fall and can be attributed in part to higher average array operating temperatures. The affects of snow cover are apparent in the efficiency results during January when the site experienced 28 cm (11 in) of snow fall. The annual average DC and AC efficiency was found to be 11.3 and 10.7 percent, respectively.

System efficiency was also evaluated and quantified against solar irradiance. The system efficiency curve was generated by using the ratio of average hourly AC power output to average hourly total solar insolation incident upon the array. Average hourly system efficiencies for all daylight hours of the monitoring period are shown in Figure 2.10.

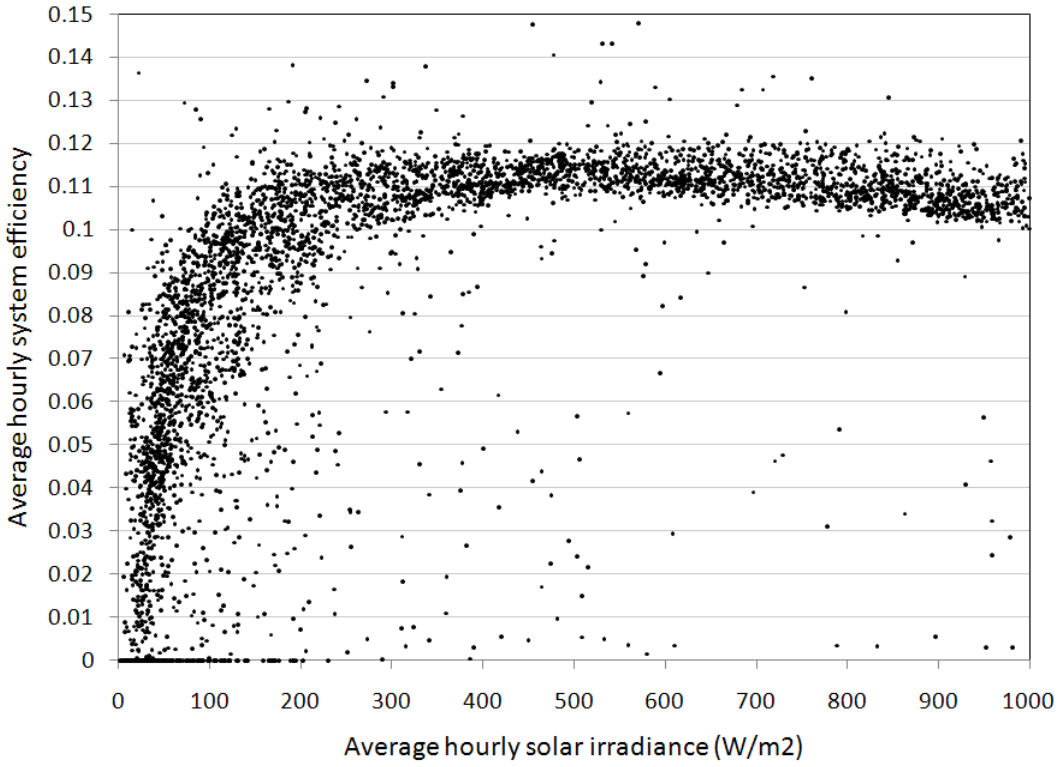

Figure 2.10. System efficiency (conversion of solar energy to AC electrical energy) vs. solar irradiance

The effects of influences such as array temperature, AOI, and solar spectrum on system efficiency can be seen by the variation of values within the main trend line. Snow cover on the array also significantly affected hourly average system efficiency, which can be seen by the data points lying below the main trend. Points that lie above the main trend line are most likely due to the intermittency of snow covering the pyranometer.

Inverter performance was quantified in terms of conversion efficiency from DC to AC electrical power. The DC and AC electrical data collected to calculate this instantaneous inverter efficiency was measured by using an independent power logger in a stand-alone test. The conversion efficiency of each inverter was found as a function of DC power input. A plot showing results for one of the three inverters can be seen in Figure 2.11. This plot shows instantaneous inverter efficiency using data at one-minute time steps. The inverters were found to operate at a fairly consistent efficiency for solar irradiances ranging from 200 to 1,200 W/m^2, which represents a large portion of the operating range. The annual average conversion efficiency of each inverter was calculated as the ratio of annual AC energy to the annual DC energy, which was found to be approximately 94 percent.

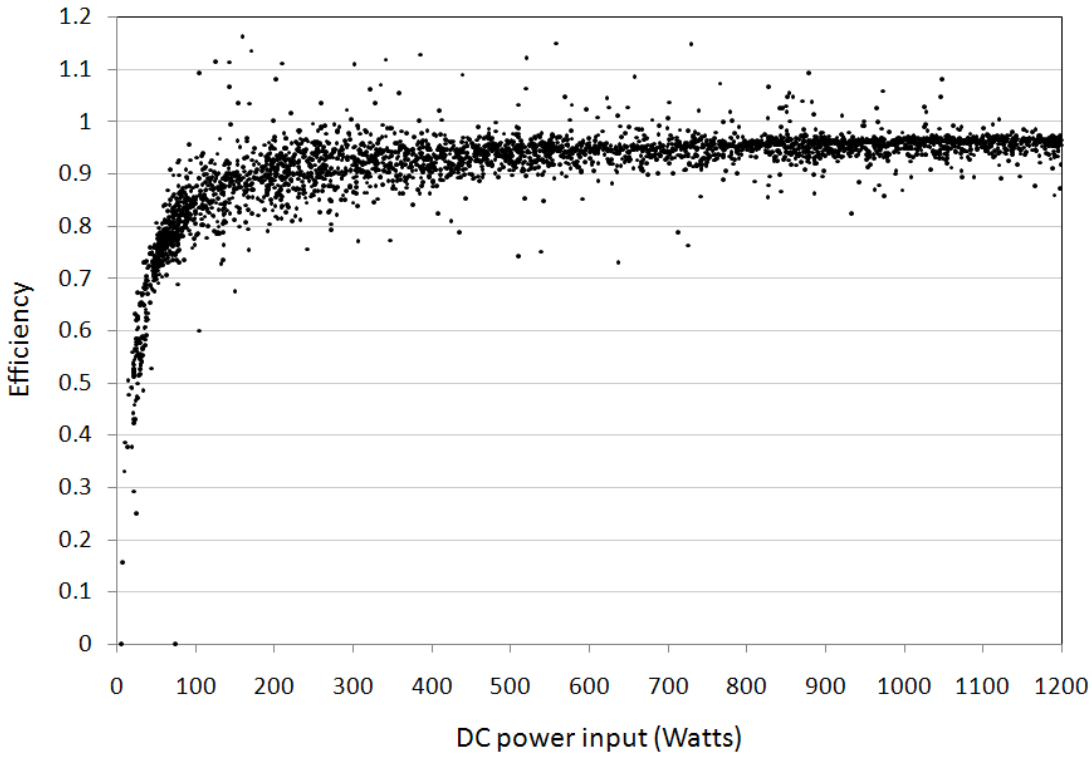

Figure 2.11. Inverter efficiency vs. DC power input from array

The performance ratio, PR, is a parameter that is normalized with respect to irradiance and quantifies the overall effect of all losses on the rated output due to system inefficiencies, losses, and operating conditions [72]. Performance ratio values are commonly quantified on annual, monthly, weekly, and daily bases. Longer term (e.g., annual and monthly) PR values can be used to assess performance of a system or compare performance of systems with similar or dissimilar characteristics and locations. Additionally, long term PR values can be estimated rather than measured to predict the energy performance of a PV system. Shorter term (e.g., weekly and daily) PR values can be used to identify component failures and other operating conditions that significantly degrade system performance such as excessive soiling or snow cover. The performance ratio can be calculated by

$$PR = \frac{Y_f}{Y_r} \tag{2.2}$$

where Y_f is the system yield (kWh/kWp) and Y_r, is the reference yield (hours) [72]. The system yield is found by dividing the net AC energy output by the installed DC capacity of the array (defined at STC). The reference yield represents the number of peak sun hours seen by the system evaluated over the same time period used for determining the system yield. Annual, monthly, and daily PR values were determined with daily PR values throughout the one-year monitoring period shown in Figure 2.12.

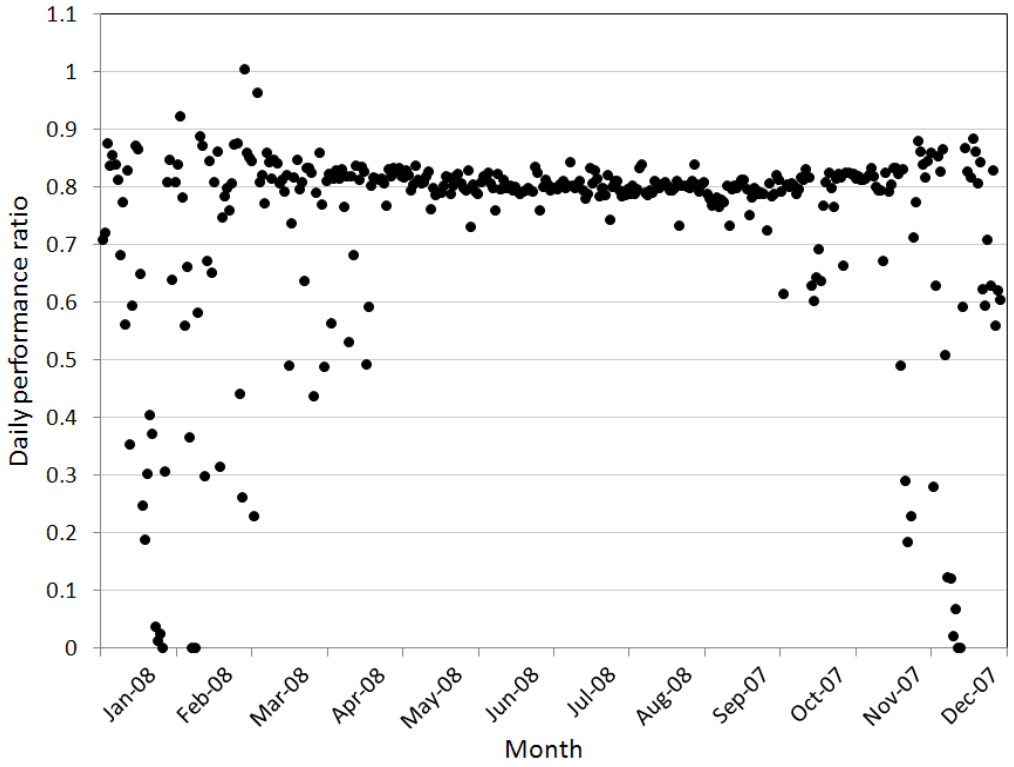

Figure 2.12. Daily performance ratios

All performance ratios calculated on monthly and annual bases are shown in Table 2.8.

Table 2.8. Monthly performance ratio

Month	Ave PR
Jan-08	0.629
Feb-08	0.786
Mar-08	0.805
April-08	0.814
May-08	0.806
June-08	0.800
July-08	0.800
Aug-08	0.800
Sep-07	0.790
Oct-07	0.804
Nov-07	0.810
Dec-07	0.796
Annual	0.792

Daily PR values during the winter months were found to be vary sporadic; the days yielding irregular PR values coincided with times the array and/or pyranometer was fully or partially covered with snow. Seasonal variations in losses due to operating temperature can be seen in the slightly higher values in the Spring and Fall in comparison to the summer in both Figure 2.12 and Table 2.8. Throughout the

year, monthly PR values varied from 0.629 to 0.814. The annual average performance ratio was found to be 0.792.

A frequency distribution of daily PR values is shown in Figure 2.13.

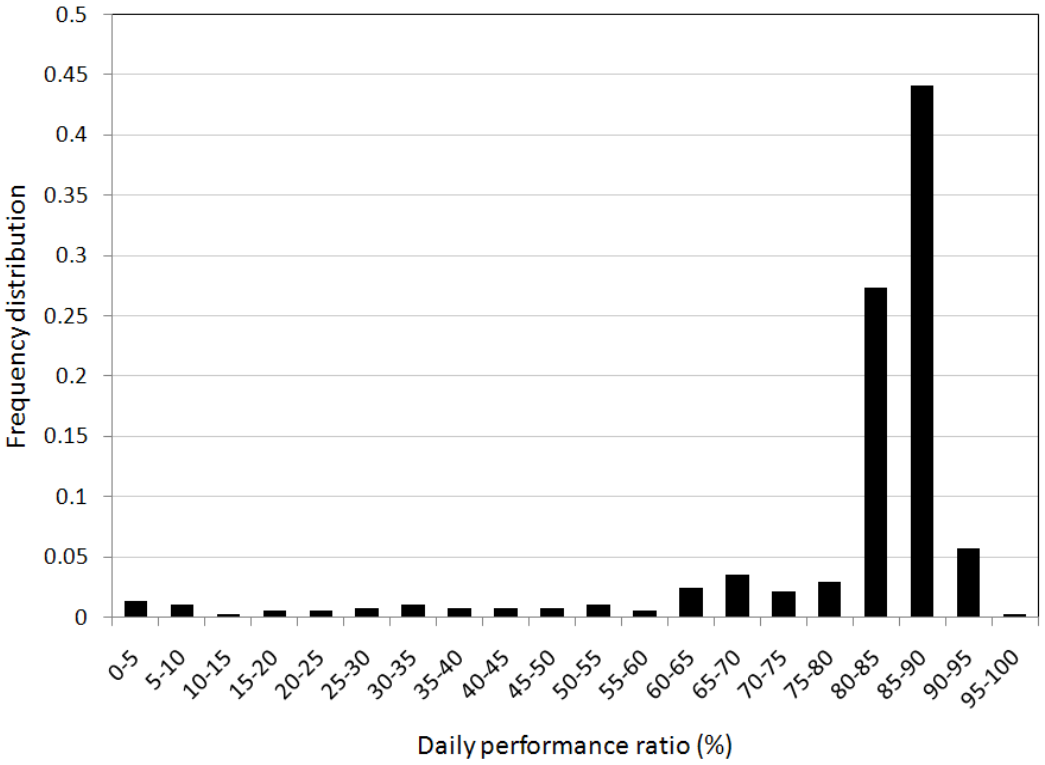

Figure 2.13. Frequency distribution of PR

The system was found to operate at a performance ratio level between 80 and 90 percent for 261 of 365 days during the monitoring period.

SUMMARY

A 4.59 kWp grid-connected, stationary PV system was installed, operated, and monitored in the Upper Midwest for one year. The array was oriented at a slope of 36 degrees and faced south in order to maximize annual energy generation. All PV and Balance-Of-System (BOS) equipment used in the installations are “off-the-shelf” components and considered standard for residential and commercial applications. The outdoor experimental performance of the system was quantified for one year of collected data. Experimental results reflect performance of a PV system exposed to a wide-range of operating conditions inherent to the climate in the Upper Midwest.

The annual average daily solar insolation incident upon the array was found to be 4.37 kWh/m^2. During the first year of operation, the PV system provided 5,801 kWh (1,264 kWh/kWp) of usable AC electrical energy. The system was found to operate at an annual average conversion efficiency and PR of 10.6 percent and 0.79, respectively. Slight seasonal variations in system efficiency were observed and can be attributed in part to variations in average array operating temperatures and snow fall throughout the year. The annual average DC to AC conversion efficiency of the inverter was found to be 94 percent.

The research reported herein serves several important purposes aimed at alleviating some of the current barriers to the widespread use of PV. This research can be used to set appropriate expectations for PV systems operating in the Upper Midwest allowing design professionals and consumers to make more informed decisions. The test systems serve as demonstrations of real-world PV applications for building energy generation and are used for research, demonstration, and education purposes. The test systems and performance data are available to the public for observation and to the scientific community for future research. The interactive data interface, webcam, and general project information can be found online through the Iowa Energy Center's website at [68].

ACKNOWLEDGEMENTS

The authors would like to thank the Iowa Energy Center for providing personnel, administrative, and financial support for this project.

CHAPTER 3 - EXPERIMENTAL PERFORMANCE OF A GRID-CONNECTED DUAL-AXIS TRACKING PHOTOVOLTAIC SYSTEM IN THE UPPER MIDWEST

A paper in preparation for submission to *American Society of Mechanical Engineers – Journal of Solar Energy Engineering*

Ryan Warren, Michael Pate, Ron Nelson

ABSTRACT

Two grid-connected photovoltaic (PV) systems comprised of multicrystalline silicon (mc-Si) modules with different mounting schemes were installed in central Iowa and monitored for one year; one roof-mounted stationary system and one pole-mounted dual-axis tracking system. These systems serve as real-world applications of PV for building energy generation in the Upper Midwest and are used for research, demonstration, and education purposes. Both systems are equipped with extensive data acquisition capable of collecting performance and meteorological data and visually displaying real-time and historical data through an interactive online interface. Additionally, web cameras and general project information are also available online (www.energy.iastate.edu/Renewable/solar).

Experimental performance and economic analyses of the systems were performed and the results are presented in a five-part series of studies. Experimental data was collected and analyzed for the systems over a one-year period from September 2007 through August 2008. This paper presents the performance of the dual-axis tracking system, and primarily focuses on measures of power production, energy generation, and efficiency. The tracking system, comprised flat-plate multicrystalline PV modules, has an installed capacity of 1.02 kWp (7.56 m^2 of PV) and is located in Nevada, Iowa. During the first year of operation, the PV system received 2,173 kWh/m2 (5.95 kWh/m^2 on average per day) of solar insolation and generated 1,815 kWh (1,779 kWh/kWp) of usable AC electrical energy. The system was found to operate at an annual average conversion efficiency and performance ratio of 11 percent and 0.82, respectively. The annual average DC to AC conversion efficiency of the inverter was found to be 92 percent.

INTRODUCTION

Two grid-connected PV systems with different mounting schemes were installed in central Iowa, USA; one roof-mounted stationary system and one pole-mounted dual-axis tracking system. Both systems were designed as “turn-key” installations for building energy generation applications. The orientation of the stationary system was selected to optimize for annual energy generation. All PV and Balance-Of-

System (BOS) equipment used in the installations are “off-the-shelf” components and considered standard for residential and commercial applications. For example, flat-plate PV modules made of silicon nitride multicrystalline silicon cells were used. The PV systems are equipped with extensive data acquisition (DAQ) systems capable of collecting accurate performance and meteorological data, archiving data in a central repository, and visually displaying real-time and historical data through an interactive online interface. Additionally, webcams are installed at each site to show real-time and historical streaming video and photographs that can be compared to the data presented in the interface.

The experimental performance and economics of both systems have been analyzed in detail based on experimental data taken over one full year and are presented in a five-part series of papers. The performance analysis of the systems primarily focuses on measures of power production, energy generation, and efficiency. Results are shown on instantaneous, daily, monthly, and annual bases. Two papers of the series present performance results for the stationary system and dual-axis tracking system, respectively [63, 64]. A third paper presents a comparison of normalized measures between the two systems by highlighting the performance differences due to the different mounting schemes [65]. The fourth paper presents an economic analysis of both systems by focusing on life-cycle-cost, payback period, internal rate of return, and the incremental cost of solar energy [66]. The final study investigates heat transfer characteristics of the stationary and tracking arrays and quantifies the affects of operating temperature on PV system performance [67]. Further, simulations were performed to estimate how each system might perform while operating at lower temperatures. Metrics used to assess heat transfer characteristics and affects of operating temperature on PV system performance include overall heat transfer coefficients and the temperature coefficient for power.

This work serves several important purposes aimed at alleviating some of the current barriers to the widespread use of PV discussed in [63]. The PV systems serve as demonstrations of real-world stationary and tracking PV applications for building energy generation and are used for research, demonstration, and education purposes. The performance and economic results of this research are based on onsite experimental testing and reflect what would be experienced in practice as opposed to model-based or laboratory generated simulations and predictions. These results can be used to set appropriate expectations for PV systems operating in the Upper Midwest allowing design professionals and consumers to make more informed decisions. Additionally, the experimental data collected can be used in the development, validation, and improvement of computer simulation tools. The test systems

are available to the public for observation and to the scientific community for future research. The interactive data interface, webcam, and general project information can be found online through the Iowa Energy Center's website at [68].

PV SYSTEM DESCRIPTION

The tracking system is located in Nevada, Iowa, 42 degrees 1 minutes north latitude and 93 degrees 27 minutes west longitude. The system has an installed capacity of 1.02 kW_p (rated at standard operating conditions) and total PV array area of 7.56 m^2 (81.38 ft^2). This system uses six, 170 Watt modules wired in series to a single inverter. The pole-mounted array follows the sun throughout the day using an actively controlled dual-axis, azimuth drive solar tracker. The azimuth range of the tracker is 270 degrees. The tracker is controlled using an electronic transducer that is mounted on top of the array. The transducer has sensors on all sides and adjusts position until an equal amount of sun is sensed on all sides. The photograph of the tracking system can be seen in Figure 3.1.

Figure 3.1. Photograph of tracking PV system

The system configuration presented in a one-line diagram is shown in Figure 3.2.

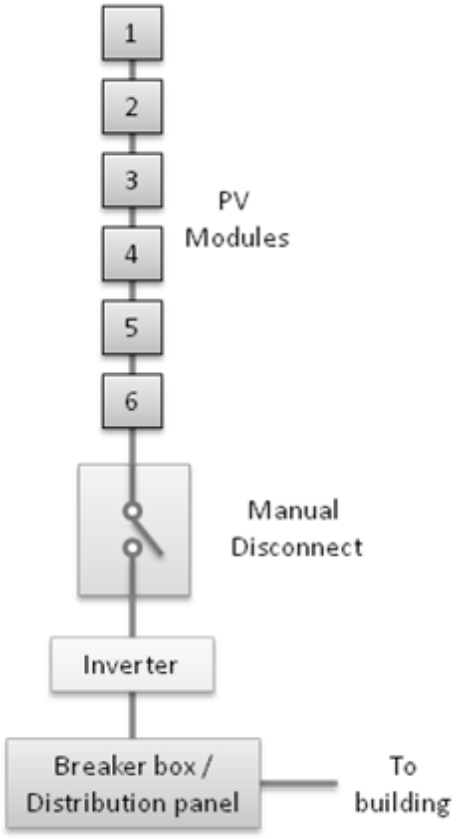

Figure 3.2. One-line diagram of PV system

The flat-plate PV modules are made of silicon nitride multicrystalline silicon cells. Electrical and mechanical specifications for these modules can be seen in Table 3.1.

Table 3.1. Electrical and mechanical characteristics of photovoltaic modules

Rated power	170 Watts
Voltage at rated power	35.4 VDC
Current at rated power	4.8 Amps
Short-circuit current	5.0 Amps
Open-circuit voltage	44.2 VDC
Temperature coefficient of short circuit current	(0.065 $\pm$ 0.015)%/^{o}C
Temperature coefficient of open circuit voltage	-(160 $\pm$ 20) mV/^{o}C
Temperature coefficient of power	(0.5 $\pm$ 0.05)%/^{o}C
NOCT (Air 20 ^{o}C; sun 0.8 kW/m^{2}, wind 1 m/s)	47 $\pm$ 2 ^{o}C (116.6 $\pm$ 3.6 ^{o}F)
Size (length x width x depth)	1593 x 790 x 50 mm (62.8 x 31.1 x 1.97 in.)
Weight	15.0 kg (33.1 lb.)
Solar Cells	72 cells (125 mm x 125 mm) in a 6 x 12 matrix connected in series

The grid-tied inverter utilizes maximum power point tracking during operation. The inverter accepts the DC electricity from the PV array and outputs single phase AC electricity to the building and utility at a nominal 120 volts AC. Electrical and mechanical specifications of the inverters can be found in Table 3.2.

Table 3.2. Electrical and mechanical characteristics of inverter

Maximum PV input power	2,200 Watts
Operating DC voltage range	156 – 400 Volts DC
Maximum DC input voltage	400 Volts DC
Maximum DC input current	12.0 Amps DC
Maximum output power	1,800 Watts
Nominal output voltage	120 Volts AC
Utility output voltage range	106 – 132 Volts AC
Maximum current	15.0 Amps AC
Nominal operating frequency range	60 Hz
Power factor	1
Peak efficiency	93.6%
Power consumption in stand-by	< 0.25 Watts (night)
Power consumption during operation	< 7 Watts
Size (length x width x height)	295 x 434 x 213 mm. (11.6 x 17.1 x 8.4 in.)
Weight	26.94 kg. (59.4 lbs.)
Certifications and compliance	UL 1741, E210376, UL 1998, IEEE 519, IEEE 929, ANSI C62.41 C1 & C3, FCC part 15 A & B

The PV system is equipped with an extensive data acquisition system (DAQ). The DAQ is capable of collecting accurate data at a high sampling rate, archiving data in a central repository, and visually displaying real-time and historical data through an online interactive interface. All data is measured at ten second intervals, and stored as one-minute averages. To adequately characterize the performance of the PV system, both operating parameters of the array and meteorological conditions were monitored. The specific performance parameters that were monitored include the following:

- DC voltage produced by the array of modules (measured at input of inverters)
- DC current produced by the array of modules (measured at input of inverters)
- AC voltage output by the inverter (measured at output of inverters)
- AC current output by the inverter (measured at output of inverters)
- Module temperatures

The meteorological parameters that were monitored include:

- Solar irradiance (measured at plane of array)
- Ambient air temperature

The placement of each instrument within the system can be seen in Figure 3.3.

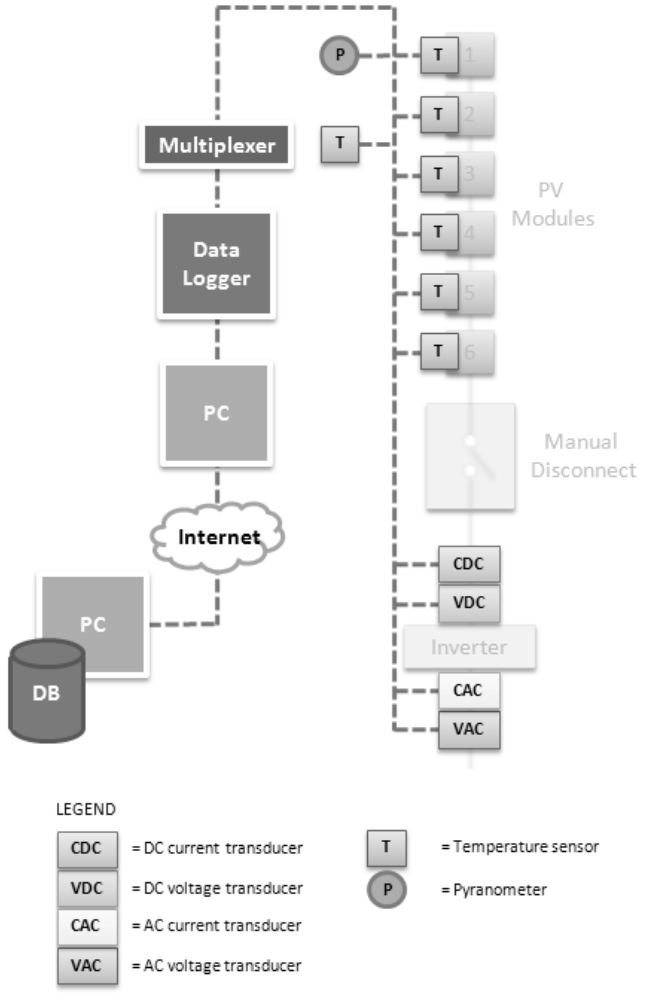

Figure 3.3. One-line diagram of data acquisition system

The operating range and specified accuracy of each instrument can be seen in Table 3.3.

Table 3.3. Instrument specifications

Measurement	Operating Range	Accuracy
AC current to utility	0 – 10 AAC	0.5% of full scale
DC current to inverter	0 – 5 ADC	1% of full scale
AC voltage to utility	0 – 150 VAC	0.5% of full scale
DC voltage to inverter	0 – 300 VDC	0.5% of full scale
Module temperatures	0 – 260 ^{0}C (0 – 500 ^{0}F)	$\pm$0.083 ^{0}C at 0 ^{0}C ($\pm$0.15^0 F at 32 ^{0}F)
Ambient air temperature	0 – 260 ^{0}C (0 – 500 ^{0}F)	$\pm$0.083 ^{0}C at 0 ^{0}C ($\pm$0.54^0 F at 32 ^{0}F)
Solar irradiance	0 – 1,500 W/m^2	Temp: $\pm$1% from -20 – 40 ^{0}C (-4 – 104 ^{0}F) Linearity: $\pm$5% from 0 – 1,500 W/m^2 Cosine: $\pm$1% from 0^0 – 70^0 or $\pm$3%

The DC wiring length between the modules and inverter is 19 m (62 ft). The length of DC wiring is important due to resistive losses that decrease the usable power generated by the array; however, a relatively large diameter wire was specified to minimize these effects. All DC wiring is insulated, uncoated 8 gauge stranded (7 conductors) copper wiring. The DC voltage and current transducers were installed at the input to the inverter. Thus, data collected by these instruments represent the actual "usable" DC electricity that could be input to an inverter, battery bank, or DC powered device and include all losses and inefficiencies between the array and inverter. The AC voltage and current were measured at the output of the inverter. However, due to the presence of reactive power in the AC current measurement, this data was not used for performance characterizations. Instead, inverter efficiency curves were generated using data taken in a stand-alone test from a power logger capable of individually measuring working, reactive, and apparent power. The inverter efficiency model calculates instantaneous inverter DC to AC conversion efficiency as a function of DC power input. Consequently, the working AC power generated by the system was calculated for each data point as a function of DC power input and inverter conversion efficiency.

Module temperatures were measured using flexible surface stick-on type three-wire 100 Ohm RTDs. One RTD was affixed to the backside of each module in the array. A small amount of foam insulation was applied to the back of each temperature sensor to reduce influences from outdoor air on the temperature measurement. All array temperature data presented in this work represent an average of all six measurements. The ambient air temperature was measured using a three-wire platinum 100 Ohm RTD (DIN B). The sensor is mounted vertically in a PVC weather resistant housing with a sun shield and open slots allowing air flow across the sensor. A thermopile-type pyranometer was used to measure the solar irradiance incident upon the array and was mounted on the tracker in-plane to the array. This type of pyranometer is commonly used for establishing the solar resource for PV systems [69, 70]. This device measures irradiance over the entire solar spectrum (0.285 to 2.8 μm). All findings in this work for solar resource are presented in terms of the total solar resource measured by this pyranometer.

EXPERIMENTAL ANALYSIS AND RESULTS

Experimental data was collected for one full year with performance parameters and meteorological conditions being monitored from September 2007 through August 2008. Data was sampled at 10 second intervals and stored as one-minute averages. The PV system was new at the onset of data collection. During the test period, the system was allowed to operate as a real-world system; modules

were never cleaned of snow or soiling, and system operation was not purposely interrupted for any reason.

A detailed analysis of system performance is presented. Meteorological conditions experienced at the site during the one-year monitoring period are shown and include solar resource, ambient air temperature, wind speed and direction, and snow fall. Experimental performance of the PV system is quantified in terms of array current-voltage characteristics, power production, energy generation, and system and inverter efficiencies. Results are presented on hourly, daily, monthly, and annual bases where applicable.

Meteorological Conditions

To assess and characterize the performance of a PV system, it is important to first establish the solar resource available to the system. The in-plane solar resource available to the test system was evaluated on monthly and annual bases. Monthly solar resource is presented in terms of average daily solar insolation, seen in Figure 3.4.

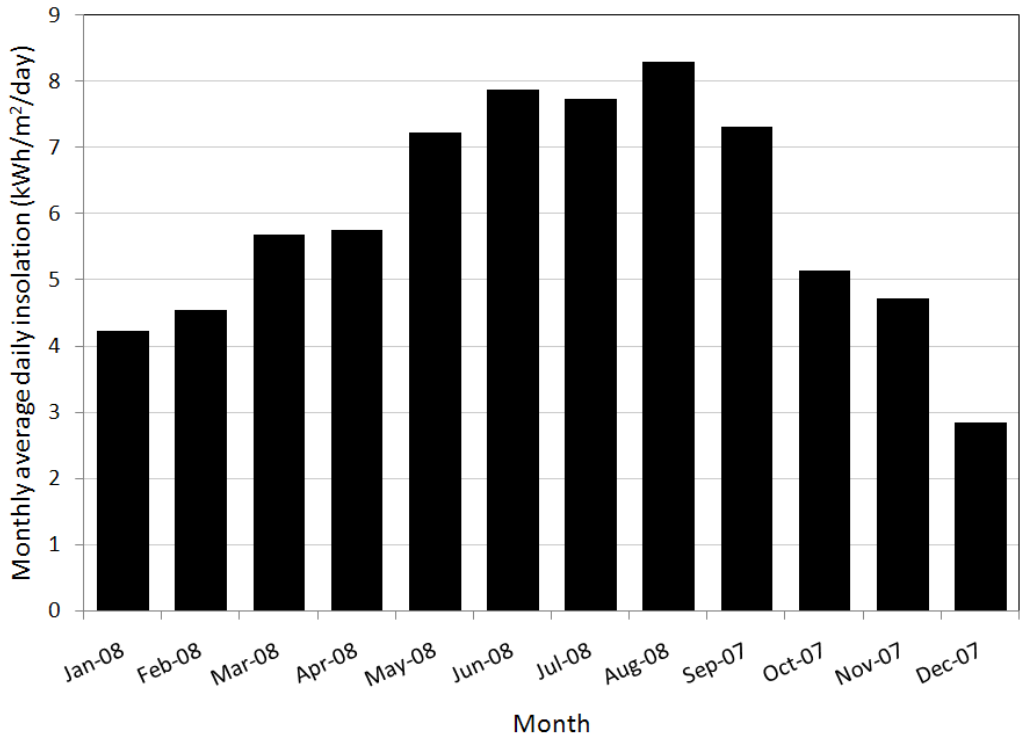

Figure 3.4. Monthly average daily solar insolation

Monthly average daily solar insolation ranged from 2.8 kWh/m^2 in December to 8.3 kWh/m^2 in August. The annual average daily solar insolation for the system was found to be 5.95 kWh/m^2.

Ambient air temperature and wind affects module/array operating temperatures, which in turn influences PV system performance. The hourly average ambient air temperature experienced during the monitoring period is shown in Figure 3.5.

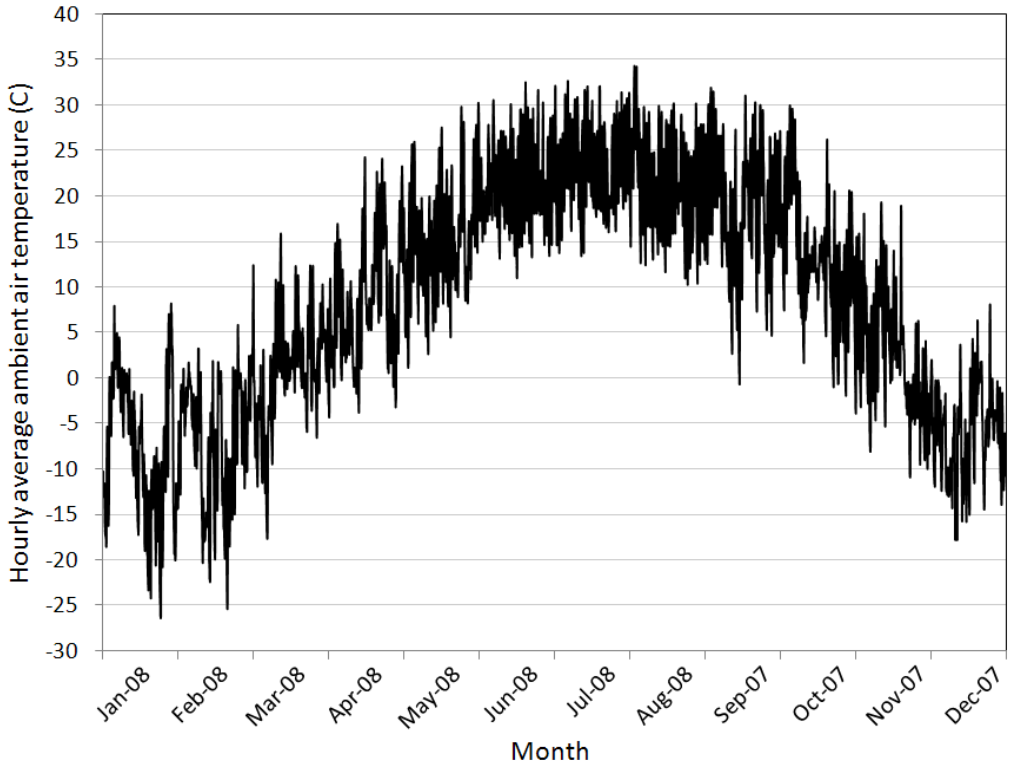

Figure 3.5. Hourly average ambient air temperature

The average monthly wind speed and prevailing direction (at a height of 10 meters) during the year of monitoring measured in Des Moines, Iowa is shown in Table 3.4.

Table 3.4. Average monthly wind speed

Month	Average wind speed at 10 meters, m/s (mph)
Jan-08	4.5 (10.0)
Feb-08	4.3 (9.7)
Mar-08	4.2 (9.5)
Apr-08	5.1 (11.3)
May-08	4..5 (10.1)
Jun-08	3.9 (8.8)
Jul-08	3.3 (7.3)
Aug-08	2.9 (6.4)
Sep-07	3.8 (8.6)
Oct-07	4.2 (9.4)
Nov-07	4.5 (10.1)
Dec-07	3.9 (8.6)

Source: National Weather Service Forecast Office [71]

Snow significantly affects PV system performance. Snow cover surrounding a PV array can increase the available solar energy incident upon the array via reflection. However, snow covering the array can degrade system performance considerably. Monthly snow fall measured in Des Moines, Iowa (which is 56 kilometers (35 miles) from the site of the stationary system) is documented in Table 3.5.

Table 3.5. Monthly snow fall

Month	Snow fall, cm. (in.)
Jan-08	28 (11)
Feb-08	57.7 (22.7)
Mar-08	12.2 (4.8)
Apr-08	2.8 (1.1)
May-08	0
Jun-08	0
Jul-08	0
Aug-08	0
Sep-07	0
Oct-07	0
Nov-07	12.2 (4.8)
Dec-07	35.8 (14.1)

Source: National Weather Service Forecast Office [71]

System Performance at Standard Test Conditions

Manufacturers rate the performance of PV modules under conditions known as Standard Reporting Conditions (SRC) or Standard Test Conditions (STC) [54]. The rated capacity of a PV system (multiple modules) is then found by summing the rated DC power of each module in the array operating under STC. The specific standard test conditions used by manufacturers are: solar irradiance of 1,000 W/m^2, reference air mass of 1.5 (ASTM Standard Spectrum), a zero-degree angle of incidence (AOI), and cell junction temperature of 25^oC. However, operating conditions experienced in practice rarely occur at STC. Additionally, systems do not output rated DC power to the inverter at STC due to losses and inefficiencies. Furthermore, the inverter, and AC-side wiring and connections introduce additional losses causing AC power output to the building or grid to be less than DC power input to the inverter.

During the one year of monitoring, 17 instances were found where the system was operating at full-sun ($\pm$ 3 W/m^2) and 25^oC ($\pm$ 0.25^oC). The measured DC and AC electrical performance data for all instances were averaged to a single value and results are presented in Table 3.6.

Table 3.6. Performance of PV system operating at 1,000 W/m^2, 25^{o}C, and AOI ≈ 0 degrees

Parameter description	Value at STC	Units
System DC power output (system rating 1,020 Watts DC)	926	Watts DC
Average DC power output per square meter (per m^2 rating 134.92 Watts DC)	123	Watts DC/m^2
Average DC power output per module (module rating 170 WDC)	154	Watts DC/module
System output voltage DC	202	Volts DC
Average output voltage DC per module	34	Volts DC
System output current DC	4.6	Amps DC
System AC power output	839	Watts AC
Average AC power output per square meter	111	Watts AC/m^2
Average AC power output per module (module rating 170 WDC)	140	Watts AC/module
Derate factor to inverter (DC side)	0.908	fraction of rated cap.
Derate factor to utility (System)	0.823	fraction of rated cap.
Conversion efficiency of sun energy to electrical energy to inverter (DC side)	0.123	%/100
Conversion efficiency of sun energy to electrical energy to utility (System)	0.111	%/100

The DC electrical parameters were measured at the input of the inverter. Thus, these values represent the actual "usable" DC electricity that could be input to an inverter, battery bank, or DC powered device and include losses and inefficiencies before the inverter. Data in this study indicates the system outputs DC power at roughly 91 percent of its rated capacity when subjected to near STC.

System Current-Voltage Curves

System I-V curves were generated to show actual operating performance when the array is subjected to outdoor conditions and when it is affected by inverter power point tracking. Array DC voltage and current were monitored at the input of the inverter. Array operating I-V curves were generated for solar irradiance values of 200, 400, 600, 800, and 1,000 W/m^2 ($\pm$ 3 W/m^2) and include data for all other operating conditions experienced throughout the year. Data points on Figure 3.6 that do not follow the general trends correspond to times where snow partially or fully covered the array and/or the pyranometer, which was verified by comparing the data points to days the site experienced snow fall [71].

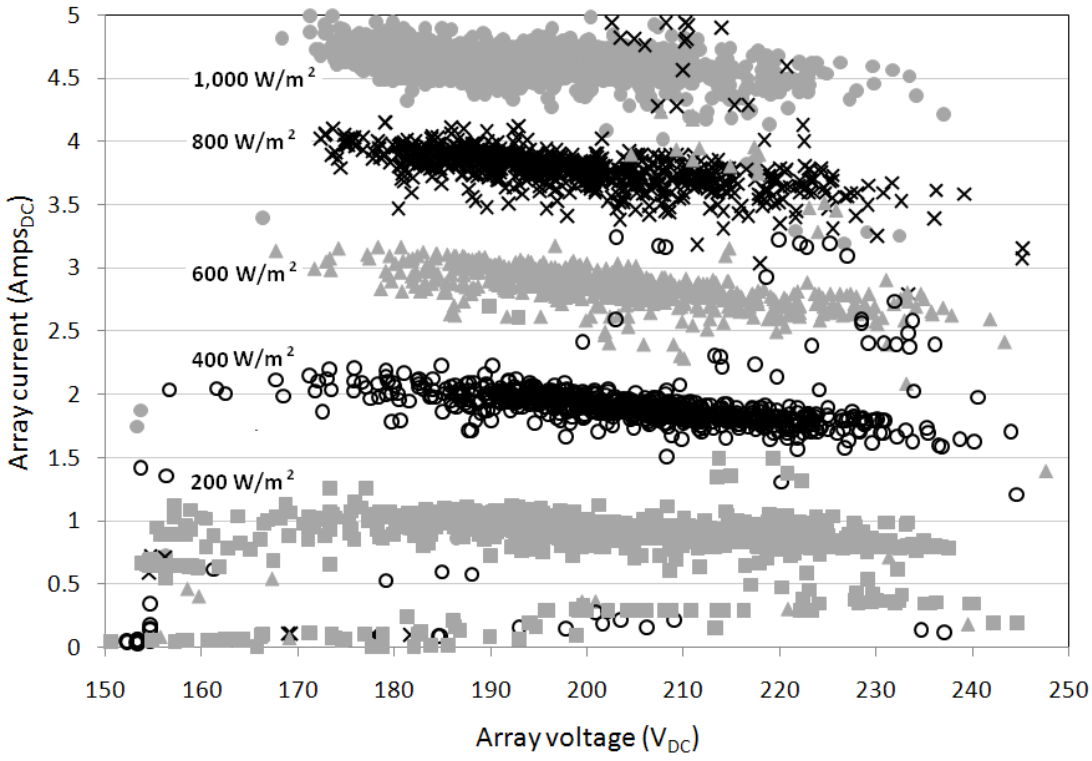

Figure 3.6. I-V curves for various levels of solar irradiance

Power Production

The instantaneous DC and AC power production of the array was calculated from data rather than being directly measured by a single instrument. The DC power output of the array, P_{DC}, was determined by the product of DC current and DC voltage. The AC power output of the array, P_{AC}, was found using the DC power input to the inverter and the inverter efficiency model by

$$P_{AC} = P_{DC}(\eta_{inverter}) \tag{3.1}$$

where $\eta_{inverter}$ is the instantaneous inverter efficiency to the corresponding DC power input. The method used for calculating inverter efficiency discussed in the section, Efficiency Measures.

The average DC power output of the system for each hour of the one-year monitoring period is plotted against corresponding hourly average in-plane solar irradiance values, seen in Figure 3.7. The AC power output would be slightly lower for all data points due to the inverter efficiencies.

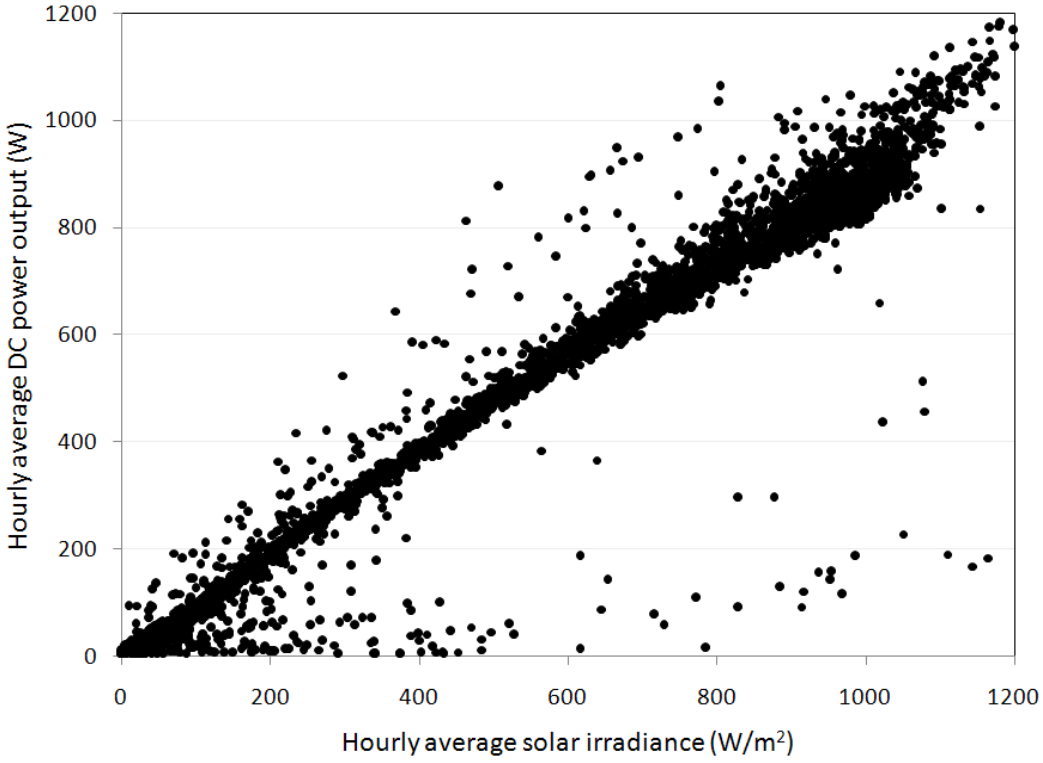

Figure 3.7. Power production vs. solar irradiance

The data shown in Figure 3.7 represents power production of the system for all operating conditions and solar irradiance values experienced at the site throughout the year. Figure 3.7 shows data points that deviate from the general trend; these particular points correspond to times where snow partially or fully covered the array and/or pyranometer and illustrate its effect on power production or measured irradiance. The maximum hourly average AC and DC power output by the system was measured to be 797 and 1,184 Watts (corresponding to a solar irradiance of 1,181 W/m^2 and an average array temperature of 1.6 ^{o}C), respectively. The average AC and DC power output of the system at full sun (i.e., 1,000 W/m^2) was found to be 800 and 854, respectively.

Energy Generation

The array performance was also characterized in terms of energy generation. Energy generation was evaluated for different time intervals (i.e., monthly and annually) and against solar energy input to the system. Monthly and annual AC and DC energy generation was calculated by multiplying the instantaneous power production value by the time-interval for which the power was produced, and then summing those values over the month or year. Results for monthly energy generation can be seen in Figure 3.8.

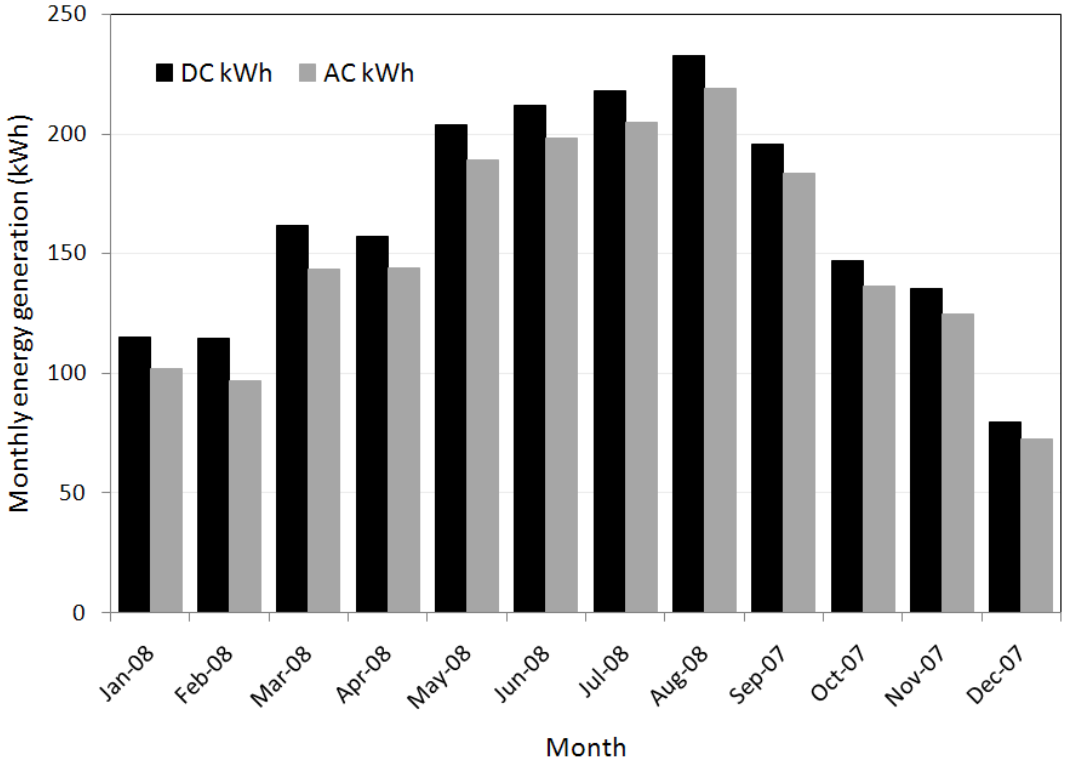

Figure 3.8. Monthly energy generation

The annual AC and DC energy generation for the system was found to be 1,815 and 1,973 kWh (1,179 and 1,934 kWh/kWp), respectively. The daily DC energy generation of the system was evaluated against the daily in-plane solar insolation incident on the array, shown in Figure 3.9. The effects of snow cover can be seen by points below the main trend line. The relationship between daily DC energy generation and daily solar insolation was observed to be approximately linear.

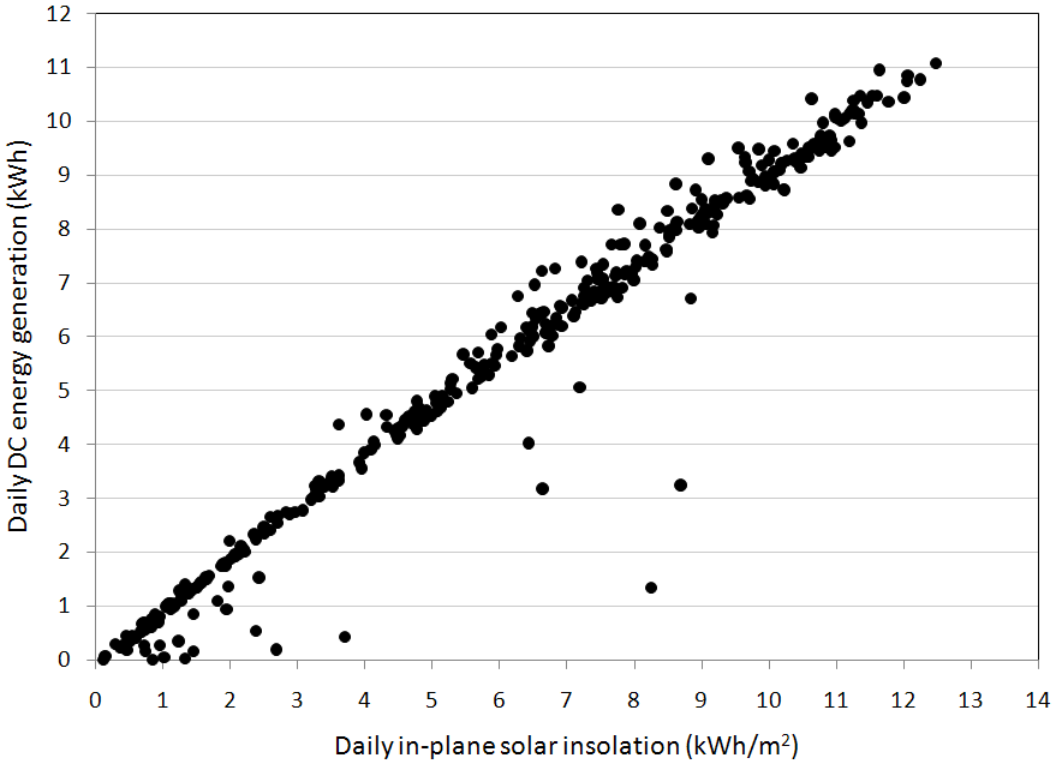

Figure 3.9. Daily DC energy generation vs. daily in-plane solar insolation

Efficiency Measures

As shown in Table 3.7, system efficiency was quantified in terms of average monthly and annual DC and AC system conversion efficiency. System conversion efficiency is defined as the ratio of the total DC or AC generated energy to the total solar insolation incident on the array.

Table 3.7. Monthly and annual average system conversion efficiencies

Month	Conversion efficiency from sun energy to DC electrical energy	Conversion efficiency from sun energy to AC electrical energy
Jan-08	0.116	0.103
Feb-08	0.119	0.100
Mar-08	0.121	0.108
Apr-08	0.121	0.110
May-08	0.120	0.112
Jun-08	0.119	0.111
Jul-08	0.120	0.113
Aug-08	0.120	0.113
Sep-07	0.118	0.111
Oct-07	0.122	0.113
Nov-07	0.127	0.117
Dec-07	0.119	0.109
Annual	0.120	0.110

Slight seasonal variations in system efficiency can be observed in this study. System efficiencies in the summer months were found to be slightly lower when compared to Spring and Fall and can be attributed in part to higher average array operating temperatures. The affects of snow cover on monthly average system efficiency were relatively insignificant. During the months of December 2007 and January 2008 the site experienced 35.8 cm (14.1 in) and 28 cm (11 in) of snow fall, respectively. However, the tracking system was observed to shed the snow cover fairly quickly. The annual average DC and AC efficiency was found to be 12 and 11 percent, respectively.

System efficiency was also evaluated and quantified against solar irradiance. The system efficiency curve was generated by using the ratio of average hourly AC power output to average hourly total solar insolation incident upon the array. Average hourly system efficiencies for all hours of the monitoring period are shown in Figure 3.10.

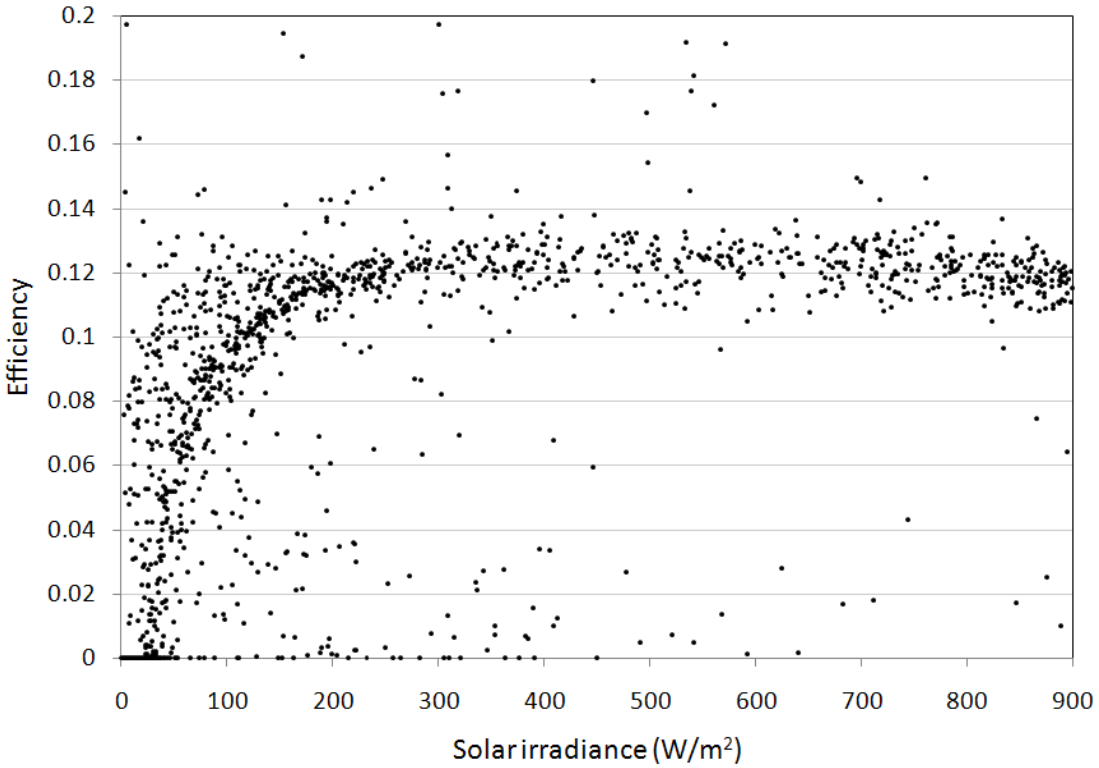

Figure 3.10. System efficiency (conversion of solar energy to AC electrical energy) vs. solar irradiance

The effects of influences such as array temperature, AOI, and solar spectrum on system efficiency can be seen by the variation of values within the main trend line. Snow cover on the array also significantly affected hourly average system efficiency, which can be seen by the data points lying below the main trend.

Inverter performance was quantified in terms of conversion efficiency from DC to AC electrical power. The DC and AC electrical data collected to calculate this instantaneous inverter efficiency was measured by using an independent power logger in a stand-alone test. The conversion efficiency of the inverter was then calculated as a function of DC power input, shown in Figure 3.11. This plot shows instantaneous inverter efficiency using data at one-minute time steps.

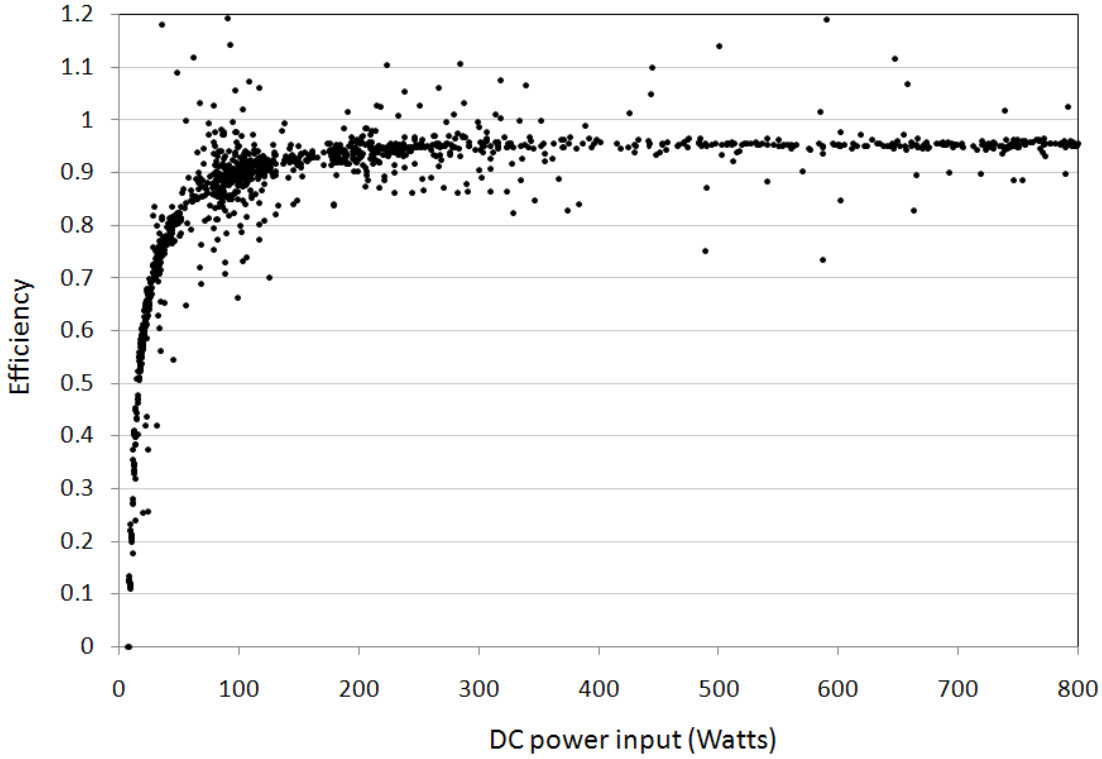

Figure 3.11. Inverter efficiency vs. DC power input from array

The inverter was found to operate at a fairly consistent efficiency for solar irradiances ranging from 200 to 1,200 W/m^2, which represents a large portion of the operating range. Lastly, the annual average conversion efficiency of the inverter was calculated as the ratio of annual AC energy to the annual DC energy, which was found to be approximately 92 percent.

The performance ratio, PR, is a parameter that is normalized with respect to irradiance and quantifies the overall effect of all losses on the rated output due to system inefficiencies, losses, and operating conditions [72]. Specific uses of PR values are documented elsewhere [63]. The performance ratio can be calculated by

$$PR = \frac{Y_f}{Y_r} \tag{3.2}$$

where Y_f is the system yield (kWh/kWp) and Y_r, is the reference yield (hours). The system yield is found by dividing the net AC energy output by the installed DC capacity of the array (defined at STC). The reference yield represents the number of peak sun hours seen by the system evaluated over the same time period used for determining the system yield. Annual, monthly, and daily PR values were determined with daily PR values throughout the one-year monitoring period shown in Figure 3.12.

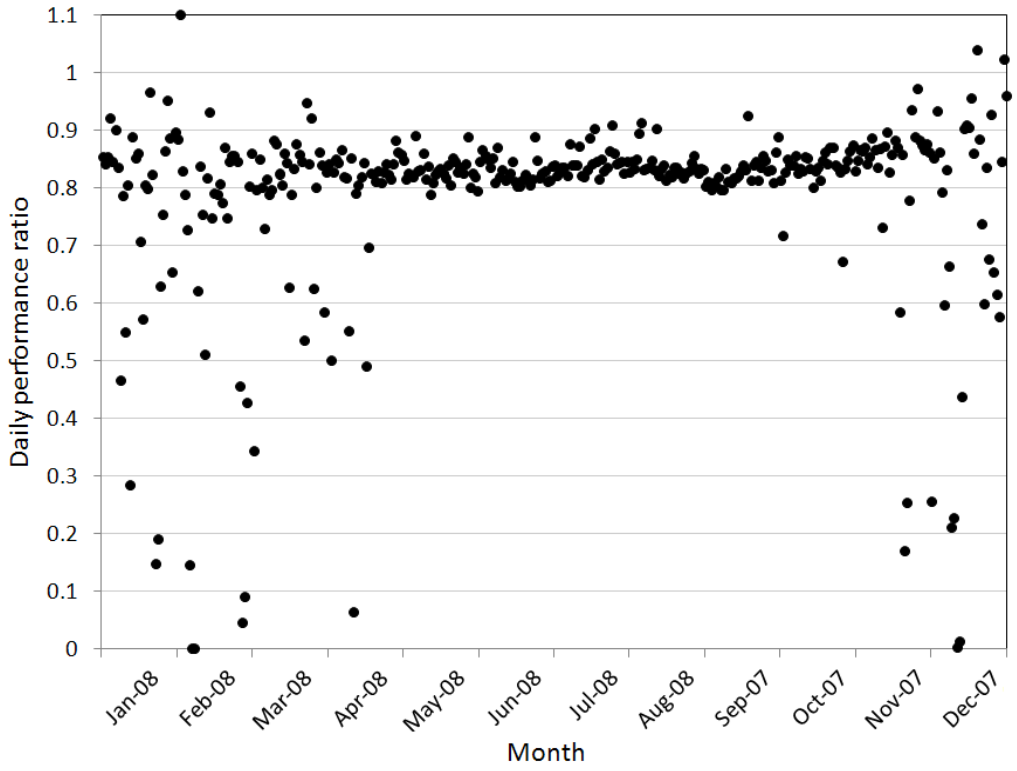

Figure 3.12. Daily performance ratios

All performance ratios calculated on monthly and annual bases can be found in Table 3.8.

Table 3.8. Monthly performance ratios

Month	Ave PR
Jan-08	0.764
Feb-08	0.744
Mar-08	0.799
April-08	0.819
May-08	0.827
June-08	0.822
July-08	0.839
Aug-08	0.834
Sep-07	0.820
Oct-07	0.838
Nov-07	0.866
Dec-07	0.807
Annual	0.819

Daily PR values during the winter months were found to be vary sporadic; the days yielding irregular PR values coincided with times the array and/or pyranometer was fully or partially covered with snow. Throughout the year, monthly PR values varied from 0.744 to 0.866. The annual average performance ratio was found to be 0.819.

A frequency distribution of daily PR values is shown in Figure 3.13.

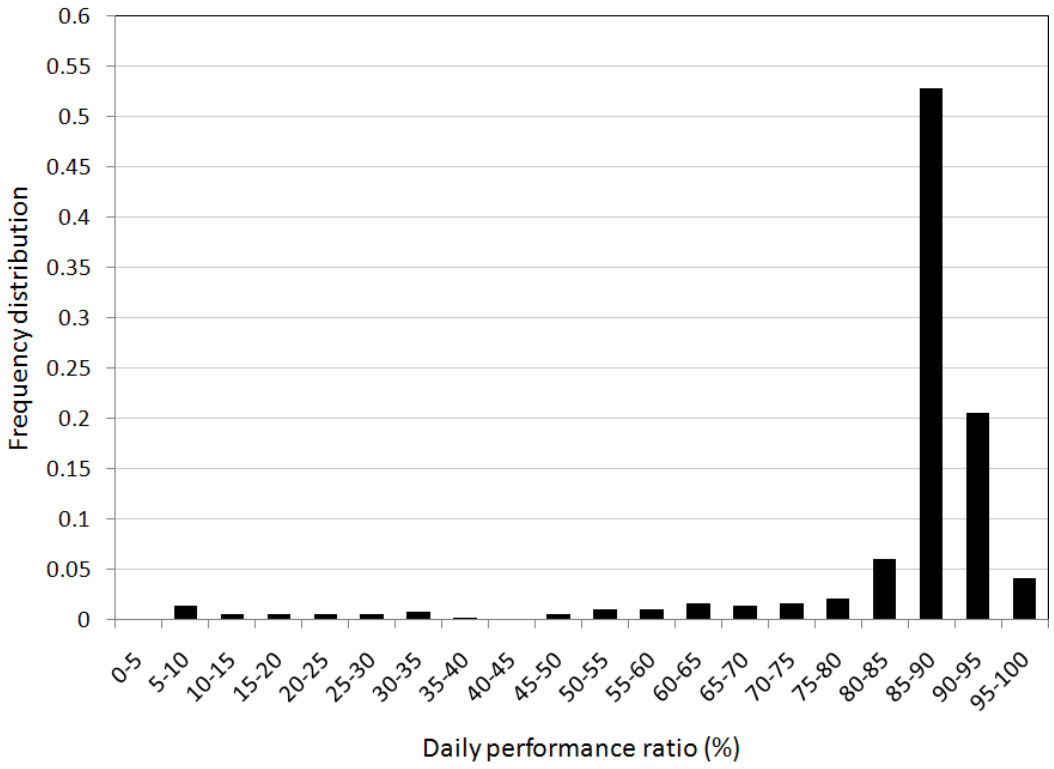

Figure 3.13. Frequency distribution of PR

The system was found to operate at a performance ratio level between 85 and 95 percent for 268 of 365 days during the monitoring period.

SUMMARY

A 1.02 kWp grid-connected, dual-axis tracking PV system was installed, operated, and monitored in the Upper Midwest for one year. All PV and Balance-Of-System (BOS) equipment used in the installations are “off-the-shelf” components and considered standard for residential and commercial applications. The outdoor experimental performance of the system was quantified for one year of collected data. Experimental results reflect performance of a PV system exposed to a wide-range of operating conditions inherent to climate in the Upper Midwest.

The annual average daily solar insolation incident upon the array was found to be 5.95 kWh/m^2. During the first year of operation, the PV system provided 1,815 kWh (1,779 kWh/kWp) of usable AC electrical energy. The system was found to operate at an annual average conversion efficiency and PR of 11 percent and 0.819, respectively. Slight seasonal variations in system efficiency were observed and can be attributed in part to variations in average array operating temperatures throughout the year. The affects of snow cover on monthly average system efficiency were found to be relatively insignificant. The annual average DC to AC conversion efficiency of the inverter was found to be 92 percent.

The research herein serves several important purposes aimed at alleviating some of the current barriers to the widespread use of PV. This research can be used to set appropriate expectations for PV systems operating in the Upper Midwest allowing design professionals and consumers to make more informed decisions. The test systems serve as demonstrations of real-world PV applications for building energy generation and are used for research, demonstration, and education purposes. The test systems are available to the public for observation and to the scientific community for future research. The interactive data interface, webcam, and general project information can be found online through the Iowa Energy Center's website at www.energy.iastate.edu/Renewable/solar/.

ACKNOWLEDGEMENTS

The authors would like to thank the Iowa Energy Center for providing personnel, administrative, and financial support for this project. Additionally, the authors acknowledge Iowa State University for providing the site and administrative support.

CHAPTER 4 - PERFORMANCE COMPARISON OF STATIONARY AND DUAL-AXIS TRACKING GRID-CONNECTED PHOTOVOLTAIC SYSTEMS IN THE UPPER MIDWEST

A paper in preparation for submission to *American Society of Mechanical Engineers – Journal of Solar Energy Engineering*

Ryan Warren, Michael Pate, Ron Nelson

ABSTRACT

Two grid-connected photovoltaic (PV) systems comprised of multicrystalline silicon (mc-Si) modules with different mounting schemes were installed in central Iowa and monitored for one year; one roof-mounted stationary system and one pole-mounted dual-axis tracking system. These systems serve as real-world applications of PV for building energy generation and are used for research, demonstration, and education purposes. Both systems are equipped with extensive data acquisition capable of collecting performance and meteorological data, visually displaying real-time and historical data, and simultaneously comparing performance through an interactive online interface. Additionally, web cameras and general project information are also available online (www.energy.iastate.edu/Renewable/solar).

Experimental performance and economic analyses of the systems were performed and the results are presented in a five-part series of studies. Experimental data was collected and analyzed for the systems over a one-year period from September 2007 through August 2008. This paper presents a comparison of performance between the two systems, and primarily focuses on measures of power production, energy generation, and efficiency. The tracking system harvested approximately 36 percent more solar energy than the stationary system throughout the year. The annual average daily solar insolation seen by the stationary and tracking systems were found to be 4.37 and 5.95 kWh/m^2, respectively. Annually, the tracking system generated 41 percent more AC electrical energy than the stationary system per kWp of installed capacity; normalized annual energy generation for the tracking and stationary systems were found to be 1,779 and 1,264 kWh/kWp, respectively. The annual average conversion efficiencies of the tracking and stationary systems were found to be 11 and 10.7 percent, respectively. Both systems operated at annual average performance ratios near 0.8.

INTRODUCTION

There are many options to consider when designing or selecting a photovoltaic (PV) system to generate electrical energy. One major decision to be considered is the type of mounting scheme. The most

common types of mounting schemes used are stationary (or fixed) and tracking. Factors that influence the decision for what type of mounting scheme to use can include: space limitations, initial cost, operating savings, aesthetics, and performance. In stationary systems, the PV array is affixed directly to a static structure (e.g., roof or rack) and the orientation of the array is constant throughout the daylight period and life of the system. The orientation of these systems is most often selected to maximize for annual energy generation and depends of the geographical location and site of the system. In tracking systems, the azimuth and/or slope of the PV array is continuously adjusted during operation to maintain, as close as possible, a perpendicular orientation to solar beam radiation.

Two grid-connected PV systems with different mounting schemes were installed in central Iowa, USA; one roof-mounted stationary system and one pole-mounted dual-axis tracking system. Both systems were designed as "turn-key" installations for building energy generation applications. The orientation of the stationary system was selected to optimize for annual energy generation. All PV and Balance-Of-System (BOS) equipment used in the installations are "off-the-shelf" components and considered standard for residential and commercial applications. For example, flat-plate PV modules made of silicon nitride multicrystalline silicon (mc-Si) cells were used. The PV systems are equipped with extensive data acquisition (DAQ) systems capable of collecting accurate performance and meteorological data, archiving data in a central repository, and visually displaying real-time and historical data through an interactive online interface. Additionally, webcams are installed at each site to show real-time and historical streaming video and photographs that can be compared to the data presented in the interface.

The experimental performance and economics of both systems have been analyzed in detail based on experimental data taken over one full year and are presented in a five-part series of papers. The performance analysis of the systems primarily focuses on measures of power production, energy generation, and efficiency. Results are shown on instantaneous, daily, monthly, and annual bases. Two papers of the series present performance results for the stationary system and dual-axis tracking system, respectively [63, 64]. This paper presents a comparison of normalized measures between the two systems by highlighting the performance differences due to the different mounting schemes. The fourth paper presents an economic analysis of both systems by focusing on life-cycle-cost, payback period, internal rate of return, and the incremental cost of solar energy [66]. The final study investigates heat transfer characteristics of the stationary and tracking arrays and quantifies the affects of operating temperature on PV system performance [67]. Further, simulations were performed to estimate how

each system might perform while operating at lower temperatures. Metrics used to assess heat transfer characteristics and affects of operating temperature on PV system performance include overall heat transfer coefficients and the temperature coefficient for power.

This work serves several important purposes aimed at alleviating some of the current barriers to the widespread use and adoption of PV discussed in [63]. The PV systems serve as demonstrations of real-world stationary and tracking PV applications for building energy generation and are used for research, demonstration, and education purposes. The performance and economic results of this research are based on onsite experimental testing and reflect what would be experienced in practice as opposed to model-based or laboratory generated simulations and predictions. These results can be used to set appropriate expectations for PV systems operating in the Upper Midwest allowing design professionals and consumers to make more informed decisions. Additionally, the experimental data collected can be used in the development, validation, and improvement of computer simulation tools. The test systems are available to the public for observation and to the scientific community for future research. The interactive data interface, webcam, and general project information can be found online through the Iowa Energy Center's website at [68].

EXPERIMENTAL TEST SYSTEMS

The two systems have a few differences in equipment and installation. The systems have different inverters, number of modules per string, DC wiring lengths, and surrounding ground cover. Different inverters were necessary due to differing building AC line voltages; the stationary and dual-axis tracking systems are coupled to electrical systems having nominal 208 VAC and 120 VAC, respectively. Additionally, due to size constraints, the tracking system was limited to six modules wired in series where the stationary system consists of three strings of nine modules in series, each wired to a different but identical inverter. The DC wiring lengths for the stationary and dual-axis tracking system are 64 m (210 ft) (average of three subsystems) and 19 m (62 ft), respectively. A summary of the differences between the stationary and dual-axis tracking systems is shown in Table 4.1.

Table 4.1. Summary of differences between stationary and dual-axis tracking systems

System	Stationary	Dual-axis tracking
Location	Ames, Iowa	Nevada, Iowa
Latitude	42 degrees 2 minutes north	42 degrees 1 minute north
Longitude	93 degrees 48 minutes west	93 degrees 27 minutes west
Installed capacity (kWp)	4.59	1.02
Total PV array area (m2)	34.02	7.56
Mount	roof-mounted	pole-mounted
Orientation	slope of 36 degrees facing due south	dual-axis tracking
Number of inverters	3	1
Number of strings of modules	1 per inverter	1
Number of modules per string	9	6
Average DC wiring length (m)	64	19
Surrounding ground cover	Rock covering rubber membrane roof	Grass and nearby pond
Building line voltage (VAC)	208	120

The stationary system is located in Ames, Iowa, at a latitude of 42 degrees 2 minutes north and a longitude of 93 degrees 48 minutes west. The system has a total installed capacity of 4.59 kW_p and total PV array area of 34.02 m^2 (366.2 ft^2). This system is designed as three side-by-side, identical, and independently operating sub-systems. Each subsystem consists of nine, 170 Watt modules operated at their peak power point and wired in series to a single inverter; all three inverters are identical. All modules are attached directly to a south-facing standing-seam white metal roof at a slope of 36 degrees (oriented for maximum annual energy generation). A complete description of the stationary system can be found in [63].

The tracking system is located in Nevada, Iowa, 42 degrees 1 minutes north latitude and 93 degrees 27 minutes west longitude and was approximately 14 kilometers (8.7 miles) from the stationary system. The system has an installed capacity of 1.02 kW_p and total PV array area of 7.56 m^2 (81.38 ft^2). This system uses six, 170 Watt modules wired in series to a single inverter. The pole-mounted array follows the sun throughout the day using an actively controlled dual-axis, azimuth drive solar tracker. The azimuth range of the tracker is 270 degrees. The tracker is controlled by using an electronic transducer that is mounted on top of the array. The transducer has sensors on all sides and adjusts position until an equal amount of sun is sensed on all sides. A complete description of the tracking system can be found in [64].

Both systems use the same PV modules made of silicon nitride multicrystalline silicon (mc-Si) cells. Electrical and mechanical specifications for these modules can be seen in Table 4.2.

Table 4.2. Electrical and mechanical characteristics of photovoltaic modules

Rated power	170 Watts
Voltage at rated power	35.4 VDC
Current at rated power	4.8 Amps
Short-circuit current	5.0 Amps
Open-circuit voltage	44.2 VDC
Temperature coefficient of short circuit current	$(0.065 \pm 0.015)\%/^{o}C$
Temperature coefficient of open circuit voltage	$-(160 \pm 20)$ mV/^{o}C
Temperature coefficient of power	$(0.5 \pm 0.05)\%/^{o}C$
NOCT (Air 20 ^{o}C; sun 0.8 kW/m^2, wind 1 m/s)	$47 \pm 2\ ^{o}C$ (116.6 $\pm$ 3.6 ^{o}F)
Size (length x width x depth)	1593 x 790 x 50 mm (62.8 x 31.1 x 1.97 in.)
Weight	15.0 kg (33.1 lb.)
Solar Cells	72 cells (125 mm x 125 mm) in a 6 x 12 matrix connected in series

The PV systems are equipped with extensive data acquisition systems (DAQ). Each DAQ is capable of collecting accurate data at a high sampling rate, archiving data in a central repository, and visually displaying real-time and historical data of both systems simultaneously through an online interactive interface. All data is measured at ten second intervals, and stored as one-minute averages. To adequately characterize the performance of the PV systems, both operating parameters of each array and meteorological conditions were monitored. The specific performance parameters that were monitored include the following:

- DC voltage produced by the arrays of modules (measured at input of inverters)
- DC current produced by the arrays of modules (measured at input of inverters)
- AC voltage output by the inverters (measured at output of inverters)
- AC current output by the inverters (measured at output of inverters)
- Module temperatures

The meteorological parameters that were monitored include:

- Solar irradiance (measured at plane of array)
- Ambient air temperature (tracking system only)
- Wind speed (stationary system only)
- Wind direction (stationary system only)

The placement of each instrument and design of the data acquisition system can be seen in Figure 4.1. Specific details of the data acquisition system and instrumentation for both systems are given in [63, 64].

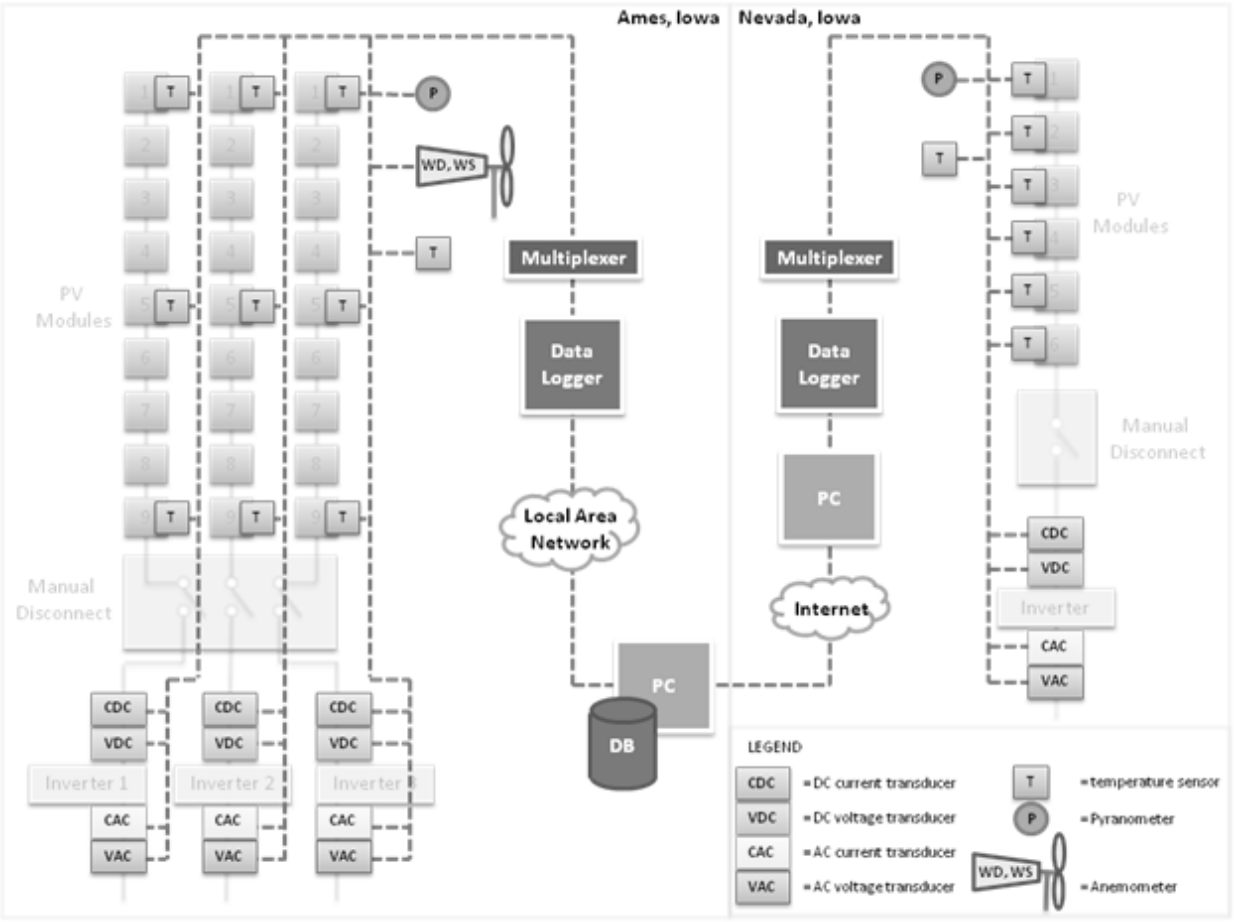

Figure 4.1. One-line diagram of data acquisition system

EXPERIMENTAL ANALYSIS AND RESULTS

Both systems were operated and monitored simultaneously for one year. Experimental data was collected for performance parameters and meteorological conditions from September 2007 through August 2008. Data was sampled at 10 second intervals and stored as one-minute averages. The PV systems were new at the onset of data collection. During the test period, the systems were allowed to operate as real-world systems; modules were never cleaned of snow or soiling and the systems were not purposely taken off-line or interrupted for any reason.

A detailed comparison for system performance of the stationary and tracking systems is presented herein. Meteorological conditions experienced at the sites during the one-year monitoring period are shown and include solar resource, ambient air temperature, wind speed and direction, and snow fall.

Performance comparisons are made for measures of solar resource, energy generation, power production, and efficiency. Results are presented on hourly, daily, monthly, and annual bases where applicable.

Meteorological Conditions

To compare performance measures between the systems, it is necessary to first establish the available solar resource to each system. The amount of solar energy that can be utilized by a PV system at any given time is dependent upon the beam radiation angle of incidence relative to the array surface. The inherent advantage of a tracking system when compared to a stationary system is its ability to orient the array perpendicular to the solar beam radiation to maximize the collection of available solar energy at all times. The solar resource available to a PV system is also a function of geographical location, surrounding ground cover, and atmospheric/meteorological conditions. For this research, the in-plane solar resource available to each PV system was compared in terms of average daily solar insolation on monthly and annual bases, seen in Table 4.3.

Table 4.3. Monthly and annual average daily solar insolation

Month	Stationary system	Dual-axis tracking system	Percent difference*
Jan-08	2.90	4.22	46
Feb-08	3.23	4.55	41
Mar-08	4.37	5.69	30
Apr-08	4.43	5.75	30
May-08	5.33	7.23	36
Jun-08	5.47	7.88	44
Jul-08	5.55	7.73	39
Aug-08	5.89	8.30	41
Sep-07	5.62	7.31	30
Oct-07	3.89	5.14	32
Nov-07	3.56	4.71	32
Dec-07	2.11	2.84	35
Annual	4.37	5.95	36

*percent difference calculated relative to stationary system

The annual average daily solar insolation seen by the stationary and dual-axis tracking systems was found to be 4.37 and 5.95 kWh/m^2, respectively. On an annual basis the tracking system harvested 36 percent more solar energy than the stationary system. Seasonally, the tracking system showed the most benefit in comparison to the stationary system during summer and winter months.

Ambient air temperature and wind affects module/array operating temperatures, which in turn influences PV system performance. The hourly average ambient air temperature experienced during the monitoring period can be seen in Figure 4.2.

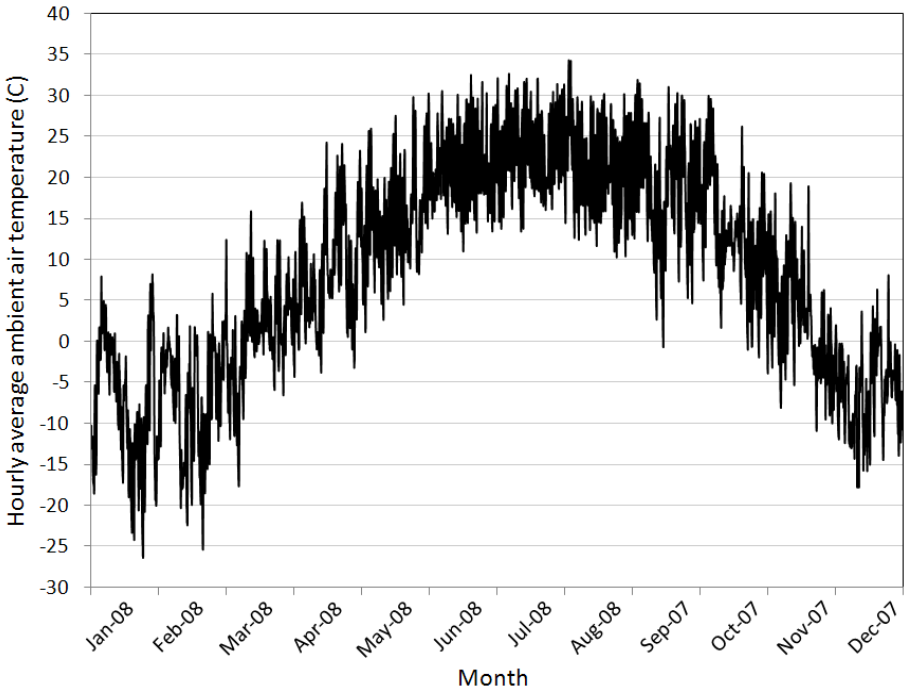

Figure 4.2. Hourly average ambient air temperature

The average monthly wind speed and prevailing direction (at a height of 10 meters) during the year of monitoring measured in Des Moines, Iowa is shown in Table 4.4.

Table 4.4. Average monthly wind speed

Month	Average wind speed at 10 meters, m/s (mph)
Jan-08	4.5 (10.0)
Feb-08	4.3 (9.7)
Mar-08	4.2 (9.5)
Apr-08	5.1 (11.3)
May-08	4..5 (10.1)
Jun-08	3.9 (8.8)
Jul-08	3.3 (7.3)
Aug-08	2.9 (6.4)
Sep-07	3.8 (8.6)
Oct-07	4.2 (9.4)
Nov-07	4.5 (10.1)
Dec-07	3.9 (8.6)

Source: National Weather Service Forecast Office [71]

Snow significantly affects PV system performance. Snow cover surrounding a PV array can increase the available solar energy incident upon the array via reflection. However, snow covering the array can degrade system performance considerably. Monthly snow fall measured in Des Moines, IA is documented in Table 4.5.

Table 4.5. Monthly snow fall

Month	Snow fall, cm. (in.)
Jan-08	28 (11)
Feb-08	57.7 (22.7)
Mar-08	12.2 (4.8)
Apr-08	2.8 (1.1)
May-08	0
Jun-08	0
Jul-08	0
Aug-08	0
Sep-07	0
Oct-07	0
Nov-07	12.2 (4.8)
Dec-07	35.8 (14.1)

Source: National Weather Service Forecast Office [71]

Energy Generation

The primary function of a photovoltaic system is to generate electrical energy, thus, one of the most important performance measures assessed in this work is the difference in energy generation resulting from stationary and tracking mounting schemes. Assessments and comparisons of energy generation are also important because it sets expectations for system performance and associated economic return. Both AC and DC energy generation on monthly and annual bases were considered. Monthly and annual AC and DC energy generation was calculated for each system by multiplying the instantaneous power production value by the time-interval for which the power was produced, and then summing those values over the month or year. Since the two systems are different sizes, the data was normalized per kilowatt of installed capacity at Standard Test Conditions (STC) to allow for a direct comparison. Results for monthly average daily AC and DC energy generation for both systems are shown in Figure 4.3.

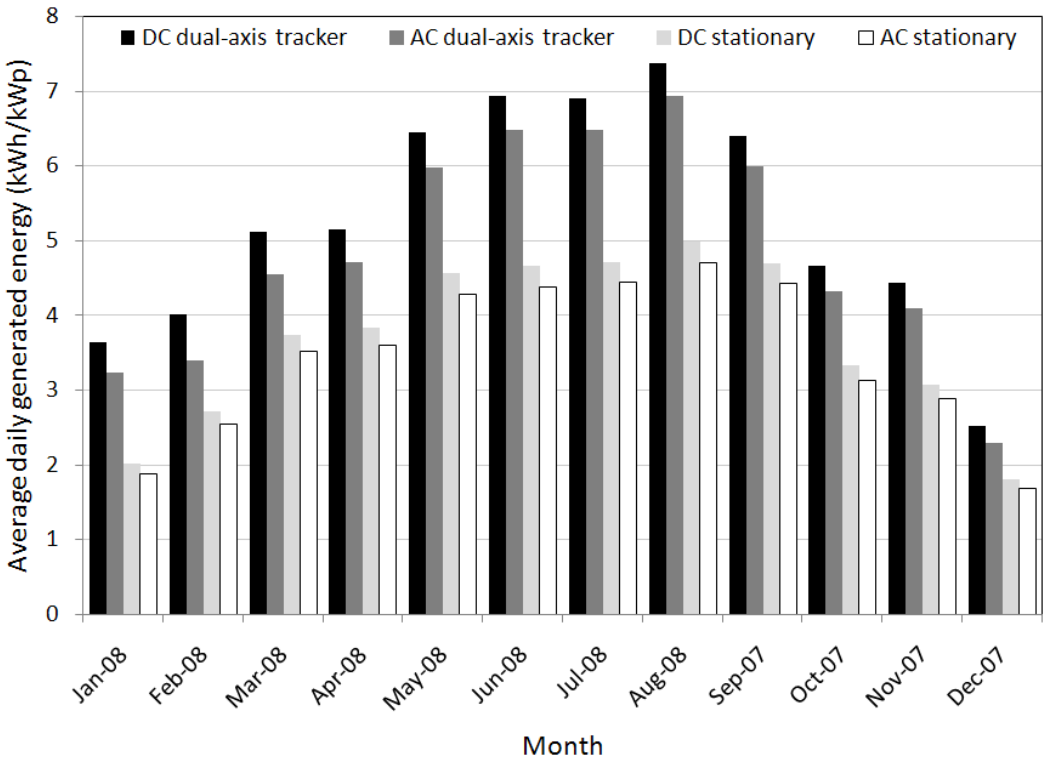

Figure 4.3. Stationary and tracking monthly average daily AC and DC generated energy per kWp of installed PV at STC

Comparisons for normalized annual AC and DC energy generation from both systems can be seen in Table 4.6.

Table 4.6. Normalized annual AC and DC energy generation

System	Stationary	Tracking
Annual AC energy generated per kWp (kWh/kWp)	1,264	1,779
Annual DC energy generated per kWp (kWh/kWp)	1,342	1,934
Annual AC energy generated per square meter of PV (kWh/m^2)	171	240
Annual DC energy generated per square meter of PV (kWh/m^2)	181	261

Annually, the tracking system generated 41 and 44 percent more AC and DC electrical energy than the stationary system per kWp, respectively. Seasonally, the tracking system showed the greatest benefit in the summer and winter months when compared to Spring and Fall.

The daily DC energy generation of each system was evaluated against the daily in-plane solar insolation incident on each array, shown in Figure 4.4.

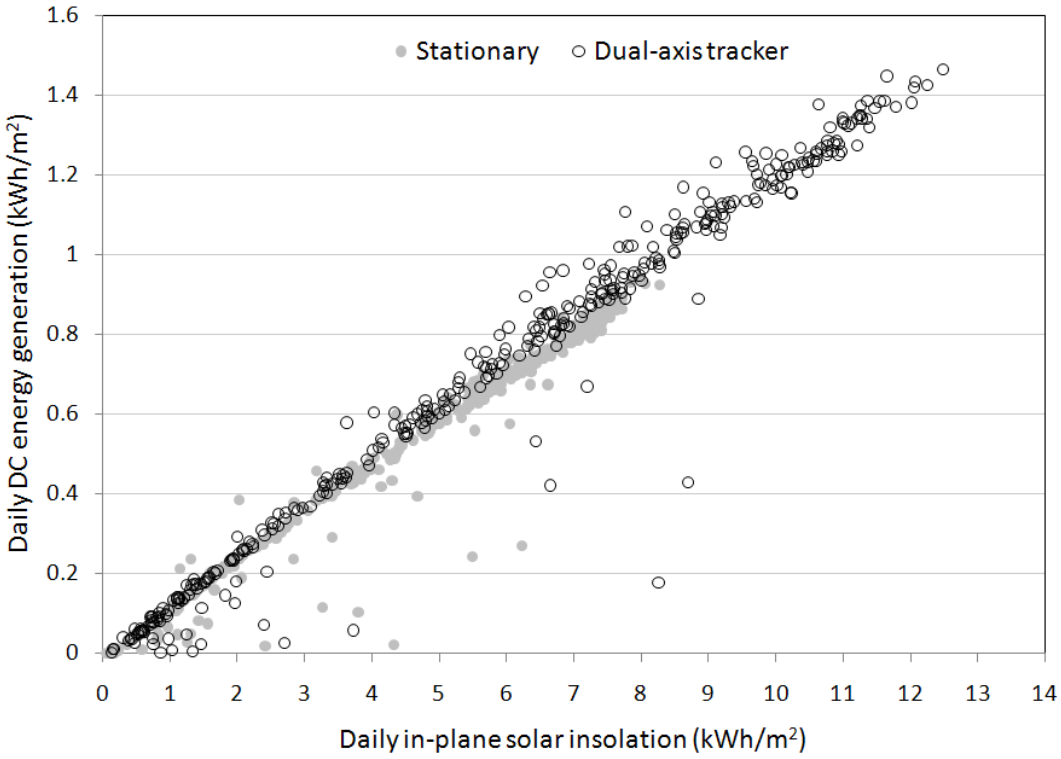

Figure 4.4. Daily DC energy generation vs. daily in-plane solar insolation

Power Production

Power production of a PV system is directly related to the amount of solar irradiance incident on the array. On average, tracking systems yield a higher average normalized power output under sunny conditions when compared to stationary systems since they are always oriented nearly perpendicular to direct beam radiation. However, during cloudy conditions, the advantages of a tracking system to a stationary system are diminished because module performance when exposed to diffuse solar irradiance is largely independent of orientation [56]. For this research, power production was compared between systems on daily and annual bases. For the daily comparison, days with no cloud cover near the summer and winter solstice were used. These two days represent the longest day where the sun has the greatest solar altitude angle and the shortest day where the sun has the lowest solar altitude angle at the sites during the year. Minute-by-minute power production was plotted for these two days for both systems, seen in Figure 4.5.

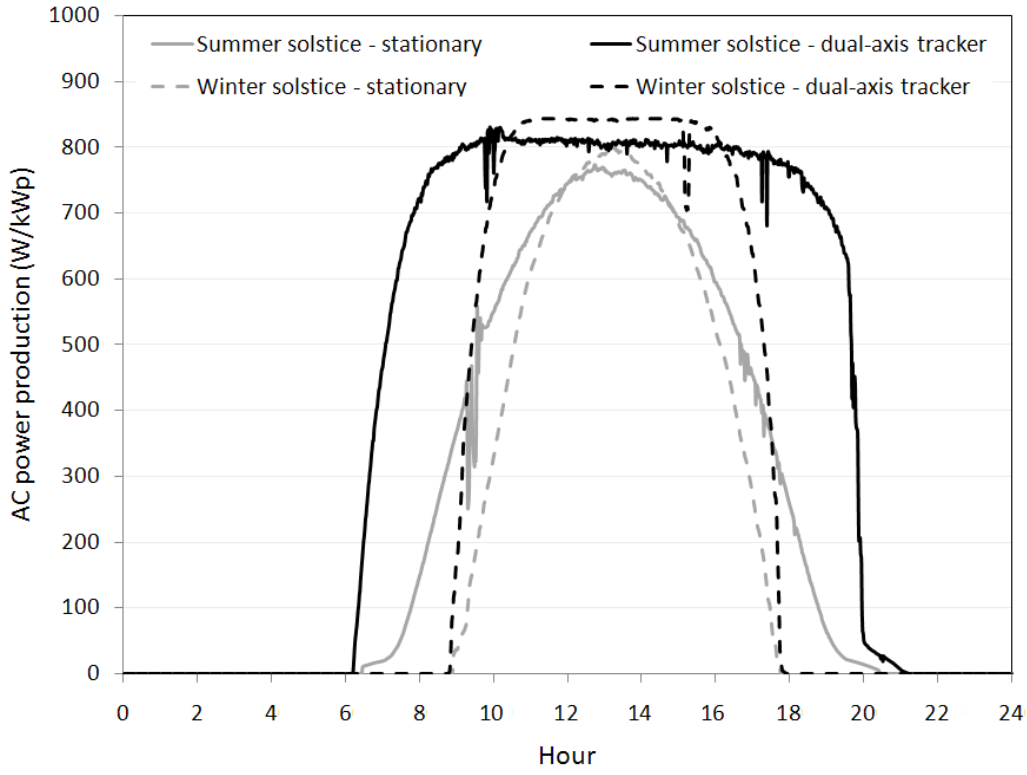

Figure 4.5. Stationary and tracking power production for summer and winter solstices

As expected, both systems yielded power outputs close to capacity for a longer period near the summer solstice than the winter solstice due to the additional solar energy available during the longer day. Additionally, it was noted that peak power output was higher for both systems during the winter solstice; this result is most likely due to lower array operating temperatures and additional solar radiation incident on the arrays due to increased reflectance from snow covered surroundings. Approximately 13 cm (5 in.) of snow covered the ground during the day shown for winter solstice results [71]. Near the summer solstice the tracking system maintained power production levels within 2 percent of full output (806 W_{AC}/kW_p) for approximately 7.7 hours of the day; whereas the stationary system output at peak levels (764 W_{AC}/kW_p) approximately 2 hours of the day.

Power production was also compared on an annual basis considering all meteorological and operating conditions. For this comparison, the power production data in one-minute intervals were divided into ten bins; each bin represents 10 percent of installed capacity for each system (e.g., for the tracking system with installed capacity of 1,020 Wp the fist bin represents power outputs between 0 and 102 Watts). Subsequently, the number of occurrences where each system output power at levels corresponding to each bin range was counted. The number of observations for each bin was then

divided by the total number of observations throughout the year to find the fraction of time each system operated in each power range. A bar chart showing the results can be seen in Figure 4.6.

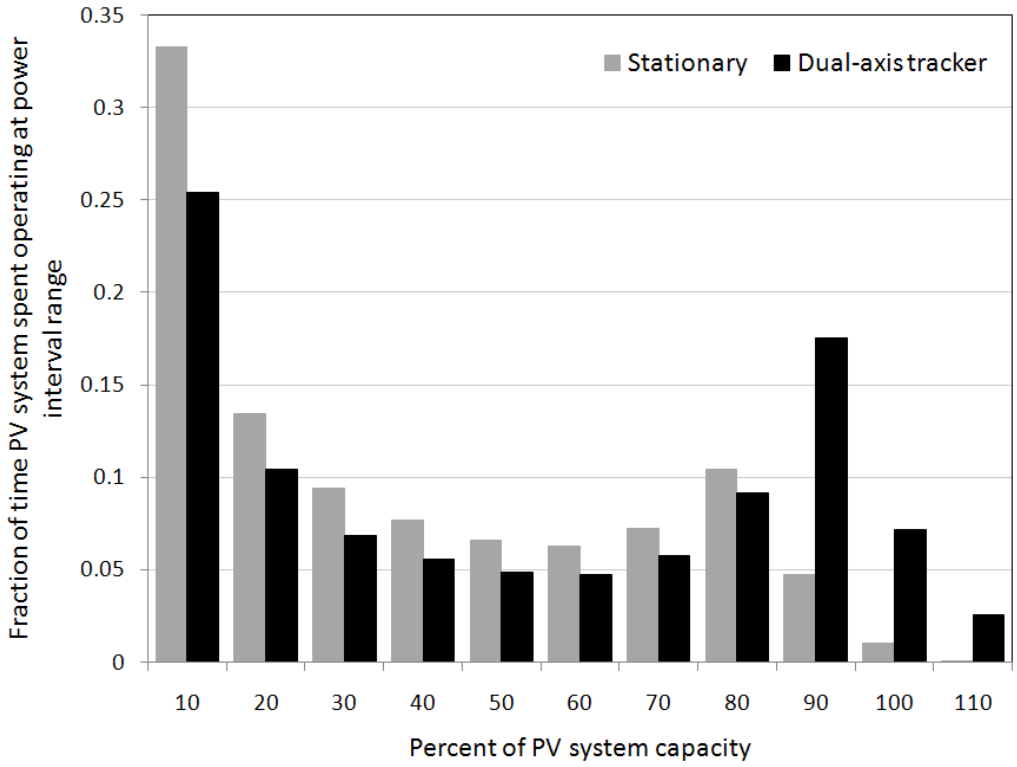

Figure 4.6. Stationary and tracking frequency distribution of power production

Figure 4.6 shows the tracking system operated closer to capacity more often that the stationary system, as expected.

Efficiency Measures

The effectiveness of converting solar energy to usable electrical energy for each system is important to consider when comparing performance. Two measures for comparing energy conversion are assessed; system conversion efficiency and performance ratio (PR). These two parameters quantify how well a system converts available solar insolation to usable electrical energy and how well a system performs relative to rated capacity. Losses that affect conversion efficiency and PR can occur in module mismatch, diodes, wiring, connections, snow cover, soiling, high operating temperatures, and the conversion of DC to AC electricity in the inverter. In addition to these sources of losses, systems may not perform at rated capacity under STC due to age and inaccurate nameplate ratings.

System conversion efficiency for this research is defined as the ratio of the total AC energy generated to the total insolation incident on the array over a particular time period. Monthly and annual conversion efficiencies for both systems are shown in Figure 4.7.

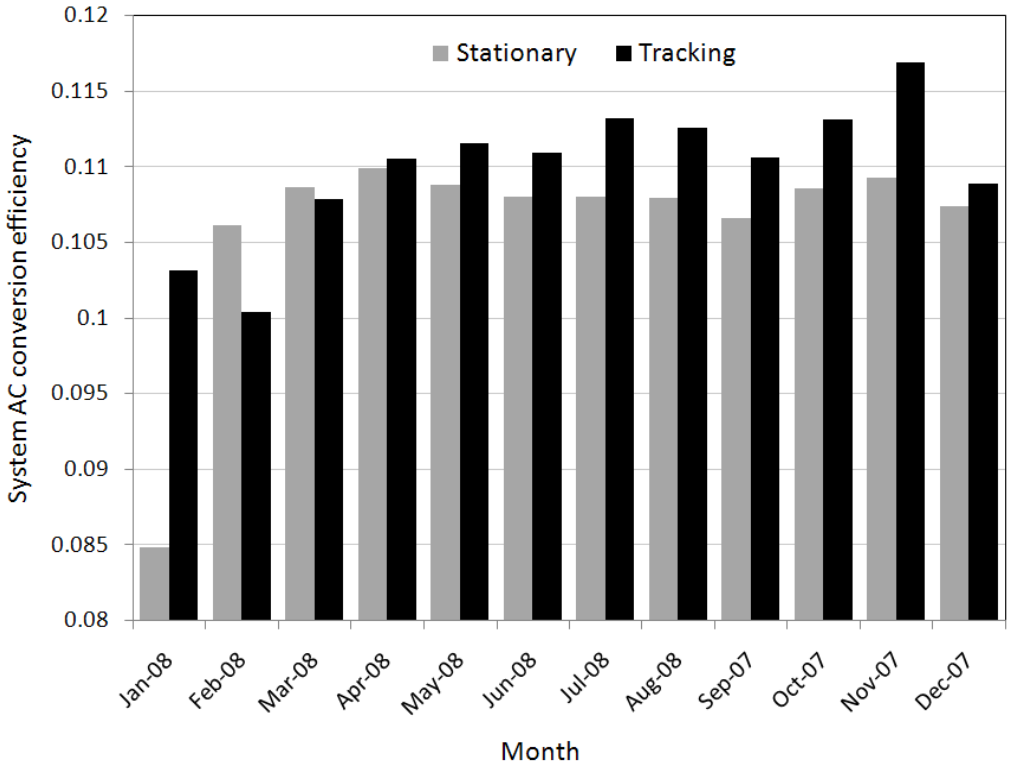

Figure 4.7. Monthly and annual average system conversion efficiencies

The annual average conversion efficiencies of the stationary and tracking systems were found to be 10.7 and 11 percent, respectively. Snow cover significantly affected conversion efficiencies in December, January, and February where the sites received 35.8, 28, and 57.7 cm (14.1, 11, and 22.7 in.) of snow fall, respectively.

The performance ratio is normalized with respect to solar irradiance and quantifies the net effect of all losses on the rated output due to system inefficiencies, losses, and operating conditions [1]. Performance ratio values can be found over any time period and have many applications. The performance ratio can be calculated by

$$PR = \frac{Y_f}{Y_r} \tag{4.1}$$

where Y_f is the system yield (kWh/kWp) and Y_r, is the reference yield (hours). The system yield is found by dividing the net AC energy output by the installed DC capacity of the array (defined at STC). The reference yield represents the number of peak sun hours seen by the system evaluated over the same time period used for determining the system yield. Daily, monthly, and annual PR values for both systems were determined. Daily PR values for each system throughout the one-year monitoring period can be seen in Figure 4.8. Performance ratios calculated on monthly and annual bases can be found in Table 4.7.

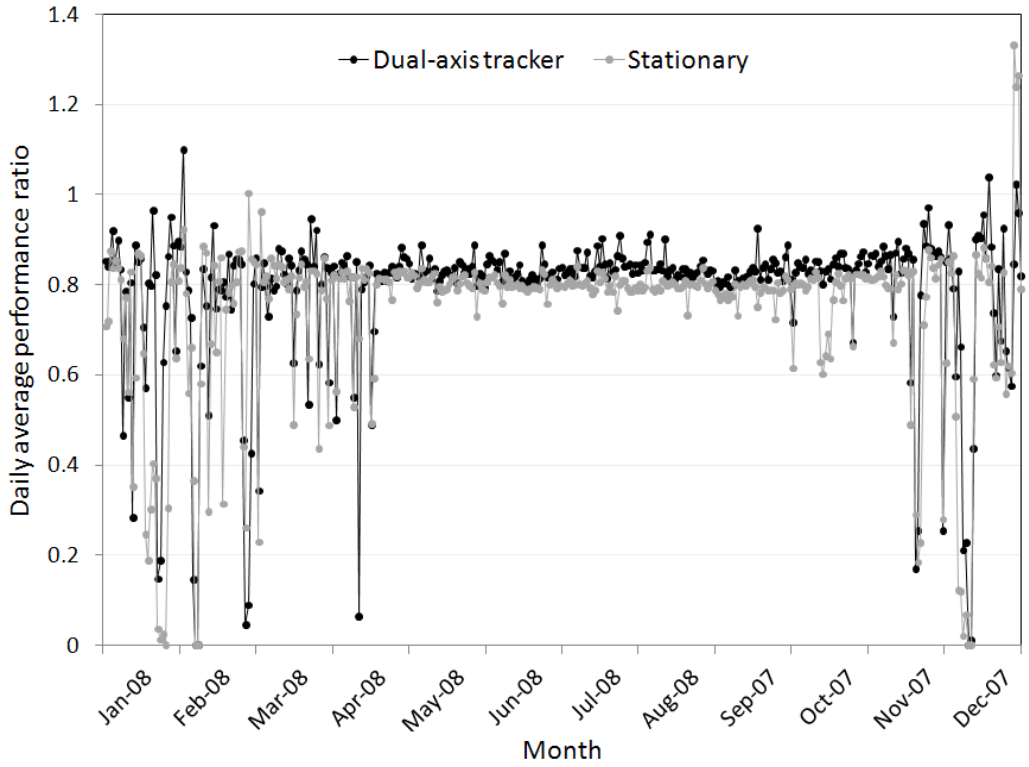

Figure 4.8. Stationary and tracking daily Performance Ratios

Daily PR values during the winter months were found to be vary sporadic for both systems; the days yielding irregular PR values coincided with times the array and/or pyranometer was fully or partially covered with snow. Snow cover was found to degrade performance for the stationary system slightly more so than the tracking system. It was found that the snow melted and/or fell from the tracking system quicker than the stationary system. Snow cover also affected monthly PR values, however, to a lesser extent. Both systems showed slight seasonal variations in PR values due to losses in higher operating temperatures in the summer months when compared to lower operating temperatures in the winter months. The annual PR of the stationary and tracking system were calculated to be 0.792 and

0.819, respectively. The tracking system was found to operate closer to rated capacity more often on average. On the whole, the tracking system was found to consistently operate at slightly higher PR values.

Table 4.7. Monthly performance ratio

Month	Stationary average PR	Dual-axis tracker average PR
Jan-08	0.629	0.764
Feb-08	0.786	0.744
Mar-08	0.805	0.799
April-08	0.814	0.819
May-08	0.806	0.827
June-08	0.800	0.822
July-08	0.800	0.839
Aug-08	0.800	0.834
Sep-07	0.790	0.820
Oct-07	0.804	0.838
Nov-07	0.810	0.866
Dec-07	0.796	0.807
Annual	0.792	0.819

SUMMARY

The main objective of this paper was to directly compare the experimental performance of a stationary (oriented for maximum annual energy generation) and a dual-axis tracking system operating in the Upper Midwest, highlighting the differences resulting from the use of different mounting schemes. Experimental performance was compared between systems for measures of solar resource, energy generation, power production, operating temperature, and efficiency.

The tracking system collected approximately 36 percent more solar energy than the stationary system throughout the year. The annual average daily solar insolation seen by the stationary and tracking systems were found to be 4.37 and 5.95 kWh/m^2, respectively. In terms of energy generation, the tracking system outperformed the stationary system on daily, monthly, and annual bases. Annually, the tracking system generated 41 percent more AC electrical energy than the stationary system per kWp of installed capacity; normalized annual energy generation for the tracking and stationary systems were found to be 1,779 and 1,264 kWh/kWp, respectively. Seasonally, the tracking system showed the most benefit in comparison to the stationary system during summer and winter months. The benefit of the tracking system in the summer and winter months is due in part to the orientation of the stationary array – oriented for maximum *annual* energy production. In the summer months during times of high

solar irradiance levels the stationary system is oriented with less slope than optimal, and conversely in the winter months. Additionally, the tracking system was found to "shed" snow quicker than that of the stationary system making it less sensitive to the negative effects of snow cover on performance. Moreover, benefits of the tracking system in terms of energy generation and power production were realized primarily during sunny conditions given that the response of PV modules to diffuse solar irradiance is largely independent of module orientation [56]. The annual average conversion efficiencies of the tracking and stationary systems were found to be 11 and 10.7 percent, respectively. Annual performance ratio values of the tracking and stationary system were found to be 0.819 and 0.792, respectively. Snow cover and operating temperature were found to affect performance of both systems.

An interactive online interface was developed to simultaneously display and compare real-time and historical performance data of both systems side-by-side. Real-time performance and meteorological data presented in the interface include: solar irradiance, power production, conversion efficiency, average array temperature, ambient air temperature, and wind speed and direction. Historical data on daily, weekly, monthly, and annual bases include: solar irradiance, power production, and energy generation. The interface has the ability to display normalized (per kW_p) and actual data. Additionally, webcams were installed at each site to show real-time and historical streaming video and photographs that can be compared to the data presented in the interface. The interface, webcam, and additional general project information can be found online through the Iowa Energy Center's website at [68].

ACKNOWLEDGEMENTS

The authors would like to thank the Iowa Energy Center for providing personnel, administrative, and financial support for this project.

CHAPTER 5 - ECONOMIC ANALYSES OF STATIONARY AND DUAL-AXIS TRACKING GRID-CONNECTED PHOTOVOLTAIC SYSTEMS IN THE UPPER MIDWEST

A paper in preparation for submission to *American Society of Mechanical Engineers – Journal of Solar Energy Engineering*

Ryan Warren, Michael Pate, Ron Nelson

ABSTRACT

Two grid-connected photovoltaic (PV) systems comprised of multicrystalline silicon (mc-Si) modules with different mounting schemes were installed in central Iowa and monitored for one year; one roof-mounted stationary system and one pole-mounted dual-axis tracking system. These systems serve as real-world applications of PV for building energy generation. Both systems are equipped with extensive data acquisition capable of collecting performance and meteorological data. The experimental performance and economic analysis of the systems are presented in a five-part series of papers. This paper presents an economic analysis of both systems in terms of life-cycle costs, payback period, internal rate of return, and the incremental cost of solar energy. Both systems use similar equipment and operate under net metering agreements with a local utility. All initial costs were documented and first-year performance and energy savings were experimentally found using data collected from September 2007 through August 2008. Future PV performance, energy savings, and operating and maintenance costs were then estimated over an assumed life of twenty-five years. Under the given assumptions and discount rates, the life-cycle savings of both systems were found to be negative. Further, neither system was found to have payback periods less than the assumed system life. The lifetime average incremental costs of solar energy generated by the stationary and dual-axis tracking systems were estimated to be $0.31 and $0.37 per kWh generated, respectively. Rates of return on investments in the stationary and dual-axis tracking system are projected to be -3.3 and -4.9 percent, respectively. Finally, potential economic feasibility of grid-connected stationary PV systems used for building energy generation and operating in the Upper Midwest was assessed using assumptions of varying utility energy costs, initial installed costs, and metering agreements. Economic analyses were performed for a PV system under different scenarios, each having a unique set of assumptions for costs and metering. Results show a potential for economic feasibility under certain conditions when compared to alternative investments with assumed yields.

INTRODUCTION

Two grid-connected PV systems with different mounting schemes were installed in central Iowa, USA; one roof-mounted stationary system and one pole-mounted dual-axis tracking system. Both systems were designed as "turn-key" installations for building energy generation applications. The orientation of the stationary system was selected to optimize for annual energy generation. All PV and Balance-Of-System (BOS) equipment used in the installations are "off-the-shelf" components and considered standard for residential and commercial applications. For example, flat-plate PV modules made of silicon nitride multicrystalline silicon cells were used. The PV systems are equipped with extensive data acquisition (DAQ) systems capable of collecting accurate performance and meteorological data.

The experimental performance and economics of both systems have been analyzed in detail based on experimental data taken over one full year and are presented in a five-part series of papers. The performance analysis of the systems primarily focuses on measures of power production, energy generation, and efficiency. Results are shown on instantaneous, daily, monthly, and annual bases. Two papers of the five-part series presented performance results for the stationary system and dual-axis tracking system, respectively [63, 64]. A third paper presented a comparison of normalized measures between the two systems by highlighting the performance differences due to the different mounting schemes [65]. This paper presents a detailed economic analysis comparing life-cycle costs (LCC), payback period, internal rate of return (IRR), and average costs of energy generated by the PV systems. Additionally, potential economic feasibility of grid-connected PV systems in the Upper Midwest was assessed assuming varying levels of incremental energy costs, installed costs, and metering agreements. An economic analysis was performed for a PV system under different scenarios; each scenario having a unique set of assumptions for costs and metering. The final study investigates heat transfer characteristics of the stationary and tracking arrays and quantifies the affects of operating temperature on PV system performance [67]. Further, simulations were performed to estimate how each system might perform while operating at lower temperatures. Metrics used to assess heat transfer characteristics and affects of operating temperature on PV system performance include overall heat transfer coefficients and the temperature coefficient for power.

One of the most important issues surrounding the application of PV for building energy generation is that of economic feasibility. The economics of PV systems can be estimated in terms of many different measures. However, the basic economic premise for an investment in PV is comparing a known initial investment and estimated future operating/maintenance expenses with projected future savings in

energy costs generated by the system [57]. The economics of a grid-connected PV system can vary significantly depending on the solar resource, site, performance of the system, interconnection agreement type, operation and maintenance costs, financial incentives, costs of energy, and initial equipment and installation costs of the system.

Economic results of this study for both the stationary and tracking systems include LCC, payback period, IRR, and average incremental cost of solar energy. Each economic parameter presented within this study allows for comparisons to be made to other investments or alternative sources of energy and can offer insight to the attractiveness of an investment in PV. A LCC analysis is a method of analyzing the initial and future annual expenses and savings associated with a system over the life of the equipment; this method normalizes the annual cash flow to an overall net present value (NPV) assuming a particular discount rate [73]. The life-cycle cost can be defined as "the total discounted dollar cost of owning, operating, maintaining, and disposing of a system" over a given period of time [74]. Payback period can be useful for assessing the amount of time required for the PV system to pay itself back or "break-even." Estimating the economic internal rate of return on an investment in a PV system allows for a direct comparison to other types of financial investments with associated expectations of return. Finally, approximating the cost of energy generated by a PV system over its assumed life is useful for comparing options of other alternative sources of energy such as energy supplied by a local utility.

EXPERIMENTAL TEST SYSTEMS

The stationary system is located in Ames, Iowa, at a latitude of 42 degrees 2 minutes north and a longitude of 93 degrees 48 minutes west. The system has a total installed capacity of 4.59 kW_p and total PV array area of 34.02 m^2 (366.2 ft^2). This system is designed as three side-by-side, identical, and independently operating sub-systems. Each subsystem consists of nine, 170 Watt modules operated at their peak power point and wired in series to a single inverter; all three inverters are identical. All modules are attached directly to a south-facing standing-seam white metal roof at a slope of 36 degrees (oriented for maximum annual energy generation). A complete description of the stationary system can be found in [63].

The tracking system is located in Nevada, Iowa, 42 degrees 2 minutes north latitude and 93 degrees 27 minutes west longitude and was approximately 9 miles from the stationary system. The system has an installed capacity of 1.02 kW_p and total PV array area of 7.56 m^2 (81.38 ft^2). This system uses six, 170 Watt modules wired in series to a single inverter and operated at their peak power point. The pole-mounted array follows the sun throughout the day using an actively controlled dual-axis, azimuth drive

solar tracker. The azimuth range of the tracker is 270 degrees. The tracker is controlled using an electronic transducer that is mounted on top of the array. The transducer has sensors on all sides and adjusts position until an equal amount of sun is sensed on all sides of the transducer. A complete description of the tracking system can be found in [64].

Both PV systems are equipped with extensive data acquisition systems (DAQ). Each DAQ is capable of collecting accurate data at a high sampling rate, archiving data in a central repository, and visually displaying real-time and historical data of both systems simultaneously through an online interactive interface. The online interface can be publically accessed at [68]. All data is measured at ten second intervals, and stored as one-minute averages. To adequately characterize the first year performance of the PV systems, both operating parameters of the array and meteorological conditions were monitored. A complete description of the data acquisition system and instrumentation can be found in [63, 64].

ANALYSIS

An economic analysis is presented for both systems. The analysis focuses on measures of LCC, payback period, IRR, and average incremental cost of solar energy. For the LCC analysis, three discount rates are assumed; the first representing general inflation, the second essentially representing a risk-free investment and the last indicative of long-term liquidity and risk one may be subjected to in competitive market conditions. These specific discount factors will allow the systems to be compared to a wide-range of alternative investment risk levels and also compared to each other directly. The LCC analysis is performed over an assumed useful system life period of twenty-five years. Payback period is defined as the number of years that it takes for the accumulated annual savings to equal to or become greater than the accumulated annual expenses of the system. Internal rate of return estimated in this research is defined as the discount rate at which the NPV of the investment in PV over the assumed life of the system is zero. The average incremental cost of solar energy generated by the systems were also estimated considering all expenses related to the PV systems and estimated lifetime energy generation. Finally, the potential economic feasibility of the systems was assessed assuming more favorable economic conditions in that the incremental energy cost of utility supplied energy was varied and initial rebates and feed-in tariffs were considered.

All initial and future expenses and revenues were quantified including: initial costs, operating and maintenance costs, energy savings, and end-of-life salvage value. However, the costs of the DAQ system and other expenses considered “non-typical” for residential and commercial applications were omitted from the analysis. Initial costs and first-year energy savings for stationary and dual-axis tracking systems

were attained experimentally with the results of the experimental performance analysis being presented in detail in [63-65]. All future expenses and revenues for both PV systems were estimated over their assumed useful life on an annual basis. Incentives applicable to this project include sales tax exemption and net-metering. The economic analysis neglects all tax considerations; the PV systems evaluated in this research were not financed, and no initial or operating costs will be claimed as business expenses.

Incentives

Several financial incentives targeting the use of PV systems for energy generation are available in the Upper Midwest. Incentives are offered at federal, state, and local levels and may vary depending on the system location, type, size, and end-use sector (e.g., residential, commercial, industrial, agricultural, etc.). Incentives applicable to qualified PV systems in Iowa may include: property and sales tax exemption, accelerated depreciation tax deductions, production tax credits, low interest financing, rebates (in limited areas), net-metering, and the exclusion of subsidies provided by utilities from gross income [44]. However, given the specific arrangements and ownership of this project, only sales tax exemption and net-metering were applicable.

Electrical loads in buildings with grid-connected PV systems are met in one of three ways: (i) all of the load is met with utility supplied power (e.g., during non-sunlight periods), (ii) a portion of the load is met with utility supplied power and a portion of the load is met with power produced by the PV system (e.g., when building load is greater than power output of PV system), (iii) or all of the load is met with power produced by the PV system (e.g., when the load of the building is either equal to or less than the output power of the PV system). When the PV system is generating more power than is demanded by the building, the excess power is fed into the utility grid. The excess quantity of energy fed back into the grid is then accounted for by either measuring it directly (using a second meter) or crediting it in terms of net energy usage at the site (using one meter with the ability to turn backwards), depending on the specific grid-connect agreement with the local utility.

Quantifying the excess energy generated in terms of net energy usage is known as “net metering” (also known as net billing). The net energy is typically measured using an electric meter that has the ability to run backwards during periods where the renewable energy system is generating more power than what is demanded onsite. In a net metering agreement, the utility credits the accumulated excess energy to the consumer for later use to offset future electrical energy consumption. The credited excess electrical energy is credited to the consumer at retail prices. However, not all states and utilities offer net

metering agreements to consumers. As of August 2008, 42 states including the District of Columbia have adopted net metering for renewable energy systems. Net metering programs offered in the U.S. vary considerably [34]; specific restrictions and rules for net metering agreements by state are well documented [35].

Some utilities are opposed to net metering due to potential negative financial impacts [36]. Yet, under federal law, if net metering is not offered, utilities are obligated to allow independent power producers to interconnect with the grid and purchase excess generated energy [36]. However, excess energy may only be purchased by the utility at their wholesale cost of electricity, which may be significantly less than the retail rate imposed to the customer [37]. Under this type of agreement, excess energy is typically quantified using a second meter to monitor only energy fed into the grid.

Costs

Expenses considered in this analysis include initial and future estimated annual operating and maintenance costs of the PV system only. All costs associated with data acquisition hardware, instrumentation, and software were omitted to attain results that would be applicable to typical residential and commercial systems in the Upper Midwest.

Initial Costs

Initial costs of typical grid-connected PV systems consist of equipment, installation, and interconnection fees; additional expenses can include system design, site preparation, and engineering work. The initial costs of the systems used in this study varied significantly. Differences in cost were attributed to hardware, installation labor, and engineering fees. Mounting hardware required for the stationary system consisted of mounting clamps to attach the modules directly to the existing roof structure. The tracking system required a concrete foundation, pole, aluminum support frame for the modules, gear drive assembly, and controller. A structural analysis was performed for the stationary system to verify the roof strength and mounting hardware was adequate to support static and wind loading of the array; whereas the tracking system required the design of a concrete foundation. Labor costs were also different. Installation costs of the tracking system were twice that of the stationary system on a peak watt (W_p) basis. Additionally, the tracking system required the installation of the foundation and trenching for electrical wiring from the system to the building. Initial costs of the stationary and dual-axis tracking systems were \$41,218 and \$16,147 (\$8.98 and \$15.83 \$/W_p), respectively. Breakdowns of the initial expenses for both systems are documented in Table 5.1.

Table 5.1. Initial costs for stationary and dual-axis tracking PV systems

Initial PV expenses	Stationary system costs ($)	Dual-axis tracking system costs ($)
Utility interconnection fee	**$125**	**$125**
Engineering	**$1,285**	**$800**
Equipment / labor	**$39,808**	**$15,222**
PV modules	*$28,282*	*$6,882*
Inverters	*$7,089*	*$1,538*
Mounting hardware (Stationary – mounting clips Tracker – frame, gear-drive, and controller)	*$1,200*	*$2,448*
Misc. (wiring, fuses, conduit, etc.)	*$1,237*	*$750*
PV installation labor	*$2,000*	*$900*
Concrete foundation/trenching/pole materials/labor	-	*$2,704*
Total cost	**$41,218**	**$16,147**
Normalized total cost ($/$W_p$)	**$8.98**	**$15.83**

Operation and Maintenance Costs

Operation and maintenance costs for typical grid-connected PV systems (without battery backup) are minimal. Maintenance tasks may include visually inspecting and cleaning the array annually, checking fastening hardware and wiring to ensure tightness every few years, verifying that sealants around building penetrations and outdoor electrical boxes are intact, and performing periodic checks of energy yield and power output [75]. Often, maintenance requirements for PV systems are preventative in nature and can be performed by the owner. For this research it was assumed that annual operating and maintenance costs were equal to 0.1 percent of the initial installed costs of the systems.

A common expense that is often neglected with PV systems (or in PV system economic analysis) is the potential future replacement cost of the inverter(s). Studies have shown that inverters may fail requiring replacement every five to ten years [43]. Thus, a new inverter may be required two to five times over the life of a PV system (assuming a twenty-five year system life). Furthermore, major inverter manufacturers do not foresee increasing inverter lifetime to twenty years as a practical goal [43]. The current cost of an inverter in the one to three kilowatt range is approximately 1 $/Watt [43]. Cost predictions for similar sized inverters in 2020 are 0.58 $/Watt [43]. Inverter prices are predicted to decrease by approximately thirty-five percent in ten years and fifty percent in twenty years [43]. For this research it was assumed that inverter replacement would be required every ten years. Future inverter costs were assumed to be consistent with the mentioned projections. Labor costs for the installation of the inverters were assumed to be 30 percent of the equipment costs.

Revenues/Savings

Revenues generated from the grid-connected PV systems came from two sources: savings incurred by offsetting electrical energy otherwise purchased from a local utility, and assumed life-end salvage value. No rebates or other financial incentives were applicable to this project at the time of purchase. Additionally, neither system generated a surplus of energy over the year that could potentially be sold to the local utility. First-year energy savings as well as future estimated energy savings are presented. Predictions of future performance of both systems were based on experimental performance data in the first year and typical levels of solar insolation experience at each site.

First-year experimental energy generation and savings

The experimental AC electrical energy generation of the stationary and dual-axis tracking systems is shown in Table 5.2.

Table 5.2. Experimental monthly and annual AC electrical energy generation

Month	Stationary system AC energy generation (kWh)	Dual-axis tracking system AC energy generation (kWh)
Jan-08	267.5	102.1
Feb-08	326.5	96.7
Mar-08	501.0	143.8
Apr-08	496.5	144.1
May-08	610.7	189.0
Jun-08	603.2	198.2
Jul-08	631.5	204.9
Aug-08	670.7	219.1
Sep-07	610.9	183.5
Oct-07	445.8	136.3
Nov-07	397.5	124.9
Dec-07	239.1	72.5
Annual	5800.8	1815.0

In the first year of operation the PV systems reduced building energy costs by offsetting electrical energy that would have otherwise been purchased from the utility. First-year monthly and annual energy savings for both systems were quantified. The energy savings yielded by each system was determined as the product of monthly AC energy generation and monthly incremental rate of electricity for each respective site. The incremental rate of electricity is the cost of one additional unit of energy in kWh. Thus, this rate excludes all constant charges and charges not related to energy usage. The incremental cost of a kWh of AC electrical energy for the stationary and dual-axis tracking systems were found to be 0.1171 and 0.0976 $/kWh, respectively. Monthly utility electric costs and energy savings can be seen in Table 5.3.

Table 5.3. Monthly incremental electric costs and energy savings

Month	Stationary system		Dual-axis tracking system	
	Incremental electric costs ($/kWh)	Energy savings ($)	Incremental electric costs ($/kWh)	Energy savings ($)
Jan-08	$0.102	$27.24	$0.080	$8.18
Feb-08	$0.106	$34.58	$0.084	$8.14
Mar-08	$0.110	$55.26	$0.089	$12.73
Apr-08	$0.114	$56.66	$0.092	$13.32
May-08	$0.115	$70.49	$0.094	$17.71
Jun-08	$0.122	$73.88	$0.108	$21.39
Jul-08	$0.137	$86.44	$0.121	$24.72
Aug-08	$0.129	$86.43	$0.113	$24.70
Sep-07	$0.122	$74.50	$0.100	$18.37
Oct-07	$0.107	$47.73	$0.085	$11.63
Nov-07	$0.105	$41.58	$0.083	$10.35
Dec-07	$0.102	$24.37	$0.080	$5.82
Annual	$0.1171	$679.16	$0.0976	$177.05

The first-year energy savings for the stationary and tracking systems were found to be $679 and $177 (148 and 174 $/ kW_p), respectively.

Future estimated energy generation and savings

To approximate future energy savings of each system, the future energy generation of both PV systems was first estimated. Future energy generation for each system was estimated based on first-year performance. However, first-year solar insolation received by both systems was found to be less than the expected solar insolation based on 30-year averages. Additionally, crystalline silicon PV modules have been shown to degrade in performance due to age over their useful life. Therefore, future energy generation of both systems are estimated using first-year energy generation normalized to solar insolation and then derated on an annual basis to account for performance degradation due to age.

Experimental AC electrical energy generation of the stationary and dual-axis tracking systems was found to be 5,801 and 1,815 kWh during the first year of operation, respectively. Further, the annual solar insolation seen by the stationary system was found to be 1,594 kWh/m^2, whereas the tracking system received 2,173 kWh/m^2. Thus, during the first year of operation, the stationary and tracking system generated an average of 3.637 and 0.836 kWh of AC electrical energy per kWh/m^2 of solar insolation, respectively. The 30-year average (from 1961-1990) annual solar insolation for Des Moines, Iowa for fixed tilt (slope of 36 degrees) and dual-axis tracking flat-plate collectors are 1,753 and 2,338 kWh/m^2 (uncertainty $\pm$9%), correspondingly [16]. Therefore, the annual energy generation of the stationary and

tracking systems before derating for performance degradation due to age are estimated to be 6,372 and 1,952 kWh/year of AC electrical energy, respectively.

Performance of a PV module degrades over time; as a result, annual energy generation will decrease correspondingly over the life of the system. Warranties offered by manufacturers typically allow for twenty percent output degradation over the module's twenty to twenty-five year warrantee life. Long-term performance and reliability studies of multicrystalline PV modules have shown degradation rates typically ranging from 0.5-0.7 percent per year [76, 77]. For this research, the future energy generation performance for both systems was assumed to degrade at 0.5 percent annually. Using the estimated annual AC electrical energy generated by both systems for average levels of solar insolation and the performance degradation factor of 0.5 percent per year, the annual energy generation for the stationary and tracking systems was estimated, shown in Table 5.4.

Table 5.4. Estimated energy generation for stationary and dual-axis tracking PV systems

End of period	End of year	Performance degradation factor	Stationary system annual AC energy production (kWh)	Dual-axis tracking system annual AC energy production (kWh)
1	2008	1.000	5,801	1,815
2	2009	0.995	6,340	1,942
3	2010	0.990	6,308	1,933
4	2011	0.985	6,277	1,923
5	2012	0.980	6,246	1,913
6	2013	0.975	6,214	1,904
7	2014	0.970	6,183	1,894
8	2015	0.966	6,152	1,885
9	2016	0.961	6,122	1,875
10	2017	0.956	6,091	1,866
11	2018	0.951	6,060	1,857
12	2019	0.946	6,030	1,847
13	2020	0.942	6,000	1,838
14	2021	0.937	5,970	1,829
15	2022	0.932	5,940	1,820
16	2023	0.928	5,910	1,811
17	2024	0.923	5,881	1,802
18	2025	0.918	5,852	1,793
19	2026	0.914	5,822	1,784
20	2027	0.909	5,793	1,775
21	2028	0.905	5,764	1,766
22	2029	0.900	5,735	1,757
23	2030	0.896	5,707	1,748
24	2031	0.891	5,678	1,739
25	2032	0.887	5,650	1,731

To estimate future energy savings, the predicted annual energy generation is multiplied by the forecasted retail incremental electricity rates. Future retail electricity rates were estimated by using energy price indices formulated by the National Institute of Standards and Technology (NIST) which are based on the Department of Energy (DOE) energy price projections [49]. Energy price indices are useful for estimating future operational energy costs (or savings) [49]. These Indices are estimated for the residential, commercial, and industrial sectors at various levels of assumed general price inflation rates that affect the purchasing power of the dollar. Energy price indices are shown in Table 5.5 and represent the multiplier used to estimate the cost of electricity for the commercial market for twenty-five years into the future at the general price inflation rate of four percent. For this study, the long-term average inflation rate of four percent was assumed. The average incremental retail rate of electricity for the stationary and dual-axis tracking PV systems were 0.1171 and 0.0976 $/kWh during the first year of operation, respectively. Using the corresponding price indices, the future retail electricity rates for both systems were estimated, shown in Table 5.5.

Table 5.5. Electricity projected fuel price indices [49] and incremental electric rates

End of period	End of year	Electric price indices	Incremental estimated future electric rates ($/kWh)	
			Stationary system	Dual-axis tracking system
1	2008	1	$0.117	$0.098
2	2009	1.07	$0.125	$0.104
3	2010	1.12	$0.131	$0.109
4	2011	1.15	$0.135	$0.112
5	2012	1.17	$0.137	$0.114
6	2013	1.19	$0.139	$0.116
7	2014	1.21	$0.142	$0.118
8	2015	1.25	$0.146	$0.122
9	2016	1.3	$0.152	$0.127
10	2017	1.35	$0.158	$0.132
11	2018	1.42	$0.166	$0.139
12	2019	1.48	$0.173	$0.144
13	2020	1.54	$0.180	$0.150
14	2021	1.59	$0.186	$0.155
15	2022	1.66	$0.194	$0.162
16	2023	1.73	$0.203	$0.169
17	2024	1.8	$0.211	$0.176
18	2025	1.87	$0.219	$0.182
19	2026	1.95	$0.228	$0.190
20	2027	2.02	$0.237	$0.197
21	2028	2.12	$0.248	$0.207
22	2029	2.21	$0.259	$0.216
23	2030	2.33	$0.273	$0.227
24	2031	2.42	$0.283	$0.236
25	2032	2.53	$0.296	$0.247

Using the forecasted retail electricity rates and energy generation by both systems, future energy savings for the stationary and tracking systems was estimated, shown in Table 5.6 and Table 5.7, respectively.

Salvage Value

The residual value of PV system components at the end of the expected service life is the salvage value. It is common practice to assign a salvage value of 20 percent of the initial cost for PV equipment that can be sold and relocated [78]. The initial costs of salvageable equipment for the stationary and tracking system were $31,825 and $10,100, respectively. Thus, the salvage value of the stationary system is estimated to be $6,365; whereas the salvage value of the dual-axis tracking system is approximated to be $2,020.

Life-Cycle Cost

Cash flow tables were constructed for the purpose of examining the economics of a PV system over its assumed life in terms of a LCC analysis. These cash flow tables display the costs, revenues, net cash flow, and the NPV revenues associated with the PV system investment on an annual basis. Annual net cash-flows are found as the difference between all annual expenses and revenues. All anticipated future operating expenses, energy savings, and net cash-flows are estimated in terms of future dollars. Subsequently, the net cash-flows are discounted to an annual present value in today's dollars by:

$$PV_n = \frac{A_n}{(1+i)^n} \tag{5.1}$$

where PV_n = present value of net cash flow at end of year n,

A_n = net cash flow at the end of year n,

i = assumed discount rate, and

n = year ($1 \leq n \leq 25$).

The discount rate represents the assumed yield on an alternative investment. For this analysis, three discount rates are assumed; the first representing general inflation, the second essentially representing a risk-free investment and the last indicative of long-term liquidity and risk one may be subjected to in competitive market conditions. The first discount factor was assumed to be equal to the 30 year average inflation rate (as of August 19, 2008) as defined by the consumer price index (CPI) at 3.78 percent [79]. The benchmark used for the risk-free investment is the yield of a 30 year treasury bill at

4.44 percent (as of August 19, 2008) [80]; the total annualized return of the S&P 500 index is used as a proxy for market investment returns at 10.74 percent (from 1975 to 2008).

The LCC is then found as the sum of the annual net cash flows in present value terms:

$$LCC = \sum_{n=0}^{n=25} PV(n) \tag{5.2}$$

Involved or complex project cash flows presented in terms of NPV permits simple comparisons between alternate investment options [81]. The cash flow tables for the stationary and dual-axis tracking systems are presented in Table 5.6 and Table 5.7, respectively.

Table 5.6. Stationary system cash flow table

End of period	End of year	Annual avoided cost/energy savings ($)	Annual O&M costs ($)	Initial cost and salvage value ($)	Net cash flow ($)	Present value ($) DR = 3.78%	Present value ($) DR=4.44%	Present value ($) DR=10.74%
1	2008	$679.16	$41.22	$41,218.20	($40,580.26)	($39,102.20)	($38,855.10)	($36,644.63)
2	2009	$794.26	$41.22	$0.00	$753.04	$699.19	$690.38	$614.06
3	2010	$827.22	$41.22	$0.00	$786.00	$703.21	$689.96	$578.78
4	2011	$845.13	$41.22	$0.00	$803.91	$693.03	$675.68	$534.55
5	2012	$855.53	$41.22	$0.00	$814.31	$676.43	$655.32	$488.95
6	2013	$865.80	$41.22	$0.00	$824.59	$660.02	$635.38	$447.10
7	2014	$875.95	$41.22	$0.00	$834.74	$643.80	$615.86	$408.71
8	2015	$900.39	$41.22	$0.00	$859.17	$638.51	$606.94	$379.88
9	2016	$931.72	$41.22	$0.00	$890.50	$637.69	$602.33	$355.54
10	2017	$962.72	$41.22	$0.00	$921.50	$635.86	$596.80	$332.24
11	2018	$1,007.57	$6,031.42	$0.00	($5,023.85)	($3,340.31)	($3,115.31)	($1,635.64)
12	2019	$1,044.90	$41.22	$0.00	$1,003.68	$643.03	$595.93	$295.08
13	2020	$1,081.82	$41.22	$0.00	$1,040.60	$642.40	$591.58	$276.26
14	2021	$1,111.36	$41.22	$0.00	$1,070.14	$636.58	$582.51	$256.55
15	2022	$1,154.49	$41.22	$0.00	$1,113.27	$638.11	$580.23	$241.01
16	2023	$1,197.15	$41.22	$0.00	$1,155.93	$638.43	$576.85	$225.98
17	2024	$1,239.36	$41.22	$0.00	$1,198.15	$637.64	$572.50	$211.51
18	2025	$1,281.12	$41.22	$0.00	$1,239.91	$635.83	$567.26	$197.65
19	2026	$1,329.25	$41.22	$0.00	$1,288.03	$636.45	$564.23	$185.41
20	2027	$1,370.08	$41.22	$0.00	$1,328.87	$632.71	$557.37	$172.74
21	2028	$1,430.72	$4,649.07	$0.00	($3,218.35)	($1,476.54)	($1,292.49)	($377.78)
22	2029	$1,484.00	$41.22	$0.00	$1,442.78	$637.82	$554.79	$152.93
23	2030	$1,556.76	$41.22	$0.00	$1,515.54	$645.58	$557.99	$145.07
24	2031	$1,608.81	$41.22	$0.00	$1,567.59	$643.43	$552.62	$135.49
25	2032	$1,673.52	$41.22	$6,365.00	$7,997.31	$3,163.02	$2,699.43	$624.21

The undiscounted loss of the stationary system over the assumed life is estimated to be $-18,370. The life-cycle cost of the stationary system at discount rates of 3.78, 4.44, and 10.74 percent were estimated as $-27,100, $-27,940, and $-31,400, respectively.

Table 5.7. Dual-axis tracking system cash flow table

End of period	End of year	Annual avoided cost/energy savings ($)	Annual O&M costs ($)	Initial cost and salvage value ($)	Net cash flow ($)	Present value ($) DR = 3.78%	Present value ($) DR=4.44%	Present value ($) DR=10.74%
1	2008	$177.06	$16.15	$16,146.60	($15,985.69)	($15,403.44)	($15,306.10)	($14,435.34)
2	2009	$202.73	$16.15	$0.00	$186.59	$173.24	$171.06	$152.15
3	2010	$211.14	$16.15	$0.00	$195.00	$174.46	$171.17	$143.59
4	2011	$215.72	$16.15	$0.00	$199.57	$172.04	$167.74	$132.70
5	2012	$218.37	$16.15	$0.00	$202.22	$167.98	$162.74	$121.43
6	2013	$220.99	$16.15	$0.00	$204.85	$163.96	$157.84	$111.07
7	2014	$223.58	$16.15	$0.00	$207.44	$159.99	$153.04	$101.57
8	2015	$229.82	$16.15	$0.00	$213.67	$158.80	$150.94	$94.47
9	2016	$237.82	$16.15	$0.00	$221.67	$158.74	$149.94	$88.50
10	2017	$245.73	$16.15	$0.00	$229.58	$158.42	$148.69	$82.77
11	2018	$257.18	$1,317.45	$0.00	($1,060.27)	($704.96)	($657.48)	($345.20)
12	2019	$266.70	$16.15	$0.00	$250.56	$160.53	$148.77	$73.66
13	2020	$276.13	$16.15	$0.00	$259.98	$160.50	$147.80	$69.02
14	2021	$283.67	$16.15	$0.00	$267.52	$159.14	$145.62	$64.14
15	2022	$294.68	$16.15	$0.00	$278.53	$159.65	$145.17	$60.30
16	2023	$305.57	$16.15	$0.00	$289.42	$159.85	$144.43	$56.58
17	2024	$316.34	$16.15	$0.00	$300.20	$159.76	$143.44	$52.99
18	2025	$327.00	$16.15	$0.00	$310.85	$159.41	$142.22	$49.55
19	2026	$339.29	$16.15	$0.00	$323.14	$159.67	$141.55	$46.52
20	2027	$349.71	$16.15	$0.00	$333.56	$158.82	$139.91	$43.36
21	2028	$365.18	$1,036.65	$0.00	($671.46)	($308.06)	($269.66)	($78.82)
22	2029	$378.78	$16.15	$0.00	$362.64	$160.31	$139.44	$38.44
23	2030	$397.35	$16.15	$0.00	$381.21	$162.39	$140.35	$36.49
24	2031	$410.64	$16.15	$0.00	$394.49	$161.92	$139.07	$34.10
25	2032	$427.16	$16.15	$2,020.00	$2,431.01	$961.49	$820.57	$189.75

The undiscounted loss of the tracking system over the assumed life is estimated to be $-9,670. The life-cycle cost of the tracking system at discount rates of 3.78, 4.44, and 10.74 percent were estimated as $-12,050, $-12,260, and $-13,020, respectively.

Neither system was found to be the most attractive investment when compared to the three alternatives. Thus, investments in either system would result in the loss of money and purchasing power.

Payback Period

For this research, the payback period is defined as the number of years that it takes for the accumulated annual savings to be equal to or become greater that the accumulated annual expenses of the system in present value dollars. In other words, the payback period can be defined as the "number of years required to recover the investment from discounted cash flows" [73]. Under the given assumptions and discount rates, neither system was found to have a payback period less than the assumed system life.

According to a survey administered by the Iowa Department of Natural Resources (DNR), respondents express that acceptable payback periods for renewable energy systems are six to ten years [50]. Given the comparatively inexpensive energy costs in the Upper Midwest, minimal financial incentives, and relatively high initial costs for solar PV systems, payback periods are typically found to be greater than the assumed life of the system. The payback period for a grid-connected PV system is most sensitive to: initial cost of the installed PV system, annual energy output of the system, local electric rate, and the type of interconnection agreement with the utility.

Rate of Return

Internal rate of return is defined as the discount rate at which the NPV of the investment in PV over the assumed life of the system is zero. This metric is a measure of the quality of an investment. Specific to this work, the IRR is the annualized effective compounded rate return earned (or lost) on an investment in a PV system used for building energy generation. The IRR can be found by finding the value of *i* that satisfies the following equation:

$$NPV = \sum_{n=0}^{n=25} \frac{A_n}{(1+i)^n} = 0 \tag{5.3}$$

Economic analysis of both systems yielded negative IRR values. The IRR found for the stationary and dual-axis tracking system were -3.3 and -4.9 percent, respectively.

Lifetime Average Cost of Energy

One metric commonly used to assess the economic feasibility of a renewable energy system is comparing the average lifetime incremental costs of energy generated by a PV system to the incremental costs of energy otherwise purchased from the local utility. The incremental costs of energy otherwise purchased by the utility can be estimated by:

$$C_{i,utility,lifetime} = \frac{\sum_{n=0}^{n=25}\left[\left(C_{i,utility}\right)_n (E)_n\right]}{\sum_{n=0}^{n=25}(E)_n} \tag{5.4}$$

where: $C_{i,utility,lifetime}$ = average incremental cost of energy otherwise purchased from utility over assumed system life,

$C_{i,utility,n}$ = average incremental cost of utility supplied energy during year *n*,

E_n = estimated energy that would otherwise be purchased from utility in year n,

The average incremental costs of energy supplied by the utility for the stationary and dual-axis tracking systems are estimated to be 0.19 and 0.16 $/ kWh over the life of the systems, respectively.

The incremental cost of energy supplied by the PV system can then be estimated as:

$$C_{i,solar,lifetime} = \frac{\sum_{n=0}^{n=25}\left[(C_{i,utility})_n (E_{PV})_n\right] - (SV)_{n=25}}{\sum_{n=0}^{n=25}(E_{PV})_n} \quad (5.5)$$

where: $C_{i,solar,lifetime}$ = average incremental cost of PV generated energy over assumed system life,

$C_{i,utility,n}$ = average incremental cost of utility supplied energy during year *n*,

$E_{PV,n}$ = estimated energy generated by PV system in year n, and

SV = salvage value of PV equipment at the end of useful life.

The average incremental costs of energy supplied by the stationary and dual-axis tracking PV systems are estimated to be 0.31 and 0.37 $/kWh over the life of the systems, respectively. Therefore, over the life of the systems, energy generated by the stationary and dual-axis tracking systems will cost a premium of 0.11 and 0.21 $/ kWh relative to utility supplied energy, correspondingly.

Potential Economics of PV Systems in the Upper Midwest

Results of this study demonstrate that grid-connected PV systems used for building energy generation in the Upper Midwest are not yet economically feasible compared to a range of alternative investment options, or competitive with conventional sources of energy. Main contributors to the economic results are relatively high initial costs of PV systems, relatively low incremental costs of utility supplied electricity, and the lack of significant financial incentives supporting implementation and operation of PV. Unfavorable economics are one of the primary reasons the use of PV is not widespread in the Upper Midwest.

The use of PV for building energy generation is more prominent in locations having more favorable incentive programs and/or higher energy costs. Incentive programs supporting the installation and/or implementation of qualified PV systems may include: initial cost incentives such as rebates; tax incentives such as sales tax exemption, personal or corporate tax credits, or property tax exemption; low

interest loans; production incentives such as feed-in tariffs; metering agreements with the local utility; among others. The specific incentives that apply to each project are often typically dependent upon the location of the system, local utility, system size and type, end-use sector, date of which the system is put into operation, etc.

To assess the potential economic feasibility of PV in the Upper Midwest, economic analyses were performed for a 1 kW_p grid-connected stationary PV system operating in Iowa under assumptions of various incremental energy costs, initial installed PV system costs, and metering agreements with or without feed-in tariffs. Economic analyses were performed for twelve different scenarios, shown in Table 5.8. Results for each scenario include metrics of LCC, payback period, and IRR. The PV system was assumed to generate 1,388 kWh of usable AC electrical energy per year, which is representative of normalized (per kW_p) experimental performance of the stationary PV system analyzed in this study and average solar expected insolation [63]. Additionally, system performance was assumed to degrade by 0.5 percent per year over a system life of 25 years. Lastly, annual operating and maintenance costs were assumed to be 0.1% of initial costs in addition to two inverter replacements.

Incremental costs of electricity were assumed to be \$0.10, \$0.15, or \$0.20 per kWh of AC energy; these values represent an approximate range for the average retail price of electricity to the residential sector in the U.S. for June 2008 [53]. The incremental costs of electricity represent the savings per kWh of electrical energy generated by the PV system under a net metering agreement. The initial installed costs of the PV system were assumed to be \$9.00, \$7.00, or \$5.00 per peak watt. Nationally, the average installed cost of a grid-connected PV system in the U.S. is approximately \$9 per peak watt [40]. Installed costs less than \$9 per peak watt represent different levels of initial rebates potentially offered to the system owner. For example, an initial cost of \$7.00 per W_p would represent a \$2.00 per W_p rebate for a consumer that would otherwise pay \$9.00 per W_p. For the analysis, initial costs were assumed to be \$9.00, \$7.00, or \$5.00 per peak watt. Finally, the means in which the electrical energy generated by the PV system is metered and credited at the site was varied. The first metering agreement that was assumed is a net metering agreement. In this situation, the consumer is essentially credited the incremental retail rate of electrical energy by offsetting energy that would otherwise be purchased from the local utility. The second metering agreement assumes that all electrical energy generated by the PV system is fed directly into the grid and credited at a feed-in tariff rate of \$0.50 per kWh. This agreement represents a production or performance based incentive.

Table 5.8. Economic analysis scenarios

Scenario	Incremental cost of electricity ($/kWh)	Initial installed PV system cost ($/$W_p$)	Metering agreement	Feed-in tariff ($/kWh)
1	$0.10	$9.00	Net meting	-
2	$0.10	$7.00	Net meting	-
3	$0.10	$5.00	Net meting	-
4	$0.15	$9.00	Net meting	-
5	$0.15	$7.00	Net meting	-
6	$0.15	$5.00	Net meting	-
7	$0.20	$9.00	Net meting	-
8	$0.20	$7.00	Net meting	-
9	$0.20	$5.00	Net meting	-
10	-	$9.00	Direct feed	$0.50
11	-	$7.00	Direct feed	$0.50
12	-	$5.00	Direct feed	$0.50

Results for LCC, payback period, and IRR for each scenario are shown in Table 5.9.

Table 5.9. Economic results for scenarios

Scenario	Life-cycle cost, DR=3.78 ($)	Life-cycle cost, DR=4.44 ($)	Life-cycle cost, DR=10.74 ($)	Payback period (yrs.)	Internal rate of return (%)
1	($5,826.54)	($6,033.19)	($6,894.37)	> 25	-2.89%
2	($4,025.61)	($4,223.39)	($5,102.39)	> 25	-1.99%
3	($2,224.68)	($2,413.59)	($3,310.41)	> 25	-0.50%
4	($4,257.69)	($4,585.22)	($6,133.89)	> 25	-0.78%
5	($2,456.76)	($2,775.42)	($4,341.91)	25	0.52%
6	($655.83)	($965.62)	($2,549.93)	23	2.62%
7	($2,688.84)	($3,137.25)	($5,373.42)	25	1.05%
8	($887.91)	($1,327.45)	($3,581.44)	22	2.67%
9	$913.02	$482.35	($1,789.46)	17	5.29%
10	$1,036.01	$426.54	($2,915.19)	16	4.95%
11	$2,836.95	$2,236.34	($1,123.22)	13	7.87%
12	$4,637.88	$4,046.13	$668.76	8	13.17%

The analysis suggests that an investment in a grid-connected stationary PV system used for building energy generation and operating in the Upper Midwest could show economic feasibility for scenarios assuming relatively higher energy costs and lower installed costs, or under available production based incentives. Results indicate that payback periods may be attained within the assumed system life for scenarios five through twelve. However, attaining acceptable payback periods of six to ten years [50] may require low initial costs and direct feed metering with feed-in tariffs. Scenario nine shows a PV

investment may be competitive with an investment in treasury bills and maintain purchasing power relative to inflation; further, similar results are shown for scenarios ten through twelve assuming direct feed agreements.

SUMMARY

Two grid-connected PV systems with different mounting schemes were installed in central Iowa, USA; one roof-mounted stationary system and one pole-mounted dual-axis tracking system. Both systems were operated and monitored for one year. Economic analyses were performed for both systems focusing on measures of life-cycle cost, payback period, internal rate of return, and average incremental cost of solar energy. Initial costs and first-year energy savings for stationary and dual-axis tracking systems were attained experimentally. All future expenses and revenues for both PV systems were estimated over their assumed useful life on an annual basis. Incentives applicable to this project include sales tax exemption and net-metering. The economic analysis neglects all tax considerations; the PV systems evaluated in this research were not financed, and no initial or operating costs were claimed as business expenses. Additionally, the potential economic feasibility of grid-connected stationary PV systems used for building energy generation and operating in the Upper Midwest was assessed for assumptions of higher utility energy costs, lower initial installed costs, and metering agreements. Economic analyses were performed for a PV system under twelve different scenarios, each having a different set of assumptions for costs and metering. Metrics used in assessing economic feasibility included LCC, payback period, and IRR.

Initial costs of the stationary system totaled $41,218 ($8.98 per peak watt); whereas initial costs of the dual-axis tracking system was found to be $16,147 ($15.83 per peak watt). Experimental first-year energy savings for the stationary and dual-axis tracking systems totaled $679 and $177 ($148 and $174 per peak kW), respectively. The life-cycle cost of each system was calculated by using three different discount rates: the first representing general inflation, the second essentially representing a risk-free investment and the last indicative of long-term liquidity and risk one may be subjected to in competitive market conditions. However, the net present values of both systems under all assumed discount rates were determined to be negative. Further, neither system was found to have a payback period less than the assumed system life of 25 years. The annual rate of return of the stationary and tracking systems were found to be -3.3 and -4.9 percent, respectively. Furthermore, the average incremental cost of energy provided by the stationary system over its useful life is projected to be $0.31 per kWh, compared to an estimated average of $0.19 per kWh of electrical energy supplied by the utility. Approximated

incremental costs of solar energy provided by the dual-axis tracking system over its useful life is projected to be $0.37 per kWh, which is more than twice the cost of electrical energy provided by the utility at an estimated $0.16 per kWh.

Economic analyses performed under the various scenarios suggest that an investment in a grid-connected stationary PV system used for building energy generation and operating in the Upper Midwest could show economic feasibility for scenarios assuming relatively higher incremental energy costs and lower installed costs, or under a direct-feed metering agreement with production based incentives. Payback periods within the assumed system life and within a seven to ten year period are shown to be possible. Additionally, positive LCC and IRR results for certain scenarios indicate an investment in PV could potentially be competitive with other alternative investments with assumed yields. However, inherent risks associated with alternative investments should be considered when comparing IRR values.

Results of this study suggest that grid-connected PV systems used for building energy generation in the Upper Midwest are not yet economically feasible. However, they could be feasible under different economic scenarios. Poor economic results for the stationary and dual-axis tracking systems are primarily due to high initial costs of PV systems, relatively low incremental costs of utility supplied electrical energy, and insufficient financial incentives for the implementation and/or operation of PV systems. However, due to the volatile nature and unpredictability of future energy costs, actual economics of the systems may vary significantly from estimations presented here. Additionally, the performance and economics of grid-connected PV systems are very sensitive to the specific site and applicable circumstances (e.g., solar resource, incremental electric rates, available incentives, etc.); results presented here may not apply to other similar systems.

ACKNOWLEDGEMENTS

The authors would like to thank the Iowa Energy Center for providing personnel, administrative, and financial support for this project.

CHAPTER 6 - EXPERIMENTAL ASSESSMENT OF HEAT TRANSFER CHARACTERISTICS AND AFFECTS OF OPERATING TEMPERATURE FOR STATIONARY AND DUAL-AXIS TRACKING PHOTOVOLTAIC SYSTEMS IN THE UPPER MIDWEST

A paper in preparation for submission to *American Society of Mechanical Engineers – Journal of Solar Energy Engineering*

Ryan Warren, Michael Pate, Ron Nelson

ABSTRACT

Two grid-connected photovoltaic (PV) systems comprised of multicrystalline silicon (mc-Si) modules with different mounting schemes were installed in central Iowa and monitored for one year; one roof-mounted stationary system and one pole-mounted dual-axis tracking system. These systems serve as real-world applications of PV for building energy generation. Both systems are equipped with extensive data acquisition capable of collecting performance and meteorological data. Experimental performance and economic analyses of the systems were performed and the results are presented in a five-part series of studies. Experimental data was collected and analyzed for the systems over a one-year period from September 2007 through August 2008. This paper presents heat transfer characteristics of the stationary and tracking arrays and quantifies the affects of operating temperature on PV system performance. Further, simulations were performed to estimate how each system might perform while operating at lower temperatures.

Throughout the year of monitoring, array operating temperatures ranged from -24.7 ^{o}C (-12.4^{o}F) to 61.7 ^{o}C (143.1 ^{o}F) for the stationary system and -23.9 ^{o}C (-11 ^{o}F) to 52.7 ^{o}C (126.9 ^{o}F) for the dual-axis tracking system during periods of system operation. Average monthly and annual operating temperatures of the two systems were found to be within 2 ^{o}C (3.6^{o}F) of each other. On a daily basis, the stationary system ran up to 6.7 ^{o}C (12.1 ^{o}F) hotter than the tracking system; however, throughout the year, daily average operating temperatures averaged to be within 1 ^{o}C (1.8^{o}F) of each other. Additionally, the stationary system was found to operate at higher average array temperatures relative to ambient air temperatures at levels of solar irradiance greater than approximately 120 W/m^{2}.

The hourly average overall heat transfer coefficients considering data sampled for solar irradiance levels greater than 200 W/m^{2} for the stationary and dual-axis tracking systems were found to be 20.8 and 29.4 W/m^{2o}C, respectively. The experimental temperature coefficients for power at a solar irradiance level of

1,000 W/m^2 were -0.30 and -0.38 %/^{o}C for the stationary and dual-axis tracking systems, respectively, which are lower than the manufacture's specified value for the modules. Simulations of the stationary and dual-axis tracking systems suggest that annual conversion efficiency could potentially be increased by up to approximately 4.3 and 4.6 percent, respectively if they were operating at lower temperatures.

INTRODUCTION

During operation, photovoltaic (PV) systems accumulate unwanted heat from the surroundings and through the absorption of solar energy that is not converted to usable electricity. Consequently, the operating temperature of the array is increased which causes a degradation in system performance and shortens the usable life of the PV modules. The net amount of heat transferred to a PV array during operation and corresponding array temperatures are primarily functions of the type, orientation, and installation of the array and meteorological conditions under which the array operates. An understanding of the heat transfer characteristics of a PV array and the affects of operating temperature on a PV system during operation is important when considering different PV technologies, installation practices, and performance.

Two grid-connected PV systems with different mounting schemes were installed in central Iowa, USA; one roof-mounted stationary system and one pole-mounted dual-axis tracking system. Both systems were designed as turn-key installations for building energy generation applications. The orientation of the stationary system was selected to optimize for annual energy generation. All PV and Balance-Of-System (BOS) equipment used in the installations are off-the-shelf components and considered standard for residential and commercial applications. For example, flat-plate PV modules made of silicon nitride multicrystalline silicon (mc-Si) cells were used. The PV systems are equipped with extensive data acquisition (DAQ) systems capable of collecting accurate performance and meteorological data, and archiving data in a central repository.

The experimental performance and economics of both systems have been analyzed in detail based on experimental data taken over one full year and are presented in a five-part series of studies. The performance analysis of the systems primarily focuses on measures of power production, energy generation, and efficiency. Results are shown on instantaneous, daily, monthly, and annual bases. Two papers of the series present performance results for the stationary system and dual-axis tracking system, respectively [63, 64]. A third paper presents a comparison of normalized measures between the two systems by highlighting the performance differences due to the different mounting schemes [65]. The fourth paper presents an economic analysis of both systems by focusing on life-cycle-cost, payback

period, internal rate of return, and the incremental cost of solar energy [66]. This paper investigates heat transfer characteristics of the stationary and tracking arrays and quantifies the affects of operating temperature on PV system performance. Further, simulations were run to estimate how each system might perform while operating at lower temperatures. Metrics used to assess heat transfer characteristics and affects of operating temperature on PV system performance include overall heat transfer coefficients and the temperature coefficient for power.

EXPERIMENTAL TEST SYSTEMS

The stationary system is located in Ames, Iowa, at a latitude of 42 degrees 2 minutes north and a longitude of 93 degrees 48 minutes west. The system has a total installed capacity of 4.59 kW_p and total PV array area of 34.02 m^2 (366.2 ft^2). This system is designed as three side-by-side, identical, and independently operating sub-systems. Each subsystem consists of nine, 170 Watt modules operated at their peak power point and wired in series to a single inverter; all three inverters are identical. All modules are attached directly to a south-facing standing-seam white metal roof at a slope of 36 degrees (oriented for maximum annual energy generation). A complete description of the stationary system can be found in [63].

The tracking system is located in Nevada, Iowa, at a latitude of 42 degrees 1 minutes north and a longitude of 93 degrees 27 minutes west which is approximately 14 kilometers (8.7 miles) from the stationary system. The system has an installed capacity of 1.02 kW_p and total PV array area of 7.56 m^2 (81.38 ft^2). This system uses six, 170 Watt modules wired in series to a single inverter. The pole-mounted array follows the sun throughout the day using an actively controlled dual-axis, azimuth drive solar tracker. The azimuth range of the tracker is 270 degrees. The tracker is controlled using an electronic transducer that is mounted on top of the array. The transducer has sensors on all sides and adjusts position until an equal amount of sun is sensed on all sides. A complete description of the tracking system can be found in [64].

Both systems use the same PV modules made of silicon nitride multicrystalline silicon (mc-Si) cells. Electrical and mechanical specifications, including temperature coefficients, for these modules can be seen in Table 6.1.

Table 6.1. Electrical and mechanical characteristics of photovoltaic modules

Rated power	170 Watts
Voltage at rated power	35.4 VDC
Current at rated power	4.8 Amps
Short-circuit current	5.0 Amps
Open-circuit voltage	44.2 VDC
Temperature coefficient of short circuit current	$(0.065 \pm 0.015)\%/^{o}C$
Temperature coefficient of open circuit voltage	$-(160 \pm 20)$ mV/^{o}C
Temperature coefficient of power	$(0.5 \pm 0.05)\%/^{o}C$
NOCT (Air 20 ^{o}C; sun 0.8 kW/m^2, wind 1 m/s)	$47 \pm 2\ ^{o}C$ (116.6 $\pm$ 3.6 ^{o}F)
Size (length x width x depth)	1593 x 790 x 50 mm (62.8 x 31.1 x 1.97 in.)
Weight	15.0 kg (33.1 lb.)
Solar Cells	72 cells (125 mm x 125 mm) in a 6 x 12 matrix connected in series

The PV systems are equipped with extensive data acquisition systems (DAQ). Each DAQ is capable of collecting accurate data at a high sampling rate, and archiving data in a central repository. All data is measured at ten second intervals, and stored as one-minute averages. The specific performance parameters that were monitored include the following:

- DC voltage produced by the arrays of modules (measured at input of inverters)
- DC current produced by the arrays of modules (measured at input of inverters)
- AC voltage output by the inverters (measured at output of inverters)
- AC current output by the inverters (measured at output of inverters)
- Module temperatures

The meteorological parameters that were monitored include:

- Solar irradiance (measured at plane of array)
- Ambient air temperature (tracking system only)
- Wind speed (stationary system only)
- Wind direction (stationary system only)

The placement of each instrument and design of the data acquisition system can be seen in Figure 6.1.

Module temperatures were measured using flexible surface stick-on type three-wire 100 Ohm RTDs. These RTD's were affixed to the backside of six modules in the array. A small amount of foam insulation was applied to the back of each temperature sensor to reduce influences from the roof and outdoor air on the temperature measurement. All array temperature data presented in this research represent an average of all six module temperature measurements. The outdoor air temperature was measured

using a three-wire platinum 100 Ohm RTD (DIN B). The sensor is mounted vertically in a PVC weather resistant housing with a sun shield and open slots allowing air flow across the sensor. The ambient air temperature is measured in Nevada, Iowa (site of the dual-axis tracking system) which is located approximately 14 kilometers (8.7 miles) from the stationary PV system. The specified accuracy of the module and ambient air temperature sensors is $\pm$0.083 ^{o}C from 0-260 ^{o}C. A thermopile-type pyranometer was used to measure the solar irradiance incident upon the arrays and was mounted at an in-plane orientation for each array. These types of pyranometers are commonly used for establishing the solar resource for PV systems [69, 70]. This device measures irradiance over the entire solar spectrum (0.285 to 2.8 µm). All findings in this research for solar resource are presented in terms of the total solar resource measured by this pyranometer. Other specific details of the data acquisition system and instrumentation for both systems are given in [63, 64].

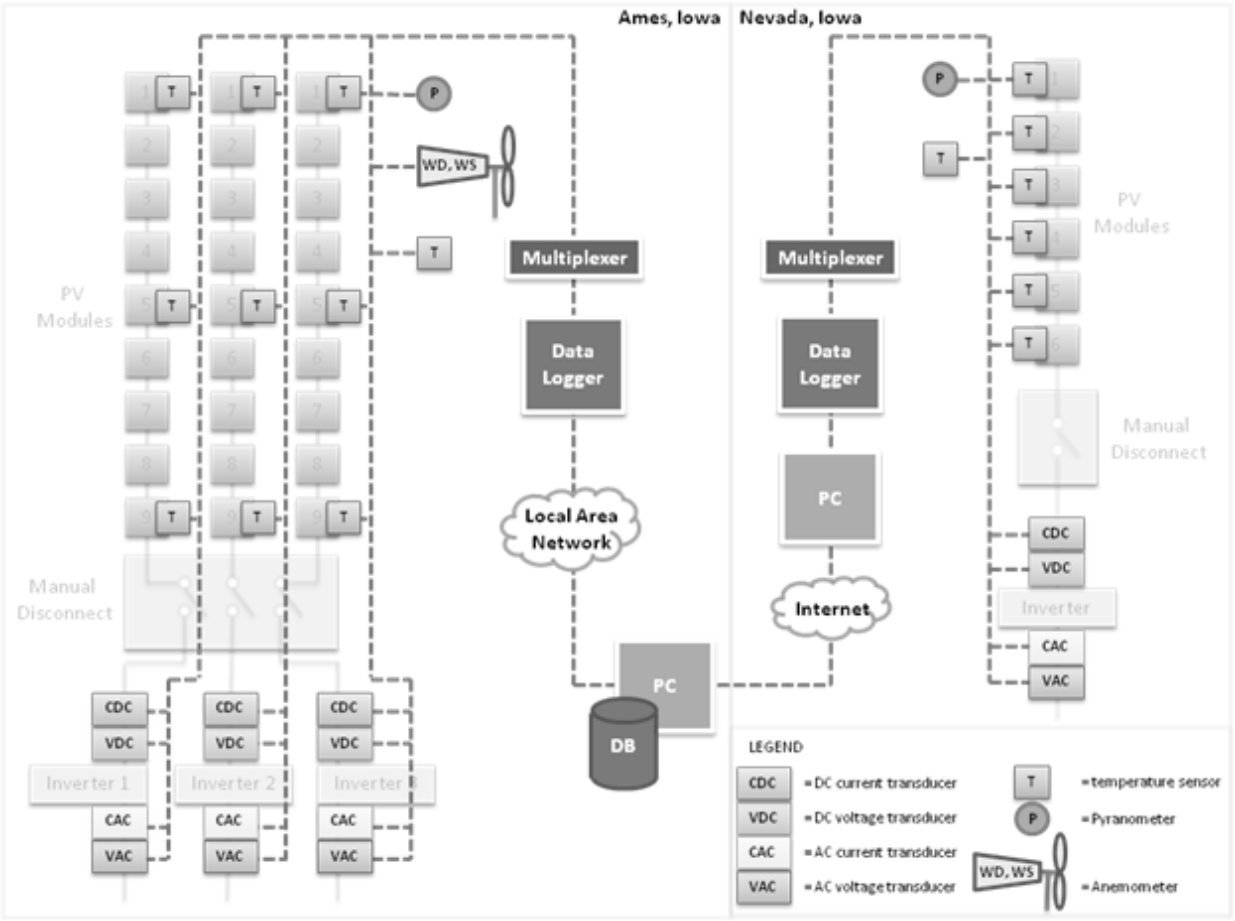

Figure 6.1. One-line diagram of data acquisition system

ANALYSIS

Experimental data was collected for each system for one full year with performance parameters and meteorological conditions being monitored from September 2007 through August 2008. Data was sampled at 10 second intervals and stored as one-minute averages. During the test period, the systems were allowed to operate as real-world systems; modules were never cleaned of snow or soiling and system operation was not purposely interrupted for any reason.

A detailed analysis of the heat transfer characteristics of the arrays and the affects of operating temperature on system performance is presented. Additionally, meteorological conditions experienced at the site and observed operating temperatures of both systems are shown in detail. Heat transfer characteristics of the arrays are quantified in terms of overall heat transfer coefficients while the affects of operating temperature on performance is assessed by examining temperature coefficients of power. Potential performance of stationary and dual-axis tracking PV systems in the Upper Midwest operating at cooler temperatures was estimated; this analysis was conducted using experimental temperature coefficients to adjust PV power output under simulations of the systems at lower temperatures. Monthly and annual energy generation and efficiencies were estimated for each simulation and compared to experimental data of actual performance to quantify potential performance benefits.

Meteorological Conditions

For this research, the in-plane solar resource available to each PV system was evaluated on monthly and annual bases. Monthly and annual solar resource is presented in terms of average daily solar insolation, shown in Table 6.2.

Table 6.2. Monthly and annual average daily solar insolation

Month	Stationary system	Dual-axis tracking system	Percent difference*
Jan-08	2.90	4.22	46
Feb-08	3.23	4.55	41
Mar-08	4.37	5.69	30
Apr-08	4.43	5.75	30
May-08	5.33	7.23	36
Jun-08	5.47	7.88	44
Jul-08	5.55	7.73	39
Aug-08	5.89	8.30	41
Sep-07	5.62	7.31	30
Oct-07	3.89	5.14	32
Nov-07	3.56	4.71	32
Dec-07	2.11	2.84	35
Annual	4.37	5.95	36

*percent difference calculated relative to stationary system

The annual average daily solar insolation seen by the stationary and dual-axis tracking systems was found to be 4.37 and 5.95 kWh/m^2, respectively.

Ambient air temperature and wind affects module/array operating temperatures, which in turn influences PV system performance. The hourly average ambient air temperature experienced during the monitoring period can be seen in Figure 6.2.

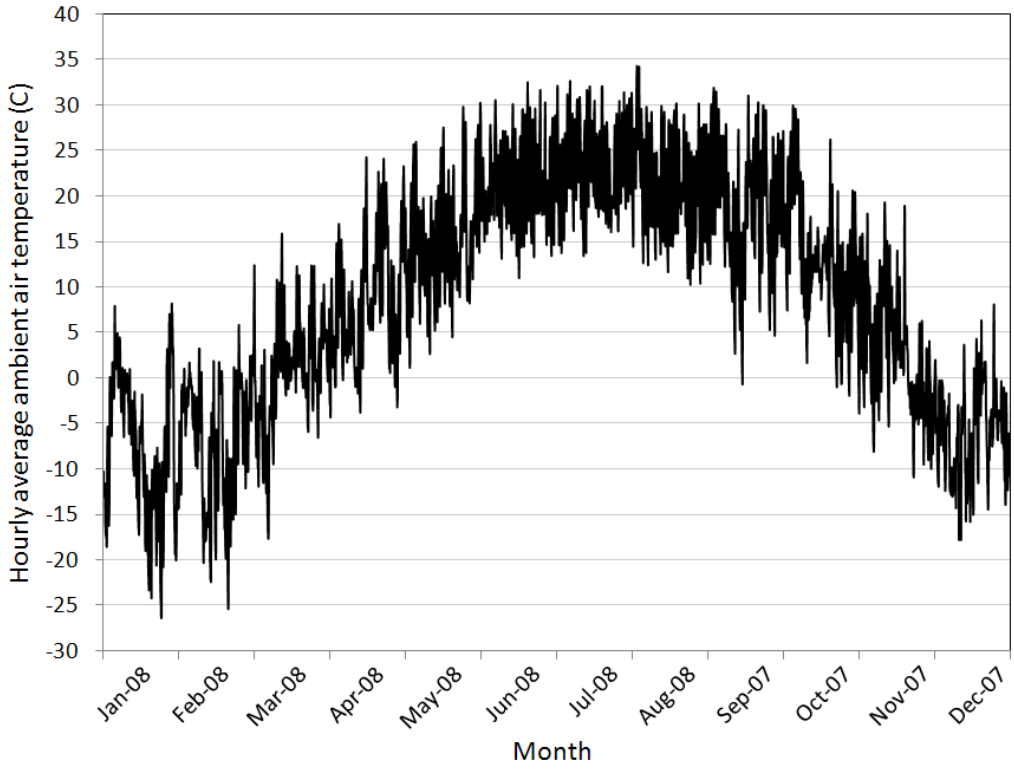

Figure 6.2. Hourly average ambient air temperature

The average monthly wind speed and prevailing direction (at a height of 10 meters) during the year of monitoring measured in Des Moines, Iowa (which is 56 kilometers (35 miles) from the site of the stationary system) is shown in Table 6.3.

Table 6.3. Average monthly wind speed

Month	Average wind speed at 10 meters, m/s (mph)
Jan-08	4.5 (10.0)
Feb-08	4.3 (9.7)
Mar-08	4.2 (9.5)
Apr-08	5.1 (11.3)
May-08	4..5 (10.1)
Jun-08	3.9 (8.8)
Jul-08	3.3 (7.3)
Aug-08	2.9 (6.4)
Sep-07	3.8 (8.6)
Oct-07	4.2 (9.4)
Nov-07	4.5 (10.1)
Dec-07	3.9 (8.6)

Source: National Weather Service Forecast Office [71]

Snow significantly affects PV system performance. Snow cover surrounding a PV array can increase the available solar energy incident upon the array via reflection. However, snow covering the array can degrade system performance considerably. Monthly snow fall measured in Des Moines, Iowa is documented in Table 6.4.

Table 6.4. Monthly snow fall

Month	Snow fall, cm. (in.)
Jan-08	28 (11)
Feb-08	57.7 (22.7)
Mar-08	12.2 (4.8)
Apr-08	2.8 (1.1)
May-08	0
Jun-08	0
Jul-08	0
Aug-08	0
Sep-07	0
Oct-07	0
Nov-07	12.2 (4.8)
Dec-07	35.8 (14.1)

Source: National Weather Service Forecast Office [71]

Experimental Operating Temperature

The operating temperature of a PV module/array affects several performance characteristics of a PV system; the parameters affected include: current, voltage, and thus, power production, energy generation, and conversion efficiency. The operating temperature of a PV module or array can be

influenced by ambient air temperature, wind speed and direction, solar irradiance characteristics, and installation.

The stationary system array is mounted directly to the roof structure and offset by approximately 7 cm (2.8 in) from the white metal standing-seam paneling. Thus, airflow across the backside of the array will typically be less than that of the topside and the temperature of the array is affected by roof conditions. The tracking system array is mounted on an open rack and exposed to ambient conditions on both sides. The open rack installation on the tracking system is more conducive to convective cooling affects from wind. Additionally, the tracking system is exposed to solar irradiance at lower angles of incidence, on average. Thus, generally, the tracking system will experience higher levels of incident solar energy. The average hourly array temperatures throughout the year of monitoring can be seen in Figure 6.3. Hourly temperatures are only presented for times during daylight periods.

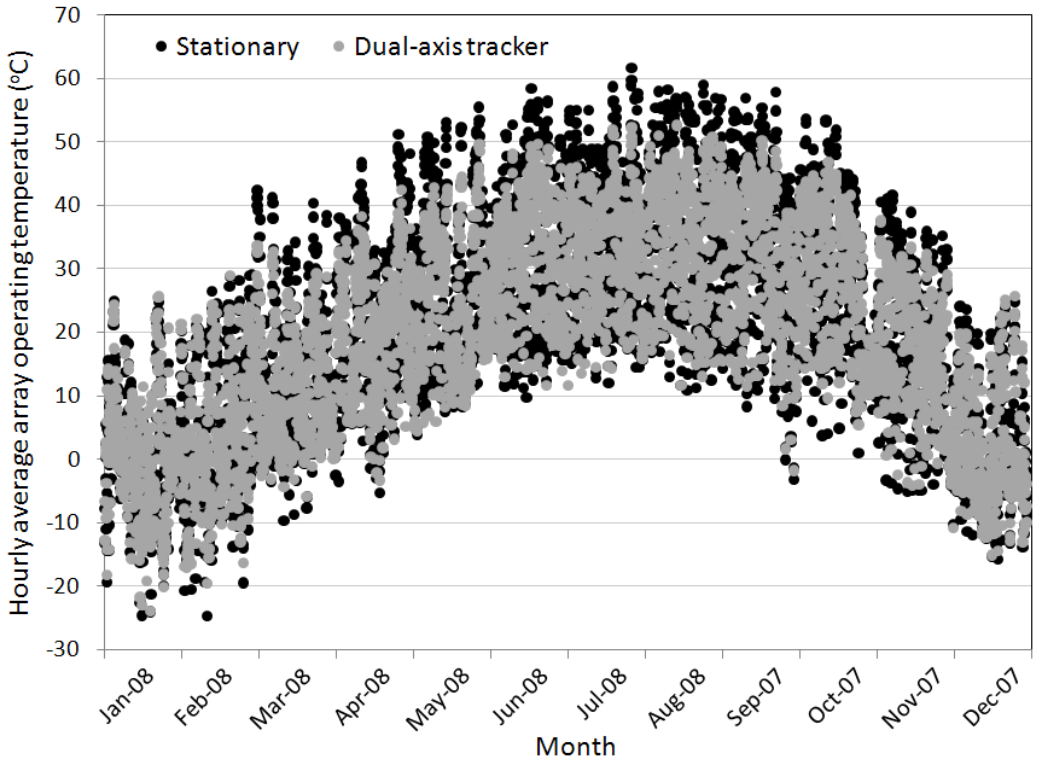

Figure 6.3. Hourly average array temperature for stationary and dual-axis tracking systems

Throughout the year of monitoring, module temperatures were observed to range from -24.7 °C (-12.4°F) to 61.7 °C (143.1 °F) for the stationary system and -23.9 °C (-11 °F) to 52.7 °C (126.9 °F) for the dual-axis tracking system. The stationary system was observed to have greater swings in hourly average

temperature than the tracking system. The discrepancies in average array temperatures between the systems are primarily attributed to differences in heat transfer rates from the array to the surrounding due to dissimilar approaches in installation.

Experimental array temperatures for both systems as well as average ambient air temperature in terms of monthly average temperatures are presented in Table 6.5.

Table 6.5. Average monthly array and ambient temperatures for daylight hours

Month	Stationary average array temperature, ^{o}C (^{o}F)	Tracking average array temperature, ^{o}C (^{o}F)	Average ambient air temperature, ^{o}C (^{o}F)
Jan-08	3.3 (37.9)	1.3 (34.3)	-6.2 (20.8)
Feb-08	2.7 (36.8)	2.1 (35.7)	-5.8 (21.6)
Mar-08	12.1 (53.7)	10.1 (50.2)	2.6 (36.7)
Apr-08	17.1 (62.7)	15.8 (60.4)	9.7 (49.4)
May-08	26.2 (79.2)	24.8 (76.6)	17.2 (62.9)
Jun-08	33.3 (92)	32.2 (90)	23.5 (74.3)
Jul-08	35.5 (96)	34.5 (94.2)	25.4 (77.7)
Aug-08	36.6 (97.9)	35.6 (96.1)	24.5 (76)
Sep-07	32.1 (89.7)	31.6 (88.9)	21.9 (71.4)
Oct-07	24.3 (75.8)	23.3 (73.9)	16.0 (60.7)
Nov-07	14.3 (57.7)	13.2 (55.8)	5.7 (42.2)
Dec-07	2.9 (37.2)	1.1 (33.9)	-4.3 (24.3)
Annual	22.6 (72.7)	20.8 (69.5)	12.7 (54.9)

The monthly and annual average array temperatures between systems were observed to be within two degrees Centigrade of each other.

Differences in heat gain for each array is compared by subtracting the hourly average ambient air temperature from the hourly average array temperature during periods of operation and plotting against hourly average solar irradiance for both systems, shown in Figure 6.4. This plot shows that the average hourly array temperature for the stationary system is hotter than the tracking system relative to ambient air temperature for solar irradiance levels ranging from approximately 120-1,200 W/m^2. It can also be seen that the difference becomes greater at higher solar irradiance values. Thus, the tracking system was observed to transfer heat from the system at a higher rate under similar solar irradiance levels. At the solar irradiance level of 1,000 W/m^2, the average array temperature of the stationary and tracking systems are 25.3 ^{o}C (45.5 ^{o}F) and 16 ^{o}C (28.8 ^{o}F) hotter than the ambient air temperature, respectively.

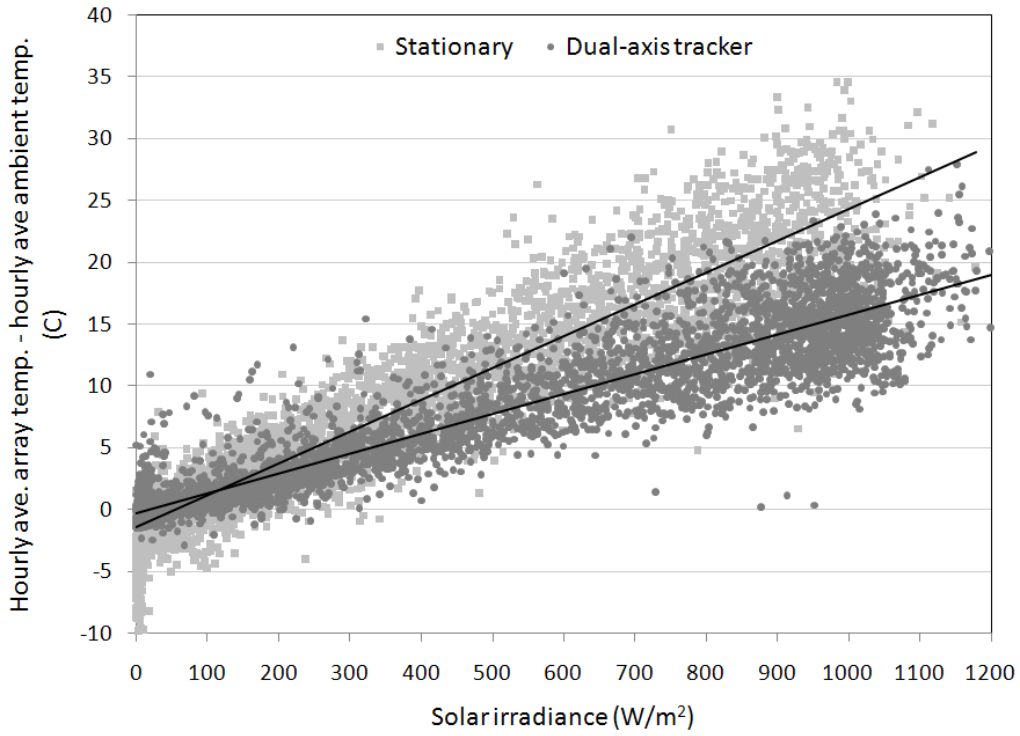

Figure 6.4. Array temperature less ambient air temperature for daylight hours vs. solar irradiance

A comparison for the fraction of time each system operated with various temperature ranges throughout the year was also made, seen in Figure 6.5.

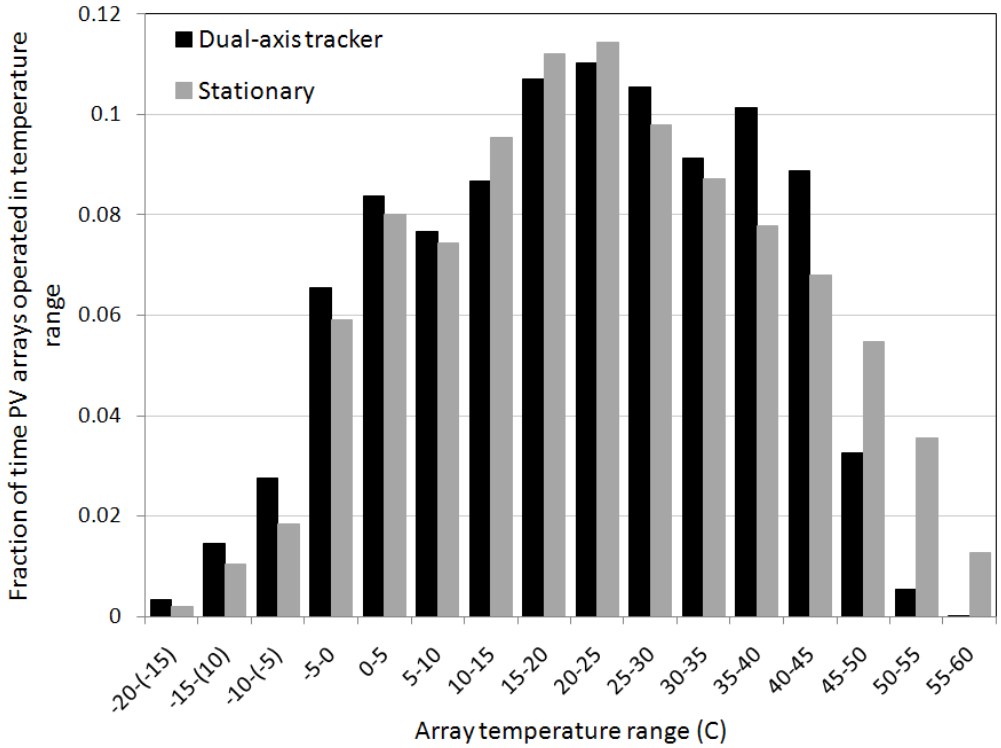

Figure 6.5. Array operating temperature frequency distributions

The frequency distributions of both systems yield similar trends; however, the stationary system was found to operate at higher temperatures more often when compared to the dual-axis tracking system.

Overall Heat Transfer Coefficient

Solar energy that strikes a PV module is either reflected off the surface or absorbed into the module and converted into electrical and thermal energy. The amount of energy converted to electrical energy can be relatively easily determined through power output measurements. Moreover, through the simultaneous measurement of solar insolation striking the module, conversion efficiency can be estimated. The remainder of the energy that is not reflected from the system or converted to usable electrical energy is converted into thermal energy and then cooled by losses to the surroundings. The rate at which the absorbed solar energy converted to thermal energy is transferred to the surroundings can be quantified in terms of an overall heat transfer coefficient.

Heat transfer from a module or array can occur via convection and radiation primarily from the top and bottom surfaces of the module or array and conduction through connection hardware to the supporting framework. The overall heat transfer coefficient of a PV array can be estimated by using an energy balance based on knowing the solar insolation striking the surface, PV array conversion efficiency, surrounding air temperature, and average operating temperature of the array. An energy balance per unit area of a module or array cooled by the surroundings can be expressed in terms of these components as [57]:

$$\tau\alpha G_T = \eta_c G_T + U_L(T_c - T_a) \tag{6.1}$$

where τ = Module cover transmittance

α = Fraction of absorbed solar radiation incident upon module surface

η_c = Module conversion efficiency (%/100)

G_T = Solar irradiance incident on array surface (W/m^2)

T_c = Module temperature (^{o}C)

T_a = Ambient air temperature (^{o}C)

U_L = Loss coefficient (W/m^{2o}C)

The energy balance can be rewritten to solve for the overall heat transfer coefficient as:

$$U_L = \frac{G_T(\tau\alpha - \eta_c)}{(T_c - T_a)} \tag{6.2}$$

Typically, the value for $\tau\alpha$ is unknown; however, it can be closely approximated as 0.9 without significantly compromising the accuracy of the model [57]. This is supported when considering the energy balance written in the following form:

$$T_c = T_a + \left(\frac{G_T \tau\alpha}{U_L}\right)\left(1 - \frac{\eta_c}{\tau\alpha}\right) \tag{6.3}$$

An estimate can be used for the value of $\tau\alpha$ without introducing significant error given that the term $\eta_c/\tau\alpha$ is small when compared to unity [57].

Values for the overall heat transfer coefficients for both systems were determined on a minute-by-minute and hourly basis. Trends in how the overall heat transfer coefficients are affected by the climate for both systems were analyzed by plotting the hourly average heat transfer coefficient during periods of operation in sequential order relative to time throughout the year. However, for hourly average heat transfer coefficients, only data sampled during periods the solar irradiance level was above 200 W/m^2 were considered. At low solar irradiance levels the difference between the array and ambient air temperatures is generally small. As a result, heat transfer coefficients estimated by using the energy balance equation approaches infinity yielding invalid and misleading values. Average hourly heat transfer coefficients observed throughout the year of monitoring for the stationary and dual-axis tracking systems can be seen in Figure 6.6 and Figure 6.7, respectively.

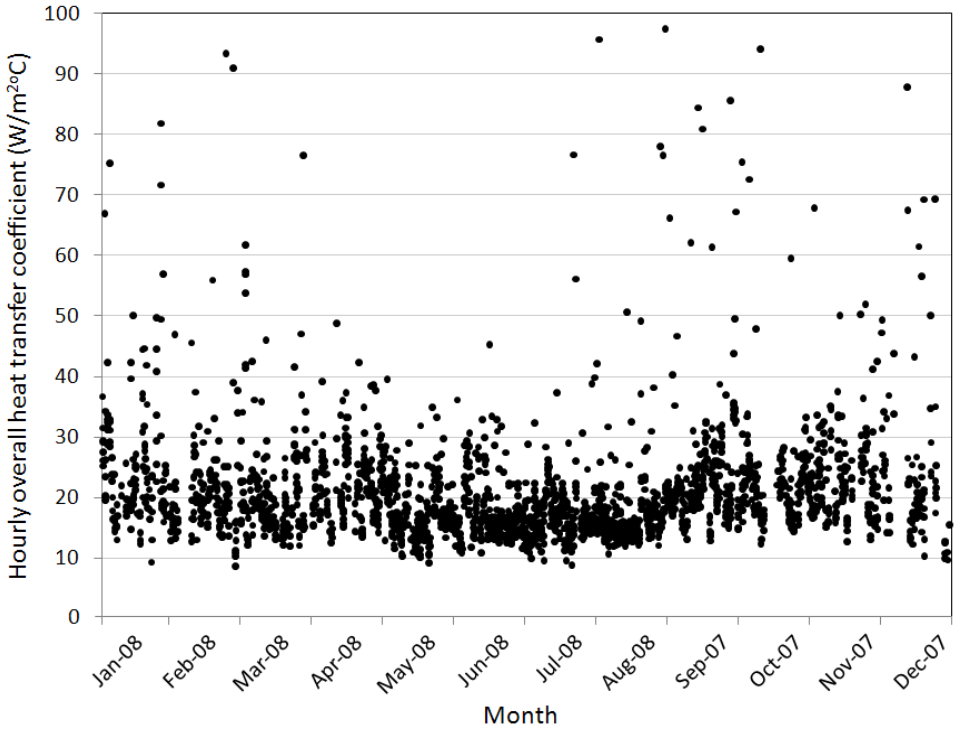

Figure 6.6. Hourly overall heat transfer coefficient for stationary system

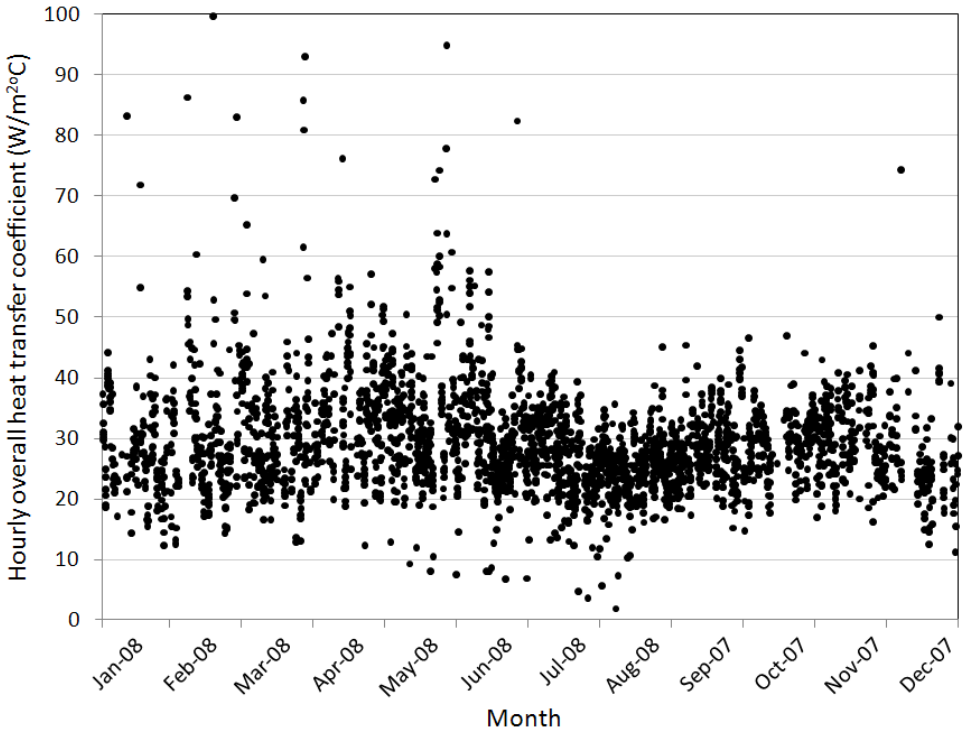

Figure 6.7. Hourly overall heat transfer coefficient for dual-axis tracking system

In general, the stationary system was found to transfer heat to the surroundings at a lesser rate per square meter of PV than the dual-axis tracking system. To gain a better understanding for overall heat transfer coefficient values of the PV systems, frequency distributions were constructed. Data used in the frequency distribution plots again only include data sampled during periods the solar irradiance level was above 200 W/m^2, as explained previously. The frequency distribution plot for both systems is shown in Figure 6.8.

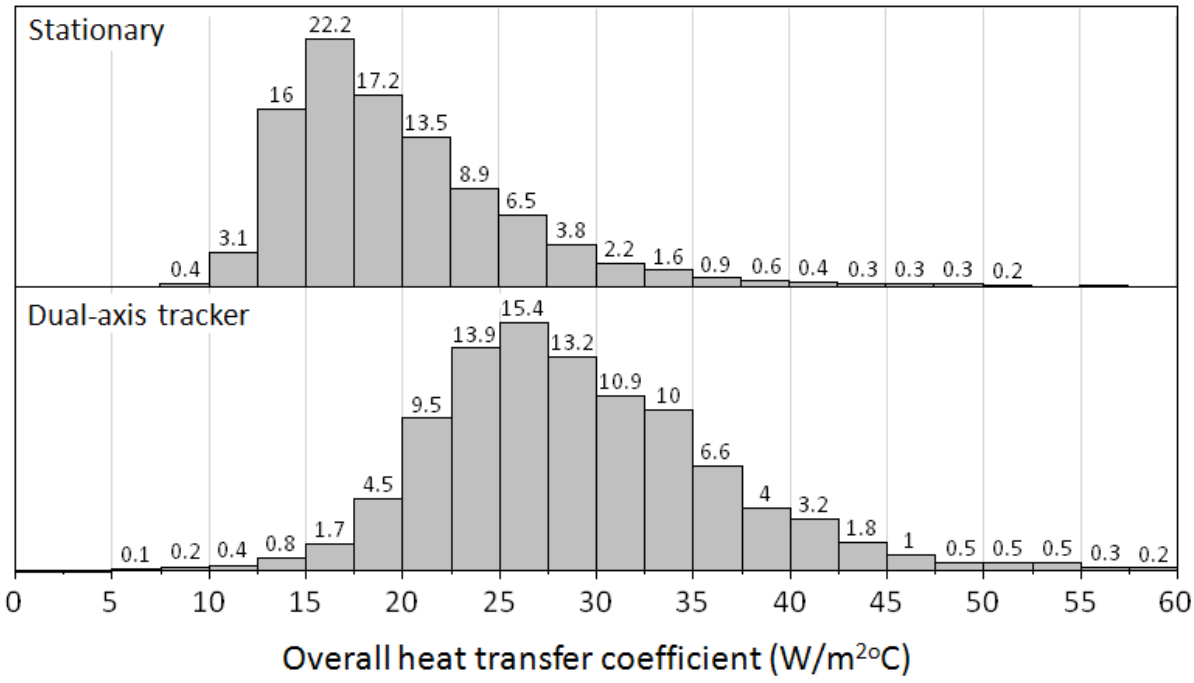

Figure 6.8. Frequency distribution of overall heat transfer coefficients for the stationary and dual-axis tracking systems

The frequency distribution shows the dual-axis tracking system overall tends to transfer heat to the surroundings more effectively. Overall heat transfer coefficients for the dual-axis tracking system appear to be normally distributed, but skewed slightly to the right. In contrast, the frequency distribution for the stationary system is clearly positively skewed, which, the greatest frequency occurrences for the overall heat transfer coefficients in lower ranges. The mean, median, and standard deviation of the overall heat transfer coefficient data for the stationary and dual-axis tracking system are shown in Table 6.6.

Table 6.6. Statistical measures for overall heat transfer coefficient for the stationary and dual-axis tracking systems

Overall heat transfer coefficient statistic (W/m^{2o}C)	Stationary system	Dual-axis tracking system
Mean	20.8	29.4
Median	18.6	28.1
Std Dev	9.1	8.7

The average (i.e., mean) overall heat transfer coefficient for the stationary and dual-axis tracking systems were found to be 20.8 and 29.4 W/(m^{2o}C), respectively.

Experimental Temperature Coefficient for Power

The affects of temperature on PV performance can be expressed in terms of a temperature coefficient. Temperature coefficients represent the change in a performance measure with respect to temperature. PV performance measures that are affected by operating temperature are current, voltage, and power. To assess net PV performance in terms of energy generated and conversion efficiency, the temperature coefficient for power is of most interest. Temperature coefficients are often stated on manufacturer's specifications for PV modules at Standard Test Conditions (STC) for short-circuit current, open-circuit voltage, and power. Temperature coefficients for these parameters measured at STC are typically assumed to be constant over the range of operating conditions PV systems experience in a real-world environment [54]. However, operating and meteorological conditions experienced in practice rarely reflect STC.

The temperature coefficients for DC power were estimated directly from data collected at solar irradiance values of 200, 400, 600, 800, and 1,000 W/m^2 ($\pm$ 3 W/m^2) throughout the year of monitoring. Power output data for each solar irradiance level was plotted against operating temperature for both systems. Using simple linear regression analysis, the temperature coefficient for DC power at each level of solar irradiance was found by determining the slope of each linear trend line. A plot showing DC power output per module verses average array operating temperature for each level of solar irradiance considered for the stationary system is shown in Figure 6.9. A plot showing DC power output per module verses average array operating temperature for each level of solar irradiance considered for the dual-axis tracking system can be seen in Figure 6.10. The slope of each trend line was then plotted against the corresponding level of solar irradiance for each system. Again, using simple linear regression analysis, a trend line was fit to the data for each system to obtain an equation relating the temperature coefficient of power to solar irradiance, shown in Figure 6.11.

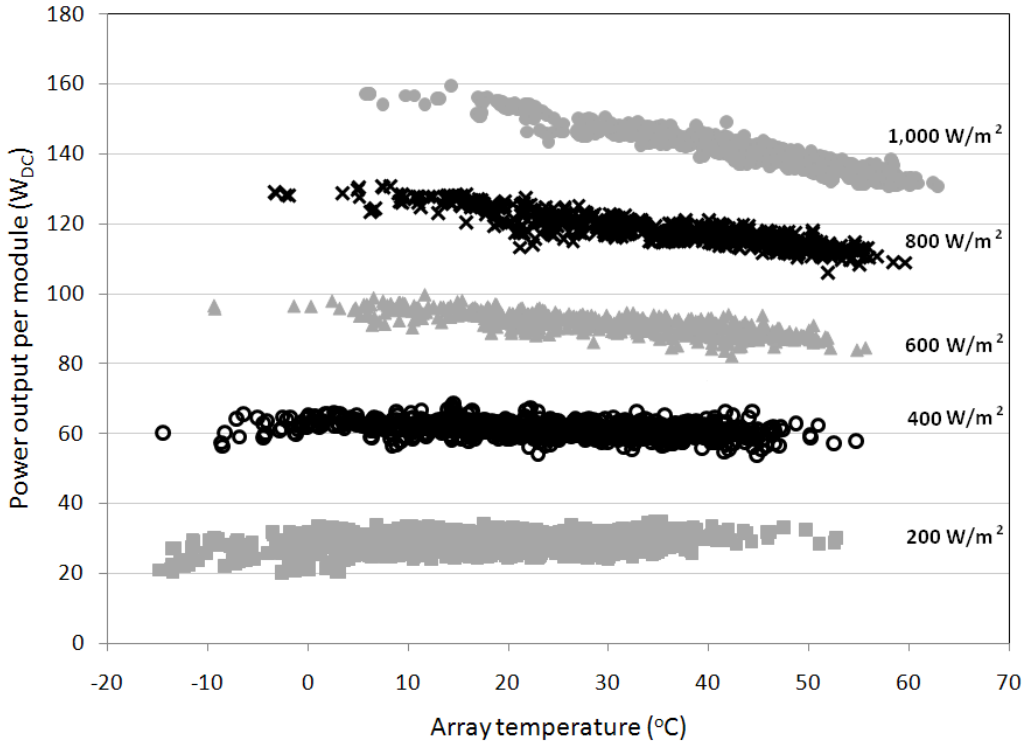

Figure 6.9. DC power output per module vs. module temperature for stationary system for different levels of solar irradiance

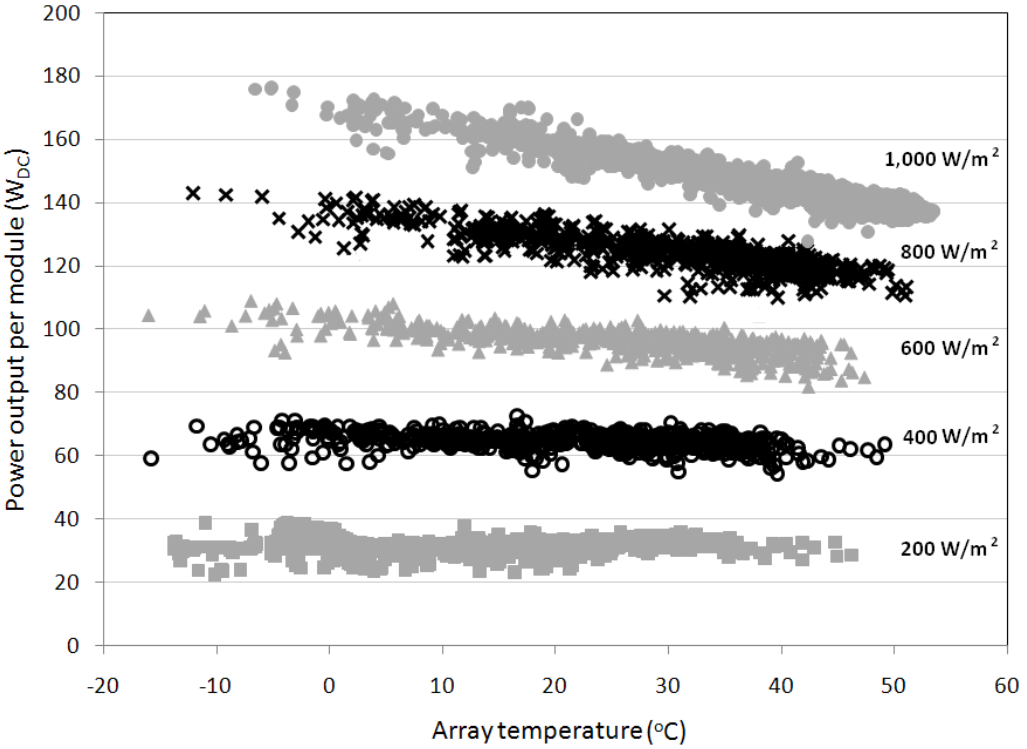

Figure 6.10. DC power output per module vs. module temperature for dual-axis tracking system for different levels of solar irradiance

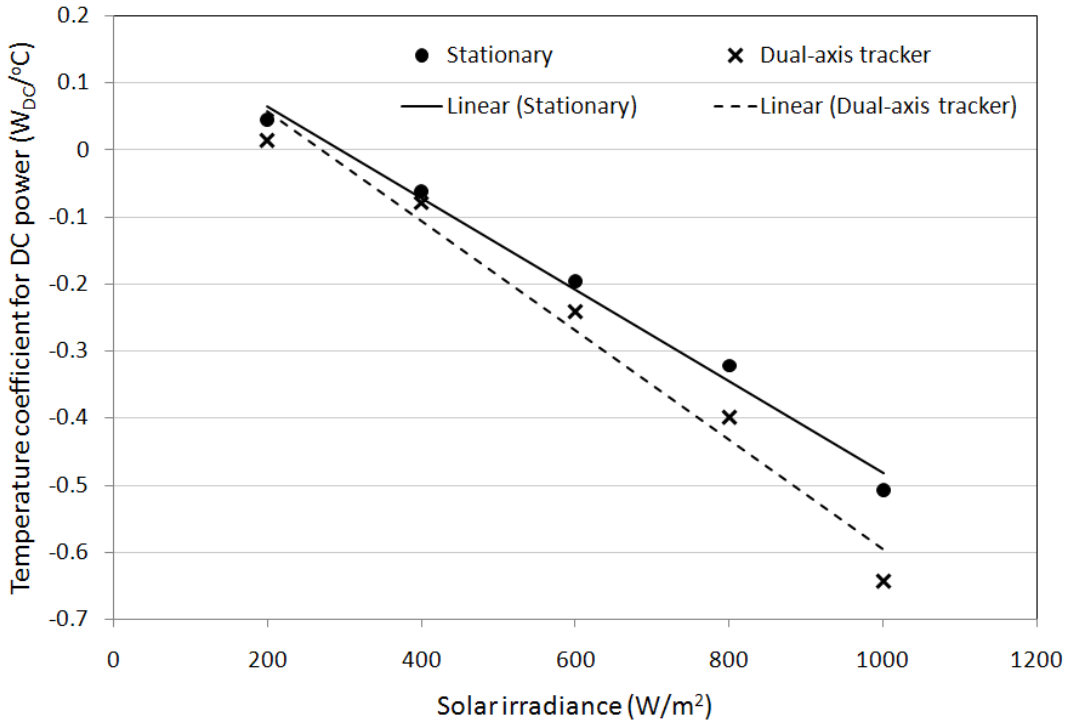

Figure 6.11. Temperature coefficients of power for stationary and dual-axis tracking systems

The resulting equations for temperature coefficient for power, β (W_{DC}/°C), as a function of solar irradiance were found to be

$$Dual-axis\ tracking\ system: \quad \beta = -8.1815 * 10^{-4}(G_T) + 0.22171 \tag{6.4}$$

$$Stationary\ system: \quad \beta = -6.8425 * 10^{-4}(G_T) + 0.20205 \tag{6.5}$$

Temperature coefficients for power were experimentally observed to be a function of solar irradiance level. Additionally, experimental data suggests that PV performance is actually enhanced as operating temperatures increase at low levels of solar irradiance, indicated by positive temperature coefficient values. Specifically, the stationary and dual-axis tracking systems show positive values for the temperature coefficient of power at solar irradiance levels less than 295 and 270 W/m^2, respectively. This phenomenon in experimental data taken for systems operating in outdoor conditions has been previously reported [54]. Some possible explanations for these observations that have been suggested include: spectral effects, soiling, dew, and instrumentation idiosyncrasies [54]. In general, however, the temperature coefficient of power for polycrystalline silicon PV modules has been estimated to be approximately -0.4 %/°C [54]. Experimental temperature coefficients at 1,000 W/m^2 for the stationary and dual-axis tracking system found in this study are -0.30 and -0.38 %/°C, respectively; these values are lower than the manufacturer's specified coefficient for power of (-0.5 $\pm$ 0.05) %/°C.

Simulations of Performance at Lower Operating Temperatures

To assess the potential for enhancing system performance by operating a PV system at cooler temperatures, two scenarios were assumed. The first scenario assumes the PV system operates at the surrounding ambient air temperature for all periods for one year. This simulation is considered a best-case scenario essentially assuming that the system is equipped with an infinite heat exchanger that transfers heat to the surrounding ambient air temperature, or that some means of moving ambient air effectively across the PV panels is arranged so that thermal equilibrium is achieved between the panels and ambient air. The second scenario assumes the PV system operates at 5.5 ^{o}C (10 ^{o}F) higher than the surrounding ambient air temperature for all periods throughout one year. This scenario was included to represent more reasonable and achievable operating temperatures without the application of complicated and costly equipment.

For the simulations, minute-by-minute experimental data that was collected from both systems was used which included: average array operating temperature, ambient air temperature, solar irradiance, and system DC power output. Using the average array operating temperatures of each system and ambient air temperature, the number of degrees each system would need to be cooled to reach the operating temperature assumed in each scenario for each minute in the simulation was determined. The experimental temperature coefficients of power for both systems were then used to estimate a new power output of each system operating at the lower temperatures simulated for each scenario:

$$P_{T,L} = P_{T,M} - \beta \Delta T \tag{6.6}$$

where $P_{T,L}$ = Estimated power output of system at the assumed lower temperature (W_{DC})

$P_{T,M}$ = Experimental power output of system at measured temperature (W_{DC})

ΔT = Temperature difference between measured and assumed temperature (^{o}C)

Monthly and annual DC energy generation for each scenario were then calculated by multiplying the instantaneous power production value by the time-interval for which the power was produced, and then summing those values over the month or year. Correspondingly, annual conversion efficiencies of the system for each scenario were estimated as the ratio of annual DC energy generated by the system to the total solar insolation received by the system. A summary of annual energy generation, and conversion efficiencies for each scenario compared to actual performance for the stationary and dual-axis tracking systems can be seen in Table 6.7.

Table 6.7. Summary of annual energy performance for each scenario

System	Field	Experimental data (no cooling)	Scenario 1: Cooling to ambient	Scenario 2: Cooling to 5.5 °C (10 °F) above ambient
Stationary system	Annual energy generation per kWp (kWh_{DC}/kWp)	1341	1399	1382
	Annual average conversion efficiency (%)	11.3%	11.8%	11.7%
	Conversion efficiency increase (%)	-	4.3%	3.1%
Dual-axis tracking system	Annual energy generation per kWp (kWh_{DC}/kWp)	1933	2021	1987
	Annual average conversion efficiency (%)	12.0%	12.6%	12.4%
	Conversion efficiency increase (%)	-	4.6%	2.8%

Simulations performed under the best-case scenario assuming both systems operate at the ambient air temperature suggest that annual conversion efficiencies could be increased from 11.3 to 11.8 percent (4.3 percent increase) for the stationary system and 12.0 to 12.6 percent (4.6 percent increase) for the tracking system. The increased in conversion efficiencies translate into approximately 58 and 88 kWh_{DC}/kWp/yr of additional energy generation from the stationary and dual-axis tracking system, respectively.

Estimated performance for each scenario and system was also analyzed on a monthly basis. Monthly performance results for the stationary and dual-axis tracking system can be seen in Table 6.8 and Table 6.9, respectively.

Table 6.8. Monthly energy performance for stationary system

Month	Experimental Data	Scenario 1: Cooling array to ambient air temperature		Scenario 2: Cooling array to 5.5 °C (10 °F) above ambient air temperature	
	Energy Generation (kWh/kWp)	Estimated energy generation (kWh/kWp)	% diff from experimental	Estimated energy generation (kWh/kWp)	% diff from experimental
Jan-08	62.3	64.8	4.1%	63.9	2.6%
Feb-08	75.7	78.7	4.0%	77.8	2.8%
Mar-08	115.8	120.8	4.4%	119.4	3.1%
Apr-08	115	119.3	3.8%	117.9	2.6%
May-08	141.1	148.1	4.9%	146.3	3.7%
Jun-08	139.4	145.8	4.6%	144.1	3.4%
Jul-08	145.9	152.5	4.5%	150.7	3.3%
Aug-08	154.6	162.6	5.2%	160.6	3.9%
Sep-07	140.6	147.1	4.6%	145.1	3.2%
Oct-07	103	107.1	3.9%	105.8	2.7%
Nov-07	91.8	94.9	3.4%	93.8	2.2%
Dec-07	55.7	57.2	2.7%	56.6	1.7%

Table 6.9. Monthly energy performance for dual-axis tracking system

Month	Experimental Data	Scenario 1: Cooling array to ambient air temperature		Scenario 2: Cooling array to 5.5 °C (10 °F) above ambient air temperature	
	Energy Generation (kWh/kWp)	Estimated energy generation (kWh/kWp)	% diff from experimental	Estimated energy generation (kWh/kWp)	% diff from experimental
Jan-08	112.6	118.1	4.9%	116.1	3.1%
Feb-08	112.1	117.9	5.2%	116.0	3.5%
Mar-08	158.4	165.5	4.5%	162.8	2.7%
Apr-08	154.3	160.2	3.9%	157.6	2.1%
May-08	199.8	208.4	4.3%	204.8	2.5%
Jun-08	207.6	217.4	4.7%	213.5	2.8%
Jul-08	213.5	223.0	4.5%	219.2	2.6%
Aug-08	228.3	240.2	5.2%	235.9	3.3%
Sep-07	191.7	201.5	5.1%	197.8	3.2%
Oct-07	144.2	150.6	4.4%	148.0	2.6%
Nov-07	132.6	138.0	4.0%	135.7	2.3%
Dec-07	77.9	80.7	3.6%	79.6	2.2%

Trends in the estimated monthly benefits of cooling each system did not show direct correlations to solar irradiance, ambient air temperature, or snow fall. However, the differences between monthly benefit in energy generation for each system were found to be within two percent.

SUMMARY

Two grid-connected PV systems with different mounting schemes were installed in central Iowa, USA; one roof-mounted stationary system and one pole-mounted dual-axis tracking system. Both systems were operated and monitored simultaneously under similar climatic conditions for one year. Heat transfer characteristics of both arrays were evaluated in terms of overall heat transfer coefficients. Further, the affects of operating temperature on PV system performance was assessed through the determination of temperature coefficients of power. Results presented here reflect operating characteristics of two real-world systems subjected to outdoor conditions. Lastly, models were built to predict performance of the PV systems operating in a climate inherent to the Upper Midwest at lower temperatures. System performance was simulated under two scenarios: the first scenario assumed the systems operated at the ambient air temperature and the second scenario modeled the systems operating at 5.5 °C (10 °F) above the ambient.

Throughout the year of monitoring, array operating temperatures ranged from -24.7 °C (-12.4°F) to 61.7 °C (143.1 °F) for the stationary system and -23.9 °C (-11 °F) to 52.7 °C (126.9 °F) for the dual-axis tracking

system during periods of system operation. Average monthly and annual operating temperatures of the two systems during daylight periods were found to be within 2 ^{o}C (3.6^{o}F) of each other. On a daily basis, the stationary system ran up to 6.7 ^{o}C (12.1 ^{o}F) hotter than the tracking system; however, throughout the year, daily average operating temperatures averaged to be within 1 ^{o}C (1.8^{o}F). Additionally, the stationary system was found to operate at higher average array temperatures relative to ambient air temperatures at solar irradiance levels greater than approximately 120 W/m^{2}. At 1,000 W/m^{2}, the stationary system operated on average 9.3 ^{o}C (16.7 ^{o}F) degrees hotter than the tracking system relative to ambient air temperature.

The dual-axis tracking system was found to transfer heat to the surroundings more effectively on average when compared to the stationary system. The hourly average overall heat transfer coefficients considering data sampled for solar irradiance levels greater than 200 W/m^{2} for the stationary and dual-axis tracking systems throughout the year of monitoring were found to be 20.8 and 29.4 W/m^{2o}C, respectively. Contrary to common convention, experimentally determined temperature coefficients of power were found to be sensitive to solar irradiance levels; however, this phenomenon has been previously observed in experimental studies conducted in outdoor conditions for polycrystalline silicon modules/arrays. The experimental temperature coefficients for power found here for the stationary and dual-axis tracking systems at a solar irradiance level of 1,000 W/m^{2} were -0.30 and -0.38 %/^{o}C, respectively, which are lower than the manufacture's specified value for the modules used. This discrepancy could be a result of more conservative testing performed by the manufacturer which would include a greater margin of error. The relationship between experimental temperature coefficients for power and solar irradiance levels was found to be approximately linear. Simulations of the stationary and dual-axis tracking systems operating at lower temperatures suggest that annual conversion efficiency could potentially be increased by up to approximately 4.3 and 4.6 percent, respectively.

ACKNOWLEDGEMENTS

The authors would like to thank the Iowa Energy Center for providing personnel, administrative, and financial support for this project.

CHAPTER 7 - TOOLS DEVELOPED TO DEMONSTRATE AND PREDICT THE PERFORMNACE OF STATIONARY AND DUAL-AXIS TRACKING PHOTOVOLTAIC SYSTEMS AND FOR INFORMATION DISSEMINATION

ABSTRACT

Two grid-connected photovoltaic (PV) systems comprised of multicrystalline silicon (mc-Si) modules with different mounting schemes were installed in central Iowa and monitored for one year; one 4.6 kW_p roof-mounted stationary system and one 1.02 kW_p pole-mounted dual-axis tracking system. Both systems are equipped with extensive data acquisition capable of collecting performance and meteorological data. Tools were developed to demonstrate the performance and operation of these systems, to predict the performance and economics of other grid-connected PV systems, and to facilitate the dissemination and access of these tools and information to the public. This paper describes the design and use of the following tools: an online interactive interface showing real-time and historical performance data of real-world stationary and dual-axis tracking PV systems operating in the Upper Midwest, an online interactive interface showing real-time streaming video and photographs of real-world stationary and dual-axis tracking PV systems operating in the Upper Midwest, and a PV calculator to predict performance and economics of PV systems operating in the Upper Midwest and elsewhere. The PV calculator was used to predict performance of the stationary and dual-axis tracking systems and results were compared to actual experimental data. Differences between modeled predictions and actual experimental results for annual energy generation for the stationary and dual-axis tracking systems were found to be 4.1 and 5.2 percent, respectively. Monthly differences in energy generation between predicted and experimental results ranged from 1.2 to 35.2 percent for the stationary system and 0.6 to 26.4 percent for the dual-axis tracking systems. The discrepancies between modeled and experimental results in terms of energy generation were attributed in part to the site receiving less solar insolation that expected based on 30-year averages and to influences due to snow cover.

INTRODUCTION

The utilization and adoption of PV for building energy generation applications is not currently widespread in the Upper Midwest. Studies indicate the general public possesses little knowledge in regards to most aspects of PV [50]; the unfamiliarity with and lack of understanding of PV technology and performance have been suggested by many sources to be reasons the use of PV for building energy generation is not more widespread [47, 50, 51, 82]. In addition, it has been suggested that consumers

are in general skeptical about the performance and reliability of PV systems; this skepticism by consumers needs to be overcome before the use of PV for building energy generation is widespread [47, 82].

This work aims to address the general unawareness, lack of understanding, and skepticism of PV performance, operation, and reliability by developing tools to (I) demonstrate the actual performance, reliability, and operation of real-world PV systems installed in the Upper Midwest, (II) predict the performance and economics of PV systems in the Upper Midwest and elsewhere, and (III) effectively disseminate applicable, objective, accurate, and understandable information focusing on the performance and general operation of PV to the public. Increasing awareness of PV through the use of these tools by further educating the social, academic, and scientific communities may lead to a more widespread use of PV. Consequently, negative impacts resulting from conventional methods of energy generation using fossil-fuel based sources may be reduced.

TOOLS DEVELOPED

Tools developed as part of this work include: an online interactive interface showing real-time and historical performance data of real-world stationary and dual-axis tracking PV systems operating in the Upper Midwest, an online interactive interface showing real-time streaming video and photographs of real-world stationary and dual-axis tracking PV systems operating in the Upper Midwest, a PV calculator to predict performance and economics of PV systems operating in the Upper Midwest and elsewhere, and a website to disseminate the results of the overall project as well as facilitate public access to the tools developed.

Data Acquisition System and Interface

The real-time and historical data software tool interfaces with data acquisition systems (DAQ) installed on two grid-connected PV systems used for building energy generation; one roof-mounted stationary system, and one pole-mounted dual-axis tracking system. Specifics of these systems are presented in [63, 64]. The DAQ and interface can be divided into four main components: (I) the instruments used to take measurements, (II) the hardware used to convert the analog signals from the instruments into digital values, and (III) software used to collect the digital data, send all data to a repository, and archive the data for future use, and (IV) the graphical user interface used to view the real-time and historical data.

Instrumentation

Both operating parameters of each array and meteorological conditions were monitored. The specific performance parameters that were monitored include the following:

- DC voltage produced by the arrays of modules (measured at input of inverters)
- DC current produced by the arrays of modules (measured at input of inverters)
- AC voltage output by the inverters (measured at output of inverters)
- AC current output by the inverters (measured at output of inverters)
- Module temperatures

The meteorological parameters that were monitored include:

- Solar irradiance (measured at plane of array)
- Ambient air temperature (tracking system only)
- Wind speed and direction (stationary system only)

The placement of each instrument and design of the data acquisition system can be seen in Figure 7.1.

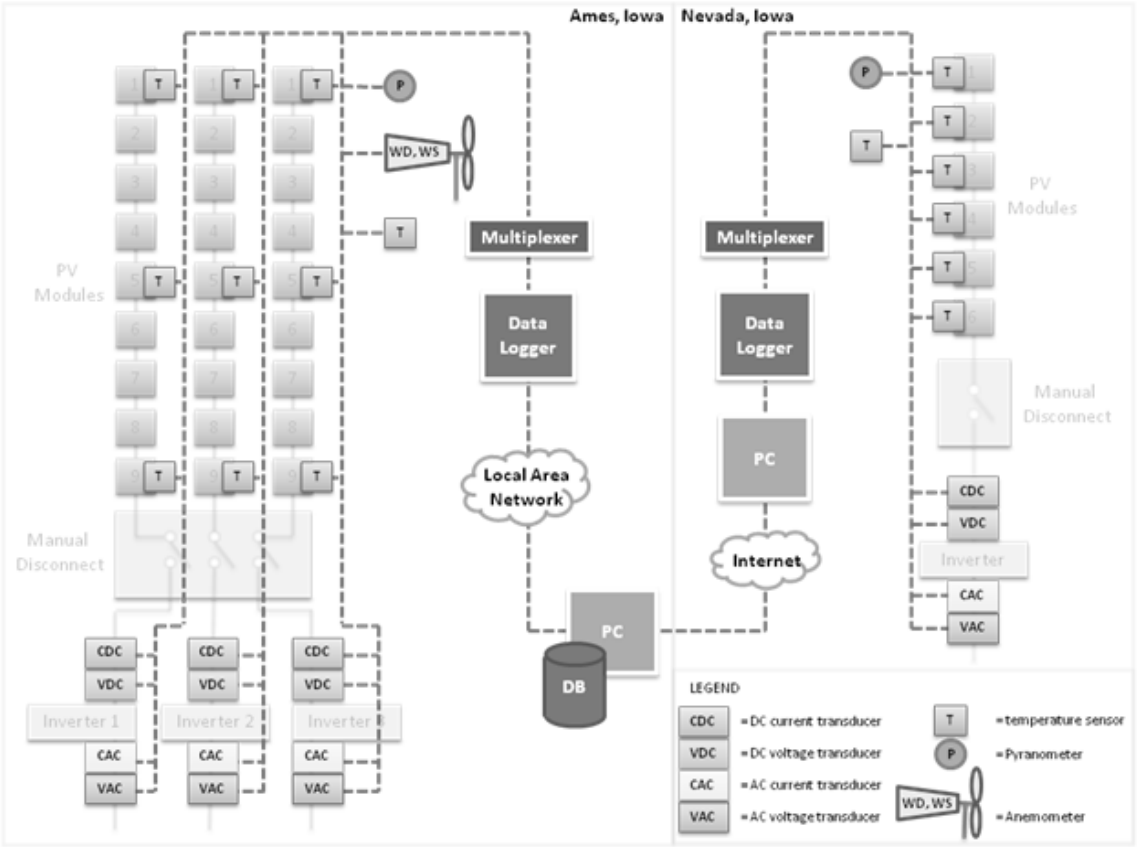

Figure 7.1. Data acquisition system diagram

Data Acquisition Hardware

The data acquisition hardware primarily functions as a system that digitizes the incoming analog signals from the instrumentation so that the data can be interpreted. The data acquisition hardware deployed at each site consists of a data logger, multiplexer, power supply, and communication cable to the local area network and/or Internet. All data acquisition equipment was manufactured by Campbell Scientific. The data acquisition equipment used for the project is considered to be of research grade.

All sensors/transducers are connected to a multiplexer. The multiplexer expands the number or analog inputs to the data logger. The number of analog inputs is increased to that of the data logger by sequentially multiplexing sensor leads into common leads. The individual common leads are then connected to the data logger's analog inputs, excitation channels, or ground, depending on the particular sensor(s). This device is positioned between the sensors and data logger as seen in Figure 7.1. The model number AM16/32 relay multiplexer used at both locations is capable of hosting 16 additional differential sensors to that of the data logger that require excitation.

Both sites use a Campbell Scientific CR1000 data logger. This particular data logger was selected due to the type, number, precision, and speed of the measurements taken for the project. The data logger accepts the analog signals from the multiplexer, converts these values to digital data, and pushes the data to the web services for archiving. The CR1000 is powered by a Campbell Scientific PS100 power supply. This power supply converts 120 VAC power to 12 VDC power and has battery backup.

Data Collection and Archival Software

The data acquisition software functions can be split into three categories: software to control the data loggers, software to push data from both sites to a central location, and software to archive data into a single database. All software applications were developed by Quality Attributes Software. Figure 7.2 shows a simplified diagram of the software applications and their basic function(s).

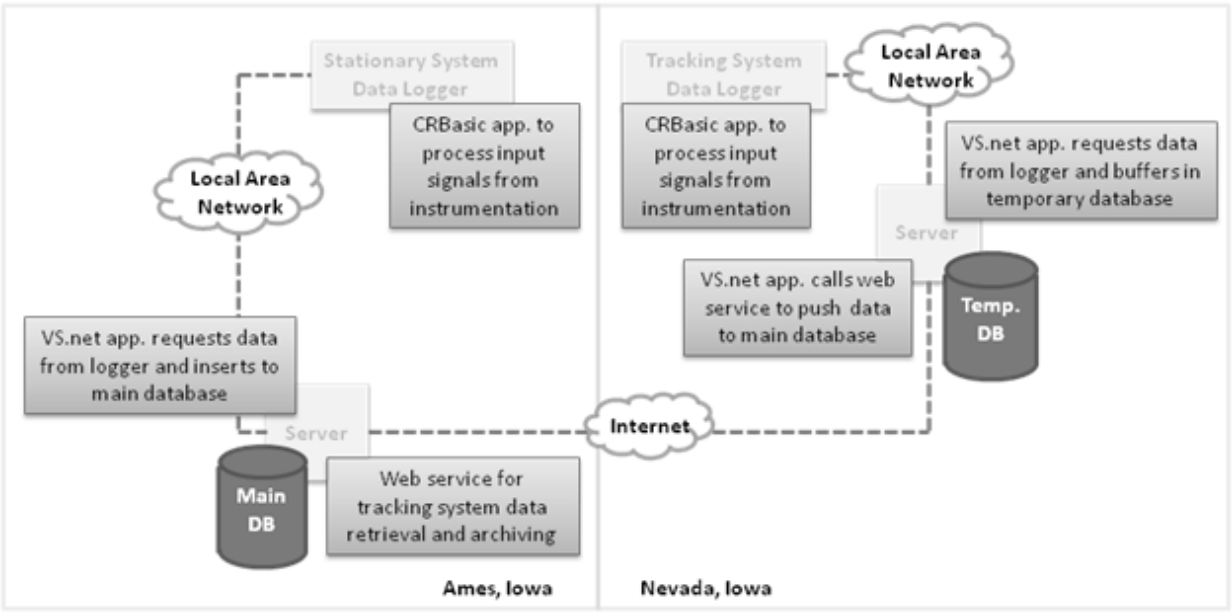

Figure 7.2. Software component diagram

The data loggers run on a PakBus® operating system. All programs controlling the data loggers are written in a proprietary language to Campbell Scientific known as CRBasic. The CRBasic programs tell the data logger what type of signal to expect from each sensor, what the conversion factors are to convert the analog signals to digital data, and how often to sample and store data from each instrument. All data is sampled (measured) every ten seconds and temporarily stored on the data logger as one-minute averages.

Since the tracking system resides at a different geographical location than the central database, some additional steps are necessary to ensure no data is lost while being pushed to the data repository. A Visual Studio.net application was put in place to move data from the data logger into a temporary Microsoft SQL Server Desktop Engine (MSDE) database. This database resides on a server located in Nevada, Iowa and has a buffer of 80,640 data records (approximately 2.5 days of data collection). After each data point is stored in the temporary database, the application uses a web service to push the data in Xml format to the central database located in Ames. If the connection between Ames and Nevada is severed, data is kept in the temporary database and sent at a later time.

The web service used to retrieve data from the tracking system is hosted on a server at the location of the stationary system and central database (in Ames, Iowa). This web service uses the Internet Information Services (IIS) 6.0 infrastructure on a Windows Server 2003 operating system platform. This web service is a Visual Studio.net application written in Visual Basic.net. Additionally, the service uses

the Service Oriented Architecture Protocol (SOAP) to exchange the Xml based files containing PV data from the tracking system at BECON.

Data storage for the stationary system is much simpler since the system and database reside at the same location. As with the tracking system, data from the stationary system is buffered in the logger. Subsequently, a Visual Studio.net application written in Visual Basic.net pulls data from the logger and archives it into the central database. The main data repository is a SQL Server 2000 database. This database is used to store the PV performance and weather data so that the data can be analyzed for research and additionally accessed by the online interface.

Graphical User Interface

An interactive online web-interface was created to present the real-time and historical performance of both PV systems as well as current meteorological conditions. Both actual measured values and normalized values (per square meter of PV) are presented. The normalized values allow a direct comparison between the two inherently different system types since the installed capacities of each system are different.

Real-time parameters for both systems available for viewing on the interface include:

- Solar irradiance
- Power production (actual and normalized available)
- Energy generation for the current day viewed (actual and normalized available)
- Energy generation since system conception (actual and normalized available)
- System efficiency (defined as the conversion of light to electricity)
- Average array temperature
- Ambient air temperature
- Wind speed
- Wind direction

The real-time portion of the interface has a “dashboard” look and feel. Solar irradiance and power production values are presented in gauges to give the user a feel for the magnitude of the current value. The solar irradiance gauges are presented with a range from 0 to 1,000 watts per square meter. The power production gauges are shown with ranges from zero to the rated capacity of the array (or square meter of PV in the normalized case). A green range is drawn on the power production gauges and represents the power output between the system’s maximum expected production (considering all

losses on rate power output), and its rated capacity. The remainders of the performance and meteorological parameters are displayed as digital values. Tool tips are available to aid the user in the understanding of each parameter presented. A screen-shot of the real-time tab of the interface can be seen in Figure 7.3.

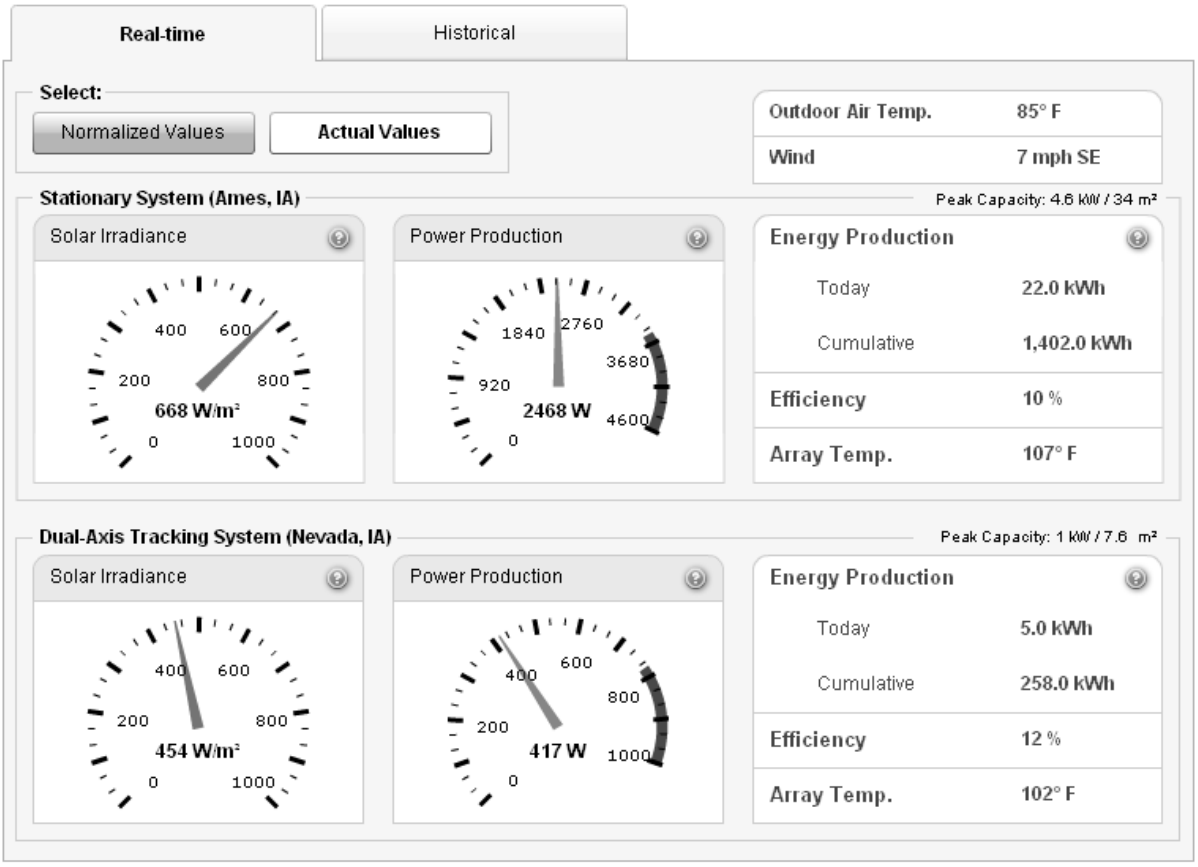

Figure 7.3. Screen-shot of real-time tab on web-interface

Historical performance parameters for both systems available for viewing on the interface include:

- Power production (actual and normalized available)
- Energy generation (actual and normalized available)
- Solar irradiance

A power production verses solar irradiance plot and an energy generation plot for both systems can be found in the historical tab of the interface. Both plots can be viewed as actual values or normalized values for easy comparison of the stationary and tracking systems. Data can be displayed from system conception to the current date in time-spans of a day, week, month, year, or custom range input by the

user. Additionally, a scroll bar is available for both plots to show the user the exact value for each trend when moved across the plot.

Historical power production and solar irradiance for both systems are all plotted together on a single line plot. When viewing this data with a time-span of a day, hourly values are plotted. Whereas, a data point at least every two hours is plotted when viewing time-spans of greater than a day but less than or equal to a month. The peak weekly power production and solar irradiance is shown when viewing a year or more of data. A screen-shot of the historical tab showing power production and solar irradiance can be seen in Figure 7.4.

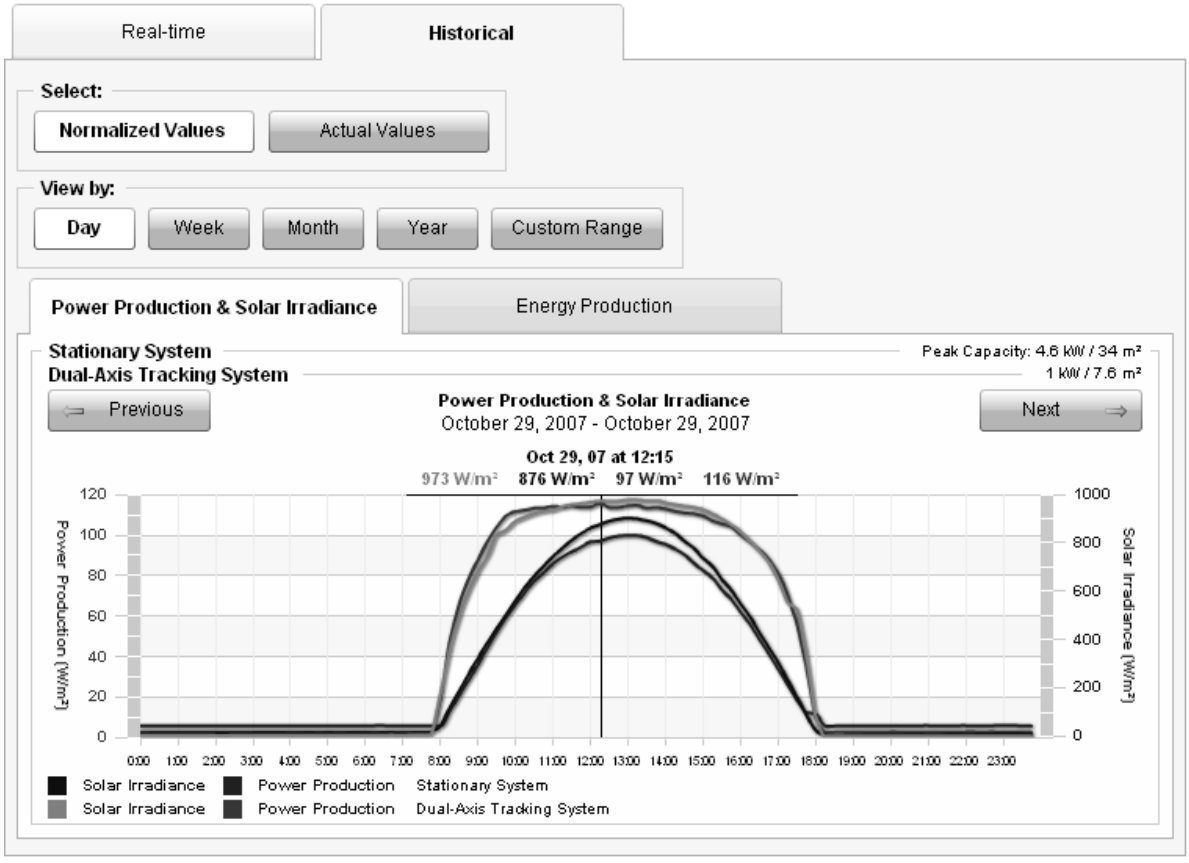

Figure 7.4. Screen-shot of historical tab on web-interface showing power production and solar irradiance

Historical energy generation of both systems are plotted in the form of a bar chart. When viewing daily data, the energy production for each hour of the day is shown. Whereas, when viewing weekly data, the energy production for each day is shown. Correspondingly, if a user requests to see data of a month or year, the energy production produced each week and month is displayed, respectively. A screen-shot of the historical tab showing energy production can be seen in Figure 7.5.

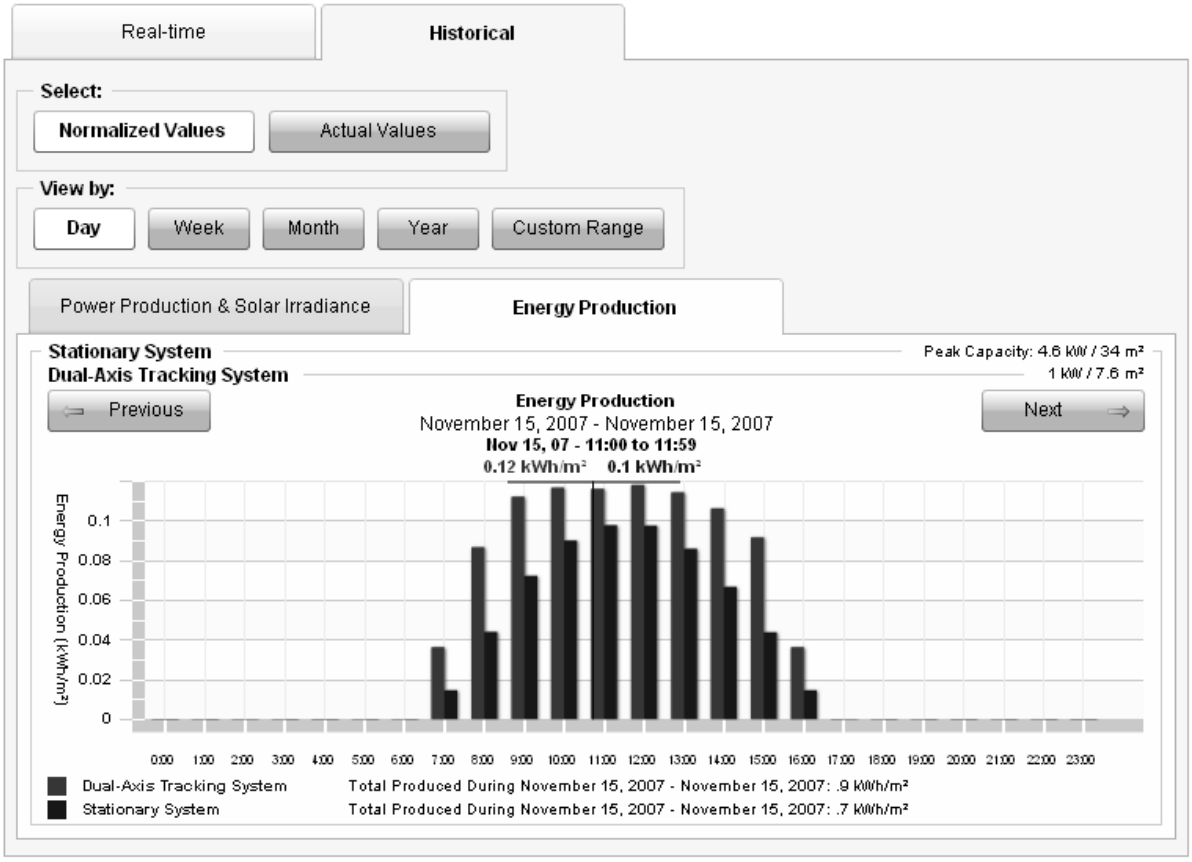

Figure 7.5. Screen-shot of historical tab on web-interface showing energy production

Network/Web cameras

Web cameras were installed at each site to allow remote monitoring of both systems. Software was developed using HyperText Markup Language (HTML) and integrated into the website to allow a user to view real-time and historical photographs and steaming video of each system. The web cameras and software interface offer a unique opportunity for a user to simultaneously compare real-time and historical performance of the PV systems with real-time and historical photographs and video of the meteorological conditions experienced at the sites.

Both webcams installed at each site are identical and are Axis 211 fixed network cameras. The cameras present photographs and video in MPEG-4 format, respectively. Frame rates for video are supported up to 30 frames per second. The maximum resolution of the cameras at all frame rates is 640 by 480 pixels. Each network camera is installed in an Axis ACH13HB outdoor housing for weather protection. The camera installed at the site of the stationary system was mounted on the southwest corner of the building. The camera installed at the tracking system site is pole-mounted directly south of the system.

The software interface is designed using a conventional tab structure, with one tab for each system. Within each tab, four buttons are available allowing access to the photographs and video. The first section can be accessed with the "*Live Photo"* button and shows a real-time photograph of the system, shown in Figure 7.6.

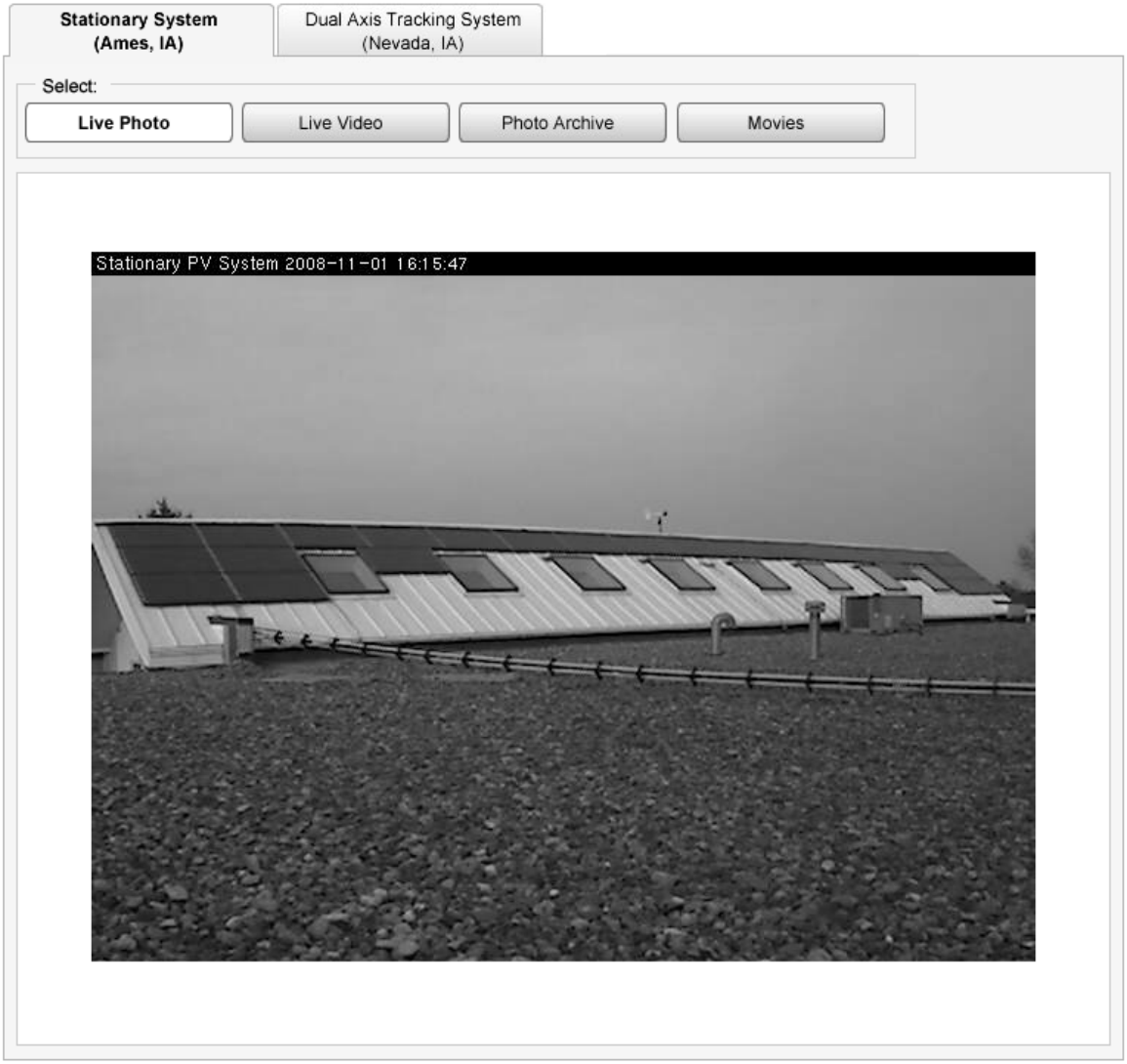

Figure 7.6. Webcam real-time photograph page

The second section can be accessed with the *"Live Video"* button and shows a real-time streaming video of the system, seen in Figure 7.7.

Figure 7.7. Webcam real-time video page

The third section can be accessed with the *"Photo Archive"* button and shows historical photographs of the system, shown in Figure 7.8. Historical photographs are archived at two-hour increments between 6:00 AM and 10:00 PM for seven days trailing the current time. The software automatically purges and permanently deletes all files from the system that date back further than seven calendar days.

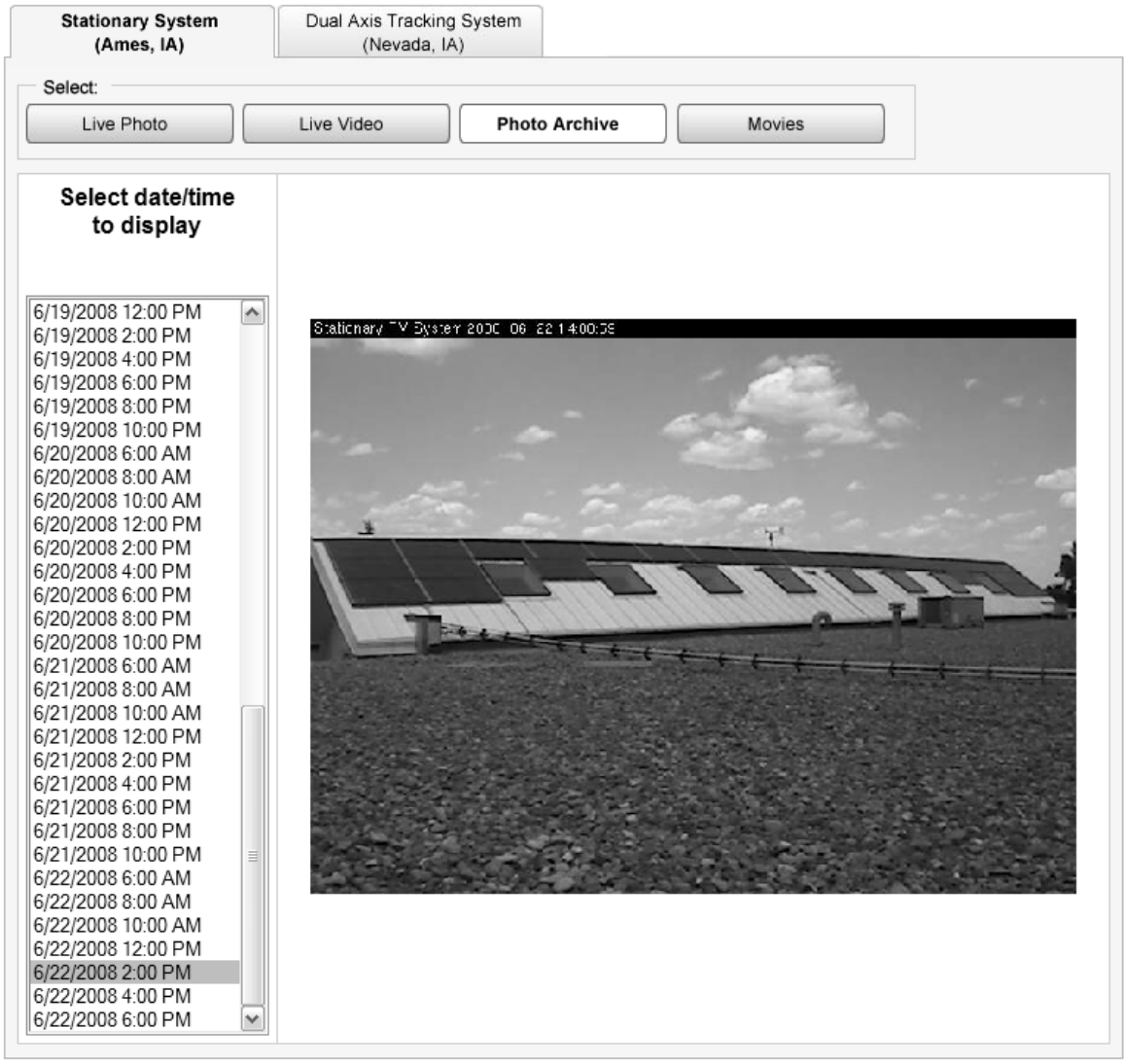

Figure 7.8. Webcam historical photograph archive page

The fourth section can be accessed with the *"Movies"* button and shows historical video of the systems, seen in Figure 7.9. Historical videos of each system are available for viewing or download from the current time and day and the six days prior. The software was developed to be compatible with several web browsers; namely, Internet Explorer, Firefox, and Safari. All movies that can be downloaded from the site are in Moving Picture Experts Group (MPEG) format and can be viewed in a variety of software packages (e.g., Windows Media Player and QuickTime).

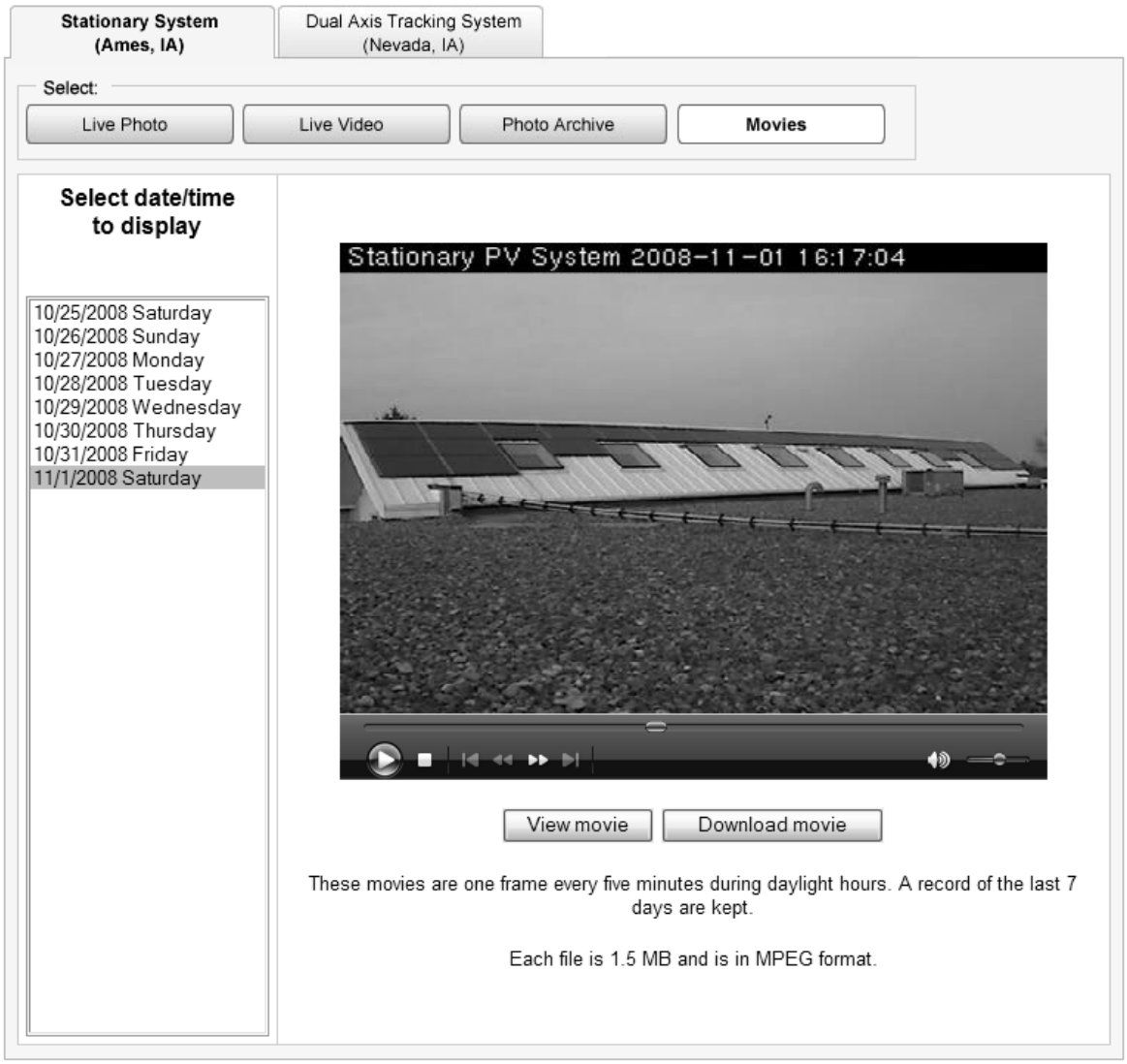

Figure 7.9. Webcam historical video archive page

PV Calculator

The PV calculator developed as part of this work is a tool that can be used to predict performance and economic parameters for grid-connected stationary and dual-axis tracking PV systems. The model can predict performance of a PV system given a geographical location, system type, array orientation (if stationary system). The calculator can be used to predict performance of PV systems located in or near 239 cities in the U.S. Well informed users have the ability to tweak default values in the model for system losses to more accurately predict performance of a particular system. Performance parameters that are modeled include monthly and annual average daily solar insolation and monthly and annual AC energy generation (kWh). Economic parameters are estimated by the model based on predicted

performance and the following input parameters: initial project installed cost (actual or per peak Watt), operating and maintenance costs (percentage of initial costs), available rebates on initial costs, incremental costs of utility supplied electrical energy ($/kWh), general inflation rate, assumed usable lifetime of the system (years), and specifics of a loan used to finance the system if one is taken. A Windows-based graphical user interface (GUI) was developed for the model to simplify its use and organize inputs and results. This application can be executed from a remote server or downloaded and installed to a local machine. The application can be accessed via remote server at http://129.186.210.47/pvdemo/publish.htm. A summary of the inputs to the model are:

- Geographical location (i.e., city and state)
- System mounting type (i.e., stationary or dual-axis tracking)
- Array orientation (if stationary system)
- Manufacturer and model of modules and inverter
- Efficiency of components and system
- System life
- Costs and incentives
    - System installation cost
    - Operation and maintenance costs
    - Rebates
    - Electric costs
    - Inflation rates
    - Loan specifics if one is to be taken to finance the system(s)
        - Interest rate on loan
        - Term of loan
        - Owners tax rate

A summary of the outputs generated by the model are:

- Average full sun hours per day striking the array for each month and annually
- System energy output (in kWh) for each month and annually
- Initial project cost
- Total lifetime cost of system
- Average cost per kWh of energy from PV system over assumed life of system
- Average cost per kWh of energy from utility over assumed life of system

- Total tax savings incurred from PV system
- Payback period (in years)

Graphical User Interface Description

The GUI to the calculator was written in the language C sharp (C#) and developed in the interactive development environment (IDE) Visual Studios.net. The application is Windows based and can be run from a remote server or downloaded and installed onto a local Windows based PC having the dot-net framework. A screen-shot of the application can be seen in Figure 7.10.

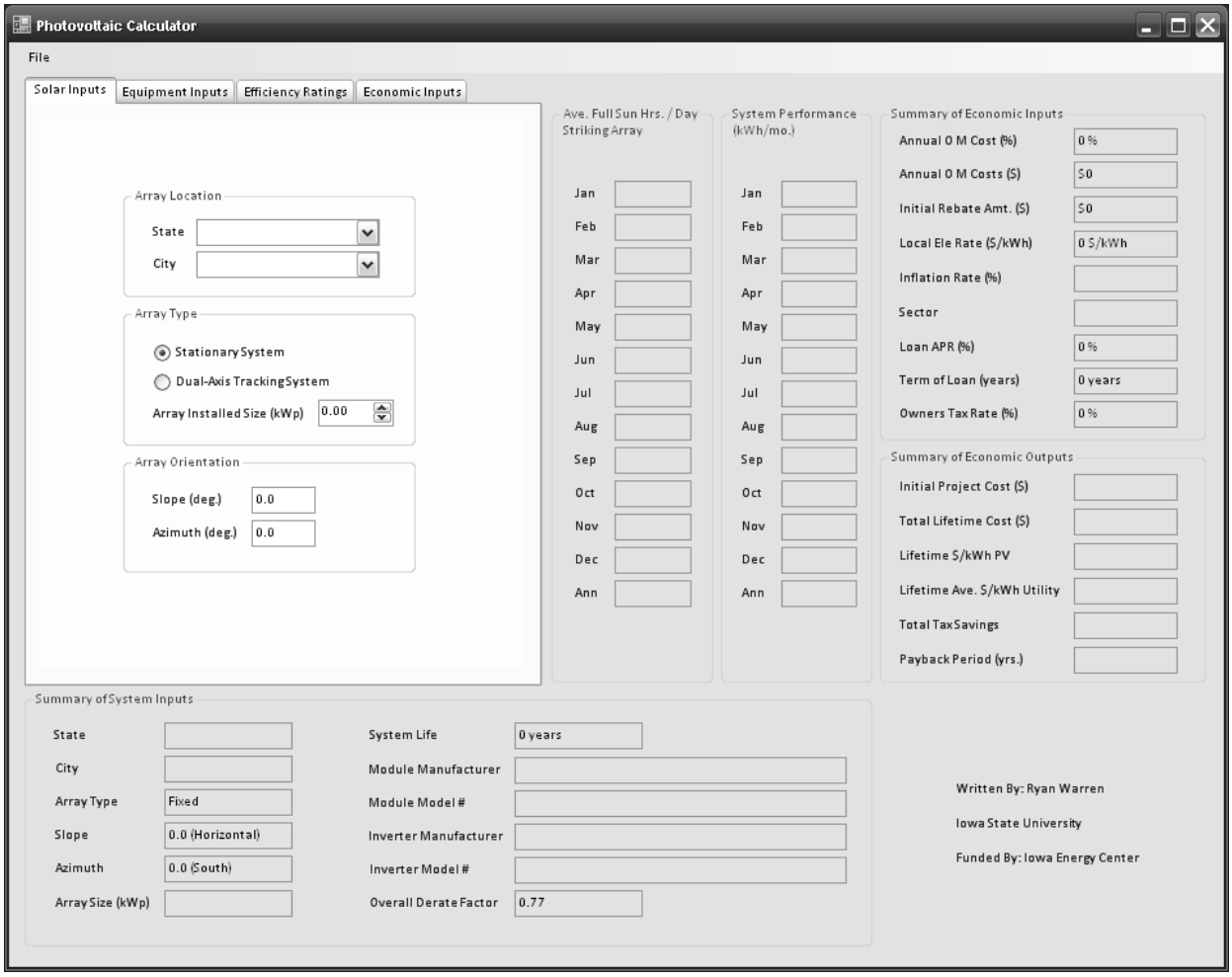

Figure 7.10. PV calculator

The GUI can be divided into three main sections: input, input summary, and output. All inputs to the model are entered by the user in the tabbed screens, which are a white color. Each input entered by the user automatically appears in the input summary section on the lower portion of the interface for

reference. Once the appropriate inputs are entered by the user, the corresponding outputs are calculated and displayed in the output sections on the right side of the interface.

Under the Solar Input tab the user can input the array location, type, and orientation (orientation inputs are only offered for stationary systems). There are 239 U.S. cities available to the user for array location. First, the user must select the state for which the array will be located. Once the state is selected, the drop down menu will populate with the cities within that state for which solar data is available. Once the location is set, the user can select the array type that they would like to model; the calculator can model both stationary and dual-axis tracking systems. For stationary systems, the user can then enter the proposed slope and azimuth of the array. With these inputs, the calculator will then estimate the average incident insolation on the array and energy generation output by the array for each month and annually.

The model also allows a user to select the specific module and inverter that they plan to use in the Equipment Inputs tab seen in Figure 7.11. The calculator contains 593 modules and 109 inverters from 31 and 16 different manufacturers, respectively. Once the user selects a particular module, a module description and PTW rating is populated in the output boxes below. Similarly, once an inverter is selected, the description, power rating, and efficiency are displayed. In addition, the efficiency for the inverter selected is input to the performance model and the energy produced by the system is adjusted and redisplayed.

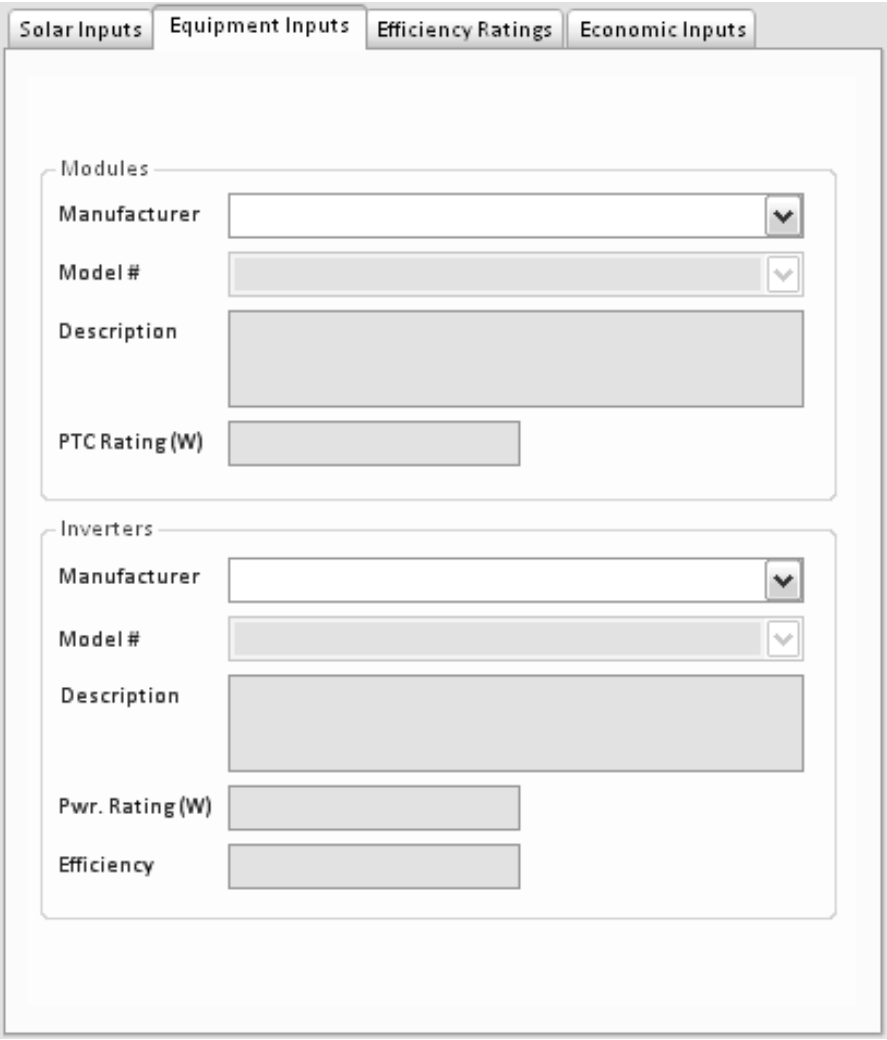

Figure 7.11. Equipment Input tab

The model considers losses due to module rating, inverter, mismatch, diodes and connections, wiring, soiling, system availability, shading, tracking, and age. Each of these losses are initially given a default derate value. However, the user can adjust any of the default values as they see fit in the Efficiency Rating tab seen in Figure 7.12. If any derate values are changed, the model recalculates estimated performance and redisplays the new values.

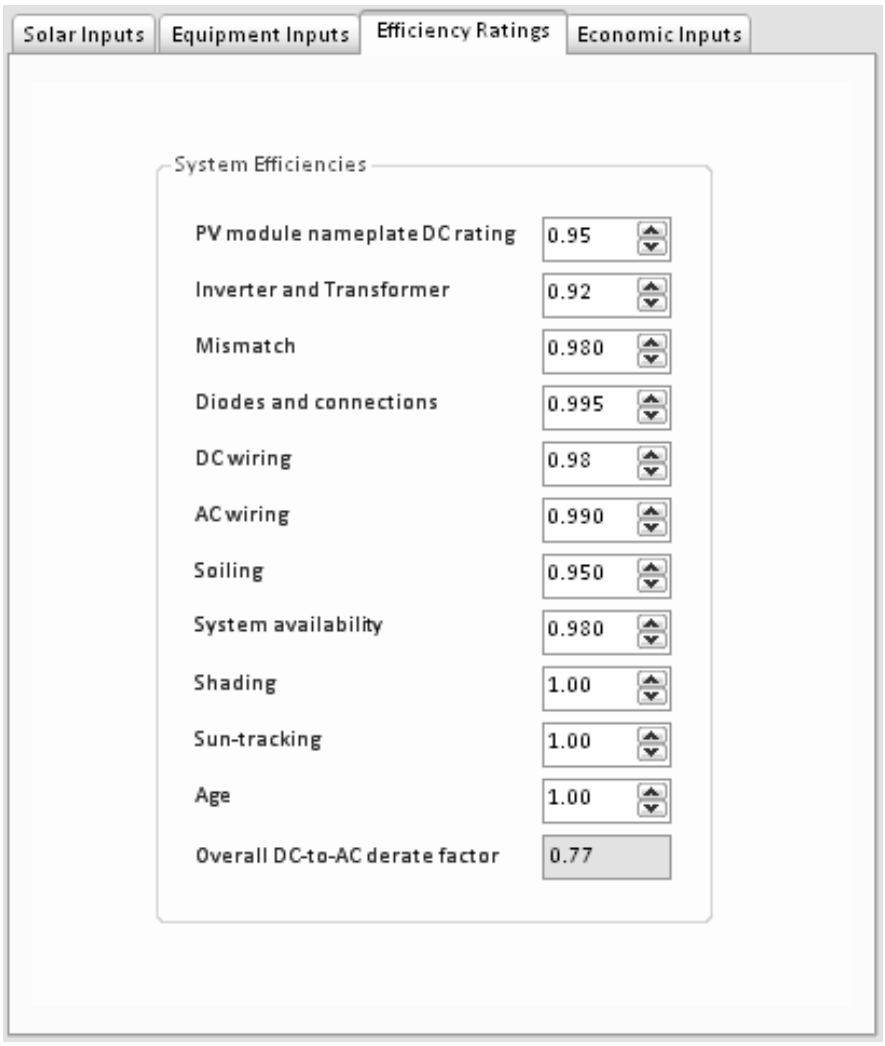

Figure 7.12. Efficiency Ratings tab

Finally, economic inputs can be entered by the user in the Economic Inputs tab seen in Figure 7.13. Within this tab, the user can input project costs and rebates, current energy costs, and specifics of a loan if one is to be taken for the project. Once the inputs are completed, all of the economic parameters are estimated and displayed in the output section of the GUI.

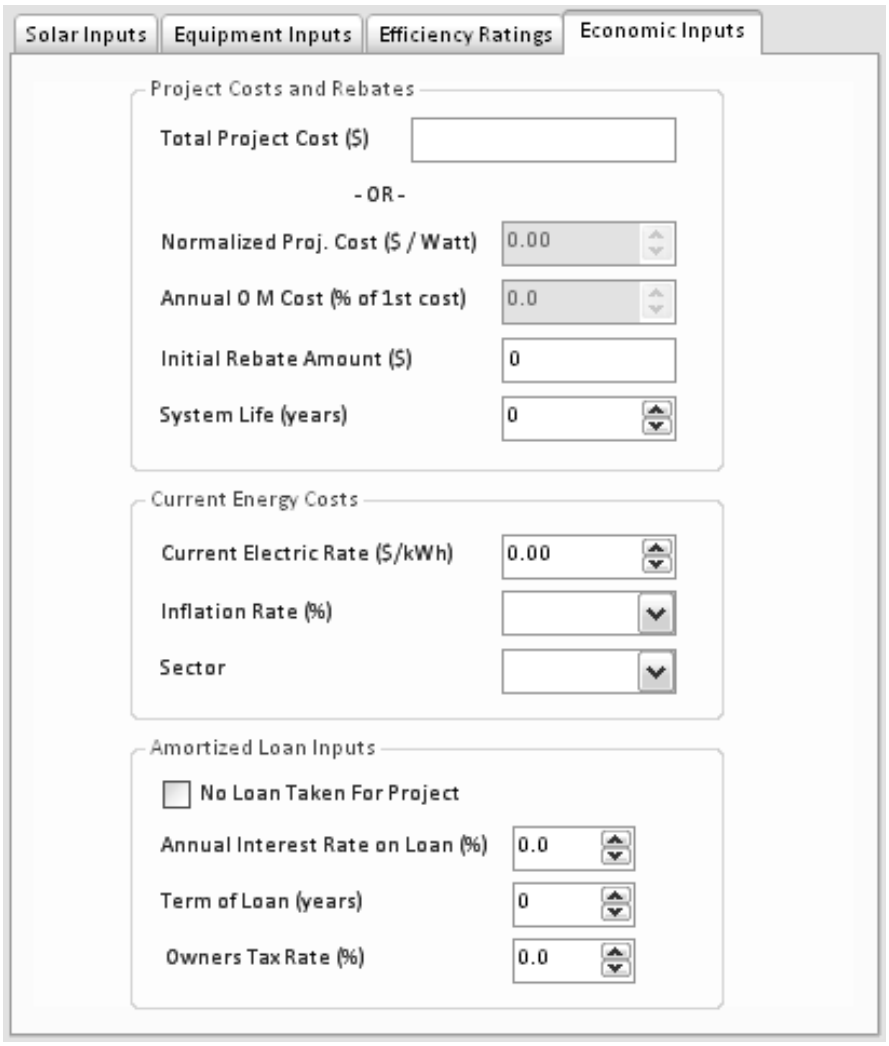

Figure 7.13. Economic Inputs tab

Performance Model

The total solar radiation striking the photovoltaic array can be split into two components, beam and diffuse radiation. The beam radiation is the portion of the total solar radiation striking the array coming from the sun without having been scattered by the atmosphere and is known as direct solar radiation [57]. The diffuse radiation is the portion of the total solar radiation striking the array from the sun after its direction has been changed due to scattering by the atmosphere, and it is known as solar sky radiation [57]. Thus, the total irradiance, which is the rate at which radiant energy is incident on a surface per unit area of surface, is the sum of the beam and diffuse radiation rates incident on the array per unit area.

All solar data for the model was obtained from the National Renewable Energy Laboratory (NREL) Typical Meteorological Year (TMY2) data set. The TMY2 data is used in a variety of energy performance software. The datasets are in a text file format and there is an individual file for 239 cities in the United States.

The TMY2 data gives solar values for a horizontal surface; therefore, the amount of solar radiation incident on a tiled surface, e.g., a fixed photovoltaic array, must be modeled. Methods for estimating solar insolation on a tilted surface used here are based on work done by Duffie and Beckman [57]. The hourly beam radiation incident on a tilted surface can be determined by

$$I_{b,T} = I_b R_b \tag{7.1}$$

The parameter R_b represents the ratio of beam radiation on a tilted surface to that on a horizontal surface for a particular hour and was determined by

$$R_b = \frac{I_{b,T}}{I_b} = \frac{\cos(\theta)_i}{\cos(\theta_z)_i} \tag{7.2}$$

The angle of incidence, ϑ, is the angle between the beam radiation on a surface and the normal to that surface; whereas, the zenith angle, ϑ_z, is the angle between the vertical and the line to the sun. The angle of incidence and the zenith angle were determined by

$$\cos(\theta)_i = \begin{bmatrix} \sin(\delta)_i \sin(\emptyset) \cos(\beta) \\ -\sin(\delta)_i \cos(\emptyset) \sin(\beta) \cos(\gamma) \\ +\cos(\delta)_i \cos(\emptyset) \cos(\beta) \cos(\omega)_i \\ +\ \cos(\delta)_i \sin(\emptyset) \sin(\beta) \cos(\emptyset) \cos(\omega)_i \\ +\cos(\delta)_i \sin(\beta) \sin(\emptyset) \sin(\omega)_i \end{bmatrix} \tag{7.3}$$

$$\cos(\theta_z)_i = \cos(\emptyset) \cos(\delta)_i \cos(\omega)_i + \sin(\emptyset) \sin(\delta)_i \tag{7.4}$$

The Greek term omega, ω, is the angular displacement of the sun east or west of the local meridian, and it is due to the rotation of the earth on its axis at 15 degrees per hour. The angular displacement value is calculated in radians where the morning values are negative and the afternoon values are positive by

$$\omega_i = (Solar\ Hour - 12) * 15^0 \tag{7.5}$$

The solar time, which is used in all of the sun-angle relationships, is the time based upon the rotation of the earth around the sun. When the sun is the highest in the sky, it is solar noon. The difference between standard time and solar time in minutes can be determined by

$$Solar\ Time - Standard\ Time\ = 4(L_{st} - L_{loc}) + E \tag{7.6}$$

where the equation of time, *E*, is

$$E = 229.2\begin{pmatrix} 0.000075 + 0.001868\ \cos(B) \\ -0.032077\ \sin(B) \\ -0.014615\ \cos(2B) \\ -0.04089\ \sin(2B) \end{pmatrix} \tag{7.7}$$

and B is

$$B_i = (n-1)\frac{360}{365} \tag{7.8}$$

The standard meridians, L_{ST}, for the continental U.S. time zones are: Eastern, 75°W; Central, 90°W; Mountain, 105°W; and Pacific, 120°W. The declination, δ, is the angular position of the sun with respect to the plane of the equator with north being positive at solar noon.

$$\delta_i = 23.45\ \sin\left(360\frac{284+n}{365}\right) \tag{7.9}$$

The latitude, φ, gives the location on the earth north or south of the equator which is expressed in degrees and minutes. The slope of the array surface is denoted using β. The surface azimuth angle, γ, is the deviation of the projection on a horizontal plane of the normal to the surface from the local meridian, with zero due south, east negative, and west positive [57]. This value can also be determined using a GPS device.

Any beam insolation values that were calculated and corresponded to a negative *cos*(θ) or *cos*(θ_z) were set to zero. This was done because negative values for these parameters indicate that either the sun has gone under the horizon or the sun is behind the surface so that there is no incident beam radiation on the surface.

The hourly diffuse radiation on a tilted surface was determined by

$$I_{d,T} = I_d\left(\frac{1+\cos(\beta)}{2}\right) + I\rho_{g,i}\left(\frac{1-\cos(\beta)}{2}\right) \tag{7.10}$$

The ground reflectance, ρ_g, was estimated assuming two conditions, grass and snow covered. The hourly snow depth values from the TMY2 data were used to determine if the ground was snow covered. If the snow depth for the hour was found to be greater than zero, then the ground reflectance was assumed to be 0.7; otherwise, the ground was assumed to be grass covered with an approximate ground reflectance value of 0.25. All of the hourly diffuse values that corresponded to a negative $cos(\vartheta_z)$ value were set to zero.

The total solar energy striking the array was found by the summation of the beam and diffuse components

$$I = I_{b,T} + I_{d,T} \tag{7.11}$$

The model estimates the monthly and annual energy production of the assumed photovoltaic system. Using the solar model, the solar insolation for each month and annually can be determined. A full-sun hour is an hour when the sun is emitting approximately 1000 W/m^2 (i.e., 3.6 MJ/m^2 in an hour). The daily average full-sun hours for each month are calculated by

$$\left(\frac{Average\ Full\ Sun\ Hours}{Day}\right)_m = \frac{1}{3.6\ u}\sum_{i=1}^{Hrs.in\ mo.}\left(I_{T,i}\right) \tag{7.12}$$

where I_T is in units of MJ/(hr*m^2)

The daily average full-sun hours over the entire year are calculated by

$$\frac{Average\ Full\ Sun\ Hours}{Day} = \frac{1}{1314}\sum_{i=1}^{8,760}\left(I_{T,i}\right) \tag{7.13}$$

where I_T is in units of MJ/(hr*m^2)

The efficiency of each of the components in the system is considered using de-rate factors. An overall de-rate factor is found by the product of the individual de-rate factors. The overall de-rate factor is calculated by [72]

$$Derate\ Factor\ = \begin{bmatrix} \eta_{DC\ rating} * \eta_{Inverter} * \eta_{Mismatch} * \eta_{Diodes} * \\ \eta_{DC\ wiring} * \eta_{AC\ rating} * \eta_{Soiling} * \eta_{System\ Availability} * \\ \eta_{Shading} * \eta_{Age} * \eta_{Sun\ Tracking} \end{bmatrix} \tag{7.14}$$

The user can choose to use their own de-rate factor or use the default values that are given.

Finally, the estimated energy output from the array is

$$\frac{Energy\ Produced\ (kWh)}{year} = \left(\frac{Ave.full\ sun\ hours}{day}\right)\left(\frac{365\ days}{year}\right)(kWp)(Derate\ Factor) \quad (7.15)$$

Economic Model

There are many factors that contribute to the economics of photovoltaic systems. To determine whether a particular photovoltaic system would be economical, several parameters must be considered. These parameters include, but are not limited to the following:

- Current fuel costs from a utility
- Future fuel costs from a utility
- Costs of a loan if a loan will be taken to finance the purchase of a photovoltaic system
- Tax implications to the consumer regarding a loan to finance the purchase of a photovoltaic system
- Initial cost of the photovoltaic system
- Available rebates for purchasing a photovoltaic system
- Size and annual energy output of the photovoltaic system
- Annual operating and maintenance costs of the photovoltaic system
- Operating characteristics of the inverter and modules
- Geographical location and physical configuration of the photovoltaic system
- Assumed life of the photovoltaic system

To estimate the future increase in electricity rates, predictions formulated by the National Institute of Standards and Technology (NIST) were used [49]. NIST has formulated projected fuel price indices. These price fuel indices are tabulated for inflation rates of 2, 3, 4, and 5 percent, end-use, sector, and fuel type. Given a state, assumed inflation rate, sector, and fuel type, the future cost of energy can be estimated using the NIST projections for thirty years into the future. The future fuel price indices can be used for estimating the cost of a particular fuel in year, *n*, by:

$$Future\ Fuel\ Cost_n = Current\ Fuel\ Cost\ \left(FFPI_{i,s,e,f}\right)_n \quad (7.16)$$

where the subscripts i, s, e, f, and n, represent the assumed inflation rate, sector, end-use, fuel type, and year, respectively.

Often, photovoltaic systems are financed using a loan from a bank or other financial source. The costs of a loan, and more specifically, the annual interest costs on the loan, can significantly increase the total cost and affect economics of the project. Often photovoltaic systems are purchased with an amortized

loan. An amortized loan is a loan in which the amount of interest owed for a specified period is calculated based on the remaining balance of the loan at the beginning of the period [73]. The amount paid per period on the loan is a constant amount, thus, the amount of interest paid and amount on the principal paid will vary with each payment.

Initially, the amount of money to be paid per year on a loan must be determined. The size of payment is equal to the net present value (cost) of the system separated into annual installments at the particular interest rate over the specified period of time [73]. The amount of each annual installment can be calculated by

$$a = K\left[\frac{i_T(1+i_T)^N}{(1+i_T)^N-1}\right] \tag{7.17}$$

The amount of interest paid on the first payment can be found using

$$I_{P,1} = Ki_T \tag{7.18}$$

Knowing that the annual payment is equal to the interest amount plus the principal amount of the payment, the amount of money paid on the principal for the first payment was found by

$$Pr_1 = a - I_{P,1} \tag{7.19}$$

The remainder of the balance can be determined at the end of the first year after the first payment using

$$B_1 = K - Pr_1 \tag{7.20}$$

Once the first values have been found, the remaining values for the term of the loan can be found using

$$B_n = K - (Pr_1 + Pr_2 + .. + Pr_n) \tag{7.21}$$

$$I_{P,n} = (B_{n-1})i_T \tag{7.22}$$

$$Pr_n = a - I_{P,n} \tag{7.23}$$

Tax savings can be accrued by loans put towards increasing the value of a building. The tax savings or will contribute to the overall savings of the project. The amount of tax savings available is dependent on the effective tax rate of the consumer and the average percentage rate (APR) of the loan. The amount of interest paid on the loan is tax deductible. The amount of annual tax savings can be estimated by

$$Tax\ Savings_n = Tax\ Rate\ (I_{P,n}) \tag{7.24}$$

The total tax savings for the project is the summation of the annual tax savings over the life of the loan.

$$Total\ Tax\ Savings = \sum_{n=1}^{N} Tax\ Savings_n \tag{7.25}$$

The total annual expenses would be determined by

$$Total\ Expenses_n = Loan\ Payment_n + O\&M\ Cost_n \tag{7.26}$$

While, the total annual savings would be determined by

$$Total\ Savings_n = Tax\ Savings_n + Rebate_n + Energy\ Savings_n \tag{7.27}$$

Payback period is estimated in the model and presented to the user. The payback period is useful for estimating the amount of time it takes for the investment to pay itself back or "break-even." Estimating the payback period, or the time it will take for the investment in a PV system to pay for itself, is one way to approximate the investment's attractiveness or rate of return [81]. For this research, the payback period is defined as the number of years that it takes for the accumulated savings to equal to or become greater that the accumulated expenses of the system. Thus, this analysis accounts for financing, maintenance, future energy costs/savings, and tax savings which can significantly affect the results of the analysis. If a financing is assumed, the payback period will never be less than the term of the loan.

Comparison of modeled results to experimental

In an effort to quantify the accuracy of the PV calculator, experimental performance and economics of the stationary and dual-axis tracking systems were compared to predictions made by the model. A simulation was done for each system; a summary of the inputs used for each system simulation is shown in Table 7.1.

Table 7.1. Model inputs for stationary and dual-axis tracking systems

Model inputs	Stationary	Dual-axis tracker
State	Iowa	Iowa
City	Des Moines	Des Moines
System type	Stationary	Dual-axis tracking
Array installed size (kWp)	4.59	1.02
Slope (deg.)	36	N/A
Azimuth (deg.)	0 (due south)	N/A
Module manuf.	BP Solar	BP Solar
Module model number	SX170B	SX170B
Inverter manuf.	Fronius USA, LLC	SMA America
Inverter model number	IG 2500-LV	SWR1800U
Overall derate factor	0.78	0.77
Normalized project cost ($/$W_p$)	8.98	15.83
Annual O&M (% of initial cost)	0.1	0.1
Initial rebate amount ($)	0	0
System life (years)	25	25
Electric rate ($/kWh)	0.12	0.1
Inflation rate (%)	4	4
Sector	Commercial	Commercial
Loan	No	No

Both systems were assumed to operate in Des Moines, Iowa, which is the closest location to the actual sites where TMY2 data is available. Actual system sizes, orientations, equipment, initial costs, and electric rates were used. The systems were both assumed to have a usable life of 25 years and be subjected to future energy costs of the commercial sector at an inflation rate of four percent. Additionally, the default overall derate factor calculated in the model was used for both simulations; actual annual average derate factors (i.e., performance ratios) were known but would not normally be known by a user without experimental data.

The experimental performance results and modeled predictions for the stationary and dual-axis tracking systems are presented in Table 7.2 and Table 7.3, respectively.

Table 7.2. Modeled vs. experimental solar insolation and energy generation for stationary system

Month	Solar insolation			AC energy generation		
	Modeled	Experimental	% diff.	Modeled	Experimental	% diff.
Jan	98	90	9.2	351	260	35.2
Feb	116	90	29.0	417	326	27.9
Mar	140	136	3.6	501	501	0.1
Apr	154	133	16.1	551	496	11.0
May	173	165	5.0	618	611	1.2
Jun	179	164	9.2	640	603	6.1
Jul	193	172	11.9	688	632	8.9
Aug	173	183	5.2	619	671	7.7
Sep	151	168	10.6	538	611	11.9
Oct	132	121	9.1	470	446	5.4
Nov	93	107	13.3	331	397	16.7
Dec	86	65	31.3	306	239	28.1
Annual	1690	1594	6.0	6031	5792	4.1

Annually, predictions of the model for the stationary system in terms of solar insolation and energy generation differed from experimental results by 6 and 4.1 percent, respectively.

Table 7.3. Modeled vs. experimental solar insolation and energy generation for dual-axis tracking system

Month	Solar insolation			AC energy generation		
	Modeled	Experimental	% diff.	Modeled	Experimental	% diff.
Jan	122	131	7.2	95	102	6.9
Feb	148	127	16.0	115	97	19.0
Mar	170	176	3.5	133	144	7.5
Apr	201	173	16.3	157	144	9.0
May	235	224	4.7	183	189	3.2
Jun	252	236	6.7	197	198	0.6
Jul	269	240	12.4	210	205	2.5
Aug	227	257	11.7	177	219	19.2
Sep	191	219	13.2	149	183	18.8
Oct	163	159	2.5	128	136	6.1
Nov	117	141	17.1	92	125	26.4
Dec	108	88	22.8	85	73	17.2
Annual	2205	2173	1.4	1720	1815	5.2

Annually, predictions of the model for the dual-axis tracking system in terms of solar insolation and energy generation differed from experimental results by 1.4 and 5.2 percent, respectively.

Discrepancies in performance between experimental and modeled energy generation can be attributed in part to snow cover affecting experimental performance and to differences in solar insolation. During the months each system was exposed to snow fall, greater differences were seen in energy generation. The average differences in energy generation for the stationary and dual-axis tracking systems for

months no snow fall occurred (May through October) were found to be 6.9 and 8.4 percent, respectively. However, during months snow fall occurred at the sites (January, February, March, April, November, and December) the average discrepancy in energy generation for the stationary and dual-axis tracking systems were found to be 19.8 and 14.3 percent, respectively. Additionally, trends in discrepancies can be seen between solar insolation and energy generation for both systems, as expected. For months where experimentally measured solar insolation differs greatly from predicted solar insolation, energy generation discrepancies are also found to be greater.

A summary of the economic outputs of the model is shown in Table 7.4.

Table 7.4. Summary of modeled economic outputs for stationary and dual-axis tracking system

Model outputs for economics	Stationary	Dual-axis tracker
Initial project cost ($)	$41,218.20	$16,146.60
Total lifetime cost ($)	$42,249.00	$16,550.00
Lifetime $/kWh PV	0.28	0.36
Lifetime ave. $/kWh utility	0.24	0.2
Payback period (years)	> 30	> 30

The economic outputs of the model are presented as reference; however, no experimental economic data exists over the life of the systems for comparison.

SUMMARY

Tools were developed in this work to demonstrate the performance and operation of two real-world PV systems installed in the Upper Midwest, predict the performance and economics of other grid-connected PV systems, and facilitate the dissemination and access of these tools and information to the public. The website and tools can be accessed at www.energy.iastate.edu. The use of the developed tools aims to address the general unawareness, lack of understanding, and skepticism of PV performance, operation, and reliability.

The interactive online interface and web camera interface developed in this work are particularly unique. The data interface is a custom designed tool that has the ability to display real-time and historical performance data of both systems. The interface can be used as a tool to visually monitor operation of both systems independently and simultaneously compare performance between the systems. The webcams and software interface offers the unique ability to visually observe the operation of each system and meteorological conditions the systems are subjected to while evaluating real-time

performance data through the interface. The interface and webcams offer a distinctive educational opportunity focused on PV performance.

The solar calculator developed in this work could benefit both PV professionals and consumers. This tool will enable dealers to quickly and efficiently estimate performance and economics of a proposed PV system. The user could then use the results to make an informed decision as to whether or not they are interested in pursuing the purchase and implementation of a photovoltaic system. The PV calculator was used to predict performance of the stationary and dual-axis tracking systems and results were compared to actual experimental data. Differences between modeled predictions and actual experimental results for annual energy generation for the stationary and dual-axis tracking systems were found to be 4.1 and 5.2 percent, respectively. Monthly differences in energy generation between predicted and experimental ranged from 1.2 to 35.2 percent for the stationary system and 0.6 to 26.4 percent for the dual-axis tracking systems. The discrepancies between modeled and experimental results in terms of energy generation were attributed in part to the site receiving less solar insolation that expected based on 30-year averages and to influences due to snow cover.

NOMENCLATURE

A = Area (ft^2)

a = Annual installment amount on loan ($)

Pr = Principal payment amount on loan ($)

i_T = Interest rate on loan (%)

N = Number of years in loan period, where N = 1, 2, 3, ….., 25

B = Remaining balance of loan ($)

I_P = Interest payment on loan ($)

K = Total amount of loan ($)

PV = Present value ($)

n = Denotation for year n, where n = 1, 2, 3, ….., 25

$I_{b,T}$ = Hourly beam radiation on a tilted surface (Btu/[ft^2*hr], MBtu/[ft^2*hr])

I_b = Hourly beam radiation on a horizontal surface (Btu/[ft^2*hr], MBtu/[ft^2*hr])

R_b = Ratio of beam radiation on a tilted surface to that on a horizontal surface (unitless)

θ = Angle of incidence of beam radiation on a surface (degrees, radians)

θ_Z = Zenith angle of beam radiation between vertical and the line to the sun (degrees, radians)

δ = Angular position of the sun at solar noon with respect to the plane of the equator with north positive, $-23.45^{o} < \delta > 23.45^{o}$ – declination (degrees)

ϕ = Latitude of location, $-90^{o} < \phi > 90^{o}$ (degrees)

β = Angle between the plane of the surface and the horizontal – slope (degrees)

ω = Angular displacement of the sun east or west of the local meridian at 15 degrees per hour with morning negative and afternoon positive (degrees)

γ = Deviation of the projection on a horizontal plane of the normal to the surface from the local meridian with zero due south and east negative, $-180^{o} < \gamma > 180^{o}$ (degrees)

L_{ST} = Local standard meridian (degrees west)

L_{loc} = Longitude of location, $0^{o} < L_{loc} > 360^{o}$ (degrees west)

i = Denotation for the hour of the year, where i = 1, 2, 3, ….., 8,760

$I_{d,T}$ = Hourly diffuse radiation on a tilted surface (Btu/[ft^2*hr], MBtu/[ft^2*hr])

I_d = Hourly diffuse radiation on a horizontal surface (Btu/[ft^2*hr], MBtu/[ft^2*hr])

I = Total hourly irradiation (Btu/[ft^2*hr], MBtu/[ft^2*hr])

ρ_g = Ground reflectance (unitless)

FFPI = Future fuel price indices

s = number of hours in month m, $1 \leq s \leq 744$

u = number of days in month m, $1 \leq u \leq 31$

m = general denotation for a particular month, $1 \leq m \leq 12$

ACKNOWLEDGEMENTS

The authors would like to thank the Iowa Energy Center for providing personnel, administrative, and financial support for this project. Additionally, the authors acknowledge Bill Haman, Keith Kutz, Amy Swenson, and Floyd Barwig for software and website design work. Other notable acknowledgements include Kim Topp and Abby Luhrs working under the direction and supervision of Amy Swenson for website design and implementation.

CHAPTER 8 - CONCLUSIONS

Conventional methods for energy generation using fossil-fuel based sources in the U.S. are negatively impacting our economy, national security, environment, natural resources, and public health. Additionally, negative impacts resulting from the use of fossil-fuels are intensifying due to the Nation's increasing demand of energy. Thus, the increasing demand of energy must be met while decreasing the use of fossil-fuels. Conventional energy generation methods must be reformed by using sources that are renewable, domestic, distributed, and environmentally friendly; solar-photovoltaic (PV) systems are an alternative to conventional methods for energy generation possessing these characteristics.

The use of PV technology for building energy generation is not currently widespread in the Upper Midwest. Performance of PV operating in the Upper Midwest and based on experimental efforts is not well-established. There currently exists a need for detailed experimental reliability, performance, and economic analyses of PV systems operating in the Upper Midwest's climate, reflecting what would be experienced in practice as opposed to model-based or laboratory generated simulations and predictions. In addition, surveys indicate the general public possesses little knowledge in regards to most aspects of PV; the unfamiliarity with and lack of understanding of PV technology, performance, and economics are suggested to be one reason the use of PV for building energy generation is not more widespread. There currently exists a lack of information on PV specific to the Upper Midwest that is applicable, objective, quantitative, accurate, publically available, and easily accessible. Moreover, the Upper Midwest possesses few grid-connected PV systems used for building energy generation available to the public for demonstration. Work for this project was focused to address each of these shortcomings inherent to the Upper Midwest and elsewhere.

Two grid-connected PV systems comprised of multicrystalline silicon (mc-Si) modules with different mounting schemes were installed in central Iowa for the preparation of this study; one 4.59 kW_p roof-mounted stationary system oriented for maximum annual energy production, and one 1.02 kW_p pole-mounted actively controlled dual-axis tracking system. Both systems were equipped with extensive data acquisition capable of collecting performance and meteorological data and were monitored for one year from September 2007 through August 2008. High-accuracy data was sampled at 10 second intervals and stored as one-minute averages.

Detailed experimental performance analyses were performed for both systems; results were quantified and compared between systems focusing on measures of solar resource, energy generation, power

production, and efficiency. Additionally, heat transfer characteristics of both arrays were evaluated in terms of overall heat transfer coefficients and the affects of operating temperature on PV system performance was assessed through the determination of temperature coefficients of power. To assess potential performance of PV in the Upper Midwest, models were built to predict performance of the PV systems operating at lower temperatures. System performance was simulated under two scenarios: the first scenario assumed the systems operated at the ambient air temperature and the second scenario modeled the systems operating at 5.5 ^{o}C (10 ^{o}F) above the ambient. Furthermore, economic analyses were performed for both systems focusing on measures of life-cycle cost (LLC), payback period, internal rate of return (IRR), and average incremental cost of solar energy. The potential economic feasibility of grid-connected stationary PV systems used for building energy generation and operating in the Upper Midwest was assessed using assumptions of higher utility energy costs, lower initial installed costs, and metering agreements. Economic analyses were performed for a PV system under twelve different scenarios, each having a different set of assumptions for costs and metering agreements.

Both the stationary and dual-axis tracking systems were found to operate very reliably; neither system failed for any reason during the year of monitoring. The annual average daily solar insolation seen by the stationary and dual-axis tracking systems was found to be 4.37 and 5.95 kWh/m^2, respectively. Therefore, the dual-axis tracking system harvested approximately 36 percent more solar energy than the stationary system throughout the year. In terms of energy generation, the tracking system outperformed the stationary system on annual, monthly, and often daily bases. The tracking system generated 41 percent more AC electrical energy throughout the year than the stationary system per peak Watt of installed capacity; normalized annual energy generation for the dual-axis tracking and stationary systems was found to be 1,779 and 1,264 kWh/kWp, respectively. Seasonally, the tracking system showed the most benefit in comparison to the stationary system during summer and winter months. The benefit of the tracking system in the summer and winter months is due in part to the orientation of the stationary array which is oriented for maximum *annual* energy production. In the summer months, the stationary system is oriented with less slope than optimal, and conversely in the winter months. Additionally, snow was found to affect performance of both systems; however, the tracking system was found to "shed" snow quicker than the stationary system making it less sensitive to the negative impacts of snow cover on performance. Benefits of the tracking system in terms of energy generation and power production were realized primarily during sunny conditions since the response of PV modules to diffuse solar irradiance is largely independent of module orientation. Slight seasonal variations in system efficiency were seen for both systems and can be attributed in part to variations in

average array operating temperatures and snow fall throughout the year. The annual average AC conversion efficiencies of the tracking and stationary systems were found to be approximately 11 and 10.7 percent, respectively. Annual performance ratio values (i.e., the ratio of energy yield to a reference yield assessed at rated capacity of the system) of the tracking and stationary system were found to be 0.819 and 0.792, respectively.

Throughout the year of monitoring, array operating temperatures ranged from -24.7 ^{o}C (-12.4^{o}F) to 61.7 ^{o}C (143.1 ^{o}F) for the stationary system and -23.9 ^{o}C (-11 ^{o}F) to 52.7 ^{o}C (126.9 ^{o}F) for the dual-axis tracking system during periods of system operation. Average monthly and annual operating temperatures of the two systems during daylight periods were found to be within 2 ^{o}C of each other. On a daily basis, the stationary system operated up to 6.7 ^{o}C (12.1 ^{o}F) hotter than the tracking system; however, throughout the year, daily average operating temperatures averaged to be within 1 ^{o}C (1.8^{o}F) of each other. Additionally, the stationary system was found to operate at higher average array temperatures relative to ambient air temperatures at levels of solar irradiance greater than approximately 120 W/m^{2}. At a solar irradiance of 1,000 W/m^{2} the stationary system operated on average 9.3 ^{o}C (16.7 ^{o}F) degrees hotter than the tracking system relative to ambient air temperature.

The hourly average overall heat transfer coefficients considering data sampled for solar irradiance levels greater than 200 W/m^{2} for the stationary and dual-axis tracking systems throughout the year of monitoring were found to be 20.8 and 29.4 W/m^{2o}C, respectively. The experimental temperature coefficients for power for the stationary and dual-axis tracking systems at a solar irradiance level of 1,000 W/m^{2} were -0.30 and -0.38 %/^{o}C, respectively, which are lower than the manufacture's specified value for the modules used. Simulations of the stationary and dual-axis tracking systems operating at lower temperatures suggest that annual conversion efficiency could potentially be increased by to up approximately 4.3 and 4.6 percent, respectively.

Initial costs of the stationary system totaled $41,218 dollars ($8.98 dollars per W_p); whereas initial costs of the dual-axis tracking system totaled $16,147 dollars ($15.83 dollars per W_p). Experimental first-year energy savings for the stationary and dual-axis tracking systems totaled $679 and $177 dollars ($148 and $174 dollar per kW_p), respectively. The life-cycle cost of each system was calculated using three different discount rates: the first representing general inflation, the second essentially representing a risk-free investment and the last indicative of long-term liquidity and risk one may be subjected to in competitive market conditions. However, the net present values of both systems under all assumed discount rates were determined to be negative. Further, neither system was found to have a payback

period less than the assumed system life of 25 years. The rate-of-return of the stationary and tracking systems were found to be -3.3 and -4.9 percent, respectively. Furthermore, the average incremental cost of energy provided by the stationary system over its useful life is projected to be $0.31 dollars per kWh, compared to an estimated average of $0.19 dollars per kWh of electrical energy supplied by the utility. Approximated incremental costs of solar energy provided by the dual-axis tracking system over its useful life is projected to be $0.37 per kWh, which is more than twice the cost of electrical energy provided by the utility at an estimated $0.16 dollars per kWh.

Economic analyses suggest that an investment in a stationary grid-connected PV system used for building energy generation and operating in the Upper Midwest could show economic feasibility for scenarios assuming relatively higher incremental energy costs and lower installed costs, or under a direct-feed metering agreement with production-based incentives. Considering only the scenarios assumed, results indicate payback periods may be attained within the assumed life of the system for incremental energy costs of 0.15 $/kWh or higher and initial costs of 7 $/$W_p$ or lower under net metering agreements. However, attaining acceptable paybacks of 6 to 10 years may require initial costs of 5 $/$W_p$ or lower and direct-feed metering with associated feed-in tariffs of 0.50 $/kWh or better. The analysis also indicates that in order to obtain rates of return competitive with inflation, treasury bills, or the general market, incremental energy costs may need to be 0.20 $/kWh or higher with initial installed costs of 5 $/$W_p$ or lower or under direct-feed agreements with feed-in tariffs of 0.50 $/kWh or higher.

In summary, economic analyses performed in this work suggest that grid-connected PV systems used for building energy generation in the Upper Midwest are not yet economically feasible when compared to a range of alternative investments; however, PV could show feasibility under more favorable economic scenarios. Poor economic results for the stationary and dual-axis tracking systems are primarily due to high initial costs of PV, relatively low incremental costs of utility supplied electrical energy, and insufficient financial incentives for the implementation and/or operation of PV systems.

Information on PV, the results of this work, as well as the tools developed in this work will be disseminated to a large and diverse audience through a publically available website. Comprehensively, the information available is likely to be understandable for someone not familiar with PV yet technical and extensive enough that it would be beneficial to those practicing/involved in the field (e.g., engineers, architects, contractors, instructors, realtors, developers, etc.). The interactive online interface developed in this work is particularly unique. The interface is a custom designed tool that has the ability to display real-time and historical performance data of both systems. The interface can be

used as a tool to visually monitor the operation of both systems and simultaneously compare performance between the systems. The webcams and software interface offer the unique ability to visually observe the operation of each system and meteorological conditions the systems are subjected to while evaluating real-time performance data through the interface. The interface and webcams offer a distinctive educational opportunity focused on PV performance and operation.

The solar calculator developed in this work could benefit both PV professionals and consumers. This tool will enable efficient estimates of the performance and economics of a proposed PV system. The user could then use the results to make an informed decision as to whether or not they are interested in pursuing the purchase and implementation of a photovoltaic system. The PV calculator was used to predict performance of the stationary and dual-axis tracking systems and results were compared to actual experimental data. Differences between modeled predictions and actual experimental results for annual energy generation for the stationary and dual-axis tracking systems were found to be 4.1 and 5.2 percent, respectively. Monthly differences in energy generation between predicted and experimental results ranged from 1.2 to 35.2 percent for the stationary system and 0.6 to 26.4 percent for the dual-axis tracking systems. The discrepancies between modeled and experimental results in terms of energy generation were attributed in part to the site receiving less solar insolation that expected based on 30-year averages and to influences due to snow cover.

Results found in this work can be used to set appropriate expectations for real-world PV systems operating in the Upper Midwest. Practicing professionals could use the results of this study to better understand PV systems which could lead to better system selection, more intelligent system design, and improved system integration/installation. The installed PV systems, online information, and tools developed in this work will provide excellent means for demonstrational and educational purposes. Increasing awareness of PV and further educating the social, academic, and scientific communities may lead to a more widespread use of PV. Consequently, negative impacts resulting from conventional methods of energy generation using fossil-fuel based sources may be reduced.

CHAPTER 9 - FUTURE WORK

This work focused on PV systems operating for one year in the Upper Midwest using multicrystalline silicon (mc-Si) modules, which based on their common use are considered to be the standard for residential and commercial building energy generation applications. Additional work could be done quantifying and comparing the performance and economics of systems utilizing other types of available PV technologies such as thin-film or building-integrated PV products. Additionally, studies could be performed assessing long-term operating and maintenance requirements and costs, reliability, and performance degradation of PV systems.

The stationary system is designed as three side-by-side, identical, and independently operating sub-systems. This unique design offers the opportunity to assess the effects of a particular variable introduced to one or more subsystems by simultaneously comparing performance in real-time to the other(s) operating in the same environment. Future studies could focus on the affects of shading or soiling, for example. Additionally, the tracking system can be controlled as a single-axis tracker; studies could be carried out to quantify performance of single-axis trackers operating in the Upper Midwest.

Temperature coefficients experimentally determined in this work were found to be sensitive to solar irradiance levels. This result has been previously observed in past studies of systems operating outdoors and potential reasons for this finding have been identified. Indoor testing of PV modules indicates temperature coefficients can be considered constant for systems operating under normal conditions. Future work could include evaluating potential sources of error in experimental measurement between indoor and outdoor testing.

The primary purpose of the website is to offer accessible, understandable, and applicable information and tools regarding PV to the general public. The information, demonstration units, and developed tools are offered to increase awareness, understanding, and acceptance of PV in the Upper Midwest and elsewhere. Additional work could include assessing the impact of these efforts through surveys or other means to determine if the awareness and acceptance of PV was increased.

The performance and economic models as well as the graphical user interface built for the PV calculator could be further developed. Future work could include further validation of the model against other experimental studies and/or data sets and also improving the model to yield more accurate results. The scope of the model could be expanded to include non-grid connected systems with battery backup, single-axis trackers, etc.

APPENDIX A - BID SPECIFICATIONS FOR DESIGN/BUILD OF STATIONARY PV SYSTEM

Bid specifications developed based on *Technical and General Bid Requirements* written by the Florida Solar Energy Center and can be accessed at: http://www.fsec.ucf.edu/en/consumer/solar_electricity/assistance/documents/EXAMPLESPECIFICATIONS.pdf

1. GENERAL INFORMATION

1.1 These design/build specifications cover the design and procurement of equipment, hardware, software, documentation, labor and supervision required for the installation of one (1) PV system as part of the Livingston South L.L.C. (Owner) Photovoltaic (PV) project.

1.2 Bids must list all the equipment necessary to complete the system installation. In addition, documentation on the designs, configurations, installations, operation and maintenance of the complete system must be included.

1.3 The system shall be designed for outdoor installation in the Central Iowa area. Central Iowa is subject to long-term high humidity and extreme temperature conditions. Annual ambient temperatures can range from -25° F to 105° F. Supplied equipment at the site must be rated and warranted to withstand and operate under these conditions.

1.4 The system to be installed shall have the following characteristics:

Location:	2521 Elwood Drive in Ames, Iowa.
System Type:	Grid-connected
Storage Devices:	None
Size:	The PV system should be sized to deliver approximately 7,950 kWh directly to the utility annually
Mounting:	Stationary array to be mounted onto the existing metal standing-seamed roof on the south side of the building atrium (see pictures in Appendix)

1.5 A total of one (1) PV system, as stated above, is to be quoted.

1.6 The stationary panels at Southgate shall be mounted onto the south face of the atrium metal standing-seamed roof.

1.7 The PV system will be connected directly to Alliant Energy's utility electric grid through a grid-interactive power conditioner (inverter).

1.8 The contractor is responsible for all commissioning duties and the system is to be fully functional upon the contractor's completion of work.

1.9 The Owner must be notified if it is necessary to deviate from the bid specifications in any way.

1.10 The contractor is encouraged to visit the Southgate site prior to submitting a bid on the project. A site-visit can be scheduled by contacting Ryan Warren at 515-294-8819 (work), 515-975-5064 (cell) or rwarren@iastate.edu (e-mail).

1.11 The professional engineer to perform the building structural analysis for the roof loading will be specified and paid for by the Owner outside the requirements of this contract.

1.12 For any technical and/or administrative questions contact Ryan Warren at 515-294-8819 (work), 515-975-5064 (cell) or rwarren@iastate.edu (e-mail).

1.13 It is in the interest of the owner to have the system installed and operating in a timely manner; completion date (to be specified in the project schedule) may be considered in the evaluation of the bids.

1.14 The Owner reserves the right to reject any or all bids received. Non-acceptance of a bid will mean that another was deemed more advantageous to the Owner or that all bids were rejected.

1.15 This request for quotation does not commit the Owner to award a contract or to pay any costs incurred in the submission of bids, or costs incurred in making necessary studies for the preparation thereof, or to procure or contract for services or supplies.

1.16 The Contractor shall secure and pay for all permits, governmental fees and licenses necessary for the proper execution and completion of the Work[1].

1.17 The Contractor shall at all times keep the site of the Work and adjacent premises as free from materials, debris, rubbish, and trash as practicable. The Owner will supply sufficient space in the parking area of the building for material and job trailer.

1.18 At the completion of the Work, the Contractor shall remove all materials, implements, barricades, equipment, debris and rubbish connected with or caused by operations for such work immediately upon the completion of that work and shall leave the premises in perfect condition insofar as affected by the work under this Contract.

1.19 The Contractor warrants to the Owner that all materials and equipment furnished under this Contract will be new unless otherwise specified and that all work will be of good quality, free from faults and defects and in conformance with the Contract Documents. All work not conforming to these standards including substitutions not authorized as provided elsewhere in the Contract Documents may be considered defective.

1.20 A contract Change Order is a written order to the Contractor issued after the award of the Contract, authorizing a change in the Work or an adjustment in the Contract Sum or the Contract Time. No change or additional work is authorized unless approved by the Owner. The Contract Sum and the Contract Time may be changed only by Contract Change Order.

1.20.1 The Owner, without invalidating the Contract, may order changes in the Work within the general scope of the Contract consisting of additions, deletions or other revisions, with the Contract Sum and the Contract Time being adjusted accordingly. All such changes in the Work shall be authorized by the Contract Change Order and shall be performed under the applicable conditions of the Contract Documents.

1.20.2 The cost or credit of the Owner resulting from a change in the Work shall be determined in one or more of the following ways:

- by mutual acceptance of a lump sum properly itemized and supported by sufficient substantial data to permit evaluation;

[1] Work is defined as the completed construction required by the Contract Documents and includes all labor necessary to produce such construction and all materials and equipment incorporated or to be incorporated in such construction.

- by cost to be determined in a manner agreed upon by the parties and a mutually acceptable fixed fee.

1.21 When the Contractor considers the work complete, notification is to be made to the Owner. An inspection to verify the status of completion will be made with reasonable promptness.

1.21.1 Should the work be considered incomplete or defective, the Contractor will be notified in writing, listing the incomplete or defective work. The Contractor shall take immediate steps to remedy the stated deficiencies.

1.22 The Owner may withhold payment in whole or in part to the extent necessary to reasonably protect the Owner. Partial or full payment could be withheld due to the following reasons:

- defective work not remedied;
- reasonable evidence that the work cannot be completed for the unpaid balance of the contract sum;
- unsatisfactory prosecution of the work by the contractor;
- damage to the Owner or another contractor

1.23 The contractor will be required to provide a Performance and Payment Bond in the full amount of this contract.

2. PV MODULE AND ARRAY SPECIFICATIONS

2.1 The overall size of the array is a consideration. The PV modules should be framed flat-plate crystalline/amorphous silicon modules. Thin-film modules will not be considered for this project.

2.2 The PV array to be installed at Southgate (stationary orientation) should be sized to deliver approximately 7,950 kWh of energy per year directly to the utility company (i.e. as would be measured at the system's point of common coupling).

2.3 The PV modules shall meet or exceed the requirements of Underwriter Laboratories (UL) Standard 1703 Standard for Safety for Flat-Plate Photovoltaic Modules and either IEEE Standard 1262-1995 IEEE Recommended Practice for Qualification of Photovoltaic (PV) Modules and Panels or IEC 1215 Crystalline Silicon Terrestrial Photovoltaic (PV) Modules- Design Qualification and Type Approval.

2.4 Each PV module shall include bypass diodes installed in the module junction box.

2.5 Each PV module shall be warranted by the manufacturer for at least 90% of its rated power at 10 years and 80% of its rated power at 20 years from the date of system acceptance.

3. POWER CONDITIONING EQUIPMENT SPECIFICATIONS

3.1 The power conditioning system (PCS) shall be designed specifically for utility grid interconnection of photovoltaic arrays and be capable of automatic, continuous, and stable operation over the range of voltages, currents, and power levels for the size and type of array used.

3.2 An interconnection agreement with the utility is the responsibility of Livingston South. The contractor should allow for time in the project schedule for Alliant Energy's approval of the interconnection agreement.

3.3 Each PCS shall be compliant with IEEE Std. 929-2000 (Recommended Practice for Utility Interface of Photovoltaic Systems) and have UL1741 (Standard for Static Inverters and Charge Controllers for Use in Photovoltaic Power Systems). The PCS shall also comply with IEEE Std. 519 (Recommended Practices and Requirements for Harmonic Control in Electrical Power Systems) and the latest applicable ANSI and FCC standards and addenda dated prior to the award of the purchase order for this procurement.

3.4 Each PCS must have an automatic visual indicator showing whether the system is on-line or not.

3.5 Each PCS must have at least a two-year repair or replacement warranty from the manufacturer covering parts and labor.

3.6 Each PCS shall be installed within Southgate's electrical room. Alternate installation locations will be considered if offered by the contractor.

3.7 The power conditioning system shall have output signals and displays for the instantaneous power production (in watts or kilowatts) and accumulated energy production (kilowatt-hours) to a data acquisition system which will update a web-interface display in real-time Further, additional output signals for DC volts and current to the power conditioning system is preferred.

4. SYSTEM INSTRUMENTATION

4.1 The following instrumentation (customer supplied) is to be installed at Southgate:

- One (1) temperature sensor for outdoor-air dry-bulb temperature
- Six (6) temperature sensors mounted to the back-side of selected modules for module operating temperature
- One (1) pyranometer for total solar irradiance striking the array

4.2 Instrumentation specification sheets for the customer supplied instruments are available to the contractor upon request.

5. DATA COLLECTION

5.1 The data points shall be collected and stored in the following time increments:

- Outdoor air temperature – 15 seconds
- Wind speed – 1 minute (value is to be an average value of all readings taken in the one-minute time interval)
- Wind direction – 1 minute (value is to be an average value of all readings taken in the one minute time interval
- Solar irradiation – 1 second
- Module temperatures – 15 second
- Instantaneous power production – 1 second

5.2 Data shall be stored on the Iowa Energy Center's network in a Microsoft SQL Server database.

5.3 Data point sample intervals can be manually adjusted instantaneously by the operator and independent of other data points.

6. REAL-TIME WEB DISPLAY

6.1 The contractor will be responsible for delivering and commissioning a web-interface software package that will display weather data and array performance in real-time. This interface must be capable of displaying the weather data and array performance data from two separate systems on a single display: the system at Southgate and from a remote system located at the Iowa Energy Center's Biomass Energy Conversion Center (BECON) in Nevada, Iowa. The data fields that will be monitored and then displayed in real-time via the Internet shall include, but is not limited to:

- Outdoor-air dry-bulb temperature from BECON system (^{o}F)
- Wind-speed (mph) from BECON system
- Wind direction from BECON system (N, NE, E, SE, S, SW, W, or NW)
- Total incident solar irradiation from BECON system (W/m^2)
- Total incident solar irradiation from Southgate system (W/m^2)
- Instantaneous power production from BECON system (Kw)
- Instantaneous power production from Southgate system (Kw)
- Instantaneous power production per unit area from BECON system (W/ft^2)
- Instantaneous power production per unit area from Southgate system (W/ft^2)
- Cumulative energy production from BECON system (kWh)
- Cumulative energy production from Southgate system (kWh)

6.2 Where necessary internal links to or within interface software shall be written to open a new browser window. Pop-ups are unacceptable.

6.3 Software shall be written in any of the following languages: ASP, JavaScript, or Cold Fusion. Other languages may be considered upon proposal.

6.4 The web-display shall be updated in a time interval that permits viewing to appear continuous and real-time without flicker or delays.

6.5 The web-display shall be capable of displaying two types of charts if requested by a user; (i) a power generation and solar irradiance line graph and a monthly and annual energy generation bar chart. All plots shall be in color.

6.6 The web-display shall be capable of displaying the charts for both the Southgate system and BECON system. The capability of displaying a single plot at a time is sufficient.

6.7 The power generation and solar irradiance line graph shall have identical axis magnitudes for both power generation and solar irradiance. The maximum axis magnitude for the power generation and solar irradiance curves shall be the installed capacity of the system (in Kw) and 1000 W/m^2, respectively. All data for both plot types shall be archived for trend presentation. The trending shall be available at various timescales (e.g., daily, monthly, annually, etc.). A daily example of this plot can be seen in Figure 1.

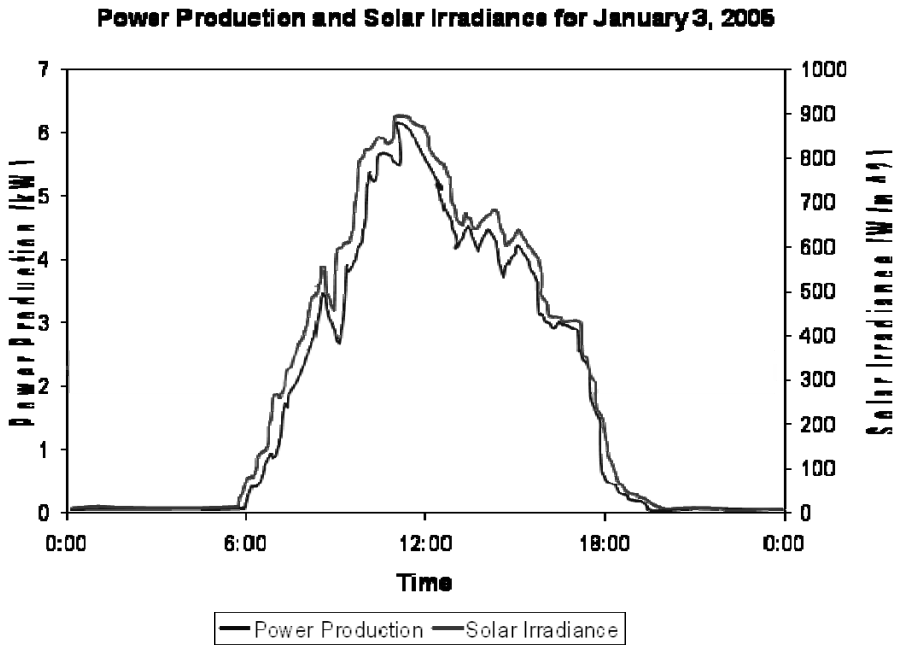

Figure A.1. Example of acceptable power production line graph

6.4 The energy production bar chart shall graph bars with values equal to the amount of energy production for each time period of the particular overall time period specified by the user. All data shall be archived for data presentation. The trending shall be available at various timescales (e.g., daily, monthly, annually, etc.). All energy production shall be expressed in units of kWh. An example of the energy production bar chart can be seen in Figure 2.

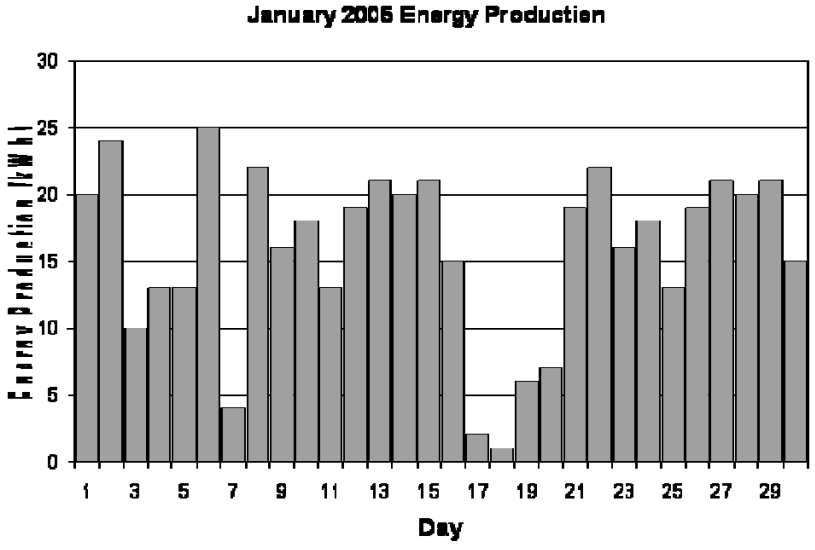

Figure A.2. Example of acceptable energy production bar chart

6.9 The contractor shall provide references and examples of at least four (2) separate similar web-interfaces to that of this project.

7. PV SYSTEM ELECTRICAL DESIGN

7.1 The electrical design and installation instructions for the PV systems shall conform to the most recent edition of the National Electric Code (NFP A 70). Article 690 of the NEC applies specifically to photovoltaic system safety, protection, control and interface with other sources. Other articles of the NEC also apply. The PV system electrical design shall also comply with the IEEE Std. 1374-1998 (Guide for Terrestrial Photovoltaic Power System Safety).

7.2 All electrical components, including overcurrent protection, disconnect, surge suppression devices, conduit, wiring and terminals must have UL or equivalent listing and have appropriate voltage, current and temperature ratings for each application. Special attention should be given to appropriate ratings for components used in the DC circuits.

7.3 All wiring shall be listed for a minimum operation of 600 volts and temperature rating of 90° C in wet locations. All current carrying conductors must be enclosed in conduit, including module interconnections.

7.4 Ampacity calculations must take into account appropriate de-ratings as required. All conductors in each system are subject to a 125% NEC de-rate, and all DC source circuit conductors and overcurrent devices must include an additional 125% de-rate for solar irradiation enhancement. Appropriate temperature de-ratings for conductors used in module junction boxes must be considered for peak module operating temperatures, as well as de-ratings for instances where more than three current-carrying conductors are enclosed in a conduit.

7.5 Voltage drop in array DC source circuits should be limited to no more than five percent (5%), including losses in conductors and through all fuses, blocking diodes, and termination points.

7.6 All overcurrent devices shall have trip ratings no greater than the de-rated ampacity of the conductors that it protects.

7.7 All series connected strings of modules (also known as panels, or source circuits) must include a series fuse as required by UL and NEC. Parallel-connected cells within individual modules are allowable as long as the module listing allows for the series fuse required for this configuration.

7.8 All series connected strings of modules (source circuits) must also include a blocking diode to prevent reverse currents. These diodes should have a low voltage drop to meet the requirements above, and have voltage and current ratings (at the design temperature) at least twice the open-circuit voltage and short-circuit ratings of the source circuits.

7.9 Array ground-fault protection devices should be included as part of the PCS packages. These devices must be capable of detecting array ground faults, shunting the fault current to ground, and disabling the array until the fault has been cleared.

7.10 All terminations must use listed box terminal or compression type connections. Twist on wire splices, crimped, soldered or taped connections are not permitted for the required field installed wiring. Proper torque specifications should be provided for all of the required field connections.

7.11 All module frames, panel/array support structures, metal enclosures, panel boards and the PCS cabinet should be provided with connections for bonding to a common grounding conductor and terminating at the ground rod at the utility service entrance point. In addition, provisions for grounding the neutral of the PCS output shall be provided. The DC negative circuit may be common to the AC neutral in the PCS design and under no circumstances should multiple connections to ground be specified for current carrying conductors in the system.

7.12 Loss of Line: Each PCS shall not operate without the line voltage present. Each PCS shall sense a “loss of line” (utility) condition and shall automatically disconnect from the line. In the event of multiple PCSs and/or balanced load on a common line, the PCS shall contain circuits (such as Sandia Voltage Shift and Sandia Frequency Shift) that will cause the PCS voltage or frequency to drift downwards under loss of line conditions and cause it to cease energizing the grid within two seconds after loss of line. The PCS restart shall occur automatically after restoration of line voltage and frequency within five minutes.

7.13 Each PCS shall be capable of completely automatic operation, including “wake-up,” “sleep” mode and shutdown after loss of utility power. In the automatic mode, the PCS shall monitor the available PV array power and voltage, and when the appropriate amount of power is available and the array voltage is within the normal starting voltage, the wake-up sequence shall be initiated. The PCS shall monitor the AC line voltage and frequency and, when the AC voltage is within the normal operating range and the frequency is between 59.5 and 60.5 Hz, the synchronization process shall be initiated prior to establishing line-tie. The DC power source

and/or the AC circuit may remain connected in the “sleep” mode to provide monitoring and instrumentation power during nighttime operation.

8. PV ARRAY MECHANICAL DESIGN

8.1 The Contractor shall provide the roof mounting for the array in a manner that is acceptable with the Owner. The Contractor shall provide all necessary mechanical hardware for mounting the photovoltaic array. The Contractor shall provide all other hardware required for assembling the photovoltaic modules and panels and structurally attaching them to the standing-seam roof.

8.2 The PV array, including modules, hardware and attachments shall be designed to withstand wind loads of 70 mph and comply with all existing local and national codes.

8.3 Array mounting hardware supplied by the bidder should be compatible with the site considerations and environment. Special attention should be paid to minimizing the risk from exposed fasteners, sharp edges, and potential damage to the modules or support structure. All fasteners shall be stainless steel and the support structure shall be aluminum for corrosion resistance and durability. The use of ferrous metals, wood or plastic components will be prohibited.

8.4 As these are high profile, educationally promoted, and publicly visible installations, the aesthetics of the overall installation is extremely important to Livingston South. To create a uniform appearance of the array, spacing between recurring roof members should be kept to a minimum. As much as possible, all mechanical hardware, conduit, junction boxes and other equipment should be concealed beneath and/or behind the array.

8.5 The array layout should be consistent with the ordering (and labeling) of source circuits in the array combiner boxes. Ease of access for array troubleshooting and maintenance is desired by allowing access to the combiner box.

8.6 A maximum of one (1) roof penetration will be allowed.

9. INFORMATION TO BE SUPPLIED WITH BID

9.1 The bid documentation must include, but not limited to, the following information for the bid to be considered responsive:

9.1.1 The bid shall include the total bid price, design cost, materials cost, and labor costs.

9.1.2 The bid shall include the required lead-time for delivery of equipment and a project schedule (Section 11.1).

9.1.3 Warranty information on individual components.

9.1.4 Proof of any relevant certifications, accreditations, qualifications, experience and/or licenses (with license number, type, and expiration date if applicable) of the contractor. In addition, a reference list of past photovoltaic projects designed and/or installed by the contractor should also be included. This section also applies to a subcontractor, if used, for the software development of the data collection and web-interface Work.

10. INFORMATION TO BE PROVIDED BY CONTRACT AWARDEE DURING CONSTRUCTION AND AFTER PROJECT COMPLETION

10.1 Shop drawings shall be provided to Livingston South prior to the system installation for review and approval. These documents shall include:

- Documentation on PV modules and inverter
- Complete parts list including all electrical components, mechanical hardware, and other equipment required for installing the system
- Drawing of roof penetration (if a roof penetration is to be made)
- Drawing layout of web-interface screen

10.2 The Contractor is responsible for providing two complete copies of all installation, operations and maintenance manuals.

10.3 As-built diagrams indicating overall layout of entire system, including PV array, and location of BOS hardware and PCS with respect to the array.

10.4 An acceptance test must be performed on the system once the installation is complete. This includes measuring the short circuit currents and open-circuit voltages on all source circuits while measuring irradiance and module temperature. This also includes measuring the instantaneous DC input and AC output of the system to determine its efficiency.

10.5 A copy of the permit obtained from the appropriate legal authority for system installation.

10.6 A copy of the minimum two-year system warranty including parts and labor.

10.7 Procedure for commissioning, operating, disconnecting, servicing and maintaining complete system and individual components.

10.8 Overview of major system components.

11. PROJECT SCHEDULE

11.1 The project schedule submitted with the bid shall include the amount of time required to complete each phase of the project in addition to a completion date for all of the Work describe within this bid document. Project schedule can be stated from time of utility agreement acceptance.

12. CONTRACTORS LIABILITY INSURANCE

12.1 The contractor shall have and maintain until final acceptance, Comprehensive General Liability Insurance and Automobile Liability Insurance in the amount not less than One Million Dollars ($1,000,000.00). This insurance shall cover injuries, including accidental death, to any one person and subject to the same limit for each person, and in an amount not less than One Million Dollars ($1,000,000.00) on account of any one occurrence. Property Damage Liability Insurance shall be in the amount not less than One Million Dollars ($1,000,000.00). Such insurance shall protect the Contractor from claims for bodily injury or property damage which may arise out of or result from the Contractor's operations under the Contract, whether such operations be by the Contractor or by any Subcontractor of by anyone directly or indirectly employed by any of them or by anyone for whose acts any of them may be liable, including but not limited to:

1. claims under workers' or workmen's compensation disability benefit and other similar employee benefit acts;

2. claims for damages because of bodily injury, occupational or otherwise sickness or disease or death of any person other than Contractor's employees;

3. claims for damages insured by usual personal injury liability coverage which are sustained (i) by any person as a result of an offense directly or indirectly related to the employment of such person by the Contractor or (ii) by any other person;

4. claims for damages, other than to the Work itself; because of injury to or destruction of tangible property, including loss of use resulting there from;

5. claims for damages because of bodily injury or death of any person or property damage arising out of the ownership, maintenance or use of any motor vehicle.

12.2 The Contractor shall either (i) require each Subcontractor, to procure and to maintain during the life of each Subcontract, Subcontractor's Liability Insurance of the type and in the same amounts as specified in this section or (ii) insures the activities of Subcontractors in the Contractor's own policy.

12.3 The contractor shall automatically renew policies which expire during the course of construction and notify the Owner of such renewal.

APPENDIX B - SCOPE OF WORK FOR DESIGN/BUILD OF PV SYSTEM AT BECON LOCATION

Bid specifications developed based on *Technical and General Bid Requirements* written by the Florida Solar Energy Center and can be accessed at: http://www.fsec.ucf.edu/en/consumer/solar_electricity/assistance/documents/EXAMPLESPECIFICATIONS.pdf

1. GENERAL INFORMATION

1.1 These design/build specifications cover the design and procurement of equipment, hardware, documentation, labor and supervision required for the installation of one (1) PV system as part of the Iowa Energy Center Photovoltaic (PV) project.

1.2 Quote should include the equipment and labor necessary to complete the system installation with the exception of the power conditioner (SMA1800U), foundation design and construction, and trenching from foundation structure to building.

1.3 Owner will be responsible for purchasing the power conditioning equipment.

1.4 Owner will be responsible for the design and construction of the foundation and mounting pole.

1.5 Owner will be responsible for the trenching work from the foundation structure to building.

1.6 Quote should include documentation on the design, configuration, installation, operation and maintenance of the complete system.

1.7 The system to be installed shall have the following characteristics:
Location: 1521 West F Avenue Nevada, Iowa.

System Type: Grid-connected

Storage Devices: None

Size: 1.02 kWp

Modules: Six (6) model #: BP SX 170B solar modules

Inverter: Sunny Boy 1800U (provided by Owner)

Mounting: 2-axis tracking mount

Tracker: Wattsun® Solar Tracker AZ-125 for six (6) BP SX 170B modules with the following additional options:

- Dual-axis tracking
- Manual controls
- IDEC PS5R-SF24 power supply
- Position feedback.

1.8 The system shall be designed for outdoor installation in the Central Iowa area. Central Iowa is subject to long-term high humidity and extreme temperature conditions. Annual ambient temperatures can range from -25° F to 105° F. Supplied equipment at the site must be rated and warranted to withstand and operate under these conditions.

1.9 A total of one (1) PV system, as stated above, is to be quoted.

1.10 The PV system will be connected directly to Alliant Energy's utility electric grid through a grid-interactive power conditioner (Owners responsibility to obtain agreement).

1.11 The Contractor is responsible for all commissioning duties and the system is to be fully functional upon the contractor's completion of Work[2].

1.12 The Owner must be notified if it is necessary to deviate from these specifications in any way.

1.13 For any technical and/or administrative questions contact Ryan Warren at 515-975-5064 (cell) or rwarren@iastate.edu (e-mail).

1.14 No construction permits are required for the BECON site.

1.15 The Contractor shall secure and pay for all governmental fees and licenses necessary for the proper execution and completion of the Work1.

[2] Work is defined as the completed construction required by the Contract Documents and includes all labor necessary to produce such construction and all materials and equipment incorporated or to be incorporated in such construction.

1.16 The Contractor shall at all times keep the site of the Work and adjacent premises as free from materials, debris, rubbish, and trash as practicable. The Owner will supply sufficient space in the parking area of the building for material and job trailer.

1.17 At the completion of the Work, the Contractor shall remove all materials, implements, barricades, equipment, debris and rubbish connected with or caused by operations for such work immediately upon the completion of that work and shall leave the premises in perfect condition insofar as affected by the work under this Contract.

1.18 The Contractor warrants to the Owner that all materials and equipment furnished under this Contract will be new unless otherwise specified and that all work will be of good quality, free from faults and defects and in conformance with the Contract Documents. All work not conforming to these standards including substitutions not authorized as provided elsewhere in the Contract Documents may be considered defective.

1.19 When the Contractor considers the work complete, notification is to be made to the Owner. An inspection to verify the status of completion will be made with reasonable promptness.

1.19.1 Should the work be considered incomplete or defective, the Contractor will be notified in writing, listing the incomplete or defective work. The Contractor shall take immediate steps to remedy the stated deficiencies.

2. PV MODULE AND ARRAY SPECIFICATIONS

2.1 Each PV module shall include bypass diodes installed in the module junction box.

2.2 Each PV module shall be warranted by the manufacturer for at least 90% of its rated power at 10 years and 80% of its rated power at 20 years from the date of system acceptance.

3. POWER CONDITIONING EQUIPMENT SPECIFICATIONS

3.1 An interconnection agreement with the utility is the responsibility of the Iowa Energy Center – ISU.

3.2 Each PCS shall be installed within BECON's electrical room. Alternate installation locations will be considered if offered by the contractor.

4. PV SYSTEM ELECTRICAL DESIGN

4.1 The electrical design and installation instructions for the PV systems shall conform to the most recent edition of the National Electric Code (NFP A 70). Article 690 of the NEC applies specifically to photovoltaic system safety, protection, control and interface with other sources. Other articles of the NEC also apply. The PV system electrical design shall also comply with the IEEE Std. 1374-1998 (Guide for Terrestrial Photovoltaic Power System Safety).

4.2 All electrical components, including overcurrent protection, disconnect, surge suppression devices, conduit, wiring and terminals must have UL or equivalent listing and have appropriate voltage, current and temperature ratings for each application. Special attention should be given to appropriate ratings for components used in the DC circuits.

4.3 All wiring shall be listed for a minimum operation of 600 volts and temperature rating of 90° C in wet locations. All current carrying conductors must be enclosed in conduit, including module interconnections.

4.4 Ampacity calculations must take into account appropriate de-ratings as required. All conductors in each system are subject to a 125% NEC de-rate, and all DC source circuit conductors and overcurrent devices must include an additional 125% de-rate for solar irradiation enhancement. Appropriate temperature de-ratings for conductors used in module junction boxes must be considered for peak module operating temperatures, as well as de-ratings for instances where more than three current-carrying conductors are enclosed in a conduit.

4.5 Voltage drop in array DC source circuits should be limited to no more than five percent (5%), including losses in conductors and through all fuses, blocking diodes, and termination points.

4.6 All overcurrent devices shall have trip ratings no greater than the de-rated ampacity of the conductors that it protects.

4.7 All series connected strings of modules must include a series fuse as required by UL and NEC. Parallel-connected cells within individual modules are allowable as long as the module listing allows for the series fuse required for this configuration.

4.8 All series connected strings of modules (source circuits) must also include a blocking diode to prevent reverse currents. These diodes should have a low voltage drop to meet the requirements above, and have voltage and current ratings (at the design temperature) at least twice the open-circuit voltage and short-circuit ratings of the source circuits.

4.9 Array ground-fault protection devices should be included as part of the PCS packages. These devices must be capable of detecting array ground faults, shunting the fault current to ground, and disabling the array until the fault has been cleared.

4.10 All terminations must use listed box terminal or compression type connections. Twist on wire splices, crimped, soldered or taped connections are not permitted for the required field installed wiring. Proper torque specifications should be provided for all of the required field connections.

4.11 All module frames, panel/array support structures, metal enclosures, panel boards and the PCS cabinet should be provided with connections for bonding to a common grounding conductor and terminating at the ground rod at the utility service entrance point. In addition, provisions for grounding the neutral of the PCS output shall be provided. The DC negative circuit may be common to the AC neutral in the PCS design and under no circumstances should multiple connections to ground be specified for current carrying conductors in the system.

4.12 Loss of Line: Each PCS shall not operate without the line voltage present. Each PCS shall sense a "loss of line" (utility) condition and shall automatically disconnect from the line. In the event of multiple PCSs and/or balanced load on a common line, the PCS shall contain circuits (such as Sandia Voltage Shift and Sandia Frequency Shift) that will cause the PCS voltage or frequency to drift downwards under loss of line conditions and cause it to cease energizing the grid within two seconds after loss of line. The PCS restart shall occur automatically after restoration of line voltage and frequency within five minutes.

4.13 Each PCS shall be capable of completely automatic operation, including "wake-up," "sleep" mode and shutdown after loss of utility power. In the automatic mode, the PCS shall monitor the available PV array power and voltage, and when the appropriate amount of power is available and the array voltage is within the normal starting voltage, the wake-up sequence shall be initiated. The PCS shall monitor the AC line voltage and frequency and, when the AC voltage is within the normal operating range and the frequency is between 59.5 and 60.5 Hz, the synchronization process shall be initiated prior to establishing line-tie. The DC power source and/or the AC circuit may remain connected in the "sleep" mode to provide monitoring and instrumentation power during nighttime operation.

5. PV ARRAY MECHANICAL DESIGN

5.1 The Contractor shall provide all necessary mechanical hardware for mounting the photovoltaic array. The Contractor shall provide all other hardware required for assembling the photovoltaic modules and panels and structurally attaching them to the tracker.

5.2 The PV array, including modules, hardware and attachments shall be designed to withstand wind loads of 70 mph and comply with all existing local and national codes.

5.3 Array mounting hardware supplied by the bidder should be compatible with the site considerations and environment. Special attention should be paid to minimizing the risk from exposed fasteners, sharp edges, and potential damage to the modules or support structure. All fasteners shall be stainless steel and the support structure shall be aluminum for corrosion resistance and durability. The use of ferrous metals, wood or plastic components will be prohibited.

5.4 As these are high profile, educationally promoted, and publicly visible installations, the aesthetics of the overall installation is extremely important to the Iowa Energy Center. As much as possible, all mechanical hardware, conduit, junction boxes and other equipment should be concealed beneath and/or behind the array.

5.5 The array layout should be consistent with the ordering (and labeling) of source circuits in the array combiner boxes. Ease of access for array troubleshooting and maintenance is desired by allowing access to the combiner box.

6. INFORMATION TO BE SUPPLIED WITH QUOTE

6.1 Please include the following information with the quote documentation:

6.1.1 The quote shall include the total price, design cost, materials cost, and labor costs.

6.1.2 The quote shall include the required lead-time for delivery of equipment and a project schedule (Section 8.1).

6.1.3 Warranty information on individual components.

7. INFORMATION TO BE PROVIDED BY CONTRACTOR DURING CONSTRUCTION AND AFTER PROJECT COMPLETION

7.1 Shop drawings shall be provided to the Iowa Energy Center prior to the system installation for review and approval. These documents shall include complete parts list including all electrical components, mechanical hardware, and other equipment required for installing the system

7.2 As-built diagrams indicating overall layout of entire system, including PV array, and location of BOS hardware and PCS with respect to the array.

7.3 An acceptance test must be performed on the system once the installation is complete. This includes measuring the short circuit currents and open-circuit voltages on all source circuits while measuring irradiance and module temperature. This also includes measuring the instantaneous DC input and AC output of the system to determine its efficiency.

7.4 A copy of the permit obtained from the appropriate legal authority for system installation.

7.5 A copy of the minimum two-year system warranty including parts and labor.

7.6 Procedure for commissioning, operating, disconnecting, servicing and maintaining complete system and individual components.

7.7 Overview of major system components.

8. PROJECT SCHEDULE

8.1 A project schedule to include the amount of time required to complete each phase of the project in addition to a completion date for all of the Work described within. Project schedule can be stated from time of utility agreement acceptance

APPENDIX C - WEB CAMERA SPECIFICATIONS

As previously discussed, the Iowa Energy Center is in the process of procuring and installing two web/network cameras. These cameras will be used to view the PV installations real-time at the Southgate and BECON locations. We would like you to quote us a price and time schedule for designing and implementing an interface for these cameras for the Energy Center's website. Quality Attributes would be responsible for everything but the physical installation of the hardware. Please incorporate the following characteristics and functionality into the quote:

- The webcam interface shall be separate (i.e., different webpage) from the real-time interface showing performance data.

- The webcam interface shall be a tab structure with a similar look and feel to the real-time interface showing performance data. There should be two tabs; one tab shall be labeled "Stationary System" and the other tab shall be labeled "Dual-Axis Tracking System".

- The webcam interface shall have similar functionality capabilities to ISU's Facilities Planning and Management's Memorial Union North webcam. This webcam can be viewed at http://www.fpm.iastate.edu/webcam/mu2/.
    - The webcam interface should not have options for both "Live Photo" and "Large Photo" as seen on example. Interface shall default to a larger image similar to what is seen in example, "Large Photo".
    - The webcam interface should not have size options for "Live Video". Interface should show live video as a larger size.
    - Photo Archive shall have the ability to show images from the current day back one week prior (i.e., seven calendar days). Each day shall archive images for 6 am, 8 am, 10 am, 12 pm, 2 pm, 4 pm, 6 pm, 8 pm, and 10 pm.
    - The interface shall allow user to download two types of movies, both daily and monthly. The daily movies shall show one frame at least every 5 minutes for the entire day (i.e., 24 hours). Daily movies shall be archived for a one week period (i.e., 7 days). Daily movies shall be updated daily.

- Navigation shall be setup so that when the user presses "Back" on the browser the user is taken back to the introduction or linked page.

- Buttons (instead of tabs) shall be used for the following:
    - Live Photo
    - Live Video
    - Photo Archive
    - Movies

- Time and date stamp shall be shown at the top of photo and video similar to example.

The camera that we will be using is the Axis 211. More information about the camera can be found at http://www.axis.com/products/cam_211/index.htm.

APPENDIX D - CONSTRUCTION CONTRACT

Construction contract developed based on template purchased at:

http://www.urgentbusinessforms.com

This Construction Agreement (Agreement) is hereby made and entered into this _____ day of _____, 2006, by and between Livingston South, L.L.C. (Owner), and Energy Engineering Solutions (Contractor).

WHEREAS

The Contractor has represented to the Owner that the Contractor has the necessary qualifications, experience and abilities to provide services to the Owner.

The Owner is agreeable to engaging the services of the Contractor, on the terms and conditions as set out in this Agreement

IN CONSIDERATION OF the matters described above and of the mutual benefits and obligations set forth in this Agreement, the receipt and sufficiency of which consideration is hereby acknowledged, the parties to this Agreement agree as follows:

SECTION ONE

STRUCTURE AND SITE

Contractor shall furnish all labor and materials necessary to construct a photovoltaic and data acquisition system with web-interface as specified within the Bid Specifications for Design/Build of PV System document upon the following described property, which owner warrants he owns, free and clear of liens and encumbrances.

The property is located at:

2521 Elwood Drive

Ames, Iowa 50010-8229

Tenant: Iowa Energy Center

2521 Elwood Drive Suite 124

Ames, Iowa 50014-8229

SECTION TWO

PLANS

Contractor shall construct the structure in conformance with the plans, specifications, and breakdown and binder receipt signed by contractor and owner, and will do so in a workmanlike manner. Contractor is not responsible for furnishing any improvements other than the structure, such as landscaping, grading, walkways, painting, etc., unless they are specifically stated in the breakdown.

SECTION THREE

PAYMENT

The Owner hereby agrees to pay the Contractor, for the aforesaid materials and labor, the sum of seventy-one thousand three hundred and twenty-five Dollars ($ 71,325), subject to adjustments for changes in the work as may be agreed upon by the Owner and the Contractor, or as may be required under this Agreement, in the following manner:

> Owner shall pay Contractor an initial amount of fifty-seven thousand five hundred and seventy-five Dollars ($57,575) within 5 business days of the agreement of this contract. This payment will cover the following expenses: One-hundred percent (100%) of equipment and materials required for the work and fifty percent (50%) of the labor costs for the data acquisition and web-interface work.
>
> Owner shall pay Contractor the remaining Contract sum of thirteen thousand seven hundred and fifty Dollars ($13,750) upon completion of the work. This final payment will be made within 5 business days of the completion of the work and Owner and tenant approval of the work. This payment will cover all other and remaining expenses not covered in the initial payment.

In the event the final payment is not paid within ten (10) days after it is due, contractor may take such action as may be necessary, including legal proceedings, to enforce its rights hereunder.

SECTION FOUR

PREPARATION

Prior to the start of construction, owner shall provide a clear and accessible building site. In the event contractor cannot obtain a building permit within thirty (30) days of the date of this agreement, contractor may declare the agreement of no further force or effect.

SECTION FIVE

UTILITIES

Prior to the start of construction, and at all times during construction, owner shall provide and maintain, at owner's sole expense, an all-weather roadway to the building site, and water and electrical service.

SECTION SIX

RESPONSIBILITY / INDEMNITY

Contractor shall not be responsible for damages to persons or property occasioned by owner or his agents, third parties, acts of God or other causes beyond contractor's control. Owner shall hold contractor completely harmless from, and shall indemnify contractor for, all costs, damages, losses, and expenses, including judgments and attorneys fees, resulting from claims arising from causes enumerated in this paragraph.

SECTION SEVEN

FINANCING

Owner agrees to promptly complete the necessary requirements to obtain financing and to prepare the site for construction.

SECTION EIGHT

FORCE MAJEURE

Neither party shall be considered in default of this Agreement or be liable for damages, for any failure of performance hereunder occasioned by an act of God, force of nature, inclement weather, war or warlike activity, insurrection or civil commotion, labor dispute, transportation delay, governmental regulatory

action whether or not with proper authority or other cause similar or dissimilar to the foregoing and beyond its reasonable control, provided the party so affected gives prompt notice to the other.

SECTION NINE

GENERAL

9.1 Assignment

Neither the Owner nor Contractor shall have the right to assign any rights or interest occurring under this agreement without the written consent of the other, nor shall the Contractor assign any sums due, or to become due, to him under the provisions of this agreement.

9.2 Termination

The Owner shall have the right to terminate the work for any reason, upon notice in writing to the Contractor. Should the Owner exercise this right in accordance with the terms of this Agreement, Contractor shall be paid its actual costs for the portion of work performed to the date of termination and for all incurred costs of termination, including but not limited to demobilization and any termination charges by vendors and subcontractors.

9.3 Notice

Any notice or other communication required or permitted hereunder shall be in writing and shall be deemed given and received on the date of delivery or on the third (3rd) business day following the day of mailing of the same, or on the day of fax transmission or other form of recorded communication service of the same, as the case may be to the party to be notified at the addresses set forth below:

If to Owner:
Paul A. Livingston
3108 Roxboro Drive
Ames, Iowa 50010

If to Contractor:
Energy Engineering Solutions
26050 200th Street
Leon, Iowa 50144
Attn: Todd Blanton

or such other address as may be designated by either party by written notice to the other as hereinabove provided.

9.4 Relationships

The parties are independent contractors, and nothing in this Agreement shall be deemed or construed to create, or have been intended to create a partnership, joint venture, employment or agency relationship between the parties. Each party agrees that it neither has nor will give the appearance or impression of possessing the legal authority to bind or to commit any other party in any way except as provided in this Agreement.

9.5 Interpretation

This Agreement has been fully reviewed and negotiated by the parties and their respective legal counsel. Accordingly, in interpreting this Agreement, no weight shall be placed upon which party or its counsel drafted the provision being interpreted.

9.6 Modification

No provision of this Agreement or the documents referred to in Sections Two and Three may be modified, waived or amended except by a written instrument duly executed by each of the parties.

9.7 Counterparts

This Agreement may be executed in two or more counterparts, each of which shall be deemed an original but all of which together shall constitute one and the same instrument.

9.8 Waiver

Any failure on the part of either party to insist upon the performance of this Agreement or any part of this Agreement, shall not constitute a waiver of any right under this Agreement.

9.9 Survival

All representations made herein shall survive the termination of this Agreement and shall remain in full force and effect. All of a party's rights and privileges, to the extent they are fairly attributable to events or conditions occurring or existing on or prior to the termination of this Agreement, shall survive termination and shall be enforceable by such party and its successors and assigns.

9.10 Attorney fees

Attorney's fees and court costs shall be paid by the defendant in the event that judgment must be, and is, obtained to enforce this agreement or any breach thereof.

9.11 Entire Agreement

This Agreement represents the entire agreement between the Contractor and the Owner regarding the work described herein, and supersedes any prior written or oral agreements, contracts or representations as to that work. There are no understandings or agreements between contractor and owner other than those set forth in this agreement and in the documents referred to in Sections Two and Three (including the bid specifications).

9.12 Own Will

The parties have entered into this Agreement in their own will and no statement, representation or promise has been made to induce either party to enter into this agreement

9.13 Confidentiality

Except as otherwise required by applicable federal and state securities laws, each party shall keep the information regarding the details of this Agreement confidential

9.14 Headings

Headings are inserted for the convenience of the parties only and are not to be considered when interpreting this Agreement.

9.15 Gender

Words in the singular mean and include the plural and vice versa. Words in the masculine mean and include the feminine and vice versa.

9.16 Severability

If any provision of this Agreement is held to be or becomes invalid, illegal, or unenforceable, such provision or provisions shall be reformed to approximate as nearly as possible the intent of the parties, and the remainder of this Agreement shall not be affected thereby and shall remain valid and

enforceable to the greatest extent permitted by law.

9.17 Choice of Law

The substantive laws of the State of Iowa applicable to contracts shall govern (i) the validity and interpretation of this Agreement, (ii) the performance by the parties of their respective obligations hereunder, and (iii) all other causes of action (whether sounding in contract or in tort) arising out of or relating to this Agreement or the termination of this Agreement.

9.18 Project Schedule

The contractor shall supply a project schedule with an estimated completion date to the Owner prior to beginning work.

IN WITNESS WHEREOF, the parties hereto set their hands and seals the day and year written above.

OWNER'S NAME:_____

OWNER'S ADDRESS:_____

_____

OWNER'S PHONE NUMBER_____

OWNER'S SIGNATURE:_____

CONTRACTOR’S NAME:_____

CONTRACTOR'S ADDRESS:_____

_____

CONTRACTOR’S LICENSE NUMBER:_____

CONTRACTOR’S PHONE NUMBER:_____

CONTRACTOR'S SIGNATURE:_____

APPENDIX E - CONTRACTOR CONTRACT

Contractor contract developed based on template purchased at:

http://www.urgentbusinessforms.com

This Construction Agreement (Agreement) is hereby made and entered into this _____ day of _____, 2006, by and between Livingston South, L.L.C. (Owner), and Energy Engineering Solutions (Contractor).

WHEREAS

The Contractor has represented to the Owner that the Contractor has the necessary qualifications, experience and abilities to provide services to the Owner.

The Owner is agreeable to engaging the services of the Contractor, on the terms and conditions as set out in this Agreement

IN CONSIDERATION OF the matters described above and of the mutual benefits and obligations set forth in this Agreement, the receipt and sufficiency of which consideration is hereby acknowledged, the parties to this Agreement agree as follows:

1. Services

1.1 The Contractor agrees to provide all of the material and labor required to perform the work described in the Bid Specifications for Design/Build of PV System document. An agreement of the work detailed in the Bid Specifications for Design/Build of PV System document is identified by the signatures of the parties to this agreement and which form a part of this agreement.

2. Payment

2.1 The Owner hereby agrees to pay the Contractor, for the aforesaid materials and labor, the sum of seventy-one thousand three hundred and twenty-five Dollars ($ 71,325), subject to adjustments for changes in the work as may be agreed upon by the Owner and the Contractor, or as may be required under this Agreement, in the following manner:

Owner shall pay Contractor an initial amount of fifty-seven thousand five hundred and seventy-five Dollars ($57,575) within 5 business days of the agreement of this contract.

This payment will cover the following expenses: One-hundred percent (100%) of equipment and materials required for the work and fifty percent (50%) of the labor costs for the data acquisition and web-interface work.

Owner shall pay Contractor the remaining Contract sum of thirteen thousand seven hundred and fifty Dollars ($13,750) upon completion of the work. This final payment will be made within 5 business days of the completion of the work and Owner approval of the work. This payment will cover all other and remaining expenses not covered in the initial payment.

2.2 If any payment is not made to Contractor as required under Paragraph 2.1 of this Agreement, Contractor may suspend work until such payment is made.

3. Time frame

3.1 The Contractor agrees that the various portions of the above-described work shall be completed on or before the following schedule:

Table E.1. Project schedule

Task Description or Project Milestone:	Time from project start:
Project Kick Off / Initial Design Meeting	1 week
Initial Content Worksheet Due From Client	3 weeks
Proof Development	4 weeks
Final Design Meeting	4 weeks
Final Content Worksheet Due From Client	5 weeks
Control System Data Available To QAS	5 weeks
Graphics Development	6 weeks
Shell On Test Site	6 weeks
Installation	14 weeks
Development Complete	15 weeks
Testing Complete	16 weeks
Verification	16 weeks
Acceptance Period	16 weeks to 20 weeks

and the entire above-described work shall be completed no later than twenty (20) weeks from the date of the project kick off / initial design meeting.

4. Materials

4.1 The Contractor agrees to provide and pay for all materials, tools and equipment required for the prosecution and timely completion of the work. Unless otherwise specified, all materials shall be new and of good quality.

5. Quality

5.1 In the prosecution of the work, the Contractor shall employ a sufficient number of workers skilled in their trades to suitably perform the work. Contractor warrants to the Owner that all materials and equipment under this Agreement shall be new unless otherwise specified and that all work will be performed in a good and workmanlike manner, shall be of good quality and shall conform to all Contract conditions and documents.

5.2 The Contractor agrees to re-execute any work which does not conform to the drawings and specifications, warrants the work performed, and agrees to remedy any defects resulting from faulty materials or workmanship which shall become evident during a period of one year after completion of the work.

6. Time

6.1 Time is of the essence of this Agreement. Should Owner request it, the Contractor shall provide the Owner with a progress and completion schedule and shall conform to that schedule, including any changes to that schedule agreed to between the Owner and the Contractor under Paragraph 7 of this Agreement or required by circumstances beyond Contractor's control.

7. Changes and deviations

7.1 All changes and deviations in the work ordered by the Owner must be in writing, the Agreement sum being increased or decreased accordingly by the Contractor. Any claims for increases in the cost of the work must be presented by the Contractor to the Owner in writing, and written approval of the Owner shall be obtained by the Contractor before proceeding with the ordered change or revision. Should an adjustment in the Agreement price be required because of errors in the plans and/or specifications, differing site conditions, lack of worksite access or other circumstances beyond the Contractor's control, the Contractor shall submit to the Owner a detailed estimate of the change to the Agreement price and the Agreement time. The Contractor shall not be obligated to perform changes in the work or additional work until the Owner has approved, in writing, the changes to the Agreement price and the Agreement time.

8. Access

8.1 The Owner, Owner's representative and public authorities shall at all times have access to the work. The Owner shall provide all necessary access to the lands upon which the work is to be performed, including access to the lands and any other lands designated herein for use by the Contractor for the purpose of completion of the work described herein. Any failure to provide such access shall entitle the Contractor to an equitable adjustment in the Agreement price and Agreement time set forth herein.

9. Insurance/Indemnity

9.1 The Owner agrees to maintain full insurance on the above-described work during the progress of the work, in his own name and that of the Contractor. Contractor shall indemnify the Owner against any and all claims, demands, lawsuits and liabilities arising out of or connected to property damage or personal injury caused, or alleged to be cause, by Contractor or its subcontractors, suppliers, employees, agents or representatives. Contractor shall not be obligated to defend Owner beyond the extent of Contractor's insurance.

9.2 The Contractor agrees to obtain insurance to protect himself against claims for property damage, bodily injury or death due to his performance of this agreement.

10. Force Majeure

10.1 In the event the Contractor is delayed in the prosecution of the work by acts of God, fire, flood or any other unavoidable casualties; or by labor strikes, late delivery of materials; or by neglect of the Owner; the time for completion of the work shall be extended for the same period as the delay occasioned by any of the aforementioned causes.

11. Delay

11.1 In the event the work is delayed due to neglect of the Contractor, the Contractor agrees to pay the Owner the sum of zero dollars and zero cents ($0.00) per day as liquidated damages until such time as the work is completed.

12. Assignment

12.1 Neither the Owner nor Contractor shall have the right to assign any rights or interest occurring under this agreement without the written consent of the other, nor shall the Contractor assign any sums due, or to become due, to him under the provisions of this agreement.

13. Termination

13.1 The Owner shall have the right to terminate the work for any reason, upon notice in writing to the Contractor. Should the Owner exercise this right in accordance with the terms of this Agreement, Contractor shall be paid its actual costs for the portion of work performed to the date of termination and for all incurred costs of termination, including but not limited to demobilization and any termination charges by vendors and subcontractors.

14. Notice

14.1 Any notice or other communication required or permitted hereunder shall be in writing and shall be deemed given and received on the date of delivery or on the third (3rd) business day following the day of mailing of the same, or on the day of transmission by fax machine or other form of recorded communication service of the same, as the case may be to the party to be notified at the addresses set forth below:

If to Owner:
Paul A. Livingston
3108 Roxboro Drive
Ames, Iowa 50010

If to Contractor:
Energy Engineering Solutions
26050 200th Street
Leon, Iowa 50144
Attn: Todd Blanton

or such other address as may be designated by either party by written notice to the other as hereinabove provided.

15. Relationships

15.1 The parties are independent contractors, and nothing in this Agreement shall be deemed or construed to create, or have been intended to create a partnership, joint venture, employment or agency relationship between the parties. Each party agrees that it neither has nor will give the appearance or impression of possessing the legal authority to bind or to commit any other party in any way except as provided in this Agreement.

16. Interpretation

16.1 This Agreement has been fully reviewed and negotiated by the parties and their respective legal counsel. Accordingly, in interpreting this Agreement, no weight shall be placed upon which party or its counsel drafted the provision being interpreted.

17. Modification

17.1 No provision of this Agreement may be modified, waived or amended except by a written instrument duly executed by each of the parties.

18. Counterparts

18.1 This Agreement may be executed in two or more counterparts, each of which shall be deemed an original but all of which together shall constitute one and the same instrument.

19. Waiver

19.1 Any failure on the part of either party to insist upon the performance of this Agreement or any part of this Agreement, shall not constitute a waiver of any right under this Agreement.

20. Survival

20.1 All representations made herein shall survive the termination of this Agreement and shall remain in full force and effect. All of a party's rights and privileges, to the extent they are fairly attributable to events or conditions occurring or existing on or prior to the termination of this Agreement, shall survive termination and shall be enforceable by such party and its successors and assigns.

21. Attorney fees

21.1 Attorney's fees and court costs shall be paid by the defendant in the event that judgment must be, and is, obtained to enforce this agreement or any breach thereof.

22. Entire Agreement

22.1 This Agreement and the Bid Specifications for Design/Build of PV System document represents the entire agreement between the Contractor and the Owner regarding the work described herein, and supersedes any other prior written or oral agreements, contracts or representations as to that work.

23. Confidentiality

23.1 Except as otherwise required by applicable federal and state securities laws, each party shall keep the information regarding the details of this Agreement confidential.

24. Headings

24.1 Headings are inserted for the convenience of the parties only and are not to be considered when interpreting this Agreement.

25. Gender

25.1 Words in the singular mean and include the plural and vice versa. Words in the masculine mean and include the feminine and vice versa.

26. Severability

26.1 If any provision of this Agreement is held to be or becomes invalid, illegal, or unenforceable, such provision or provisions shall be reformed to approximate as nearly as possible the intent of the parties, and the remainder of this Agreement shall not be affected thereby and shall remain valid and enforceable to the greatest extent permitted by law.

27. Own Will

27.1 The parties have entered into this Agreement in their own will and no statement, representation or promise has been made to induce either party to enter into this agreement.

28. Choice of Law

28.1 The substantive laws of the State of Iowa applicable to contracts shall govern (i) the validity and interpretation of this Agreement, (ii) the performance by the parties of their respective obligations hereunder, and (iii) all other causes of action (whether sounding in contract or in tort) arising out of or relating to this Agreement or the termination of this Agreement.

IN WITNESS WHEREOF, the parties hereto set their hands and seals the day and year written above.

OWNER'S NAME:_____

OWNER'S ADDRESS:_____

_____

OWNER'S PHONE NUMBER_____

OWNER'S SIGNATURE:_____

CONTRACTOR’S NAME:_____

CONTRACTOR'S ADDRESS:_____

_____

CONTRACTOR’S LICENSE NUMBER:_____

CONTRACTOR’S PHONE NUMBER:_____

CONTRACTOR'S SIGNATURE:_____

APPENDIX F - UNCERTAINTY IN EXPERIMENTAL MEASUREMENTS

Experimental measurement errors can be divided into two categories: errors due to the physical hardware that is performing the measurement (e.g., linearity, repeatability, hysteresis, sensitivity, distortion, responsiveness, etc.), and errors due to the placement/installation of this hardware. In addition, after the measurement is taken by the instrument, the signal from the sensor could be subject to error caused by distortion due to the wiring and physical terminations, the accuracy of the transducer converting the signal, the accuracy of analog to digital conversion, and the ability of the software to process, display, and record the signals.

An uncertainty analysis was performed to specifically quantify the expected error in the experimental measurements taken to characterize the performance of the stationary and dual-axis tracking PV systems. An experimental result, which will be denoted by *F*, is determined from a set of independently measured parameters, x_i, where i = 1 to n with n denoting the number of measurements used to calculate *F*.

$$F = f(x_1, x_2, \dots, x_n) \tag{F.1}$$

The uncertainty in an experimental measurement, δF, based on a set of measured variables, where each measurement has an associated error, can be found by

$$\delta F = \left[\left(\frac{\partial F}{\partial x_1}\delta x_1\right)^2 + \left(\frac{\partial F}{\partial x_2}\delta x_2\right)^2 + \cdots + \left(\frac{\partial F}{\partial x_n}\delta x_n\right)^2\right]^{1/2} \tag{F.2}$$

where, δx_i denotes the uncertainty in the measured variable x_i.

The uncertainty of measurement for each instrument used for data sampling is shown in Table F.1.

Table F.1. Instrument specifications

System	Measurement	Operating Range	Accuracy
Stationary	AC current to utility	0 – 10 AAC	0.5% of full scale
	DC current to inverter	0 – 5 ADC	1% of full scale
	AC voltage to utility	0 – 300 VAC	0.5% of full scale
	DC voltage to inverter	0 – 400 VDC	0.5% of full scale
	Module temperatures	0 – 260 ^{0}C (0 – 500 ^{0}F)	$\pm$0.083 ^{0}C at 0 ^{0}C ($\pm$0.15^0 F at 32 ^{0}F)
	Ambient air temperature	0 – 260 ^{0}C (0 – 500 ^{0}F)	$\pm$0.083 ^{0}C at 0 ^{0}C ($\pm$0.54^0 F at 32 ^{0}F)
	Solar irradiance	0 – 1,500 W/m^2	Temp: $\pm$1% from -20 – 40 ^{0}C (-4 – 104 ^{0}F) Linearity: $\pm$5% from 0 – 1,500 W/m^2 Cosine: $\pm$1% from 0^0 – 70^0 or $\pm$3%
	Wind speed	1 – 100 m/s (2.2 – 224 mph)	$\pm$ 0.27 m/s ($\pm$0.6 mph) or 1% of reading
	Wind direction	355^0 electrical	$\pm$3^0
Dual-axis tracking	AC current to utility	0 – 10 AAC	0.5% of full scale
	DC current to inverter	0 – 5 ADC	1% of full scale
	AC voltage to utility	0 – 150 VAC	0.5% of full scale
	DC voltage to inverter	0 – 300 VDC	0.5% of full scale
	Module temperatures	0 – 260 ^{0}C (0 – 500 ^{0}F)	$\pm$0.083 ^{0}C at 0 ^{0}C ($\pm$0.15^0 F at 32 ^{0}F)
	Ambient air temperature	0 – 260 ^{0}C (0 – 500 ^{0}F)	$\pm$0.083 ^{0}C at 0 ^{0}C ($\pm$0.54^0 F at 32 ^{0}F)
	Solar irradiance	0 – 1,500 W/m^2	Temp: $\pm$1% from -20 – 40 ^{0}C (-4 – 104 ^{0}F) Linearity: $\pm$5% from 0 – 1,500 W/m^2 Cosine: $\pm$1% from 0^0 – 70^0 or $\pm$3%

DC Power

The DC power, P_{DC}, generated by the PV array is calculated as the product of DC voltage, V_{DC}, and DC current, I_{DC} by

$$P_{DC} = V_{DC}\, I_{DC} \tag{F.3}$$

The uncertainty of the DC power generated by the PV array is then expressed as

$$\delta P_{DC} = \left[\left(\frac{\partial P_{DC}}{\partial I_{DC}}\delta I_{DC}\right)^2 + \left(\frac{\partial P_{DC}}{\partial V_{DC}}\delta V_{DC}\right)^2\right]^{1/2} \tag{F.4}$$

The uncertainty of DC power was determined for each system with Equation F.4 being used to determine the uncertainty in each array; however, the stationary system is comprised of three independent sub-systems. Given this design characteristic, an extra step was required to determine the uncertainty in system power output. The uncertainty in DC power output for the stationary system was determined by

$$\delta P_{DC} = \left[\left(\frac{\partial P_{DC}}{\partial P_{DC,inv\,1}}\delta P_{DC,inv\,1}\right)^2 + \left(\frac{\partial P_{DC}}{\partial P_{DC,inv\,2}}\delta P_{DC,inv\,2}\right)^2 + \left(\frac{\partial P_{DC}}{\partial P_{DC,inv\,3}}\delta P_{DC,inv\,3}\right)^2\right]^{1/2} \tag{F.5}$$

The uncertainty in DC power verses system DC power output for the stationary and dual-axis tracking systems can be seen in Figure F.1 and Figure F.2, respectively.

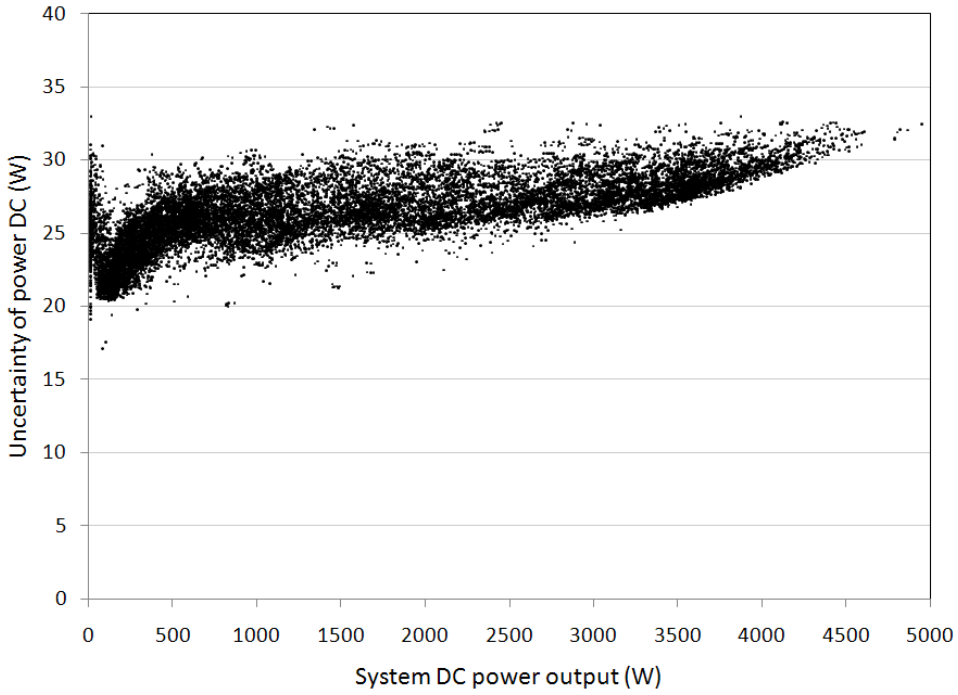

Figure F.1. Stationary system uncertainty of DC power vs. DC power output

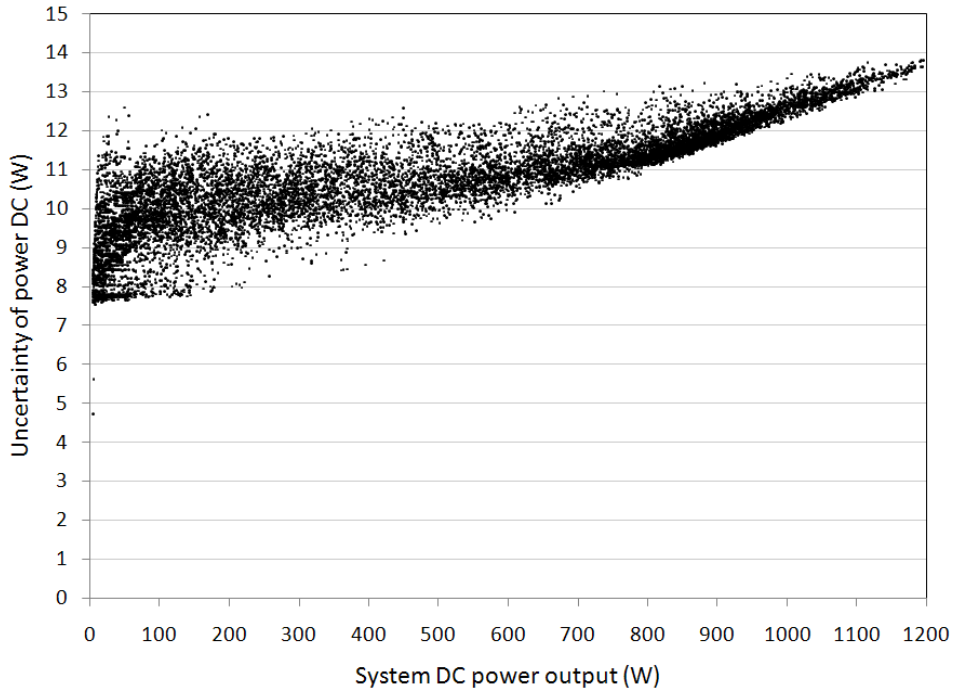

Figure F.2. Dual-axis tracking system uncertainty of DC power vs. DC power output

The uncertainty was also calculated in terms of a percentage of the system power output. Plots for the percentage of uncertainty in the DC power output verses the system DC power output for the stationary and dual-axis tracking systems can be seen in Figure F.3 and Figure F.4, respectively.

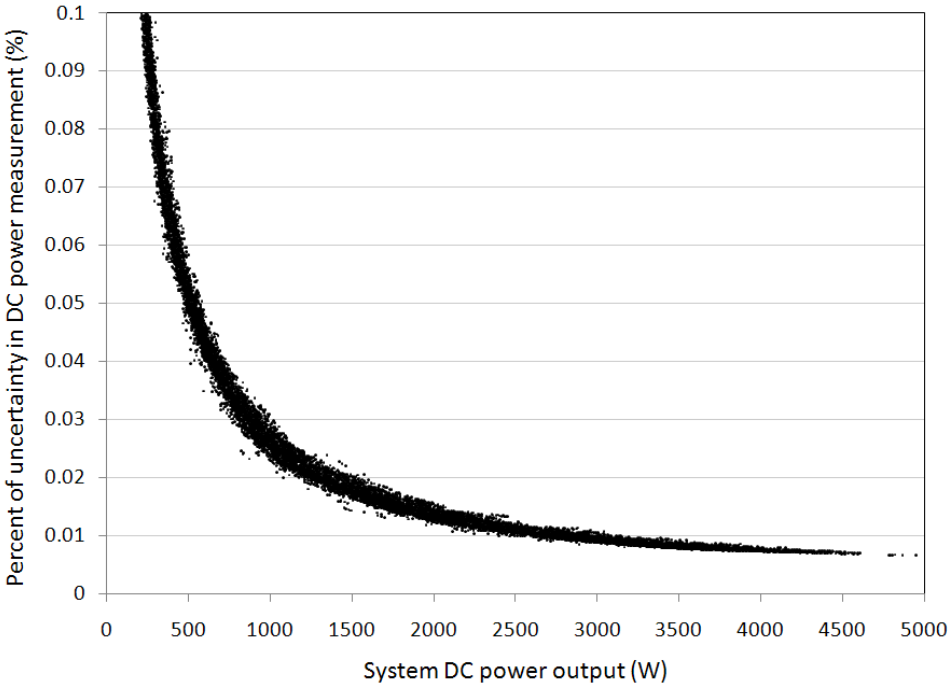

Figure F.3. Stationary system percent of uncertainty in DC power vs. DC power output

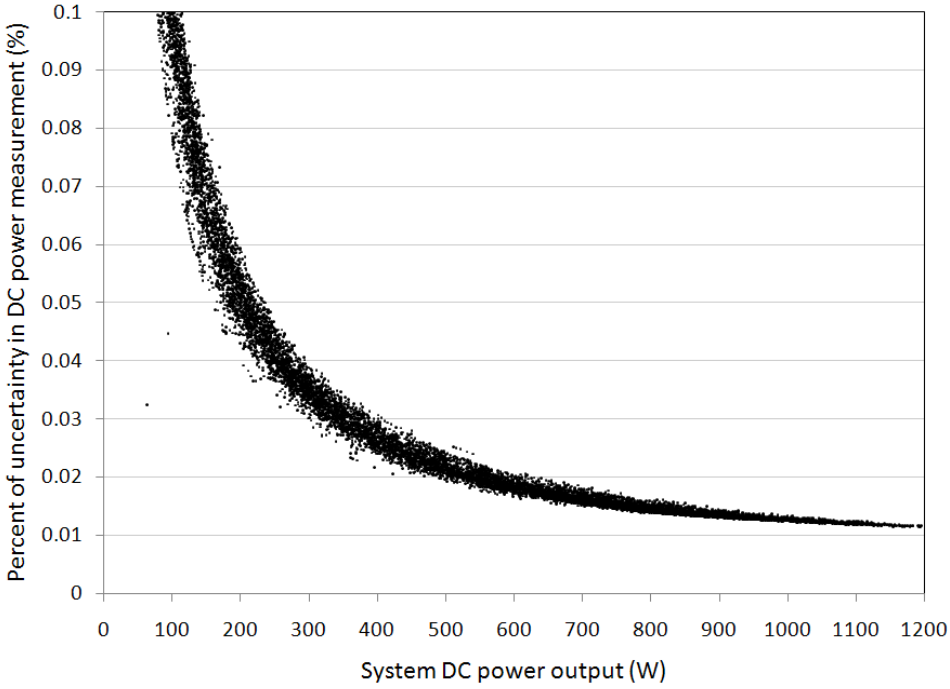

Figure F.4. Dual-axis tracking system percent of uncertainty in DC power vs. DC power output

DC Energy

The uncertainty in DC energy generation can be determined directly by knowing the uncertainty in DC power. The measured DC power and uncertainty in DC power for each data point was converted into an

energy generation value and then summed monthly and annually, as shown in Table F.2 and Table F.3, respectively for the stationary and dual-axis tracking systems.

Table F.2. Uncertainty in monthly and annual energy generation of stationary system

Month	Measured energy generation (kWh)	Energy generation uncertainty (kWh)	Energy generation uncertainty (%)
Jan-08	277.0	5.8	2.1
Feb-08	346.6	6.4	1.9
Mar-08	531.1	8.9	1.7
Apr-08	527.7	9.5	1.8
May-08	647.9	10.6	1.6
Jun-08	639.9	10.2	1.6
Jul-08	669.9	10.5	1.6
Aug-08	709.5	10.0	1.4
Sep-07	645.5	9.0	1.4
Oct-07	473.0	7.9	1.7
Nov-07	421.2	7.0	1.7
Dec-07	255.3	5.8	2.3
Annual	6144.7	101.8	1.7

Table F.3. Uncertainty in monthly and annual energy generation of dual-axis tracking system

Month	Measured energy generation (kWh)	Energy generation uncertainty (kWh)	Energy generation uncertainty (%)
Jan-08	114.9	3.1	2.7
Feb-08	114.4	2.9	2.5
Mar-08	161.6	3.8	2.4
Apr-08	157.4	4.0	2.5
May-08	203.8	4.5	2.2
Jun-08	211.8	4.4	2.1
Jul-08	217.8	4.5	2.1
Aug-08	232.9	4.4	1.9
Sep-07	195.6	3.8	2.0
Oct-07	147.1	3.4	2.3
Nov-07	135.3	3.0	2.2
Dec-07	79.5	2.7	3.4
Annual	1972.1	44.7	2.3

Solar Insolation

The pyranometer used to measure solar irradiance produces error in experimental measurement due to temperature dependence, linearity, and cosine response; accuracy statements for each source of error can be found in Table F.1. In addition, error is introduced in the conversion of the signal from the pyranometer to a digital value in the data logger; the conversion error in the data logger is $\pm$0.2 percent of full scale range and is a constant value of 5.81 W/m^2 [83].

The uncertainty in solar irradiance, *I*, for the dual-axis tracking system can be calculated by taking the square root of the sum of the squares of each individual component of error [83].

$$\delta I = [(5.81)^2 + (I * 0.01)^2 + (I * 0.005)^2 + (I * 0.01)^2]^{1/2} \quad \text{(F.6)}$$

The error due to cosine response can be assumed to be a constant value of 1 percent of the measured solar irradiance value since the tracking system is always oriented perpendicular to solar beam radiation (i.e., incidence angle is approximately 0 degrees and constant). The uncertainty in solar insolation available to the tracking system is shown in Table F.4.

Table F.4. Uncertainty in monthly and monthly average daily solar insolation for dual-axis tracking system

Month	Solar insolation (kWh/m^2)	Average daily solar insolation (kWh/m^2)	Uncertainty in solar insolation (kWh/m^2)	Uncertainty in average daily solar insolation (kWh/m^2)	Percent uncertainty (%)
1	130.96	4.22	2.77	0.09	2.1
2	127.40	4.55	2.65	0.09	2.1
3	176.40	5.69	3.61	0.12	2.0
4	172.55	5.75	3.70	0.12	2.1
5	224.13	7.23	4.48	0.14	2.0
6	236.40	7.88	4.65	0.16	2.0
7	239.58	7.73	4.69	0.15	2.0
8	257.43	8.30	4.78	0.15	1.9
9	219.42	7.31	4.14	0.14	1.9
10	159.37	5.14	3.33	0.11	2.1
11	141.45	4.71	2.87	0.10	2.0
12	88.12	2.84	2.17	0.07	2.5
Annual	2173.22	5.95	43.83	0.12	2.0

Determining the uncertainty in solar irradiance measurements for the stationary system is much more involved due to incidence angles ranging from 0 to 90 degrees. To determine the error due to cosine response, the incidence angle for each measurement was determined.

Methods for angle of incidence used here are based on work done by Duffie and Beckman [57]. The angle of incidence, ϑ, is the angle between the beam radiation on a surface and the normal to that surface. The angle of incidence can be determined by

$$\cos(\theta)_i = \begin{bmatrix} \sin(\delta)_i \sin(\emptyset) \cos(\beta) \\ -\sin(\delta)_i \cos(\emptyset) \sin(\beta) \cos(\gamma) \\ +\cos(\delta)_i \cos(\emptyset) \cos(\beta) \cos(\omega)_i \\ +\cos(\delta)_i \sin(\emptyset) \sin(\beta) \cos(\emptyset) \cos(\omega)_i \\ +\cos(\delta)_i \sin(\beta) \sin(\emptyset) \sin(\omega)_i \end{bmatrix} \quad \text{(F.7)}$$

The Greek term omega, ω, is the angular displacement of the sun east or west of the local meridian, and it is due to the rotation of the earth on its axis at 15 degrees per hour. The angular displacement value is calculated in radians where the morning values are negative and the afternoon values are positive by

$$\omega_i = (Solar\ Hour - 12) * 15^0 \tag{F.8}$$

The solar time, which is used in all of the sun-angle relationships, is the time based upon the rotation of the earth around the sun. When the sun is the highest in the sky, it is solar noon. The difference between standard time and solar time in minutes can be determined by

$$Solar\ Time - Standard\ Time\ = 4(L_{st} - L_{loc}) + E \tag{F.9}$$

where the equation of time, E, is

$$E = 229.2\begin{pmatrix} 0.000075 + 0.001868\ \cos(B) \\ -0.032077\ \sin(B) \\ -0.014615\ \cos(2B) \\ -0.04089\ \sin(2B) \end{pmatrix} \tag{F.10}$$

and B is

$$B_i = (n-1)\frac{360}{365} \tag{F.11}$$

The standard meridians, L_{ST}, for the continental U.S. time zones are: Eastern, 75°W; Central, 90°W; Mountain, 105°W; and Pacific, 120°W. The declination, δ, is the angular position of the sun with respect to the plane of the equator with north being positive at solar noon.

$$\delta_i = 23.45\ \sin\left(360\frac{284+n}{365}\right) \tag{F.12}$$

The latitude, φ, gives the location on the earth north or south of the equator which is expressed in degrees and minutes. The slope of the array surface is denoted using β. The surface azimuth angle, γ, is the deviation of the projection on a horizontal plane of the normal to the surface from the local meridian, with zero due south, east negative, and west positive [57].

Given the angle of incidence values for each data point, the uncertainty of the solar irradiance taken at the stationary system could be found as

$$\delta I = [(5.81)^2 + (I * 0.01)^2 + (I * 0.005)^2 + (I * e)^2]^{1/2} \tag{F.13}$$

Where the cosine response error, *e*, is 1 percent of full scale if the solar incidence angle is less than or equal to 70 degrees or 3 percent of full scale otherwise. The uncertainty in solar insolation available to the tracking system is shown in Table F.5.

Table F.5. Uncertainty in monthly and monthly average daily solar insolation for dual-axis tracking system

Month	Solar insolation (kWh/m^2)	Average daily solar insolation (kWh/m^2)	Uncertainty in solar insolation (kWh/m^2)	Uncertainty in average daily solar insolation (kWh/m^2)	Percent uncertainty (%)
1	89.99	2.90	1.97	0.06	2.2
2	90.31	3.23	2.07	0.07	2.3
3	135.53	4.37	3.01	0.10	2.2
4	132.81	4.43	3.27	0.11	2.5
5	165.10	5.33	3.91	0.13	2.4
6	164.24	5.47	3.86	0.13	2.3
7	171.97	5.55	3.88	0.13	2.3
8	182.73	5.89	3.91	0.13	2.1
9	168.48	5.62	3.57	0.12	2.1
10	120.71	3.89	2.79	0.09	2.3
11	106.89	3.56	2.36	0.08	2.2
12	65.42	2.11	1.69	0.05	2.6
Annual	1594.19	4.37	36.30	0.10	2.3

BIBLIOGRAPHY

[1] Energy Information Administration, 2008, "Annual Energy Outlook 2008 - with Projections to 2030," Technical Report No. DOE/EIA-0383(2008), Washington, D.C.

[2] Energy Information Administration, 2007, "Electric Power Annual 2006," Technical Report No. DOE/EIA-0348(2006), Washington, D.C.

[3] Energy Information Administration, 2008, Net Generation by Other Renewables: Total (All Sectors), October 28, 2008, http://www.eia.doe.gov/cneaf/electricity/epm/table1_1_a.html

[4] Energy Information Administration, 2008, "Annual Energy Review 2007," Technical Report No. DOE/EIA-0384(2007), Washington, D.C.

[5] Harrison Fraker, 2007, The Impact of Energy Consumption on the Environment - What Is the Biggest Culprit?, October 28, 2008, http://www.ced.berkeley.edu/images/stories/publications/ced_pubs/frameworks_5/fraker.07.fw.5.2.pdf

[6] American Society of Heating Refrigerating and Air-Conditioning Engineers, The American Institute of Architects, Illuminating Engineering Society of North America, New Buildings Institute, and United States Department of Energy, 2004, *Advanced Energy Design Guide for Small Office Buildings*, American Society of Heating Refrigerating and Air-Conditioning Engineers, Atlanta.

[7] American Society of Heating Refrigerating and Air-Conditioning Engineers, The American Institute of Architects, Illuminating Engineering Society of North America, New Buildings Institute, and United States Department of Energy, 2006, *Advanced Energy Design Guide for Small Retail Buildings*, American Society of Heating Refrigerating and Air-Conditioning Engineers, Atlanta.

[8] American Society of Heating Refrigerating and Air-Conditioning Engineers, The American Institute of Architects, Illuminating Engineering Society of North America, New Buildings Institute, and United States Department of Energy, 2008, *Advanced Energy Design Guide for K-12 School Buildings*, American Society of Heating Refrigerating and Air-Conditioning Engineers, Atlanta.

[9] American Society of Heating Refrigerating and Air-Conditioning Engineers, The American Institute of Architects, Illuminating Engineering Society of North America, New Buildings Institute, and United States

Department of Energy, 2008, *Advanced Energy Design Guide for Small Warehouses and Self-Storage Buildings*, American Society of Heating Refrigerating and Air-Conditioning Engineers, Atlanta.

[10] Frantzis L., and P. Mints, 2006, Pv Economics and Markets, November 3, 2008, http://www.abanet.org/environ/committees/renewableenergy/teleconarchives/021506/2-15-06Navigant.pdf

[11] Energy Information Administration, 2007, Annual Photovoltaic Domestic Shipments, October 28, 2008, http://www.eia.doe.gov/cneaf/solar.renewables/page/solarphotv/solarpv.html

[12] Energy Information Administration, 2008, Shipments of Photovoltaic Cells and Modules by Market Sector, End Use, and Type, 2005 and 2006, October 28, 2008, http://www.eia.doe.gov/cneaf/solar.renewables/page/rea_data/table2_23.pdf

[13] Sherwood L., 2008, U.S. Solar Market Trends 2007, November 4, 2008, http://www.irecusa.org/fileadmin/user_upload/NationalOutreachPubs/IREC%20Solar%20Market%20Trends%20August%202008_2.pdf

[14] Iowa Energy Center, 2006, Iowa Solar Maps, November 3, 2008, http://www.energy.iastate.edu/Renewable/solar/maps-index.htm

[15] National Renewable Energy Laboratory, 2008, Annual Average Daily Solar Radiation, October 28, 2008, http://rredc.nrel.gov/solar/old_data/nsrdb/redbook/atlas/serve.cgi

[16] Marion, W., and Wilcox, S., 1994, *Solar Radiation Data Manual for Flat-Plate and Concentrating Collectors*, National Renewable Energy Laboratory, Golden.

[17] Dummer G. W. A., 1997, *Electronic Inventions and Discoveries - Electronics from Its Earliest Beginnings to the Present Day*, Institute of Physics, London.

[18] Vignola F., Hocken J., and G. Grace, 2000, Pv Lesson Plan 1 - Solar Cells, November 2, 2008, http://solardat.uoregon.edu/download/Lessons/PVLessonPlan1SolarCells.pdf

[19] National Aeronautics and Space Administration, 2008, The Electromagnetic Spectrum, November 2, 2008, http://imagine.gsfc.nasa.gov/docs/science/know_l2/emspectrum.html

[20] U.S. Department of Energy, 2008, Technologies - Light and the Pv Cell, November 2, 2008, http://www1.eere.energy.gov/solar/pv_cell_light.html

[21] Schoolpowernaturally, Photocells Ii: The Photoelectric Effect in Photocells, November 3, 2008, http://www.powernaturally.org/Programs/pdfs_docs/29_Photocells_II.pdf

[22] Exell R. H. B., 2000, The Physics of Photovoltaic Cells, November 3, 2008, http://www.jgsee.kmutt.ac.th/exell/Solar/PVCells.html

[23] Petchers N., 2003, *Combined Heating, Cooling & Power Handbook: Technologies & Applications*, The Fairmont Press, Lilburn.

[24] Solarbuzz, 2008, Solar Cell Technologies, November 3, 2008, http://www.solarbuzz.com/technologies.htm

[25] Mah O., 1998, Fundamentals of Photovoltaic Materials, October 1, 2008, http://userwww.sfsu.edu/~ciotola/solar/pv.pdf

[26] U.S. Department of Energy, 2005, Technologies - Solar Cell Materials, November 3, 2008, http://www1.eere.energy.gov/solar/solar_cell_materials.html

[27] U.S. Department of Energy, 2005, Technologies - Pv Devices, November 3, 2008, http://www1.eere.energy.gov/solar/pv_devices.html

[28] Luque A., and S. Hegedus, 2003, *Handbook of Photovoltaic Science and Engineering*, John Wiley & Sons Ltd., West Sussex, England.

[29] U.S. Department of Energy, 2005, Technologies - Silicon, November 3, 2008, http://www1.eere.energy.gov/solar/silicon.html

[30] Baker R., Harry L., and B. David, 1998, *Cmos Circuit Design, Layout, and Simulation*, John Wiley & Sons, New York.

[31] Solar Century, 2008, Pv Technology Comparison, January 6, 2008, http://www.solarcentury.com/knowledge_base/articles/pv_comparison_table

[32] U.S. Department of Energy, 2006, Technologies - Polycrystalline Thin Film, November 1, 2008, http://www1.eere.energy.gov/solar/tf_polycrystalline.html

[33] U.S. Department of Energy, 2005, Technologies - Solar Cell Structures, November 1, 2008, http://www1.eere.energy.gov/solar/solar_cell_structures.html

[34] Forsyth, T. L., Pedden, M., and Gagliano, T., 2002, "Effects of Net Metering on the Use of Small-Scale Wind Systems in the United States," Technical Report No. NREL/TP-500-32471, National Renewable Energy Laboratory, Golden.

[35] North Carolina Solar Center, and Interstate Renewable Energy Council, 2008, Net Metering for Renewable Energy, August 24, 2008, http://www.dsireusa.org/library/includes/seeallincentivetype.cfm?type=Net&currentpageid=7&back=regtab&EE=0&RE=1

[36] U.S. Department of Energy, 2006, Pv Systems and Net Metering, August 21, 2008, http://www1.eere.energy.gov/solar/net_metering.html

[37] Messenger, R. A., and Ventre, J., 2004, *Photovoltaic Systems Engineering*, CRC Press LLC, Boca Raton.

[38] Wiser, R., Bolinger, M., Cappers, P., and Margolis, R., 2006, "Letting the Sun Shine on Solar Costs: An Emperical Investigation of Photovoltaic Cost Trends in California," Technical Report No. NREL/TP-620-39300, Berkeley.

[39] Solarbuzz, 2006, Solar Energy Costs and Prices, October 28, 2008, http://www.solarbuzz.com/statsCosts.htm

[40] National Renewable Energy Laboratory, 2008, "Planning for Pv - the Value and Cost of Solar Electricity," Technical Report No. DOE/GO-102008-2555, Golden.

[41] National Renewable Energy Laboratory, 2004, "Solar Energy Technologies Program - Multi-Year Technical Plan 2003-2007 and Beyond," Technical Report No. DOE/GO-102004-1775, Bolder.

[42] Solarbuzz, 2008, Solar Module Price Highlights: October 2008, November 3, 2008, http://www.solarbuzz.com/Moduleprices.htm

[43] Navigant Consulting Inc., 2006, "A Review of Pv Inverter Technology Cost and Performance Projections," Technical Report No. NREL/SR-620-38771, Golden.

[44] North Carolina Solar Center, and Interstate Renewable Energy Council, 2008, Iowa Incentives for Renewable Energy, September 4, 2008, http://www.dsireusa.org/library/includes/map2.cfm?CurrentPageID=1&State=IA

[45] Sherwood L., U.S. Solar Market Trends, October 28, 2008, http://www.arcmansolarpower.com/specs/US%20Solar%20Market%20Trend.pdf

[46] Starrs T. J., 2004, Designing a Performance-Based Incentive for Photovoltaic Markets, November 4, 2008, http://www.californiasolarcenter.org/pdfs/forum/Solar04-PerfBasedIncent-Pub.pdf

[47] Caird S., Roy R., Potter S., and Herring H., 2007, "Consumer Adoption and Use of Household Renewable Energy Technologies," Technical Report No. DIG-10, The Open University, Miltono Keynes, UK.

[48] National Renewable Energy Laboratory, 2008, A Performance Calculator for Grid-Connected Pv Systems, October 28, 2008, http://rredc.nrel.gov/solar/codes_algs/PVWATTS/

[49] Rushing, A. S., and Lippiatt, B. C., 2008, "Energy Price Indices and Discount Factors for Life-Cycle-Cost Analysis - April 2008," Technical Report No. NISTIR 85-3273-23, National Institute of Standards and Technology, Gaithersburg.

[50] Iowa Department of Natural Resources, 2000, A Midwest Study of Attitudes and Opinions toward Photovoltaic Technology: Executive Summary, November 15, 2007, http://www.iowadnr.gov/energy/renewable/files/pvsum.pdf

[51] Sandia National Laboratories, 2001, Solar Electric Power - the U.S. Photovoltaic Industry Roadmap, November 1, 2008, http://photovoltaics.sandia.gov/docs/PDF/PV_Road_Map.pdf

[52] Sharp Solar Energy Solutions Group, 2006, Growing Number of Americans Think That Solar Electricity Should Be Offered on All New Homes, October 29, 2008, http://solar.sharpusa.com/files/sol_dow_solarsurvey_062106.pdf

[53] Energy Information Administration, 2008, Average Retail Price of Electricity to Ultimate Customers by End-Use Sector, by State, October 16, 2008, http://www.eia.doe.gov/cneaf/electricity/epm/table5_6_b.html

[54] Whitaker, C. M., Townsend, T. U., Wenger, H. J., Iliceto, A., Chimento, G., and Paletta, F., 1992, "Effects of Irradiance and Other Factors on Pv Temperature Coefficients," eds., Las Vegas, NV, USA, 1, pp. 608-613.

[55] Del Cueto, J. A., 2002, "Comparison of Energy Production and Performance from Flat-Plate Photovoltaic Module Technologies Deployed at Fixed Tilt," eds., New Orleans, LA, United States, pp. 1523-1526.

[56] King, D. L., Boyson, W. E., and Kratochvil, J. A., 2002, "Analysis of Factors Influencing the Annual Energy Production of Photovoltaic Systems," eds., New Orleans, LA, United States, pp. 1356-1361.

[57] Duffie, J. A., and Beckman, W. A., 1991, *Solar Engineering of Thermal Processes*, John .Wiley & Sons, Inc., New York.

[58] Tiwari G. N., and M. K. Ghosal, 2005, *Renewable Energy Resources: Basic Principles and Applications*, Alpha Science International Ltd., Harrow, Middlesex U.K.

[59] New Solar Homes Partnership, 2007, New Solar Homes Partnership Calculator, November 1, 2008, http://www.gosolarcalifornia.ca.gov/nshpcalculator/index.html

[60] California Energy Commission, 2008, Clean Power Estimator, October 20, 2008, http://www.consumerenergycenter.org/renewables/estimator/index.html

[61] Fanney, A. H., and Dougherty, B. P., 2001, "Building Integrated Photovoltaic Test Facility," Journal of Solar Energy Engineering, Transactions of the ASME, 123(3), pp. 194-199.

[62] Hall, B. H., and Khan, B., 2003, Adoption of New Technology, http://repositories.cdlib.org/iber/econ/E03-330/

[63] Warren R. D., Pate, M. B., and R. M. Nelson, 2008, "Experimental Performance of a Grid-Connected Stationary Photovoltaic System Using Mc-Si Modules in Central Iowa," Journal of Solar Energy Engineering, Transactions of the ASME, pp. Submitted for publication.

[64] Warren R. D., Pate, M. B., and R. M. Nelson, 2008, "Experimental Performance of a Grid-Connected Dual-Axis Tracking Photovoltaic System Using Mc-Si Modules in Central Iowa," Journal of Solar Energy Engineering, Transactions of the ASME, pp. Submitted for publication.

[65] Warren R. D., Pate, M. B., and R. M. Nelson, 2008, "Performance Comparison of Stationary and Dual-Axis Tracking Grid-Connected Photovoltaic Systems Using Mc-Si Modules in Central Iowa," Journal of Solar Energy Engineering, Transactions of the ASME, pp. Submitted for publication.

[66] Warren R. D., Pate, M. B., and R. M. Nelson, 2008, "Economic Analyses of Stationary and Dual-Axis Tracking Grid-Connected Photovoltaic Systems Using Mc-Si Modules in Central Iowa," Journal of Solar Energy Engineering, Transactions of the ASME, pp. Submitted for publication.

[67] Warren R. D., Pate, M. B., and R. M. Nelson, 2008, "Experimental Assessment of Heat Transfer Characteristics and the Affects of Operating Temperature for Stationary and Dual-Axis Tracking Photovoltaic Systems Using Mc-Si Modules in the Upper Midwest," Journal of Solar Energy Engineering, Transactions of the ASME, pp. Submitted for publication.

[68] Iowa Energy Center, 2008, Demonstration Real-Time and Historical Performance Data Interface, www.energy.iastate.edu/Renewable/solar

[69] King, D. L., and Eckert, P. E., 1996, "Characterizing (Rating) the Performance of Large Photovoltaic Arrays for All Operating Conditions," eds., Washington, DC, USA, pp. 1385-1388.

[70] Myers, D. R., Reda, I., Wilcox, S., and Andreas, A., 2004, "Optical Radiation Measurements for Photovoltaic Applications: Instrumentation Uncertainty and Performance," eds., Denver, CO, United States, 5520, pp. 142-153.

[71] National Weather Service Forecast Office, 2008, Observed Weather, Des Moines, Ia., September 28, 2008, http://www.weather.gov/climate/index.php?wfo=dmx

[72] Marion, B., Adelstein, J., Boyle, K., Hayden, H., Hammond, B., Fletcher, Canada, B., Narang, D., Kimber, A., Mitchell, L., Rich, G., and Townsend, T., 2005, "Performance Parameters for Grid-Connected Pv Systems," eds., Lake Buena Vista, FL, United States, pp. 1601-1606.

[73] Park, C. S., 2002, *Contemporary Engineering Economics*, Prentice-Hall, Inc., New Jersey.

[74] Fuller, S. K., and Petersen, S. R., 1995, *Life-Cycle Costing Manual for the Federal Energy Management Program*, *Nist Handbook; 135*, U.S. Dept. of Commerce, Technology Administration, National Institute of Standards and Technology, Gaithersburg.

[75] Laukamp, H., Schoen, T., and Ruoss, D., 2002, "Reliability Study of Grid Connected Pv Systems Field Experience and Recommended Design Practice," Technical Report No. IEA-PVPS T7-08: 2002, Freiburg.

[76] Quintana, M. A., King, D. L., Mcmahon, T. J., and Osterwald, C. R., 2002, "Commonly Observed Degradation in Field-Aged Photovoltaic Modules," eds., New Orleans, LA, United States, pp. 1436-1439.

[77] Osterwald, C. R., Anderberg, A., Rummel, S., and Ottoson, L., 2002, "Degradation Analysis of Weathered Crystalline-Silicon Pv Modules," eds., New Orleans, LA, United States, pp. 1392-1395.

[78] 1995, "Stand-Alone Photovoltaic Systems: A Handbook of Recommended Design Practices," Technical Report No. SAND-87-7023,

[79] 2008, Average Annual Inflation by Decade, August 19, 2008, http://inflationdata.com/Inflation/images/charts/Articles/Decade_inflation_chart.htm

[80] U.S. Department of Treasury, 2008, Daily Treasury Yield Curve Rates, August 19, 2008, http://www.treas.gov/offices/domestic-finance/debt-management/interest-rate/yield.shtml

[81] Lange N., and W. Grant, 2001, *Landowner's Guide to Wind Energy in the Upper Midwest*, Izaak Walton League of America, St. Paul.

[82] Watson J., Sauter R., Bahaj B., James P. A., Myers L., and R. Wing, 2006, *Unlocking the Power House: Policy and System Change for Domestic Micro-Generation in the Uk*, Universities of Sussex and Southampton and Imperial College London.

[83] Campbell Scientific, 2001, "Eppley Psp Precision Spectral Pyranometer," Technical Report No. 2RA-A, Logan.

ACKNOWLEDGEMENTS

I sincerely thank my parents, Terry and Detra Warren, for their unconditional support and encouragement throughout my life; they have undoubtedly provided me every opportunity possible to peruse my dreams. I would also like to express my most sincere gratitude to my major professors, Dr. Michael Pate and Dr. Ron Nelson; they have been excellent mentors, teachers, and friends throughout my undergraduate and graduate studies. Additionally, I would like to acknowledge to the Iowa Energy Center for providing support and guidance during my graduate work. The Iowa Energy Center staff worked very hard to make my research and graduate education possible; I would like to specifically acknowledge: Curt Klaassen, Keith Kutz, Amy Myers, Floyd Barwig, William Haman, Norm Olson, Xiaohui Zhou, David Perry, Patty Prouty, Julie Charlson, and Denise Junod. Finally, I would also like to note my appreciation to each of my committee members: Dr. Michael Pate, Dr. Ron Nelson, Dr. Gregory Maxwell, Dr. Palaniappa Molian, and Dr. Howard Meeks. My personal accomplishments and character as well as my abilities as an engineer and researcher are a direct reflection of the superior support and guidance received by all those acknowledged.